

Institut für Stammzellforschung und Regenerative Medizin

Direktor: Univ.-Prof. Dr. rer. nat. James Adjaye

kumulative
Habilitationsschrift

Induced pluripotent stem cells for modelling nonalcoholic fatty liver disease (NAFLD)

zur Erlangung der Venia Legendi
im Fach Stammzellforschung und Regenerative Medizin

vorgelegt der Medizinischen Fakultät
der Heinrich-Heine-Universität Düsseldorf

von
Dr. rer. nat. Nina Graffmann

Düsseldorf, 2023

Contents

1. Zusammenfassung	4
2. Abstract	6
3. Introduction	7
3.1. Nonalcoholic fatty liver disease (NAFLD)	7
3.2. Induced pluripotent stem cells as a tool for disease modelling	9
3.3. Liver function and anatomy as a basis for modelling the organ	11
3.4. In vitro differentiation of hepatocyte like cells for disease modelling	13
3.5. Understanding lipid droplet formation and lipid metabolism	15
3.6. Regulation of lipid metabolism	18
3.6.1. Peroxisome proliferator-activated receptors (PPAR) family	18
3.6.2. Adipokines	19
3.7. The role of microRNAs in NAFLD	19
4. Aim of this study	20
5. Own research articles	21
5.1. Establishment and characterization of an iPSC line from a 35 years old high grade patient with nonalcoholic fatty liver disease (30 – 40 % steatosis) with homozygous wildtype PNPLA3 genotype	21
5.2. Establishment and characterization of an iPSC line from a 58 years old high grade patient with nonalcoholic fatty liver disease (70 % steatosis) with homozygous wildtype PNPLA3 genotype.	21
5.3. Modeling Nonalcoholic Fatty Liver Disease with Human Pluripotent Stem Cell-Derived Immature Hepatocyte-Like Cells Reveals Activation of PLIN2 and Confirms Regulatory Functions of Peroxisome Proliferator-Activated Receptor Alpha.	24
5.4. Cell fate decisions of human iPSC-derived bipotential hepatoblasts depend on cell density.	27
5.5. A stem cell based in vitro model of NAFLD enables the analysis of patient specific individual metabolic adaptations in response to a high fat diet and AdipoRon interference.	30

6.	Discussion	34
6.1	The role of iPSCs for disease modelling	34
6.2	Using iPSC to model liver diseases	35
6.2.1	Increasing maturation in iPSC-derived HLCs	36
6.3.	IPSC-based in vitro models for NAFLD	38
7.	Conclusion	40
8.	Abbreviations	42
9.	References	44
10.	Acknowledgements	61
11.	Erklärungen und Eidesstattliche Versicherungen	62
12.	Addendum	66

1 Zusammenfassung

Etwa 30 % der Gesamtbevölkerung und 70 % aller übergewichtigen Patienten sind von der nicht-alkoholischen Fettlebererkrankung (nonalcoholic fatty liver disease (NAFLD)) betroffen. Durch kalorienreiche Ernährung und Bewegungsmangel lagern Hepatozyten Fett ein. Die frühen Stadien sind gutartig und reversibel, können sich jedoch in eine nicht-alkoholische Steatohepatitis mit chronischer Entzündung und weiter zur Fibrose, Zirrhose und zum hepatozellulären Karzinom entwickeln. Bis heute ist nicht verstanden, warum die Erkrankung bei einigen Patienten in dieser Weise fortschreitet.

Induzierte pluripotente Stammzellen (induced pluripotent stem cells (iPSCs)) sind ein wertvolles Werkzeug, um Krankheiten *in vitro* nachzustellen und neue Medikamente zu entwickeln oder zu testen. Um das im ISRM vorhandene Portfolio an NAFLD-Zelllinien zu vervollständigen, wurden im Rahmen dieser Arbeit zwei neue iPSC-Linien von Fettleberpatienten mit 30-40 % bzw. 70 % Steatose generiert. Eine embryonale Stammzelllinie und iPSC-Linien von fünf Spendern wurden zu hepatozyten-ähnlichen Zellen (hepatocyte-like cells (HLCs)) differenziert. Hierbei zeigte sich, dass die Zelldichte für den Differenzierungserfolg essentiell ist. Bei geringer Zelldichte entwickelten sich statt HLCs sogenannte endodermale Epithelzellen (endoderm derived epithelial cells (EDECs)). Dies konnte durch Manipulation der Notch-, wingless-related integration site (WNT), hedgehog (Hh), and transforming growth factor (TGF) β -Signalwege nicht verhindert werden.

Nach Behandlung der HLC mit Ölsäure (oleic acid (OA)) konnten die NAFLD-Charakteristika Fetteinlagerung und erhöhte Perilipin 2 Expression in allen Linien reproduziert werden. Die HLCs wiesen ein NAFLD-assoziiertes Transkriptom und micro-RNA Profil auf, welches vergleichbar mit dem von Patienten war. Mit Hilfe der HLCs konnte gezeigt werden, dass Stoffwechselknotenpunkte wie das Peroxisome proliferator-activated receptor (PPAR) α Netzwerk unter OA-Einfluss differentiell reguliert sind. Eine Aktivierung von PPAR α mittels Fenofibrat reduzierte die Expression von Genen, die an der Biosynthese von Phospholipiden und Cholesterin beteiligt sind. Des Weiteren wurden HLCs mit AdipoRon, einem synthetischen Analogon des Adiponektins, welches einen mit positiven Einfluss auf die β -Oxidation und die Insulinsensitivität hat, behandelt. Auch hier konnten positive Veränderungen des Transkriptoms wie z.B. die Hochregulation des PI3K-AKT-Signalwegs in OA-behandelten Zellen festgestellt werden.

Aufgrund differentieller Genotypen der Spender und ihrer individuellen Krankheitsausprägung konnten Unterschiede zwischen den Zelllinien in Bezug auf Größe und Verteilung der Fetttröpfchen sowie der Genexpression beobachtet werden. Unabhängig von der Behandlung konnte ein Steatose-Phänotyp mit niedriger Expression von Genen des Fettexports, der Fett- und Cholesterinsynthese, der

Glukoneogenese, der β -Oxidation und des FGF21-Signalwegs in den HLCs aus Steatosepatienten identifiziert werden. Diese Befunde belegen die Eignung des etablierten iPSC-basierten Zellkulturmodells zur Untersuchung der Ätiologie von NAFLD und zur patientenspezifischen Testung möglicher therapeutischer Interventionen als Baustein der personalisierten Medizin.

2 Abstract

Nonalcoholic fatty liver disease (NAFLD) is a prominent condition in our modern world, affecting up to 30 % of the general population and 70 % of obese patients, with increasing incidences. It develops as a consequence of a high caloric diet and lack of physical exercise, when hepatocytes store excess fat. While the early stages are benign and reversible, patients can develop nonalcoholic steatohepatitis, characterized by chronic inflammation, which can progress to fibrosis, cirrhosis, and hepatocellular carcinoma. The phenotype is rather complex and the causes and mechanisms of disease progression are not yet understood.

Induced pluripotent stem cells (iPSCs) are a valuable tool for disease modelling as well as drug development and testing. For this study, two novel iPSC lines from steatosis patients with 30-40 % and 70 % steatosis, respectively, were derived to complement the panel of patient specific iPSC lines available at ISRM. One embryonic stem cell line and five iPSC lines from different donors were differentiated into hepatocyte like cells (HLCs).

Our work showed that cellular density is an essential factor for differentiation success. Insufficient density favoured an endoderm derived epithelial cell (EDEC) fate over HLCs, which could not be reverted by interfering with Notch, wntless-related integration site (WNT), hedgehog (Hh), and transforming growth factor (TGF) β signalling pathways, respectively. HLCs stored fat and up-regulated perilipin 2 expression in response to treatment with high levels of oleic acid (OA), thus reproducing prominent features of NAFLD. In addition, their transcriptome and micro-RNA profile recapitulated alterations seen in NAFLD patients.

The *in vitro* model revealed metabolic hubs, such as the peroxisome proliferator-activated receptor (PPAR) α signalling network, as being differentially regulated in response to OA treatment. Activation of PPAR α by Fenofibrate resulted in reduced expression of genes involved in biosynthesis of phospholipids and cholesterol. Treatment with AdipoRon, an analogue of adiponectin, which is known to improve β -oxidation and insulin sensitivity, confirmed several NAFLD specific positive effects on transcriptome level such as up-regulation of PI3K-AKT-signalling in OA treated cells.

In accordance with the various genetic backgrounds and disease phenotypes of the donors, differences between the cell lines regarding gene expression and lipid droplet profile could be observed. Overall, we identified a steatosis related phenotype, independent of OA treatment, which is characterized by low expression of genes involved in lipid export, fat and cholesterol synthesis, gluconeogenesis, β -oxidation and FGF21 signalling in the high steatosis lines. Our observations confirm the suitability of the iPSC-based *in vitro* model to study the aetiology of NAFLD and - as part of a personal medicine approach- to test intervening drugs with respect to the patient-specific genetic background.

3 Introduction

3.1 Nonalcoholic fatty liver disease (NAFLD)

NAFLD is defined by storage of more than 5 % fat inside of hepatocytes (steatosis) in the absence of other triggers such as alcohol consume, virus infection, or drug-mediated injury (Tacke et al., 2022). This disease comprises a spectrum of phenotypes, ranging from simple steatosis over nonalcoholic steatohepatitis (NASH) to liver fibrosis/cirrhosis and cancer. Initially, the fat storage is benign, reversible, and even beneficial, because it protects the cells from lipotoxicity and provides energy in times of fasting (Geltinger et al., 2020). However, 5 – 10 % of the patients develop NASH with hepatocyte ballooning, formation of Mallory-Denk-bodies and, most critically, also inflammation and massive function loss. From there on, liver fibrosis, cirrhosis, and hepatocellular carcinoma can develop, which finally result in the necessity of a liver transplant (Buzzetti et al., 2016)

Fig. 1).

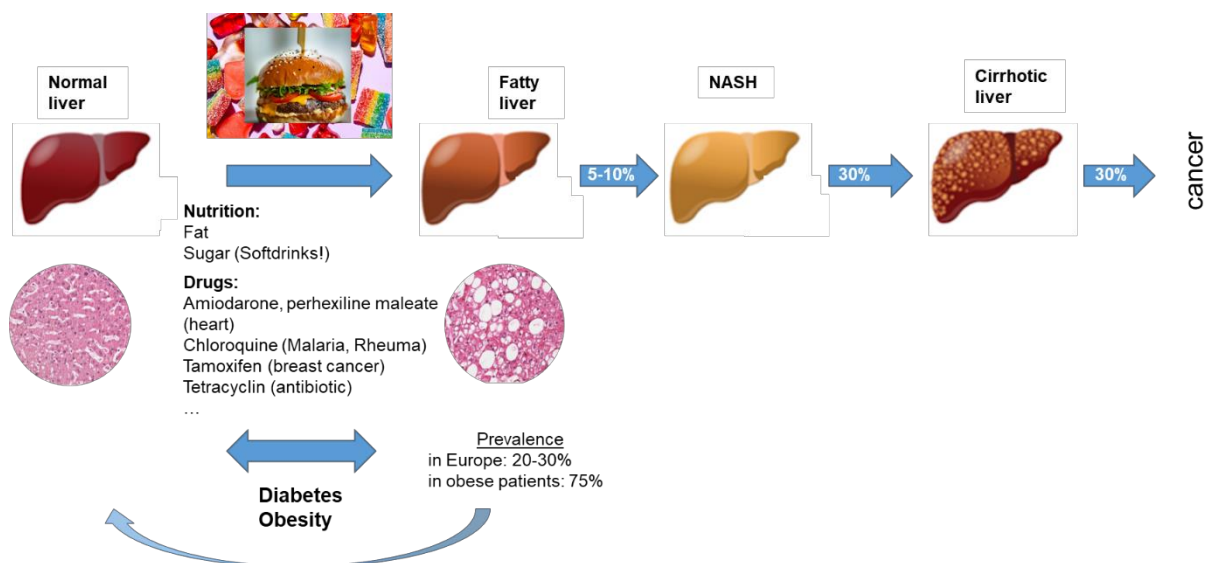


Fig. 1 Scheme of NAFLD development. NAFLD develops as a consequence of a high caloric diet and sedentary lifestyle. NAFLD is defined as > 5 % fat storage by hepatocytes. It is a multifactorial disease and additional hits lead to the development of nonalcoholic steatohepatitis (NASH), cirrhosis and finally hepatocellular carcinoma. Modified from <https://theconversation.com>¹, and Wruck et al. 2015, published under a creative commons licence <http://creativecommons.org/licenses/by/4.0> and reproduced with friendly permission of the publisher.

In the United States, NASH is already the second most common cause for liver transplantation after hepatitis C virus infection (Wong et al., 2015). As early stages of NAFLD do not cause any severe

¹ Benoit Arsenault, Université de Québec, Université Laval, and Émilie Gobeil Université Laval <https://theconversation.com/uncovering-the-genetic-causes-of-fatty-liver-disease-a-growing-health-concern-176641>, accessed on 11.09.2023

symptoms, the disease is likely to be underdiagnosed and current data on patient number are difficult to obtain (Alexander et al., 2018). A study by Younossi et al. from 2016 estimates that about 52 million people with NAFLD/non-cirrhotic NASH lived in Germany, France, Italy, and the United Kingdom, causing an approximate annual cost of about 35 billion € to the health care system (Younossi et al., 2016a). For Germany, it is predicted that NAFLD cases without NASH rise by 7.2 % from 15.12 million cases to 16.21 million in 2030. NASH cases are expected to rise within this time period by 43 % from 3.33 million cases to 4.74 million (Estes et al., 2018). Thus, NAFLD and its potential consequences are not only an individual health problem but also a burden to the economy.

NAFLD develops as a consequence of our high-caloric modern Western diet in combination with a lack of physical exercise. It affects around 25-30 % of the general population and 31.6 % of obese / overweight children (Younossi et al., 2016b, Cholongitas et al., 2021).

It is not fully understood yet, why only 5-10 % of the patients develops NASH and the majority does not (Buzzetti et al., 2016). Disease progression is attributed to several “hits” that result in liver damage, including insulin resistance, diet, hormones/adipokines secreted from the adipose tissue, gut microbiota and genetic as well as epigenetic factors (Buzzetti et al., 2016).

While NAFLD is tightly connected to type 2 diabetes mellitus and obesity, it can also occur independently of these conditions, even in lean patients. Up to now it is not known how exactly diabetes and NAFLD influence each other (Tilg et al., 2017, Stefan and Cusi, 2022). However, NAFLD patients often suffer from metabolic syndrome and cardiac failure is a main cause of death in these patients (Mantovani et al., 2022). In addition, they have a higher incidence of extrahepatic cancers, coeliac disease, osteoporosis, and bone fractures (Loosen et al., 2022, Roderburg et al., 2022a, Roderburg et al., 2022b).

The tight connection of NAFLD to the metabolic syndrome is the basis for recent approaches to re-label the disease into metabolic fatty liver disease (MAFLD) instead of NAFLD. This has been intensively discussed, because changes of the disease definition result in changes of the diagnostic criteria (Eslam et al., 2020, Mendez-Sanchez et al., 2021). MAFLD includes steatosis patients with relevant metabolic risk factors regardless of other causes such as high alcohol consumption or hepatitis C infection. In contrast, NAFLD excludes the latter patients but includes lean patients without metabolic risk factors (Kaya et al., 2022). This discordance is partly reflected in an overall reduced mortality rate in NAFLD patients compared to MAFLD patients (Huang et al., 2021, Kaya et al., 2022).

After intense debate and the evaluation of four online surveys, which assessed the opinions of 236 panellists from 56 countries, the three large pan-national liver associations (American Association for Study of Liver Disease, European Association for Study of the Liver and La Asociación Latinoamericana

para el Estudio del Hígado) agreed in June 2023 on replacing the term NAFLD with MASLD (short for metabolic dysfunction-associated steatotic liver disease) which evokes less negative associations. The term “steatotic liver disease” (SLD) will now be employed as an umbrella term for all liver diseases with steatosis phenotype regardless of their origin and steatohepatitis will be retained for the severe forms of the disease (Rinella et al., 2023).

While NAFLD is a multifactorial disease mainly related to an imbalance in calorie intake and expenditure, a few genetic polymorphisms have been described, which predispose patients for developing the disease. These are mainly patatin-like phospholipase domain containing protein (PNPLA) 3 rs738409 (I148M) (Romeo et al., 2008) and transmembrane 6 superfamily member 2 (TM6SF2) rs58542926 (E167K) (Kozlitina et al., 2014). Interestingly, the PNPLA3 M/M variant is most common in Hispanics (frequency 0.49), the ethnic group with the highest susceptibility for NAFLD and much less in European Americans (0.23) and African Americans (0.17) (Romeo et al., 2008). While the PNPLA3 mutation increases both, steatosis and fibrosis, the TM6SF2 variant seems to predominantly increase hepatic fat accumulation (Krawczyk et al., 2017).

Due to metabolic differences in rodents and humans, it has been difficult to study the molecular mechanisms of NAFLD/NASH and there exists no United States Food and Drug Administration (FDA) or European Medical Agency (EMA) approved therapy (Sumida et al., 2019, Harrison et al., 2023). Several drugs which are successful for the treatment of diabetes or elevated blood fats failed to reduce NAFLD/NASH (Boeckmans et al., 2019, Francque and Vonghia, 2019).

Currently, there are four different anti NASH drugs in phase 3 clinical trials: Obeticholic acid (Intercept Pharmaceutical), Resmetirom (Madrigal Pharmaceuticals Inc), Lanifibranor (Inventiva), and Semaglutide (Novo Nordisk) (Harrison et al., 2023). Of these, the oral pan-peroxisome proliferator-activated receptor (PPAR) agonist Lanifibranor and the glucose-like peptide (GLP)-1 receptor agonist Semaglutide are the most promising ones. Lanifibranor is the only drug in phase 3 trials that could reduce both fibrosis and NASH and might therefore be the first EMA approved anti NASH drug. Semaglutide is already approved for the treatment of type 2 diabetes and obesity and was successful in reducing NASH without worsening fibrosis (Harrison et al., 2023).

3.2 Induced pluripotent stem cells as a tool for disease modelling

To understand the molecular mechanisms underlying human diseases, cell culture models as well as animal studies are essential. Cell lines based on tumour cells are often applied. They have the advantage of unlimited proliferation and the disadvantage of chromosomal, metabolic, and epigenetic aberrations (Geraghty et al., 2014, Franzen et al., 2021). A better alternative, regarding metabolism

and physiology, are primary cells. Naturally, they are only available in limited numbers, rarely from healthy donors and always associated with ethical issues. In addition, they are only usable for short-term experiments. This is especially true for human primary hepatocytes (PHH), which dedifferentiate almost immediately in conventional monolayer cell culture (Godoy et al., 2013).

When animals are used to study human diseases, their differential metabolism, immune system, and gene function compared to humans is often problematic. This explains, why animal models fail frequently in predicting drug toxicities and why so many clinical trials must be aborted due to serious side effects and many drugs have to be withdrawn from the market (Kaplowitz, 2005, Sun et al., 2022). In 2021 drug attrition rate even reached 95% (Loewa et al., 2023).

Since the discovery of induced pluripotent stem cells (iPSCs) by Shinya Yamanaka in 2006/7 (Takahashi and Yamanaka, 2006, Takahashi et al., 2007) novel, more complex cell culture models, which better resemble the human system, have been developed. iPSCs can be obtained from every cell of the human body, by overexpressing a cocktail of pluripotency associated genes, namely octamer-binding transcription factor (OCT) 3/4, sex determining region Y-box (SOX) 2, krüppel-like factor (KLF) 4, c-MYC, or OCT4, SOX2, NANOG and LIN28 (Takahashi and Yamanaka, 2006, Takahashi et al., 2007, Yu et al., 2007). After a period of 2-4 weeks, the transcriptome and epigenome of the reprogrammed cells is profoundly remodelled, and they re-express their endogenous pluripotency factors. While initially fibroblasts have been predominantly reprogrammed, nowadays almost all cell types have been used as a source (Ray et al., 2021). Especially urine derived cells are interesting as a starting material, because of their inherent stem cell character and their non-invasive accessibility (Bento et al., 2020).

iPSCs can be differentiated into almost all cell types, and differentiation protocols are constantly improved to increase maturity and functionality of the resulting cells. However, up to now the cells differentiated from iPSC resemble more foetal than adult cells and still substantial work is necessary to obtain fully functional cells (Baxter et al., 2015, Camp et al., 2017, Wu et al., 2018). While initially the goal was to get pure populations of each isolated cell type, it became apparent that mixed cultures, containing different cell types from one tissue, reach higher levels of maturity. They are more suitable to model complex diseases, which depend on cell-cell interactions (Takebe et al., 2017, Takahashi et al., 2018, Saglam-Metiner et al., 2023). Nowadays, this is frequently combined by transferring the cells into 3D systems, where optimized cell-cell contacts, matrix conditions, and perfusion with medium give ideal support (Lancaster and Huch, 2019).

3.3 Liver function and anatomy as a basis for modelling the organ

The liver is a complex organ, which is essential for keeping up the bodies' metabolic equilibrium, for detoxifying xenobiotics, and for the synthesis of plasma proteins and bile acids (Schulze et al., 2019). Micro-anatomically, it consists of distinct functional subunits, the so-called liver lobules (Si-Tayeb et al., 2010, Godoy et al., 2013) (Fig. 2).

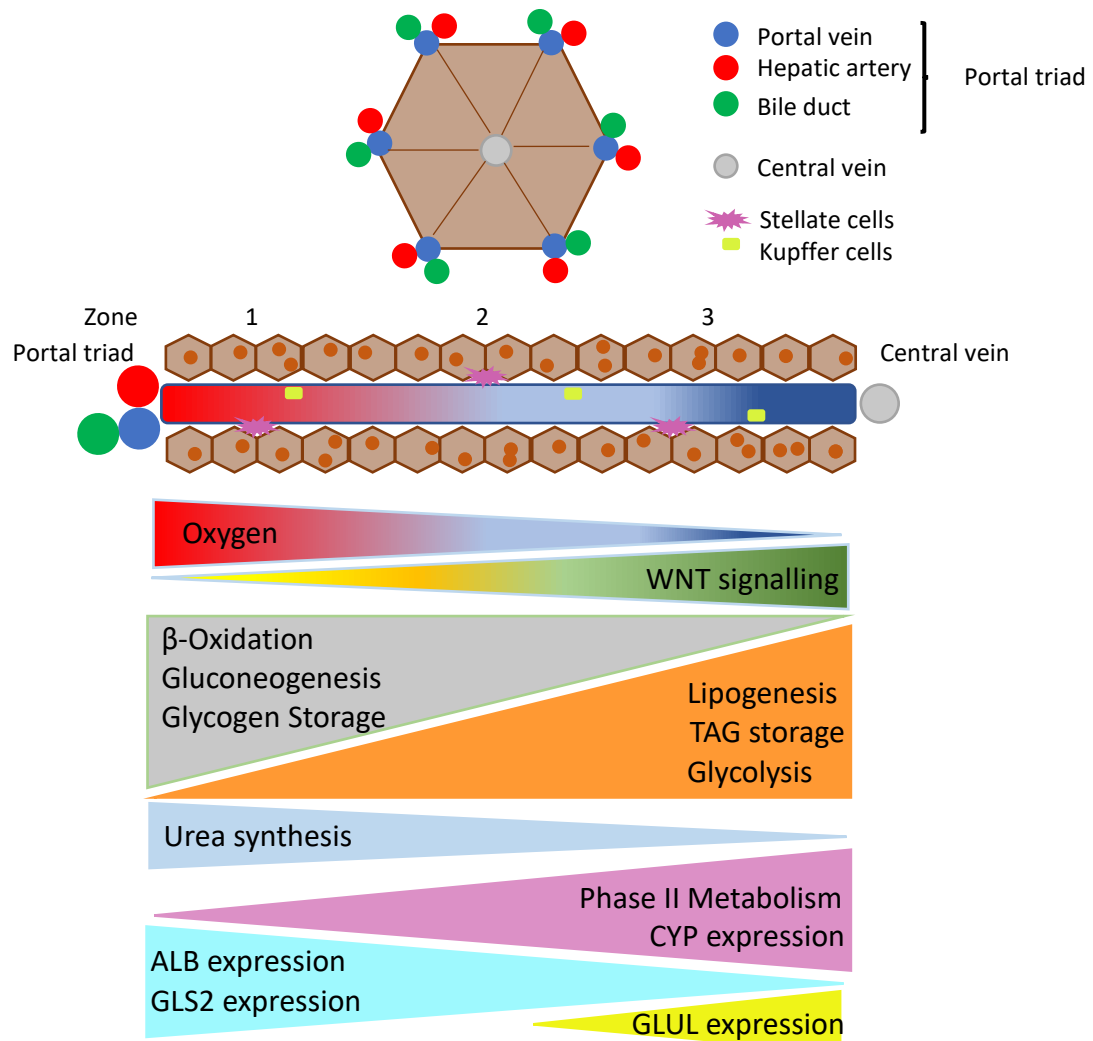


Fig. 2: Micro-anatomy, zonation and function of the liver lobules. Idealized scheme of hepatic lobules, to facilitate an understanding of the liver architecture which can only be found in this way in pig liver (upper image). Each lobule begins at a branch of the hepatic artery, portal vein, and bile duct. This ensemble is known as portal triad. Blood flows from here to the central vein, while bile flows into the opposite direction. Hepatocytes constitute about 80% of the liver mass. Cholangiocytes line the bile ducts and sinusoidal endothelial cells line the blood vessels. Kupffer cells - liver specific macrophages - are located in the blood vessels. Stellate cells reside in the Space of Disse, a gap between hepatocytes and blood vessels. Hepatocytes in zone 1, close to the portal triad (periportal hepatocytes), get into contact with oxygen rich blood (red) and have distinct functions and gene expression compared to pericentral hepatocytes in zone 3 close to the central vein, which receive blood with reduced oxygen (blue). Mid-lobular cells reside in zone 2 in the middle of the gradient. (ALB = Albumin, CYP = Cytochrome P450, GLS2 = Glutaminase, GLUL = Glutamate-Ammonia Ligase, TAG = Triacylglyceride, WNT = Wingless-related integration site). Figure credits: Own creation.

Each lobule is arranged around the central vein, which transports blood from the liver back to the heart. A branch of the hepatic artery and the hepatic vein as well as a bile duct form the so-called portal triad. While the hepatic artery supplies the liver with oxygen rich blood, the portal vein delivers blood rich of nutrients directly from the gut. The blood flows through small intrahepatic capillaries lined with fenestrated sinusoidal epithelial cells towards the central vein. It passes the hepatocytes that line the blood vessels on its way (Si-Tayeb et al., 2010, Godoy et al., 2013).

Hepatocytes are epithelial cells that show cell polarity. The basolateral membrane faces the Space of Disse, a small space between sinusoids and hepatocytes, where hepatic stellate cells reside as pericytes (Haussinger and Kordes, 2019). Hepatocytes take up nutrients and oxygen from the sinusoidal blood via their basolateral cell membrane which is equipped with microvilli. Shear stress from the blood flow is important for hepatocyte maturation and function (Rashidi et al., 2016). The apical surfaces provide contact between hepatocytes, which form bile canaliculi. Bile, that is produced by hepatocytes, flows through the bile canaliculi towards the cholangiocyte-lined bile duct and from there to the gall bladder and finally reaches the gut (Schulze et al., 2019). Bile canaliculi at the apical surface of the hepatocytes are separated by tight junctions from the basolateral membrane.

Hepatocytes are the main functional cells of the liver, which comprise about 80 % of the cell mass (Schulze et al., 2019). Depending on their position along a gradient of oxygen, nutrients, hormones, and wntless-related integration site (WNT) signalling between the portal triad and the central vein (Fig. 2), they fulfil distinct functions. Hepatocytes in zone 1, close to the portal triad, are receiving oxygen and nutrient rich blood and perform metabolic functions such as β -oxidation of fatty acids or ureagenesis. Hepatocytes in zone 3, close to the central vein, are predominantly involved in detoxifying reactions and have high levels of cytochrome P450 (CYP) activity (Cunningham and Porat-Shliom, 2021).

CYP enzymes are responsible for phase I xenobiotic metabolism. They oxidise xenobiotics and prepare them for further modification by phase II enzymes or direct excretion (Esteves et al., 2021). This process mainly detoxifies foreign molecules, but it can also activate therapeutic or toxic effects of otherwise inert molecules such as the mycotoxin aflatoxin B₁, one of the most potent hepatotoxins (Gallagher et al., 1996). As a consequence of the high CYP activity, zone 3 hepatocytes are the first ones affected in toxin-induced liver damage (Cunningham and Porat-Shliom, 2021). CYP mediated drug metabolism is of major interest for the pharma industry, as CYPs are capable to inactivate or activate pharmacologically relevant molecules. This has a major impact on their plasma concentration and thus on the efficiency of the drug (Ingelman-Sundberg et al., 2007). Phase I metabolism is followed by phase II metabolism where a plethora of enzymes is responsible for conjugating xenobiotics with small

residues such as glucuronic acid that increase their water solubility and finally prepares them for excretion via the urine or the bile (Wätjen and Fritsche, 2010).

Although the liver has a very high regenerative potential, hepatocytes cannot be functionally maintained *in vitro*. They de-differentiate within the first 24 hours and lose their important de-toxifying functions (Godoy et al., 2013) Therefore, they are of limited suitability to study long-term drug effects *in vitro* (Godoy et al., 2016).

3.4 *In vitro* differentiation of hepatocyte like cells for disease modelling

IPSC-derived hepatocyte-like cells (HLCs) have emerged as a promising tool for the effective study of human hepatic diseases (Rashid et al., 2010, Jozefczuk et al., 2011, Choi et al., 2013, Eggenschwiler et al., 2013, Graffmann et al., 2016, Matz et al., 2017, Niemietz et al., 2018, Graffmann et al., 2021, Sinton et al., 2021) .

Interestingly, there exists no generally valid protocol as a gold-standard for the *in vitro* differentiation of HLCs. On the contrary, a plethora of different protocols are being used (Fig. 3). They are mostly based on four major underlying patterns but vary substantially in the individual steps (Graffmann et al., 2022).

In general, the protocols aim to reproduce the *in vivo* development. They subdivide the whole process into either three or four steps. In three step protocols, the cells are first pushed into definitive endoderm (DE), followed by hepatic endoderm (HE) and finally HLCs (Cameron et al., 2015), while in four step protocols DE cells are guided into foregut/anterior definitive endoderm before moving on to HE and finally HLC (Hannan et al., 2013b).

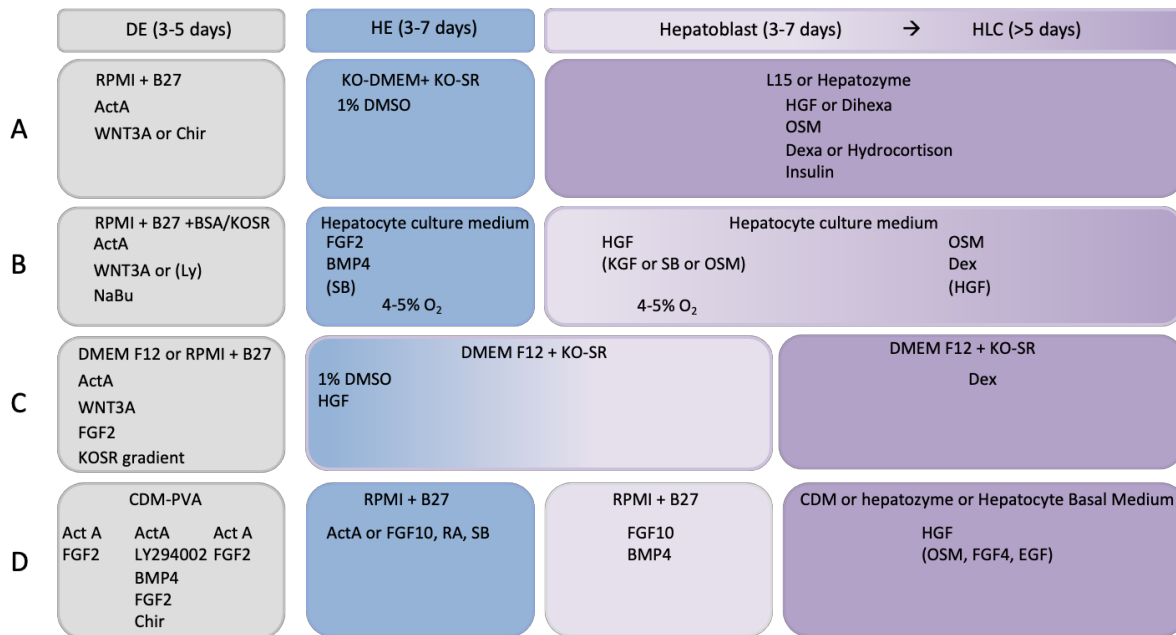


Fig. 3: Basic elements of the four most common hepatocyte-like cell (HLC) differentiation protocols. A plethora of HLC differentiation protocols have been developed during the recent years. Most of them are based on one of four distinct core protocols A-D with variation in cytokine and small molecule combination, concentration, and treatment duration. The work presented herein was performed in 2D using a variation of the 3-step protocol presented in A with L15 medium, HGF and Dexamethasone (Dexa) in the last step.

ActA = Activin A; BMP = Bone morphogenic protein; CDM-PVA = Chemically defined medium with polyvinyl alcohol; CHIR = CHIR99061; Dexa = Dexamethasone; EGF = Epidermal growth factor; FGF = Fibroblast growth factor; HGF = Hepatocyte growth factor; KGF = Keratinocyte growth factor; KOSR = knock out serum replacement; Ly = Ly294002; NaBu = Sodiumbutyrate; OSM = Oncostatin M; RA = Retinoic Acid; SB = SB431542; WNT = Wingless-related integration site. Figure taken from Graffmann et al 2022 published under the CC BY-NC-ND license (<http://creativecommons.org/licenses/by-nc-nd/4.0/>) and reproduced with friendly permission of the publisher.

Distinct cocktails of cytokines and small molecules are used to induce the differentiation steps (Graffmann et al., 2022). While Activin A (ActA) is essential for the induction of DE, it can be supplemented with either WNT 3A or fibroblast growth factor (FGF) 2 and bone morphogenic protein (BMP) 4 activation in combination with phosphoinositide 3-kinase (PI3K) inhibition. For HE induction, there exist two main strategies. It can be either achieved by exposing the cells to 1 % DMSO or by a combination of FGFs and BMPs. Cells in the HE stage resemble the biopotent hepatoblast stage *in vivo* and are capable to differentiate into either HLCs or cholangiocyte like cells (CLCs) (Fougere-Deschatrette et al., 2006, Si-Tayeb et al., 2010, Miyajima et al., 2014). For the final HLC step, three distinct media are frequently employed: Leibovitz (L)15 medium (Thermo Fisher Scientific), HepatoZYME-SFM (Thermo Fisher Scientific), or hepatocyte basal medium (Lonza). They are commonly supplemented with 10-100 ng/ml hepatic growth factor (HGF), 10 - 20 ng/ml oncostatin M (OSM), 1 µg/ml insulin, 0.1 µM dexamethasone (Dexa) or 10 µM hydrocortison alone or in various combinations. While HGF seems to be essential at this step, the effect of OSM is still under debate. It has been shown that OSM stimulates hepatic differentiation and function in primary hepatocytes as

well as in HLCs (Kamiya et al., 2001, Levy et al., 2015, Chen et al., 2018, Danoy et al., 2020) while there is also evidence that it promotes de-differentiation of HLCs as well as growth of endothelial cells (Demyanets et al., 2011, Chen et al., 2018).

Besides the medium, the coating which mimics the extracellular matrix, is important for HLC maturation. While initially cells have been grown on Matrigel, more recently also different laminins have been used which resulted in considerable increase of CYP activity (Takayama et al., 2013b, Cameron et al., 2015, Ong et al., 2018).

Another approach for increasing HLC activity is to culture them in a 3D environment which also mimics the natural situation more accurately. It is possible to build pure HLC-organoids, however, organoids that comprise several hepatic cell types have proven to be more useful in terms of HLC function and disease recapitulation (Takebe et al., 2013, Sgodda et al., 2017, Rashidi et al., 2018, Ouchi et al., 2019).

Besides disease modelling, HLCs can be useful for drug testing (Takayama et al., 2013a, Takayama et al., 2014, Wilson et al., 2015, Bircsak et al., 2021). Their low level of CYP activity still prevents them from being used systematically in pharmacology but with increasing maturity conveyed by novel protocols, these cells might soon become essential parts of the drug- and toxin-testing pipelines. Until then, they can at least be used to test drug efficiency for treatment of selected diseases (Choi et al., 2013, Lichtmanegger et al., 2016, Pastore et al., 2017).

3.5 Understanding Lipid droplet formation and lipid metabolism

Hepatocytes store fat in the form of lipid droplets (LDs). In these entities, cholesterol and triacylglycerides (TAGs) are tightly clustered inside a shell of proteins which mainly belong to the family of perilipins (PLIN). LDs grow according to the availability of TAGs up to a diameter of 5 μM in steatotic human hepatocytes (Schott et al., 2019, Brekk et al., 2020). LDs can take up a considerable space of the cells and thus impair their normal function. On the other hand, they protect the cells against lipotoxicity from free fatty acids (FFAs) and are a reservoir of high-energy containing TAGs which provide energy in starving periods (Geltinger et al., 2020). Their outer protein shell changes with their size from initially predominantly PLIN3 to PLIN1 in very big LDs (Pawella et al., 2014). One factor, which is present throughout the growth cycle of LDs, is PLIN2, an important gatekeeper for LDs, protecting them from lipases (Magne et al., 2013, Kaushik and Cuervo, 2015, Kaushik and Cuervo, 2016). PLIN2 knockout in mice prevented NAFLD and obesity and significantly improved their health status during a high fat diet (McManaman et al., 2013, Carr et al., 2014).

TAG degradation mainly follows two distinct pathways: lipolysis or lipophagy (Fig. 4). During enzymatic lipolysis, Adipose triglyceride lipase (ATGL, also known as PNPLA2) binds to its co-factor comparative

gene identification-58 (CGI-58) and docks onto the surface of an LD (Lass et al., 2006, Smirnova et al., 2006). It releases diacylglycerides (DAGs) plus FFAs which then get degraded in more steps until finally the FAs enter β -oxidation. ATGL shares its co-factor CGI-58 with the closely related PNPLA3 enzyme. The I148M single nucleotide polymorphism (SNP) in PNPLA3 is the largest genetic driver known to increase the risk of developing NAFLD. It has been shown in mice and in a human hepatic cell line, that PNPLA3 I148M binds CGI-58 more tightly than the wt version, depriving ATGL of its co-factor and thus impairing lipolysis (Wang et al., 2019).

The other way for LD degradation is a special form of autophagy, called lipophagy (Singh et al., 2009). In this case, the TAGs of the LD get digested inside lysosomes which are equipped with the enzyme Lipase A (LAL/LIPA) (Schott et al., 2019). It has long been believed that both pathways act separately from each other, but recent studies indicate that LDs are initially degraded by lipolysis until their size is reduced to a format that is suitable for lipophagy (Schott et al., 2019). Usually, autophagy levels are high during starvation and low in the fed stage. However, cells can up-regulate lipophagy as a response to acute challenges with lipids and thus prevent excessive lipid storage. If lipid overload becomes chronic, as a result of a high-caloric diet, turnover via lipophagy is reduced (Singh and Cuervo, 2011). In addition, PNPLA3 I148M also seem to impair lipophagy by reducing the interaction of LDs with the autophagosome (Negoita et al., 2019).

The proteins of the perilipin family play a major role for coordinating lipolysis and lipophagy. PLIN3, which predominantly covers smaller LDs, promotes lipophagy (Garcia-Macia et al., 2021) while PLIN2 prevents lipolysis and lipophagy (Listenberger et al., 2007, Tsai et al., 2017). PLIN2 and 3 levels on the LDs are regulated via chaperone mediated autophagy (CMA). Defects in the CMA system result in reduced levels of lipolysis and lipophagy (Kaushik and Cuervo, 2015, Garcia-Macia et al., 2021).

Recently, the PLIN2 polymorphism S251P has been described. In this protein variant, an α -helix is disrupted and it is associated with lower rates of lipolysis, higher intracellular LD content, smaller LDs and reduced plasma TG levels (Magne et al., 2013, Sentinelli et al., 2016, Faulkner et al., 2020).

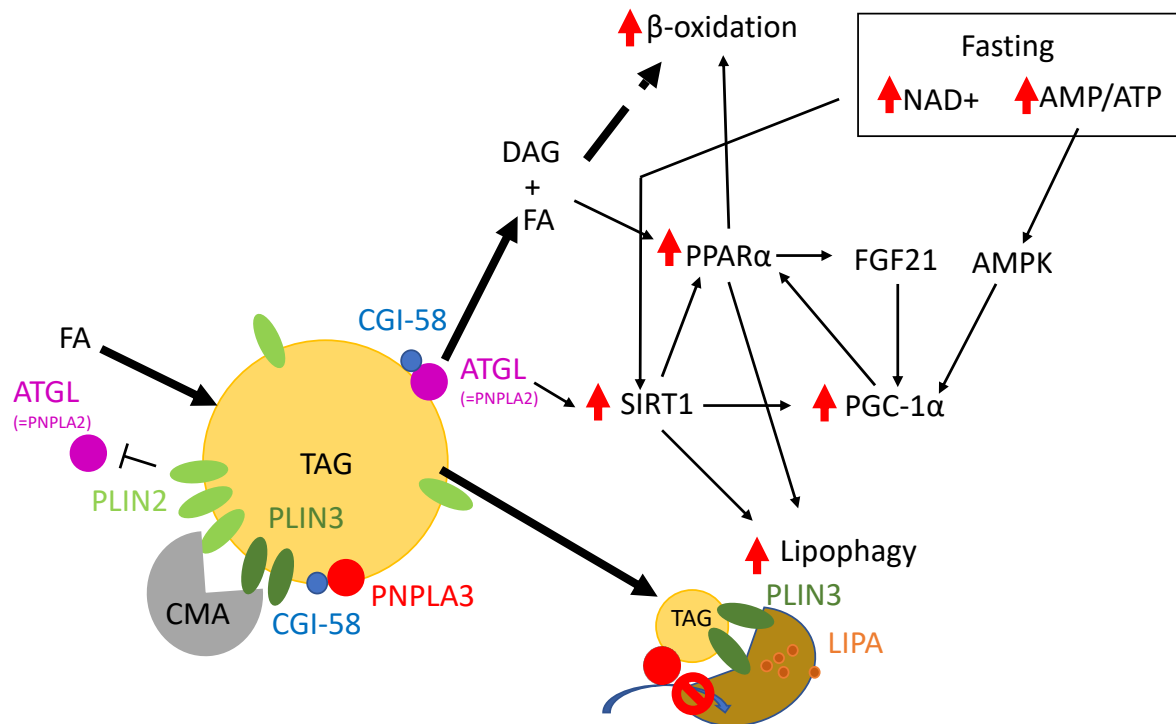


Fig. 4: Scheme of LD metabolism. Fatty acids (FA) get sequestered and stored as triacylglycerides (TAG) in lipid droplets (LDs). LDs are covered by various proteins such as Perilipin (PLIN) 2 and 3. PLIN2 prevents access of the lipase ATGL (also called PNPLA2) to the LD and thus impairs LD degradation. When ATGL can access the LD, it pairs with its co-factor CGI-58 and catalyses the hydrolyzation of TAG into diacylglyceride (DAG) and FA. These products get further metabolized until they are finally used in β -oxidation. ATGL-activity is dependent on the availability of the co-factor CGI-58 which also interacts with PNPLA3. This interaction is particularly strong for the mutant isoform I148M, which results in reduced ATGL activity.

Smaller LDs can be degraded by lipophagy and Lipase A (LIPA), which is promoted by the presence of PLIN3 on the LD surface. Chaperone-Mediated Autophagy (CMA) regulates levels of PLIN2 and 3 on the LD surface and thus influences activity levels of lipolysis and lipophagy.

Lipid catabolism is increased during fasting. Metabolic signs of energy depletion such as high NAD⁺ levels or a high AMP/ATP ratio activate SIRT1 and AMPK, respectively. They both activate PGC-1 α , which increases Peroxisome proliferator-activated receptors (PPAR) α activity. The latter enhances β -oxidation, lipophagy, and FGF21 signalling and is in a feed-forward-loop activated by FAs and by FGF21 induced PGC-1 α . While these adaptations are rather slow, SIRT1 can also be activated directly by ATGL, thus initiating the feedback loop in a faster way. (AMP = adenosine monophosphate, AMPK = AMP-activated protein kinase, ATGL = Adipose triglyceride lipase, ATP = adenosine phosphate, CGI-58 = Comparative gene identification-58, CMA = Chaperone-Mediated Autophagy, DAG = Diacylglyceride FA = Fatty Acids, FGF = Fibroblast growth factor, LD = Lipid droplet, LIPA = Lipase A, PGC-1 α = PPARY co-activator 1 α , PLIN = Perilipin, PNPLA = Patatin-like phospholipase domain containing protein, SIRT = Sirtuin). Figure credits: own creation.

3.6 Regulation of lipid metabolism

3.6.1. Peroxisome proliferator-activated receptors (PPAR) family

Metabolic regulation is a highly complex process and not yet fully understood. Peroxisome proliferator-activated receptors (PPARs) are nuclear receptors that control metabolic processes in the body. There exist three family members, PPAR α , γ , and β/δ with distinct tissue distribution and function (Moreno et al., 2010). PPAR α is mainly expressed in cells with high oxidative capacity such as hepatocytes, cardiomyocytes, renal tubular cells, and brown adipocytes. The PPAR γ splice-variant 1 can be found ubiquitously, while variant 2 is present in adipocytes and 3 in adipocytes, macrophages, and colon. While PPAR γ 2 expression is low in healthy liver, it increases during steatosis (Pettinelli and Videla, 2011). PPAR β/δ is ubiquitously present.

All three family members are bound to co-repressors and get activated by specific ligands. In the activated state, they form heterodimers with retinoid X receptor (RXR), enter the nucleus and act as transcription factors (Moreno et al., 2010).

Hepatic PPAR α gets activated by FFAs which are released from adipose tissue or hepatic LDs during fasting (Tanaka et al., 2017). In the activated state, it pairs with the co-activators PPAR γ co-activator 1 α (PGC-1 α) (Vega et al., 2000) and RXR (Kliwer et al., 1992) and thereby induces transcription of genes important for β -oxidation, gluconeogenesis, and ketogenesis. It also activates hepatic FGF21 production (Badman et al., 2007, Goto et al., 2017). FGF21 is a hormone-like factor that modulates lipid and glucose metabolism in mice (Fisher et al., 2011) and has already been used in human clinical trials against type 2 diabetes (Gaich et al., 2013).

While FFAs directly activate PPAR α , deacetylation of the co-factor PGC-1 α also increases PPAR α mediated effects. In addition, PGC-1 α also pairs with other PPAR family members, as well as hormone receptors and non-nuclear receptor transcription factors to increase mitochondrial biogenesis, respiration rates and uptake/utilization of substrates for energy production (Canto and Auwerx, 2009).

PGC-1 α is regulated on the transcriptional level and its activity is controlled by several posttranslational modifications (Fernandez-Marcos and Auwerx, 2011). During fasting, its transcription is up-regulated via glucagon and cyclic adenosine monophosphate (cAMP) signalling (Cao et al., 2005). On the posttranslational level, PGC-1 α gets activated by AMP-activated protein kinase (AMPK)-mediated phosphorylation or by deacetylation via sirtuin (SIRT) 1 and repressed by insulin-mediated AKT signalling (Moreno et al., 2010). AMPK and SIRT1 are both metabolic master regulators, which get activated in energy depleted stages. Activity of the serine/threonine kinase AMPK is regulated by the cellular AMP/ATP ratio, which is low in the fed state and high during fasting (Gonzalez et al., 2020).

SIRT1 is a member of the highly conserved family of sirtuins and regulates, amongst others, energy homeostasis, longevity, and DNA damage (Lagouge et al., 2006, Yuan et al., 2007). Like all SIRT family members, SIRT1 activity is dependent on NAD⁺ and thus has been regarded as an energy sensor, being mainly active in energy depleted conditions, characterized by high NAD⁺ levels (Canto and Auwerx, 2009).

However, activation of SIRT1 by changes in NAD⁺ levels is quite slow and very fast SIRT1 activations, which occur for example as a response to β -adrenergic signalling, cannot be explained by this effect. Instead, β -adrenergic signalling, mediated by c-AMP and protein kinase A (PKA) has recently been identified as an independent regulatory pathway (Khan et al., 2015, Sathyanarayan et al., 2017). PKA-mediated SIRT1 phosphorylation at Ser434, which is part of the active centrum, stimulates SIRT1 activity and increases deacetylation and thus activity of PGC-1 α (Gerhart-Hines et al., 2011).

3.6.2 Adipokines

Hepatic lipid storage is not only regulated independently on the cellular level, but it is influenced by metabolic processes in other organs, especially white adipose tissue (WAT). Adipocytes are not an inert reservoir for storing excess lipids in case of obesity, but they also produce a variety of signalling molecules, so called adipokines. One important factor of this family is Adiponectin, which is down-regulated in obesity (Kadowaki and Yamauchi, 2005, Vuppalanchi et al., 2005, Wruck et al., 2015). Adiponectin is associated with a variety of positive effects on hepatocytes such as increased β -oxidation, insulin sensitivity, and autophagy, as well as reduced gluconeogenesis, lipogenesis, inflammation, and fat storage. In 2013, a small molecule analogon called AdipoRon has been synthesized (Okada-Iwabu et al., 2013). Similar to Adiponectin, AdipoRon improves insulin sensitivity and reduces fasting blood glucose levels in high fat diet-induced obese mice. It could also reduce liver TAG levels in wild-type mice on a high fat diet and prolonged the lifespan of db/db mice (Okada-Iwabu et al., 2013), which are homozygous for a leptin receptor mutation associated with hyperglycemia and obesity.

3.7 The role of microRNAs in NAFLD

miRNAs are short, noncoding RNAs consisting of 20-22 nucleotides. They are synthesized by RNA polymerase II and subsequently activated by several processing steps until they reach their mature form. MiRNAs regulate their target mRNAs, which have a complementary nucleotide sequence within their 3'UTR, by binding and marking them for degradation or by repressing translation (Bartel, 2004).

Target recognition depends on the seed-sequence, a 6 nucleotides long sequence at the 5'-end of the miRNA (Bartel, 2009). MiRNA mediated regulation of gene expression is a complex process, as every miRNA can target and regulate several mRNAs and a specific mRNA can be regulated by several miRNAs (Ambros, 2004, Doench and Sharp, 2004). Interestingly, miRNAs do not only act in the cells where they have been synthesized but can also be exported to act in other cell types and are thus accessible as potential biomarkers for diseases such as NAFLD (Cermelli et al., 2011, Pirola et al., 2014, Thomou et al., 2017).

Serum levels of miRNAs such as miRNA-34a, miRNA-122, miRNA-192, and miRNA-375 have been associated with NAFLD and/or disease progression to NASH (Pirola et al., 2014, Liu et al., 2018, Lopez-Pastor et al., 2020). Counterintuitively, hepatic levels of these miRNAs do not correspond to those measured in serum and can even be inversely correlated, which might be a characteristic phenomenon for hepatic diseases (Pirola et al., 2014, Liu et al., 2018).

Especially miRNA-122 has been extensively analysed, as it is the most prevalent miRNA in the liver and is increased in serum of NASH patients but not early stage NAFLD patients (Pirola et al., 2014, Liu et al., 2018). In mice, inhibition of hepatic miRNA-122 reduced the hepatic expression of genes involved in lipogenesis, fatty acid oxidation, bile acid metabolism, lipid transport, and transcriptional regulation of lipid homeostasis (Esau et al., 2006, Tsai et al., 2012)

4 Aim of this study

The aim of this work was to establish iPSC derived HLCs to study NAFLD. The first part of this project comprised the generation of two novel iPSC lines from obese NAFLD patients to complement the panel of available patient derived and healthy cell lines at the ISRM (Graffmann et al., 2018a, Graffmann et al., 2018b). The second part consisted in the improvement of the HLC differentiation protocol to increase cellular maturity and mimic the *in vivo* situation as good as possible. Also, increasing robustness and reproducibility of the hepatic differentiation protocol was necessary, which could be partly obtained by reducing the presence of non-HLC cell types in the final culture (Graffmann et al., 2018c).

In the third part, two studies were performed to (i) reveal genome wide expression changes during early steps of NAFLD development depending on the respective genotypes of iPSC donors and to (ii) establish the cell culture model as a means to test putative anti-NAFLD drugs in the future (Graffmann et al., 2016, Graffmann et al., 2021).

5 Summaries of own research articles

5.1 Establishment and characterization of an iPSC line from a 35 years old high grade patient with nonalcoholic fatty liver disease (30 – 40 % steatosis) with homozygous wildtype PNPLA3 genotype

Graffmann, N., Bohndorf, M., Ncube, A., Kawala, M.-A., Wruck, W., Kashofer, K., Zatloukal, K., and Adjaye, J.

Stem cell research (2018) 31, 113-116

and

5.2 Establishment and characterization of an iPSC line from a 58 years old high grade patient with nonalcoholic fatty liver disease (70 % steatosis) with homozygous wildtype PNPLA3 genotype.

Graffmann, N., Bohndorf, M., Ncube, A., Wruck, W., Kashofer, K., Zatloukal, K., and Adjaye, J.

Stem cell research (2018) 31, 131-134.

In order to model diseases with iPSCs, it is important to have several cell lines from patients and healthy controls available in the laboratory. Especially a disease like NAFLD, which is of multifactorial origin, needs several cell lines to cover a variety of distinct genotypes. Therefore, the novel iPSC lines S18 (5.1) and S11 (5.2) have been generated to complement the ISRM-pool of available iPSCs for disease modelling (Table 1).

Table 1: iPSC lines from steatosis patients and controls established in the ISRM. Table modified from Graffmann et al. 2021, published under the terms of the Creative Commons Attribution License (<https://creativecommons.org/licenses/by/4.0>) and reproduced with friendly permission of the publisher. Cell lines CO2, S08, S11, and S12 were used in that same publication. PNPLA3 genotype I/I homozygote wildtype, I/M heterozygous, N.A. = not applicable.

ID	gender	age	BMI	steatosis grade	PNPLA3 genotype	diabetes type 2	reference
B4	m	0	N.A.	none	I/I	none	(Wang and Adjaye, 2011)
AF	f	0	N.A.	none	unknown	none	(Drews et al., 2015)
CO2	f	19	21	non-obese	I/M	unknown	(Kawala et al., 2016a)
S08	m	61	46	obese, high steatosis	I/I	No	(Kawala et al., 2016b)
S11	f	58	45	obese, high steatosis	I/I	No	(Graffmann et al., 2018b)
S12	f	50	35	obese, low steatosis	I/I	No	(Kawala et al., 2016c)
S18	f	35	41	obese, high steatosis	I/I	No	(Graffmann et al., 2018a)

To generate the iPSCs, fibroblasts from high steatosis patients, that were obtained in a collaboration project with Prof. Zatloukal from the University of Graz, were expanded and transfected with a cocktail of episomal plasmids coding for *OCT4*, *SOX2*, *NANOG*, *LIN28*, *c-MYC*, and *KLF4*.

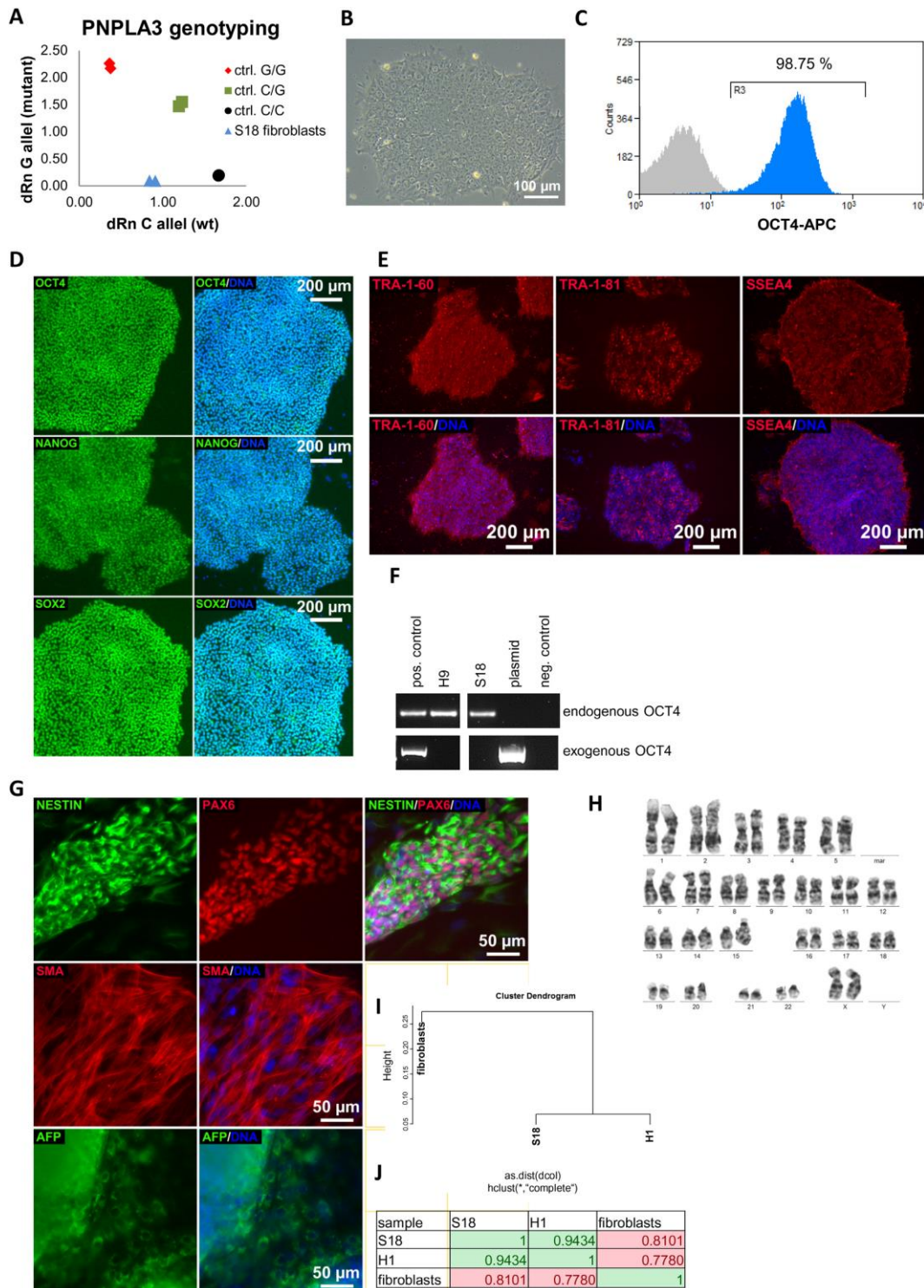


Fig. 5: Characterization of the iPSC line S18. (A) S18 cells are homozygous for the *PNPLA3* wildtype C/C (corresponding to I/I on protein level) genotype. (B) Morphology of the iPSC colonies. (C) Flow cytometric analysis revealed 98.75 % OCT4 positive cells. (D, E) Immunocytochemistry for the pluripotency associated transcription factors OCT4, NANOG, and SOX2 (D) and the surface markers TRA1-60, TRA1-81, and SSEA4 (E) was positive. (F) Fully reprogrammed cells expressed the endogenous *OCT4* while the transgene (exogenous *OCT4*) was not detectable by PCR. (G) The potential to differentiate into all three germ layers was shown by immunofluorescence for the ectoderm markers NESTIN and PAX6, the mesoderm marker smooth muscle actin (SMA), and the endoderm marker AFP. (I) Cells clustered together with the embryonic stem cell (ESC) line H1 and away from the original fibroblasts. (J) Similarity between S18 cells and H1 ESCs on transcriptome level was 0.94. Figure reproduced from Graffmann et al. 2018a under the CC BY-NC-ND license (<http://creativecommons.org/licenses/by-nc-nd/4.0/>) and with friendly permission of the publisher.

Formation of iPSCs was enforced by inhibiting TGF β -, MEK-, and ROCK-signalling as well as by activating canonical WNT-signalling with Chir99021.

As soon as colonies were visible, they were picked and transferred to Matrigel coated plates for further expansion. The resulting iPSC lines were fully characterized to confirm their pluripotency (Fig. 5, showing representative results for the cell line S18). Expression of the pluripotency associated transcription factors OCT4, SOX2, and NANOG was confirmed by immunofluorescence (Fig. 5D) and in case of OCT4 also flow cytometry (Fig. 5C) after the cells had lost the reprogramming plasmids (Fig. 5F). Likewise, expression of surface markers stage-specific embryonic antigen-4 (SSEA4), TRA-1-60, and TRA1-81 was confirmed by immunofluorescence (Fig. 5E). The cells were capable of spontaneous differentiation into all three germ layers via formation of embryoid bodies (EBs). The presence of differentiated cells was demonstrated by staining for Nestin/paired box (PAX) 6 (ectoderm), α -smooth-muscle-actin (mesoderm) and SRY-Box (SOX)17/AFP (endoderm) (Fig. 5G). The cells had no chromosomal aberrations (Fig. 5H) and their transcriptomes correlated to that of pluripotent cells with an R^2 of >0.94 (Fig. 5I, J). In addition, we could confirm that they were indeed generated from the parental fibroblast cells by small tandem repeat analysis. Thus they matched all criteria for newly generated iPSCs (Tigges et al., 2021) and could be used for further experiments.

In addition to the minimum of characterization necessary for newly generated iPSCs, we also determined the *PNPLA3* genotype of these cells (Fig. 5A). *PNPLA3* is one of the very few factors, where a genetic polymorphism has been linked to a predisposition of developing NAFLD. As expected from the low frequency of the mutant *PNPLA3* M/M allele (European Americans (0.23) and African Americans (0.17) (Romeo et al., 2008)), S11 and S18 have the wildtype form of *PNPLA3*.

5.3 Modeling Nonalcoholic Fatty Liver Disease with Human Pluripotent Stem Cell-Derived Immature Hepatocyte-Like Cells Reveals Activation of PLIN2 and Confirms Regulatory Functions of Peroxisome Proliferator-Activated Receptor Alpha.

Graffmann, N., Ring, S., Kawala, M.A., Wruck, W., Ncube, A., Trompeter, H.I., and Adjaye, J.

Stem cells and development (2016), 25, 1119-1133.

(Some of the published and herein discussed data are part of the Master Thesis of Sarah Ring and Marie-Ann Kawala, and the PhD thesis of Dr. Wasco Wruck)

In this study, a cell culture model to analyse the molecular mechanisms of NAFLD was established. Human embryonic stem cells (ESCs) as well as iPSCs derived from fibroblasts of a healthy donor (line B4 Table 1), were differentiated into hepatocyte like cells (HLCs) via the 3-step protocol (Fig. 3 A). HLCs were characterized in terms of marker expression and showed the expected functionality in terms of CYP activity, urea synthesis, and indocyanine green dye uptake.

HLCs were capable to store fat in the form of lipid droplets (LDs) when fed with 50 μ M oleic acid (OA) dissolved in Ethanol. OA treatment was associated with fundamental changes in the transcriptome with many pathways involved in lipid- and glucose metabolism being affected such as lipid oxidation, lipid homeostasis, glycolysis or glucose homeostasis. By testing the expression of selected lipid-metabolism associated genes, it was confirmed that the HLC-based model recapitulates gene expression changes characteristic for liver biopsies derived from patients with different levels of steatosis (Wruck et al., 2015).

Importantly, PLIN2, a protein covering LDs, was upregulated after OA treatment as well as many targets of the PPAR pathways such as fatty acid binding protein (*FABP*), carnitine palmitoyltransferase (*CPT1A*), and 3-hydroxy-3-methylglutaryl-CoA synthase (*HMGCS2*).

PLIN2 is important for LD growth and restrains access of triacylglyceride digesting enzymes such as ATGL to the droplets (Fig. 4). In this study, it was shown for the first time, that PLIN2 is also actively involved in LD formation in pluripotent stem cell (PSC) derived HLCs. From mouse studies, it is known that reduced PLIN2 levels prevent the formation of fatty liver and PLIN2 knockout mice have health benefits (McManaman et al., 2013, Carr et al., 2014). However, it was not possible to significantly reduce LD levels in HepG2 cells with siRNAs against PLIN2. This is probably due to other PLIN family members which still cover the LDs and can replace PLIN2. In addition, it might be necessary to extend the incubation time beyond 48 hours. Nonetheless, characteristic changes on the transcriptome level could be observed, indicating that PLIN2 has a major influence on metabolic gene transcription. For example, the AMPK complex member AMP-activated protein kinase catalytic subunit alpha (*PRKAA*) 2 was down-regulated in PLIN2 siRNA / EtOH-treated cells and up-regulated after OA induction. It is

known that AMPK is upregulated during starvation (Gonzalez et al., 2020) and at least its catalytical subunit can act as a nutrient sensor in the NAFLD *in vitro* model.

In addition, downregulation of *PPAR* α and γ after PLIN2 siRNA treatment was observed. As they are both involved in lipid metabolism, the role of *PPAR* α in the HLC based NAFLD *in vitro* model was further analysed. By using the small molecules Fenofibrate (agonist) and GW6471 (antagonist) *PPAR* α activity was modulated. Again, this had no visible influence on LD formation but on the transcriptome level major effects could be observed, especially on genes involved in lipid, glucose, and purine metabolism. It was apparent, that activation and inhibition of *PPAR* α activity had opposing effects on gene expression, which corresponded well with the beneficial effects of *PPAR* α induction in patients. Inhibition of *PPAR* α resulted for example in downregulation of genes involved in lipid catabolism such as *CPT1A*, Hydroxyacyl-CoA Dehydrogenase (*HADH*), and *LIPA*, while activation using Fenofibrate reduced expression of genes involved in biosynthesis of phospholipids and cholesterol such as 1-acylglycerol-3-phosphate O-acyltransferase (*AGPAT2*) and 3-hydroxy-3-methylglutaryl-coenzyme A reductase (*HMGCR*).

In addition, the regulation of *PPAR* α did not simply result in opposing expression changes but had effects of distinct entities of the metabolism. For example, genes of the purine metabolism were regulated in samples treated with Fenofibrate independent of OA treatment, while this group was not regulated in OA-treated cells in combination with *PPAR* α reduction. Especially aminoimidazole carboxamide ribonucleotide (AICAR), which is an intermediate product in *de-novo* purine synthesis (Warren et al., 1957, Daignan-Fornier and Pinson, 2012), seems to play a key role connecting purine synthesis to other metabolic processes. It is able to activate the starvation sensor AMPK (Asby et al., 2015) for which we already assumed increased activity in OA-treated cells after PLIN2 siRNA treatment based on increased expression of its catalytic subunit *PRKAA2*. The genome wide analysis revealed that genes directly preceding AICAR biosynthesis were upregulated or exclusively expressed after Fenofibrate mediated *PPAR* α induction, indicating the presence of a feedback loop.

While mRNAs were up- and down-regulated after OA treatment, all 84 liver specific miRNAs analysed were down-regulated in at least one cell line in response to the treatment. It has indeed been described before that miR-122 is downregulated in steatotic hepatocytes while higher levels are measured in the patients' blood (Cermelli et al., 2011, Pirola et al., 2014). Besides miR-122, this study focused on miR-106b which is highly expressed in liver cirrhosis and hepatocellular carcinoma (HCC) (Tan et al., 2014). One potential target gene for miR-122, namely C3 and PZP-like alpha-2-macroglobulin domain-containing protein 8 (*CPAMD*) 8, as well as two for miR-106b, namely atlastin (*ATL*) 3, and ephrin type-A receptor (*EPHA*) 7 were checked in more detail. While luciferase assays

confirmed that these genes were regulated by the corresponding miRNAs, they were also upregulated after OA treatment which indicate that they might play a role for disease development.

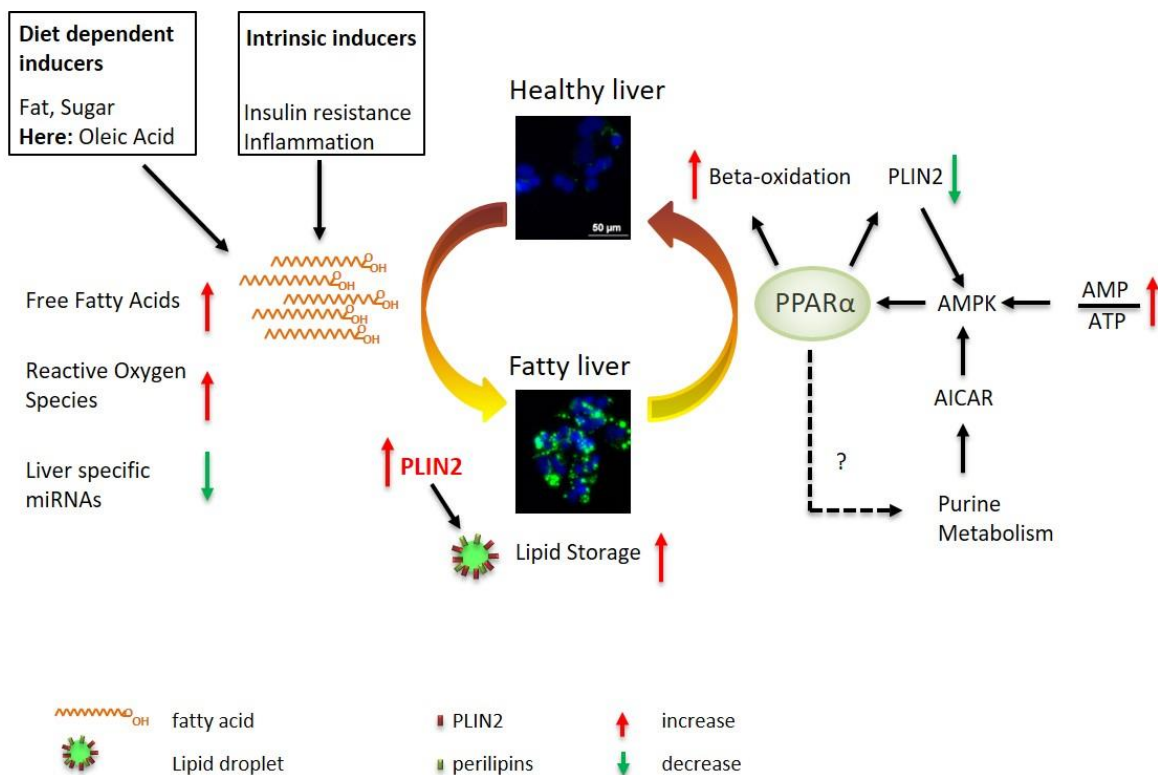


Fig. 6: Schematic overview of inducers of NAFLD and potential intervention points (taken from Graffmann et al. 2016). The transition from a healthy liver (upper panel) toward a fatty liver (lower panel) is shown. Factors that promote NAFLD are shown on the left. Besides diet related inducers that are in this study mimicked by OA addition to the medium, intrinsic factors like insulin resistance promote NAFLD. From a global perspective, the triggers result in increased free fatty acids and reactive oxygen species. A global downregulation of hepatic miRNAs such as miR-122 was also observed. Eventually, every trigger results in an upregulation of PLIN2 expression and an increase in lipid storage within hepatocytes. Beneficial processes that might reduce fat content of hepatocytes are shown on the right side. In general, PPAR α activation (here by application of Fenofibrate) decreases the amount of stored fat by inducing β -oxidation. Besides fibrates, which activate PPAR α , it is also regulated by AMPK, which senses the low energy state of a cell as measured by the ratio between AMP and ATP. AMPK expression increases in response to PLIN2 knockdown and its activity might be regulated by intermediates of purine metabolism, which is in turn regulated by PPAR α . This indicates a possible positive feedback loop that has to be verified by additional experiments. Besides PPAR α modulation, a direct reduction of PLIN2 expression could also be beneficial. AMP = adenosine monophosphate; AMPK = adenosine monophosphate-activated protein kinase; ATP = adenosine triphosphate; NAFLD = nonalcoholic fatty liver disease; OA = oleic acid; PLIN = Perilipin; PPAR α = peroxisome proliferator-activated receptor alpha. Original figure under the terms of the Creative Commons Attribution Noncommercial License (<http://creativecommons.org/licenses/by-nc/4.0/>) and with friendly permission of the publisher.

In summary, the data indicate that PSC-derived HLCs are suitable for studying NAFLD as (i) they accumulate LDs when fed with a high-fat medium and (ii) they differentially express genes of relevant metabolic hubs and NAFLD-associated miRNAs when treated with high levels of OA and (iii) some of these metabolic hubs are easily targetable with small molecules.

5.4 Cell fate decisions of human iPSC-derived bipotential hepatoblasts depend on cell density.

Graffmann, N., Ncube, A., Wruck, W., and Adjaye, J.

PloS one (2018). 13, e0200416

(Some of the published and herein discussed data are part of the Master Thesis of Audrey Ncube)

In vitro differentiation of hepatocytes from PSCs is a very delicate process, which reacts in sensitive ways to any disturbances. Here, the influence of cell density on cellular fate during HLC differentiation was studied (Graffmann et al., 2018c). During *in vivo* development, the cells first adopt definitive endoderm fate and continue to differentiate into hepatic endoderm. By the time the so-called liver bud, a three-dimensional structure invading the surrounding tissue, forms, the cells have developed into hepatoblasts, bipotential cells that can differentiate into hepatocytes and cholangiocytes (Fougere-Deschatrette et al., 2006, Si-Tayeb et al., 2010, Miyajima et al., 2014). This stage is difficult to dissect *in vitro*. Most likely bipotential cells are present during the end of HE and the first days of HLC-stage. The decision between hepatocyte and cholangiocyte fate depends on interactions of the Notch, WNT, TGF β , and Hedgehog signalling (Hh) pathways (Hussain et al., 2004, Decaens et al., 2008, Zong et al., 2009, Omenetti and Diehl, 2011, Raynaud et al., 2011, Zong and Stanger, 2011, Cordi et al., 2016). In the differentiation culture, the formation of non-hepatocyte like cells, which are still epithelial but do not foster the typical hepatic polygonal shape, can frequently be observed. These cells form predominantly in regions of low cell density and we refer to them as endoderm derived epithelial cells (EDECs).

In this study, ESCs and iPSCs derived from human fetal foreskin fibroblast (B4, Table 1) and amniotic fluid (AF, Table 1) were used for differentiation. We could show for the first time that also amniotic fluid derived iPSCs can differentiate into HLCs.

The development of EDECs was forced by splitting cells at the HE stage, where they presumably consist of bipotential hepatoblasts, into low density. EDECs grew spontaneously and consistently under low density cell culture conditions. They have an epithelial morphology and are much bigger than HLCs with distinct intracellular filamentous structures visible (Fig. 7A).

On the molecular level, they are characterized by the expression of the cholangiocyte markers SOX9, osteopontin (OPN), cystic fibrosis transmembrane conductance regulator (CFTR), and cytokeratin (CK)19 as well as the hepatocyte markers HNF4 α and CK18, but do neither express the mature hepatocyte marker ALB nor the progenitor marker AFP (Fig. 7B,C). They express both E-Cadherin, which is a marker for epithelial cells, and Vimentin, which is present on mesenchymal cells. In healthy organs,

these two markers are mutually exclusive, but they occur together during cancer (Tajima et al., 2010, Yamashita et al., 2018).

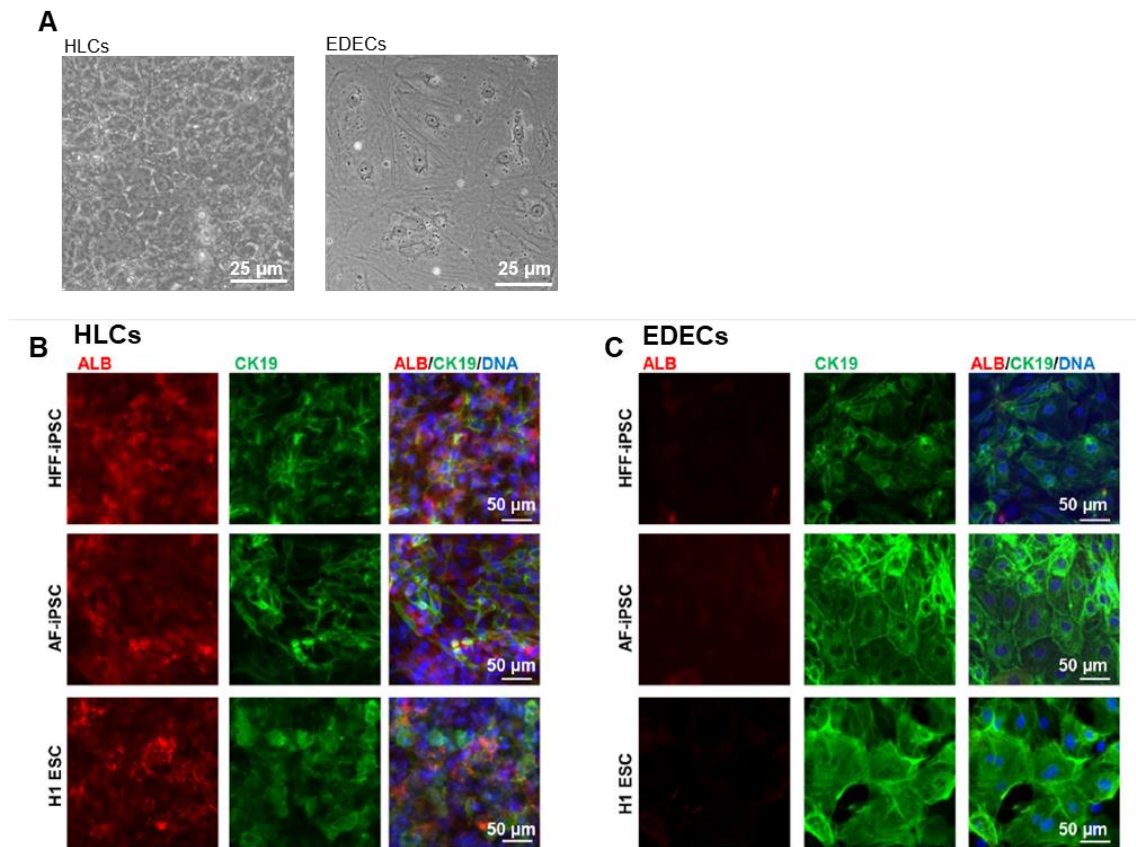


Fig. 7: Characterization of EDECs. (A) Brightfield picture demonstrates the morphological differences between HLCs and EDECs. (B,C) Representative Immunofluorescence for ALB as an HLC marker and CK19 as a Cholangiocyte marker in HLCs (left) and EDECs (right). Figure modified from Graffmann et al 2018c, under the terms of the Creative Commons Attribution License, <https://creativecommons.org/licenses/by/4.0>) and reproduced with friendly permission of the publisher.

In contrast to HLCs, EDECs did not show any classical hepatocyte functionality, such as urea synthesis and CYP3A4 activity.

In order to enforce HLC differentiation despite low-density culture conditions, several well-known signalling pathways, that are involved in cell fate decision of hepatoblasts, namely Notch, WNT, Hh, and TGF β signalling were modulated. In all cases, immunofluorescence showed that predominantly EDECs were present in the culture with marginal amounts of HLCs. This indicates that the low density gives strong differentiation cues to the cells which cannot be overcome by interfering with the above mentioned signalling pathways.

Notch signalling is an important pathway for the development of cholangiocytes *in vivo*, as known from Alagille syndrome, where mutations in the genes coding for Jagged 1 (JAG1), a canonical NOTCH ligand,

or NOTCH2 receptor, result in impaired intrahepatic bile duct formation and cholestasis development (Li et al., 1997, Oda et al., 1997, McDaniell et al., 2006).

Therefore, the consequences of blocking this signalling pathway were studied in more detail. ESC and iPSC derived EDECs were treated with one of two different γ -secretase inhibitors during differentiation in low-density. RT-qPCR demonstrated that application of the γ -secretase inhibitors down-regulated expression of hepatocyte markers (*CK18*) and the hepatocyte-associated transcription factors *FOXA2*, *PROX1*. Interestingly, the cholangiocyte-associated transcription factor *SOX9* was up-regulated after γ -secretase inhibition, while the characteristic cholangiocyte markers *CK19* and *OPN* were down-regulated. For *OPN* and *SOX9* these effects depended on the dose of applied γ -secretase inhibitor, while *CK19* expression changes were largely independent of γ -secretase inhibitor dose. We reasoned that the very early cholangiocyte marker *SOX9* might not be entirely dependent on Notch signalling, while the later markers *OPN* and *CK19* are. Especially, down-regulation of *OPN*, which was only weakly expressed in the cells, might imply impaired maturation.

The hepatocyte promoting transcription factors *PROX1* and *FOXA2* were down-regulated in EDECs derived from both cell lines after γ -secretase inhibition which supports the immunofluorescence-based data, that the cells do retain EDEC fate after NOTCH inhibition.

In contrast, the expression of *c/EBP α* changed in opposing directions after treatment with the two distinct γ -secretase inhibitors. In general, NOTCH signalling is responsible for down-regulation of *c/EBP α* expression in cholangiocytes (Tanimizu and Miyajima, 2004). As a dose-dependent up-regulation of *c/EBP α* after compound E treatment was observed, this implies an effective reduction of NOTCH signalling. *c/EBP α* is crucial for hepatocyte development. It activates the transcription of hepatocyte markers such as albumin (Tan et al., 2007) and limits their proliferation (Diehl, 1998). In parallel, it inhibits the expression of cholangiocyte-promoting transcription factors (Yamasaki et al., 2006). However, the cells were still in a very immature state so that effects of different *c/EBP α* levels were probably not visible yet.

In order to further investigate the effects of NOTCH inhibition on the cell fate, transcriptome analyses for cells with and without NOTCH inhibitor treatment was performed. Two distinct but closely related cell types were obtained via the high- and low-density differentiation paths, independent of NOTCH inhibition. The hepatocyte promoting transcription factor *c/EBP α* was higher expressed in HLCs than in EDECs, while EDECs expressed the cholangiocytes-associated marker G protein-coupled bile acid receptor 1 (*GPBAR1*) also named *TGR5* (Keitel and Haussinger, 2013) as well as *SOX17*, an early endoderm marker, which indicates an immature phenotype. In general, HLCs expressed more genes related to metabolic functions, transcription, and cell cycle as investigated by gene ontology (GO) term

analysis, while in EDECs, the predominant GO-terms were related to structural features, signalling pathways, apoptosis, and proliferation. NOTCH inhibition reduced developmental and differentiation related genes in EDECs, while it increased the expression of genes related to cell cycle. Together, this mirrors a reduced differentiation potential of the γ -secretase inhibitor-treated cells.

In conclusion, low density during HLC differentiation results in the development of EDECs rather than HLCs. This process could not be reverted by inhibiting involved signalling pathways, in particular NOTCH, WNT, Hh, or TGF β . However, it is still possible that combinations of distinct inhibitors, different concentrations or treatment at different time points might have an effect. The fact that EDECs often appear during HLC differentiation, if the starting population has not been seeded densely enough, implies that cell-cell contacts are important for the development of HLCs. Therefore, strict adherence to a high density is essential for successful HLC differentiation. Alternatively, this effect might be simulated by repressing Yes-associated protein (YAP) signalling, a well know driver of proliferation and growth whose cell-cell contact-mediated inactivation by Hippo signalling increases cellular maturation (Cai et al., 2021).

5.5 A stem cell based in vitro model of NAFLD enables the analysis of patient specific individual metabolic adaptations in response to a high fat diet and AdipoRon interference.

Graffmann, N., Ncube, A., Martins, S., Fiszl, A. R., Reuther, P., Bohndorf, M., Wruck, W., Beller, M., Czekelius, C., and Adjaye, J.

Biol Open. (2021).

Lipid metabolism in hepatocytes is controlled by a complex metabolic network, which centres around PPAR α and AMPK. One important signalling molecule that activates this network is adiponectin (Yamauchi et al., 2007, Liu et al., 2012), an adipokine which is synthesized by adipocytes. In general, adiponectin has favourable effects on the human metabolism and its synthesis is reduced with increasing bodyweight (Kadowaki and Yamauchi, 2005, Vuppalanchi et al., 2005, Wruck et al., 2015). Adiponectin is capable to reduce gluconeogenesis and lipogenesis in hepatocytes (Combs and Marliss, 2014). High fat diet-induced obese mice, that have been treated with a small-molecule analogue named AdipoRon, showed improved insulin sensitivity, reduced fasting blood glucose levels, and lowered liver triacylglycerides (Okada-Iwabu et al., 2013).

In this study, iPSCs from four donors with distinct grades of steatosis (CO2 = control, S08 and S11 = high steatosis, S12 = low steatosis, see Table 1) were differentiated into HLCs and the effect of AdipoRon on lipid storage and metabolism was elucidated (Graffmann et al., 2021).

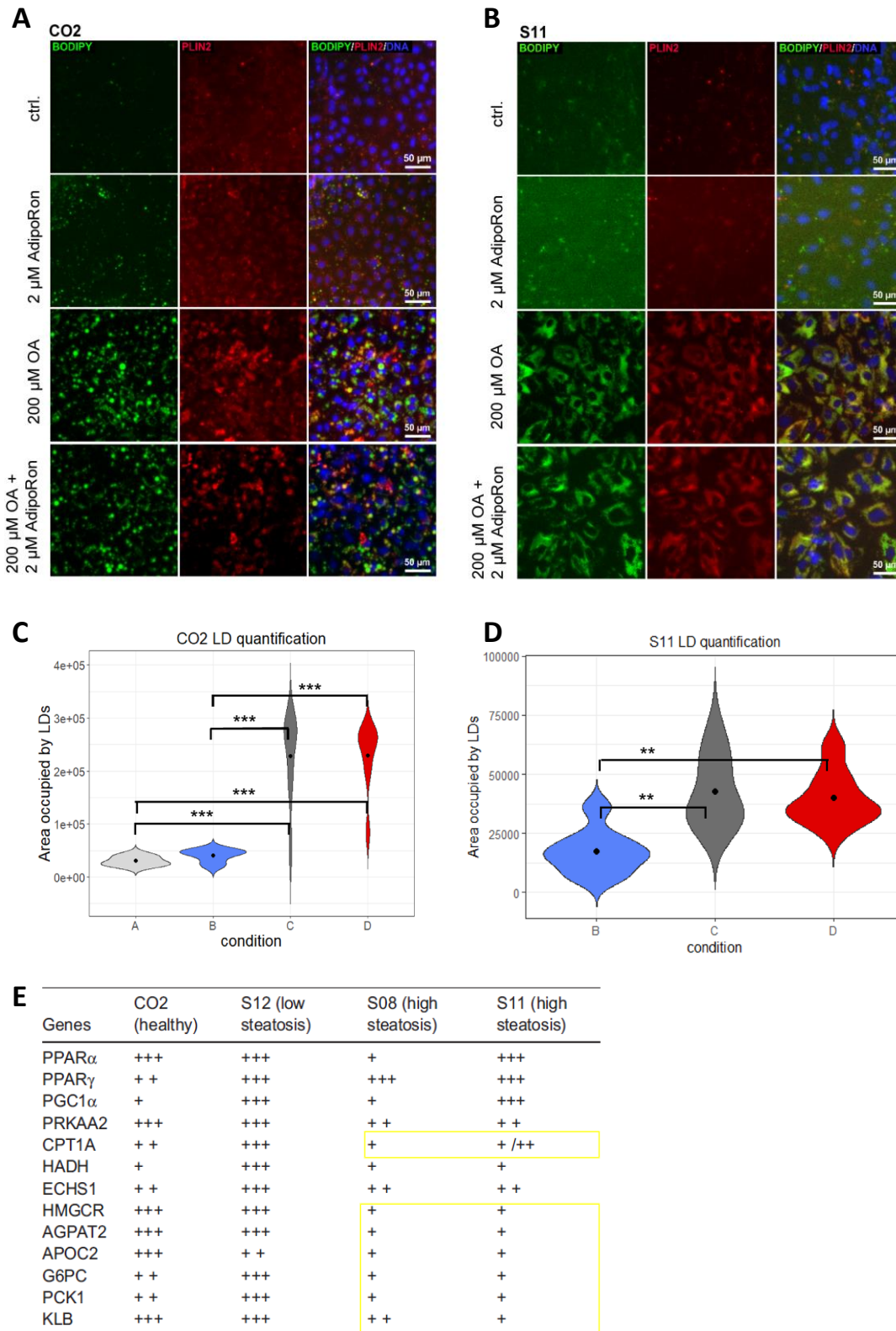


Fig. 8: OA treatment increases LD number and size in HLCs and influences their metabolism. (A,B), Representative immunofluorescence pictures for LD (BODIPY 493/593, green) formation in HLCs derived from a low steatosis cell line (CO2, A) and a high steatosis cell line (S11, B). LDs are covered by PLIN2 (red). **(C,D)** quantification of LDs in the two cell lines. Condition A = ctrl., B = 2 μ M AdipoRon, C = 200 μ M OA, D = 200 μ M OA + 2 μ M AdipoRon. **(E)** Summary of gene expression levels in the four analyzed cell lines after OA induction and with AdipoRon. Figure adapted from Graffmann et al. 2021 under the terms of the Creative Commons Attribution License (<https://creativecommons.org/licenses/by/4.0>) and reproduced with friendly permission of the publisher.

The HLCs expressed characteristic markers of hepatocytes and showed CYP3A activity. They were all capable to store lipids in LDs and up-regulated *PLIN2* expression as a response to OA overload (Fig. 8 A-D). Interestingly, the LD pattern varied from clearly separated, big round droplets in the cells from the healthy donor (Fig. 8 A) to a plethora of very tiny diffusely distributed ones in cells from the diseased donors (Fig. 8 B). However, in all cases number and size of LDs, as well as the occupied area increased after OA treatment (Fig. 8 C, D). Unexpectedly, AdipoRon treatment did not reduce the size or number of LDs in the HLCs.

The presence the of the two adiponectin receptors *ADIPOR1* and *2* was confirmed on mRNA level, while at least the liver specific *ADIPOR2* could also be detected by Western Blot. Proteins of the major Adiponectin signalling pathways, such as cAMP response element-binding protein (CREB), AMPK, and AKT, as well as their respective phosphorylated active forms were present, albeit with major variations between the four lines. RT-qPCR of metabolic regulators (*PPAR α* , *PPAR γ* , *PGC-1 α* , *PRKAA2*), β -oxidation related factors (*CPT1A*, *HADH*, enoyl-CoA hydratase, short chain (*ECHS 1*), lipid and cholesterol metabolism associated factors (*HMGCR*, *AGPAT2*), the lipid export factor apolipoprotein C2 (*APOC2*) and gluconeogenesis genes (glucose-6-phosphatase catalytic-subunit (*G6PC*) and phosphoenolpyruvate carboxykinase (*PCK 1*) revealed rather cell line and OA treatment specific expression patterns than an influence of AdipoRon.

Detailed analysis of the regulation of genes of the *PPAR α* /adiponectin network revealed a down-regulation of the important signalling factor *FGF21* after OA treatment. The expression of *FGF21* is regulated by *PPAR α* and γ , while *FGF21* itself regulates adiponectin synthesis and *PPAR γ* expression (Goetz, 2013). *FGF21* reduction after OA treatment was confirmed in Western Blot for three out of four lines while the *FGF21* receptor β -*KLOTHO* (*KLB*) was expressed in all cell lines, albeit on low levels in the high-steatosis ones. As hepatic *FGF21* expression increases in fasting periods (Inagaki et al., 2007, Galman et al., 2008), low levels after OA-overload are expected as a healthy response. The failed reduction in one of the high-steatosis lines might indicate metabolic dysregulation as for example seen in *FGF21* resistant obese patients (Zhang et al., 2008, Gallego-Escuredo et al., 2015). The general low *KLB* expression in the high steatosis lines independent of treatment, might be a sign for reduced *FGF21* signalling in these cells.

To discern the influence of AdipoRon on the cells in a setting of limited variability, microarray analysis for the CO2-HLC, which are derived from a healthy donor, were performed. The comparison of control and OA-treated cells with data from our previous study (Graffmann et al., 2016) revealed striking similarities given that different cell lines and a different induction protocol have been used. *In silico* analysis of the common significantly up-regulated pathways employing the Kyoto Encyclopedia of

Genes and Genomes (KEGG) algorithm (Kanehisa et al., 2017) pointed to a strong association with metabolism as well as with adipocytokine and AMPK signalling in both studies.

A comparison of regulated KEGG pathways in control and OA-treated CO2 cells revealed, that AdipoRon treatment of control cells reduced amongst others drug metabolism pathways and chemical carcinogenesis, while pathways related to cytokine signalling as well as amino acid and folate biosynthesis were up-regulated. Folate homeostasis is an important factor for DNA methylation and necessary for proper epigenetic transcription control (Crider et al., 2012) as well as for lipid metabolism. Reduced folate levels are associated with NAFLD (da Silva et al., 2014). Thus, AdipoRon seems to be relevant to protect transcriptomic and metabolic integrity in the control cells. Similarly, AdipoRon treatment of OA-induced cells resulted in a down-regulation of drug metabolism related pathways and chemical carcinogenesis, while it increased signalling related pathways such as MAPK, RAP1, and PI3K-AKT signalling, the latter being an important mediator of insulin action (Boucher et al., 2014). However, neither AKT nor phospho-AKT levels changed in Western Blot analyses. Although no direct, cell line independent effect of AdipoRon on any analysed pathway could be discovered by Western Blot or RT-qPCR, the array data indicated a beneficial influence on the cells.

The study demonstrated that HLCs could reproduce essential features of steatosis, independent of the donor's health situation and that AdipoRon positively affected metabolism and signalling pathways in general but could not reduce LD formation. A detailed analysis of metabolic pathways after OA treatment showed strong inter-individual variation, which could explain the differences seen in disease progression within patients. Nevertheless, we could identify a steatosis-related phenotype, independent of the treatment, which was characterized by low expression of genes involved in lipid export, fat and cholesterol synthesis, gluconeogenesis, β -oxidation, and FGF21 signalling in the high steatosis lines (Fig. 8 E).

6 Discussion

6.1 The role of iPSCs for disease modelling

Patient derived iPSC lines are an indispensable tool for modelling diseases and to study their molecular basis as well as possible treatment options. In this regard, it can be differentiated between monogenetic diseases, which are caused by an isolated genetic mutation and are frequently inborn, and multifactorial diseases such as NAFLD and most types of cancer, which arise as a consequence of the combination of genetic variants and environmental cues. iPSCs are useful in both settings. For monogenetic diseases, patient derived iPSCs can be differentiated in comparison to iPSCs from a healthy donor and different behaviour is frequently attributed to the mutation. Even better controls have been developed by using the clustered regularly interspaced short palindromic repeats (CRISPR)/cas9 technology to either revert or introduce mutations at the target locus and thus generating cell lines which differ only at this exact position (Brooks et al., 2022).

Multifactorial diseases are more difficult to capture, as it is never clear which combination of factors plays a role and how the single hits are to be weighted. Therefore, it is important to study the behaviour of cells from different donors to figure out disease-associated pathways. Only with patient-derived cells, it is ensured that the cells really contain all the prerequisites on the genetic level to develop the disease even though not all of them might be known yet.

In order to model NAFLD, we have collected fibroblasts from donors of different disease stages and selected several for reprogramming to end up with a healthy control cell line, a low steatosis and three high steatosis lines (5.1 and 5.2; Table 1) (Kawala et al., 2016a, Kawala et al., 2016b, Kawala et al., 2016c, Graffmann et al., 2018a, Graffmann et al., 2018b). Four of these lines (CO2, S08, S11, S12) were used for the experiments presented herein (5.5), alongside with human fetal foreskin (5.3) and amniotic fluid-derived iPSC (5.4) as well as embryonic stem cells (5.3).

One drawback of this multi-cell line approach is, that every iPSC line has its individual differentiation capacity (Hannan et al., 2013a, Asplund et al., 2016, Volpato and Webber, 2020). This adds another level of variability to the *in vitro* studies. In some cases, it might be useful to determine certain endpoint criteria defining the “final” state rather than just a common differentiation end-date to study the most similar cell population as possible.

6.2 Using iPSCs to model liver diseases

Pluripotent stem cells have been widely used to study hepatic development (Jozefczuk et al., 2011, Matz et al., 2017) and to model hepatic diseases, ranging from congenital diseases such as alpha-1-antitrypsin (A1AT) deficiency (Wilson et al., 2015, Werder et al., 2021) over virus infections (Schwartz et al., 2012, Wu et al., 2012) to the multifactorial metabolic disease NAFLD (Lyll et al., 2018, Sinton et al., 2021, Graffmann et al., 2022). Interestingly, several different approaches comprising at least 3 and up to 6 steps, reproducing the developmental steps with varying levels of accuracy, lead to HLCs with more or less limited functions. While most protocols rely only on small molecules and cytokines to induce HLC fate, it is also possible to push the cell into the desired direction by overexpression of hepatic transcription factors such as HEX, SOX17, FOXA2, HNF4 α , or HNF1 α (Inamura et al., 2011, Takayama et al., 2012a, Takayama et al., 2012b, Nagamoto et al., 2016, Boon et al., 2020).

Successful HLC differentiation is defined by the presence of typical hepatocyte markers such as ALB, A1AT, HNF4 α , or Transthyretin (TTR) on transcript and protein level. On a functional level, HLCs need to be able to store glycogen and fat and have active transporters as demonstrated by uptake and release of cardiogreen dye. Ideally, the cells are also polarized, which is demonstrated by localized expression of transporters such as multidrug resistance protein (MDR) 1. Most importantly, especially with regard of their usefulness for the pharmaceutical industry, is the presence of functional and inducible CYP molecules.

For our studies, we decided to focus on a straight-forward 3-step protocol, which comprises DE induction by ACTA and Chir99021 (canonical WNT signalling activation) treatment, HE induction by DMSO, and HLC induction by HGF, OSM, Dexa, and Insulin. This combination has been shown to result in decently mature cells which have cytochrome activity that can even be boosted by using laminins as a matrix instead of Matrigel (Takayama et al., 2013b, Cameron et al., 2015, Ong et al., 2018). Laminins are an attractive matrix because they are very specific for the respective cell type and -being xenofree- also suitable for good manufacturing practice (GMP) cell production. However, we realized that the culture is less stable than on Matrigel, especially in the early days of differentiation. This is possibly due to a lack of the laminin compatible integrins which only get expressed properly in later stages (Kanninen et al., 2016). Therefore, we decided to continue our work on Matrigel coated dishes.

Protocols of higher complexity tend to produce cells of higher maturity. The most sophisticated approach in this regard has been provided by Ang et al.. They apply a distinct set of cytokines almost every day, which leads to the production of pure and relatively mature HLCs (Ang et al., 2018). Unfortunately, complicated protocols are usually more expensive and much more error prone than

less complex regimen. This is mirrored by the fact that most laboratories still use much more simple protocols.

We realized that cell density in the first half of the differentiation is essential to obtain HLCs (5.4). When seeding cells in a low density after the HE stage, we obtained epithelial cells with a distinct morphology and no hepatic function, which we named EDECs. When starting the differentiation with an insufficient number of cells, EDECs inevitably occur during the differentiation process and frequently cells even lift off the culture dish during DE stage. When studying EDEC formation, we used small molecules to inhibit relevant signalling pathways, in particular Notch, WNT, Hh, or TGF β . However, none of them was capable to revert the cell fate decision. While it is possible that higher concentrations of the single factors or a combination thereof pushes the cell fate more effectively into HLCs, the most robust regimen to prevent aberrant differentiation is seeding the initial iPSCs at a very high density (> 80 % of a fully confluent plate). Interestingly, cell-cell contact also seems to be indispensable in later stages, as studies on liver bioprinting suggest, that this an essential factor for success (Goulart et al., 2019).

6.2.1 Increasing maturation in iPSC-derived HLCs

In vitro-derived HLCs resemble more foetal than adult hepatocytes (Baxter et al., 2015). This is a common problem in the field of iPSC-based disease modelling and limits the usefulness of all these models (Camp et al., 2017, Wu et al., 2018). They are very suitable to analyse developmental disorders, the impact of selected mutations on certain basic cellular functions, or drastic toxin effects but are not good yet for detecting subtle changes in very elaborate pathways, which might even need cell-cell interactions and are also only of limited use for studying diseases of higher age such as Alzheimer's disease.

There are two main approaches to improve the cellular models. First, the maturity of the cell type of interest can be enhanced by using small molecules and second, several cell types can be mixed to foster cell-cell interactions and thus increase maturity and function of all involved cell types. While the first approach can be done in 2D and 3D cultures, the latter applies predominantly to 3D cultures, as the floating environment enables the cells to form structures and interactions in a more natural way.

A good indicator of HLC maturity is the ratio of ALB and AFP expression. *In vivo*, AFP is only present in foetal HLCs as well as in cancer cells, while ALB is the mature form expressed by adult hepatocytes. In cell culture, both factors are detectable, and a reduction of AFP expression is an indicator for more maturity. The lack of maturity reflects the limitations of the current culturing protocols, which do not

provide unambiguous differentiation cues for the cells. A recent single cell study revealed, that iPSC-derived HLCs express, beside liver related genes, also intestinal ones, all in one cell. This indicates that the separation of the two lineages is not complete in culture. Enhancement of farnesoid X receptor (FXR) helped to reduce the unwanted intestinal gene expression and pushed the cells more into the hepatic direction (Nell et al., 2022).

The main goal in all approaches to increase maturity in HLCs, is to increase CYP activity, which is of tremendous interest for the pharmaceutical industry. Except for the foetal CYP3A7 and CYP19A1, expression levels of most CYP molecules are low in children and increase in adults (Robinson et al., 2020). Some small molecules have been used to increase maturation. One of the earliest factors was functional proliferation hit 1 (FPH1) which helped to mature HLCs (Shan et al., 2013). When studying treatment options for malaria infection, it turned out that this small molecule could increase CYP function, thus enabling drug activation and inhibition of parasite growth (Ng et al., 2015).

More recently, the effects of thyroid hormones triiodo-L-thyronine (T3) and L-thyroxine (T4) have been studied. Especially T3 showed a positive effect. We and others were able to reduce the expression of the foetal genes AFP and CYP3A7 and increase the expression of ALB when using T3 alone or in combination with T4 (T3/T4) (Bogacheva et al., 2021, Ncube et al., 2021, Ma et al., 2022). Withey et al. observed higher levels of the transcription factors *c/EBP α* and *HNF4 α* after treatment with a combination of T3 and a TGF- β inhibitor and did not only measure higher ALB secretion but also increased CYP activity (Withey et al., 2022). Interestingly, pathway analysis demonstrated that treatment with T3/T4 had a major impact on PPAR pathways and thus might be involved in metabolic control (Ncube et al., 2021). Beneficial PPAR pathway modulation could also be a reason for the therapeutic effect of the thyroid hormone receptor β agonist Resmetirom.

T3/T4 also affected TGF- β and mitogen-activated protein kinase/extracellular-signal-regulated kinase (MAPK/ERK) signalling (Ncube et al., 2021), two pathways that are involved in hepatic maturation (Gordillo et al., 2015, Tormos et al., 2017, Fortier et al., 2019). In particular, TGF- β activity induces de-differentiation by promoting epithelial to mesenchymal transition (EMT) and our data indicate a lower presence of mesenchymal genes after T3/T4 treatment (Ncube et al., 2021), indicating that T3/T4 might be able to replace other small molecules that are sometimes used to prevent the formation of mesenchymal cells during differentiation.

Another approach of increasing HLC maturity, which will in the future be included into our protocol, is using 3D differentiation conditions. The big advantage of this concept is that the microenvironment of the cells is closer to the *in vivo* situation. The replacement of a stiff culturing surface with soft matrices and cell-cell contact in all dimensions is much more physiological and allows the cells to engage in their natural 3-fold polarity. While it is easier to generate 3D hepatic spheroids, which only consist of HLCs,

organoids with mixed cell types usually gain higher levels of maturation (Takebe et al., 2013, Takebe et al., 2014, Collin de l'Hortet et al., 2019, Ouchi et al., 2019, Lucendo-Villarin et al., 2020). There exist almost unlimited options for forming the 3D complexes and for keeping them in culture. Cells will find each other without external support in 96 well low-attachment plates but can also be forced into structures by using nanopillars (Takayama et al., 2013a, Nagamoto et al., 2016), compressing systems (Gieseck et al., 2014), or bioprinters (Faulkner-Jones et al., 2015, Ma et al., 2016, Goulart et al., 2019). Blood flow and its associated shear stress can be simulated in microfluidic chambers (Freund et al., 2012).

3D culture can be either initiated right from the beginning, or at later, preferably during the HE stage. If 3D culture is initiated at later differentiation stages, it seems to be important that cells do not completely lose their cell-cell contact when re-seeding them (Goulart et al., 2019).

It is possible to directly generate distinct cell types from iPSCs in one culture, although this approach can lead to an undesired dominance of cells other than HLCs, especially mesenchymal stem cells (MSCs) (Rashidi et al., 2018, Ouchi et al., 2019), or to differentiate cells into HE/HLC stage and mix them later with defined numbers of cholangiocytes, endothelial cells and/or MSCs, which ideally can all be derived from iPSCs of the same donor (Takebe et al., 2013, Takebe et al., 2014, Asai et al., 2017, Camp et al., 2017, Lucendo-Villarin et al., 2020, Meseguer-Ripolles et al., 2021). HLCs can be cultured for more than one year in 3D systems (Rashidi et al., 2018) and organoids get vascularized after transplantation into mice (Takebe et al., 2013, Takebe et al., 2014, Camp et al., 2017, Takebe et al., 2017).

For future toxicological or pharmaceutical studies, it is important that the organoids have comparable sizes and are relatively small without a necrotic core. However, organoids will perform better in assays when testing lipophilic substances which can penetrate into their core and might not be suitable for hydrophilic substances which only reach the outer surface of the organoid.

6.3 IPSC-based *in vitro* models for NAFLD

Focusing on easily accessible markers such as CYP activity and ALB/AFP ratio is a straightforward means to assess if a certain treatment can increase maturation. However, depending on the disease that should be studied, this might not be the best way. *In vivo*, the function of a hepatocyte highly depends on its position along the porto-central axis of the liver lobule (Fig. 2). Only the cells close to the central vein have high CYP activity, while those close to the portal triad are more active in general metabolic pathways such as β -oxidation, gluconeogenesis, or glycogen storage (Cunningham and Porat-Shliom,

2021). Therefore, HLCs with low CYP-activity might not necessarily be too immature for modelling metabolic diseases, they might rather resemble zone 1 hepatocytes which also *in vivo* would be more involved in the metabolic processes of interest.

We and others have successfully used iPSC-derived HLCs to study distinct aspects of metabolic derailment in the context of NAFLD (Lyll et al., 2018, Collin de l'Hortet et al., 2019, Ouchi et al., 2019, Gurevich et al., 2020, Lucendo-Villarin et al., 2020, Ramli et al., 2020, Sinton et al., 2021). In 2016, we showed for the first time, that iPSC and ESC derived HLCs can recapitulate key features of NAFLD. The cells were able to store fat after treatment with oleic acid (OA) and we saw genome wide gene expression changes that mirrored those seen in NAFLD patients (Graffmann et al., 2016), although there were major differences between the two cell lines. Importantly, the cells reacted to treatment with a PPAR α agonist/antagonist in a similar way that was expected from patient data. In brief, PPAR α inhibition with GW6471 reduced expression of lipid catabolism genes, which most likely results in increased lipid storage, while the PPAR α agonist Fenofibrate could reduce enzymes for cholesterol and phospholipid synthesis, thus most likely also reducing lipid storage. Unfortunately, clinical trials showed that Fenofibrate as well as other fibrates are not capable to significantly improve NASH in patients (Fernandez-Miranda et al., 2008, Boeckmans et al., 2019). However, pan-PPAR activators such as Lanifibranor are still promising candidates (Harrison et al., 2023).

Besides gene expression, we also screened for miRNA expression and identified miR-106b and -122 as candidate factors involved in NAFLD development. We could confirm the *in silico* predicted genes *CPAMD8*, *ATL3*, and *EPHA7* as new miR-122 and miR-106b targets, respectively. None of these were described as steatosis markers at that time, while *ATL3* and *EPHA7* are meanwhile listed as human fatty liver associated genes by the harmonizome (Rouillard et al., 2016). *ATL3*, which is differentially regulated in NAFLD/NASH (Ahrens et al., 2013, Murphy et al., 2013), is known as a receptor for ER-phagy, a process where ER particles are digested by autophagosomes. As autophagic processes are important for lipid turnover, this might provide a link to NAFLD that is worth investigating in more depth in the future (Duwaerts and Maiers, 2021).

To study NAFLD in more detail and test for another possible treatment option, we next used a set of four iPSC lines (CO2, S08, S11, S12, Table 1) derived from patients with high and low levels of steatosis as well as from a healthy control (Graffmann et al., 2021). Also in this study, we observed huge inter-individual differences, which reflect the complexity of the disease that occurs in every patient cohort. Variations were observed on every level of analysis, from the size and distribution of LDs, via gene expression to the protein level. The first point confirmed observations made earlier by Gurevich et al. who also reported distinct LD patterns in HLCs derived from donors of different disease stages (Gurevich et al., 2020). Summarizing our observations, we realized that the high steatosis lines had

lower expression of genes involved in lipid export, fat, and cholesterol synthesis as well as in gluconeogenesis, β -oxidation, and FGF21 signalling than the low steatosis lines. This might contribute to the increased tendency of fat storage in these patients.

In contrast to our expectations, we could not see a clear beneficial effect of treating the cells with 2 μ M of the small molecule AdipoRon, a mimic of Adiponectin. Neither fat incorporation was reduced, nor proteins of the major Adiponectin signalling pathways, CREB, AMPK, and AKT were up-regulated in Western Blot. By analysing transcriptome data, a positive influence of AdipoRon on several pathways including folate metabolism, AKT signalling, and chemical carcinogenesis was observed, indicating effects that might become more pronounced with different treatment schemes.

Nonetheless, the iPSC-based model for NAFLD is rather robust, as transcriptome analyses revealed similar affected GOs and pathways when comparing HLCs derived from two independent healthy donors after treatment with either EtOH dissolved OA or BSA-coupled OA.

While the high inter-individual differences that we observed make it difficult to clearly identify disease-associated factors, it undoubtedly reflects the mixed phenotypes seen in patients. It is not clear yet, why only 5 - 10 % of patients develop the severe NASH phenotype with high levels of chronic inflammation from an initially mild NAFLD, which then can proceed towards fibrosis, cirrhosis, and HCC. To address this question, immune reactions and inflammation can be mimicked by the addition of pro-inflammatory cytokines into the HLC-based model.

In a next step, we will enhance the steatosis model by incorporating besides HLCs also other major cell types of the liver such as immune cells mediating inflammation, endothelial cells, and stellate cells as an important regulatory element that can also trigger the later steps of fibrosis.

7 Conclusion

NAFLD or MASLD are umbrella terms for a complex disease-spectrum that proceeds from simple steatosis to severe chronic hepatic inflammation seen in NASH towards liver cirrhosis and cancer. To increase our understanding of this disease, *in vitro* liver models are a valuable tool. For these models it is essential to keep the cells at a high density in order to get a high percentage of HLCs and not EDECs at the end of the differentiation protocol.

The studies presented herein demonstrate that HLCs derived from healthy controls as well as from NAFLD patients are capable to recapitulate the NAFLD phenotype in terms of lipid storage, gene

expression, and miRNA profile. While there were substantial inter-individual variations regarding all analysed aspects, iPSC-derived HLCs from patients with hepatic steatosis had lower expression of genes involved in lipid export, fat, and cholesterol synthesis as well as in gluconeogenesis, β -oxidation, and FGF21 signalling than the low steatosis lines, potentially contributing to a more severe phenotype.

The HLCs responded to PPAR α activity modulation by small molecules in a similar way as observed in patients. Importantly, activation of PPAR α resulted in a reduced expression of enzymes for cholesterol and phospholipid synthesis, most likely contributing to reduced fat storage. Effects detected by AdipoRon treatment were less obvious and comprised a positive influence on pathways such as folate metabolism, AKT signalling, and chemical carcinogenesis, when analysing transcriptome data.

Overall, the *in vitro* model is useful for studying NAFLD development and testing anti-NAFLD drugs. Based on the knowledge obtained over the last years, we will continuously improve it by I) employing small molecules to increase HLC maturity, II) transferring it into 3D to provide the cells with a more natural environment and III) by the incorporation of other liver cell types fostering cellular communication and also to mimic the natural environment. As more accurate liver functions will be achieved *in vitro*, the model will not only be useful to study a single disease such as NAFLD but can also stepwise complement or even replace animal experiments for drug and toxin tests and thus become part of the growing field of personalized medicine.

8 Abbreviations

2D	Two dimensional
3D	Three dimensional
A1AT	α -1-antitrypsin
AFP	Alpha-foeto protein
AGPAT	1-acylglycerol-3-phosphate O-acyltransferase
AICAR	Aminoimidazole carboxamide ribonucleotide
AMP	Adenosine-monophosphate
AMPK	AMP-activated protein kinase
APOC2	Apolipoprotein C2
ATL3	Atlastin 3
ATP	Adenosine-triphosphate
BMP	Bone morphogenetic protein
BSA	Bovine serum albumin
cAMP	Cyclic adenosine-monophosphate
CD	Cluster of differentiation
Cas9	CRISPR-associated 9
CFTR	Cystic fibrosis transmembrane conductance regulator
CK	Cytokeratin
CMA	Chaperone mediated autophagy
cDNA	Complementary DNA
c-MYC	Cellular MYC
CPAMD8	C3 and PZP-like alpha-2-macroglobulin domain-containing protein 8
CPT1A	Carnitine palmitoyltransferase
CRISPR	Clustered regularly interspaced short palindromic repeats
CYP	Cytochrome P450
DE	Definitive endoderm
Dexa	Dexamethasone
DILI	Drug-induced liver injury
DNA	deoxyribonucleic acid
e.g.	Exempli gratia (for example)
EB	Embryoid body
ECAD	E-cadherin
ECHS1	Enoyl-CoA hydratase, short chain 1
EDEC	Endoderm derived epithelial cell
EMA	European medical agency
EMT	epithelial-mesenchymal-transition
EPHA7	Ephrin type-A receptor 7
ERK	Extracellular-signal-regulated kinase
ESC	Embryonic stem cell
et al.	Et aliae (and others)
EtOH	Ethanol
FCS	Foetal calf serum
FDA	Food and Drug Agency
FGF	Fibroblast growth factor
FOXA2	Forkhead-box-protein A2
FXR	Farnesoid X
G6PC	Glucose-6-phosphatase catalytic-subunit
GLP	Glucose-like peptide

HADH	Hydroxyacyl-CoA dehydrogenase
HE	Hepatic endoderm
hESC	Human embryonic stem cell
HGF	Hepatocyte growth factor
Hh	Hedgehog
HLC	Hepatocyte-like cell
HMGCR	3-hydroxy-3-methylglutaryl-coenzyme A reductase
HNF	Hepatocyte nuclear factor
hPSC	Human pluripotent stem cell
iPSC	Induced pluripotent stem cell
JAG	Jagged canonical notch ligand
KEGG	Kyoto Encyclopedia of Genes and Genomes
KLF4	Krüppel-like factor 4
KO-SR	Knock out serum replacement
MAFLD	Metabolic associated fatty liver disease
MAPK	Mitogen-activated protein kinase
MASLD	metabolic dysfunction-associated steatotic liver disease
MET	Mesenchymal to epithelial transition
miRNA	Micro RNA
MSC	Mesenchymal stem/stromal cell
NANOG	Nanog homeobox
OCT	Octamer-binding transcription factor
OSM	Oncostatin M
OSN	Osteopontin
PAX	Paired box
PCK1	Phosphoenolpyruvate carboxykinase 1
PGC-1 α	PPAR γ co-activator 1 α
PHH	Primary human hepatocyte
PLIN	Perilipin
PPAR	Peroxisome proliferator-activated receptor
P/S	Penicillin/ Streptomycin
RbAp	Retinoblastoma protein associated protein
RNA	Ribonucleic acid
RT-qPCR	Reverse transcription quantitative polymerase chain reaction
RXR	Retinoid X receptor
SIRT	Sirtuin
SLD	steatotic liver disease
SOX	SRY-box transcription factor
SRY	Sex determining region Y
SSEA4	Stage-specific embryonic antigen-4
T3	Triiodo-L-thyronine
T4	L-Thyroxine
TGF β	Transforming growth factor β
TR	Thyroid hormone receptor
TTR	Transthyretin
VIM	Vimentin
YAP	Yes-associated protein

9 References

- Ahrens, M., Ammerpohl, O., Von Schonfels, W., Kolarova, J., Bens, S., Itzel, T., Teufel, A., Herrmann, A., Brosch, M., Hinrichsen, H., Erhart, W., Egberts, J., Sipos, B., Schreiber, S., Hasler, R., Stickel, F., Becker, T., Krawczak, M., Rocken, C., Siebert, R., Schafmayer, C. & Hampe, J. 2013. DNA methylation analysis in nonalcoholic fatty liver disease suggests distinct disease-specific and remodeling signatures after bariatric surgery. *Cell Metab*, 18, 296-302.
- Alexander, M., Loomis, A. K., Fairburn-Beech, J., Van Der Lei, J., Duarte-Salles, T., Prieto-Alhambra, D., Ansell, D., Pasqua, A., Lapi, F., Rijnbeek, P., Mosseveld, M., Avillach, P., Egger, P., Kendrick, S., Waterworth, D. M., Sattar, N. & Alazawi, W. 2018. Real-world data reveal a diagnostic gap in non-alcoholic fatty liver disease. *BMC Med*, 16, 130.
- Ambros, V. 2004. The functions of animal microRNAs. *Nature*, 431, 350-5.
- Ang, L. T., Tan, A. K. Y., Autio, M. I., Goh, S. H., Choo, S. H., Lee, K. L., Tan, J., Pan, B., Lee, J. J. H., Lum, J. J., Lim, C. Y. Y., Yeo, I. K. X., Wong, C. J. Y., Liu, M., Oh, J. L. L., Chia, C. P. L., Loh, C. H., Chen, A., Chen, Q., Weissman, I. L., Loh, K. M. & Lim, B. 2018. A Roadmap for Human Liver Differentiation from Pluripotent Stem Cells. *Cell Rep*, 22, 2190-2205.
- Asai, A., Aihara, E., Watson, C., Mourya, R., Mizuochi, T., Shivakumar, P., Phelan, K., Mayhew, C., Helmrath, M., Takebe, T., Wells, J. & Bezerra, J. A. 2017. Paracrine signals regulate human liver organoid maturation from induced pluripotent stem cells. *Development*, 144, 1056-1064.
- Asby, D. J., Cuda, F., Beyaert, M., Houghton, F. D., Cagampang, F. R. & Tavassoli, A. 2015. AMPK Activation via Modulation of De Novo Purine Biosynthesis with an Inhibitor of ATIC Homodimerization. *Chem Biol*, 22, 838-48.
- Asplund, A., Pradip, A., Van Giezen, M., Aspegren, A., Choukair, H., Rehnstrom, M., Jacobsson, S., Ghosheh, N., El Hajjam, D., Holmgren, S., Larsson, S., Benecke, J., Butron, M., Wigander, A., Noaksson, K., Sartipy, P., Bjorquist, P., Edsbacke, J. & Kuppers-Munther, B. 2016. One Standardized Differentiation Procedure Robustly Generates Homogenous Hepatocyte Cultures Displaying Metabolic Diversity from a Large Panel of Human Pluripotent Stem Cells. *Stem Cell Rev Rep*, 12, 90-104.
- Badman, M. K., Pissios, P., Kennedy, A. R., Koukos, G., Flier, J. S. & Maratos-Flier, E. 2007. Hepatic fibroblast growth factor 21 is regulated by PPARalpha and is a key mediator of hepatic lipid metabolism in ketotic states. *Cell Metab*, 5, 426-37.
- Bartel, D. P. 2004. MicroRNAs: genomics, biogenesis, mechanism, and function. *Cell*, 116, 281-97.
- Bartel, D. P. 2009. MicroRNAs: target recognition and regulatory functions. *Cell*, 136, 215-33.
- Baxter, M., Withey, S., Harrison, S., Segeritz, C. P., Zhang, F., Atkinson-Dell, R., Rowe, C., Gerrard, D. T., Sison-Young, R., Jenkins, R., Henry, J., Berry, A. A., Mohamet, L., Best, M., Fenwick, S. W., Malik, H., Kitteringham, N. R., Goldring, C. E., Piper Hanley, K., Vallier, L. & Hanley, N. A. 2015. Phenotypic and functional analyses show stem cell-derived hepatocyte-like cells better mimic fetal rather than adult hepatocytes. *J Hepatol*, 62, 581-9.
- Bento, G., Shafiqullina, A. K., Rizvanov, A. A., Sardao, V. A., Macedo, M. P. & Oliveira, P. J. 2020. Urine-Derived Stem Cells: Applications in Regenerative and Predictive Medicine. *Cells*, 9.

- Bircsak, K. M., Debiasio, R., Miedel, M., Alsebah, A., Reddinger, R., Saleh, A., Shun, T., Verneti, L. A. & Gough, A. 2021. A 3D microfluidic liver model for high throughput compound toxicity screening in the OrganoPlate(R). *Toxicology*, 450, 152667.
- Boeckmans, J., Natale, A., Rombaut, M., Buyl, K., Rogiers, V., De Kock, J., Vanhaecke, T. & R, M. R. 2019. Anti-NASH Drug Development Hitches a Lift on PPAR Agonism. *Cells*, 9.
- Bogacheva, M. S., Bystriakova, M. A. & Lou, Y.-R. 2021. Thyroid Hormone Effect on the Differentiation of Human Induced Pluripotent Stem Cells into Hepatocyte-Like Cells. *Pharmaceuticals*, 14.
- Boon, R., Kumar, M., Tricot, T., Elia, I., Ordovas, L., Jacobs, F., One, J., De Smedt, J., Eelen, G., Bird, M., Roelandt, P., Doglioni, G., Vriens, K., Rossi, M., Vazquez, M. A., Vanwelden, T., Chesnais, F., El Taghdouini, A., Najimi, M., Sokal, E., Cassiman, D., Snoeys, J., Monshouwer, M., Hu, W. S., Lange, C., Carmeliet, P., Fendt, S. M. & Verfaillie, C. M. 2020. Amino acid levels determine metabolism and CYP450 function of hepatocytes and hepatoma cell lines. *Nat Commun*, 11, 1393.
- Boucher, J., Kleinridders, A. & Kahn, C. R. 2014. Insulin receptor signaling in normal and insulin-resistant states. *Cold Spring Harb Perspect Biol*, 6.
- Brekke, O. R., Honey, J. R., Lee, S., Hallett, P. J. & Isacson, O. 2020. Cell type-specific lipid storage changes in Parkinson's disease patient brains are recapitulated by experimental glycolipid disturbance. *Proc Natl Acad Sci U S A*, 117, 27646-27654.
- Brooks, I. R., Garrone, C. M., Kerins, C., Kiar, C. S., Syntaka, S., Xu, J. Z., Spagnoli, F. M. & Watt, F. M. 2022. Functional genomics and the future of iPSCs in disease modeling. *Stem Cell Reports*, 17, 1033-1047.
- Buzzetti, E., Pinzani, M. & Tsochatzis, E. A. 2016. The multiple-hit pathogenesis of non-alcoholic fatty liver disease (NAFLD). *Metabolism*, 65, 1038-48.
- Cai, X., Wang, K. C. & Meng, Z. 2021. Mechanoregulation of YAP and TAZ in Cellular Homeostasis and Disease Progression. *Front Cell Dev Biol*, 9, 673599.
- Cameron, K., Tan, R., Schmidt-Heck, W., Campos, G., Lyall, M. J., Wang, Y., Lucendo-Villarin, B., Szkolnicka, D., Bates, N., Kimber, S. J., Hengstler, J. G., Godoy, P., Forbes, S. J. & Hay, D. C. 2015. Recombinant Laminins Drive the Differentiation and Self-Organization of hESC-Derived Hepatocytes. *Stem Cell Reports*, 5, 1250-62.
- Camp, J. G., Sekine, K., Gerber, T., Loeffler-Wirth, H., Binder, H., Gac, M., Kanton, S., Kageyama, J., Damm, G., Seehofer, D., Belicova, L., Bickle, M., Barsacchi, R., Okuda, R., Yoshizawa, E., Kimura, M., Ayabe, H., Taniguchi, H., Takebe, T. & Treutlein, B. 2017. Multilineage communication regulates human liver bud development from pluripotency. *Nature*, 546, 533-538.
- Canto, C. & Auwerx, J. 2009. PGC-1alpha, SIRT1 and AMPK, an energy sensing network that controls energy expenditure. *Curr Opin Lipidol*, 20, 98-105.
- Cao, W., Collins, Q. F., Becker, T. C., Robidoux, J., Lupo, E. G., Jr., Xiong, Y., Daniel, K. W., Floering, L. & Collins, S. 2005. p38 Mitogen-activated protein kinase plays a stimulatory role in hepatic gluconeogenesis. *J Biol Chem*, 280, 42731-7.
- Carr, R. M., Peralta, G., Yin, X. & Ahima, R. S. 2014. Absence of perilipin 2 prevents hepatic steatosis, glucose intolerance and ceramide accumulation in alcohol-fed mice. *PLoS One*, 9, e97118.
- Cermelli, S., Ruggieri, A., Marrero, J. A., Ioannou, G. N. & Beretta, L. 2011. Circulating microRNAs in patients with chronic hepatitis C and non-alcoholic fatty liver disease. *PLoS One*, 6, e23937.
- Chen, C., Soto-Gutierrez, A., Baptista, P. M. & Spee, B. 2018. Biotechnology Challenges to In Vitro Maturation of Hepatic Stem Cells. *Gastroenterology*, 154, 1258-1272.

- Choi, S. M., Kim, Y., Shim, J. S., Park, J. T., Wang, R. H., Leach, S. D., Liu, J. O., Deng, C., Ye, Z. & Jang, Y. Y. 2013. Efficient drug screening and gene correction for treating liver disease using patient-specific stem cells. *Hepatology*, 57, 2458-68.
- Cholongitas, E., Pavlopoulou, I., Papatheodoridi, M., Markakis, G. E., Bouras, E., Haidich, A. B. & Papatheodoridis, G. 2021. Epidemiology of nonalcoholic fatty liver disease in Europe: a systematic review and meta-analysis. *Ann Gastroenterol*, 34, 404-414.
- Collin De L'hortet, A., Takeishi, K., Guzman-Lepe, J., Morita, K., Achreja, A., Popovic, B., Wang, Y., Handa, K., Mittal, A., Meurs, N., Zhu, Z., Weinberg, F., Salomon, M., Fox, I. J., Deng, C.-X., Nagrath, D. & Soto-Gutierrez, A. 2019. Generation of Human Fatty Livers Using Custom-Engineered Induced Pluripotent Stem Cells with Modifiable SIRT1 Metabolism. *Cell Metabolism*, 30, 385-401.e9.
- Combs, T. P. & Marliss, E. B. 2014. Adiponectin signaling in the liver. *Rev Endocr Metab Disord*, 15, 137-47.
- Cordi, S., Godard, C., Saandi, T., Jacquemin, P., Monga, S. P., Colnot, S. & Lemaigre, F. P. 2016. Role of beta-catenin in development of bile ducts. *Differentiation*, 91, 42-9.
- Crider, K. S., Yang, T. P., Berry, R. J. & Bailey, L. B. 2012. Folate and DNA methylation: a review of molecular mechanisms and the evidence for folate's role. *Adv Nutr*, 3, 21-38.
- Cunningham, R. P. & Porat-Shliom, N. 2021. Liver Zonation - Revisiting Old Questions With New Technologies. *Front Physiol*, 12, 732929.
- Da Silva, R. P., Kelly, K. B., Al Rajabi, A. & Jacobs, R. L. 2014. Novel insights on interactions between folate and lipid metabolism. *Biofactors*, 40, 277-83.
- Daignan-Fornier, B. & Pinson, B. 2012. 5-Aminoimidazole-4-carboxamide-1-beta-D-ribofuranosyl 5'-Monophosphate (AICAR), a Highly Conserved Purine Intermediate with Multiple Effects. *Metabolites*, 2, 292-302.
- Danoy, M., Tauran, Y., Poulain, S., Arakawa, H., Mori, D., Araya, K., Kato, S., Kido, T., Kusuvara, H., Kato, Y., Miyajima, A., Plessy, C., Sakai, Y. & Leclerc, E. 2020. Analysis of hiPSCs differentiation toward hepatocyte-like cells upon extended exposition to oncostatin. *Differentiation*, 114, 36-48.
- Decaens, T., Godard, C., De Reynies, A., Rickman, D. S., Tronche, F., Couty, J. P., Perret, C. & Colnot, S. 2008. Stabilization of beta-catenin affects mouse embryonic liver growth and hepatoblast fate. *Hepatology*, 47, 247-58.
- Demyanets, S., Kaun, C., Rychli, K., Pfaffenberger, S., Kastl, S. P., Hohensinner, P. J., Rega, G., Katsaros, K. M., Afonyushkin, T., Bochkov, V. N., Paireder, M., Huk, I., Maurer, G., Huber, K. & Wojta, J. 2011. Oncostatin M-enhanced vascular endothelial growth factor expression in human vascular smooth muscle cells involves PI3K-, p38 MAPK-, Erk1/2- and STAT1/STAT3-dependent pathways and is attenuated by interferon-gamma. *Basic Res Cardiol*, 106, 217-31.
- Diehl, A. M. 1998. Roles of CCAAT/enhancer-binding proteins in regulation of liver regenerative growth. *J Biol Chem*, 273, 30843-6.
- Doench, J. G. & Sharp, P. A. 2004. Specificity of microRNA target selection in translational repression. *Genes Dev*, 18, 504-11.
- Drewe, K., Matz, P. & Adjaye, J. 2015. Generation of iPSC lines from primary human amniotic fluid cells. *Stem Cell Res*, 15, 712-4.
- Duwaerts, C. C. & Maiers, J. L. 2021. ER Disposal Pathways in Chronic Liver Disease: Protective, Pathogenic, and Potential Therapeutic Targets. *Front Mol Biosci*, 8, 804097.
- Eggenchwiler, R., Loya, K., Wu, G., Sharma, A. D., Sgodda, M., Zychlinski, D., Herr, C., Steinemann, D., Teckman, J., Bals, R., Ott, M., Schambach, A., Scholer, H. R. & Cantz, T. 2013. Sustained knockdown of a disease-causing gene in patient-specific induced

- pluripotent stem cells using lentiviral vector-based gene therapy. *Stem Cells Transl Med*, 2, 641-54.
- Esau, C., Davis, S., Murray, S. F., Yu, X. X., Pandey, S. K., Pear, M., Watts, L., Booten, S. L., Graham, M., McKay, R., Subramaniam, A., Propp, S., Lollo, B. A., Freier, S., Bennett, C. F., Bhanot, S. & Monia, B. P. 2006. miR-122 regulation of lipid metabolism revealed by in vivo antisense targeting. *Cell Metab*, 3, 87-98.
- Eslam, M., Newsome, P. N., Sarin, S. K., Anstee, Q. M., Targher, G., Romero-Gomez, M., Zelber-Sagi, S., Wai-Sun Wong, V., Dufour, J. F., Schattenberg, J. M., Kawaguchi, T., Arrese, M., Valenti, L., Shiha, G., Tiribelli, C., Yki-Jarvinen, H., Fan, J. G., Gronbaek, H., Yilmaz, Y., Cortez-Pinto, H., Oliveira, C. P., Bedossa, P., Adams, L. A., Zheng, M. H., Fouad, Y., Chan, W. K., Mendez-Sanchez, N., Ahn, S. H., Castera, L., Bugianesi, E., Ratziu, V. & George, J. 2020. A new definition for metabolic dysfunction-associated fatty liver disease: An international expert consensus statement. *J Hepatol*, 73, 202-209.
- Estes, C., Anstee, Q. M., Arias-Loste, M. T., Bantel, H., Bellentani, S., Caballeria, J., Colombo, M., Craxi, A., Crespo, J., Day, C. P., Eguchi, Y., Geier, A., Kondili, L. A., Kroy, D. C., Lazarus, J. V., Loomba, R., Manns, M. P., Marchesini, G., Nakajima, A., Negro, F., Petta, S., Ratziu, V., Romero-Gomez, M., Sanyal, A., Schattenberg, J. M., Tacke, F., Tanaka, J., Trautwein, C., Wei, L., Zeuzem, S. & Razavi, H. 2018. Modeling NAFLD disease burden in China, France, Germany, Italy, Japan, Spain, United Kingdom, and United States for the period 2016-2030. *J Hepatol*, 69, 896-904.
- Esteves, F., Rueff, J. & Kranendonk, M. 2021. The Central Role of Cytochrome P450 in Xenobiotic Metabolism-A Brief Review on a Fascinating Enzyme Family. *J Xenobiot*, 11, 94-114.
- Faulkner, C. S., White, C. M., Shah, V. H. & Jophilin, L. L. 2020. A single nucleotide polymorphism of PLIN2 is associated with nonalcoholic steatohepatitis and causes phenotypic changes in hepatocyte lipid droplets: A pilot study. *Biochim Biophys Acta Mol Cell Biol Lipids*, 1865, 158637.
- Faulkner-Jones, A., Fyfe, C., Cornelissen, D. J., Gardner, J., King, J., Courtney, A. & Shu, W. 2015. Bioprinting of human pluripotent stem cells and their directed differentiation into hepatocyte-like cells for the generation of mini-livers in 3D. *Biofabrication*, 7, 044102.
- Fernandez-Marcos, P. J. & Auwerx, J. 2011. Regulation of PGC-1alpha, a nodal regulator of mitochondrial biogenesis. *Am J Clin Nutr*, 93, 884S-90.
- Fernandez-Miranda, C., Perez-Carreras, M., Colina, F., Lopez-Alonso, G., Vargas, C. & Solis-Herruzo, J. A. 2008. A pilot trial of fenofibrate for the treatment of non-alcoholic fatty liver disease. *Dig Liver Dis*, 40, 200-5.
- Fisher, F. M., Estall, J. L., Adams, A. C., Antonellis, P. J., Bina, H. A., Flier, J. S., Kharitonov, A., Spiegelman, B. M. & Maratos-Flier, E. 2011. Integrated regulation of hepatic metabolism by fibroblast growth factor 21 (FGF21) in vivo. *Endocrinology*, 152, 2996-3004.
- Fortier, M., Cadoux, M., Boussetta, N., Pham, S., Donné, R., Couty, J. P., Desdouets, C. & Celton-Morizur, S. 2019. Hepatospecific ablation of p38 α MAPK governs liver regeneration through modulation of inflammatory response to CCl₄-induced acute injury. *Scientific Reports*, 9, 1-12.
- Fougere-Deschatrette, C., Imaizumi-Scherrer, T., Strick-Marchand, H., Morosan, S., Charneau, P., Kremsdorf, D., Faust, D. M. & Weiss, M. C. 2006. Plasticity of hepatic cell differentiation: bipotential adult mouse liver clonal cell lines competent to differentiate in vitro and in vivo. *Stem Cells*, 24, 2098-109.

- Francque, S. & Vonghia, L. 2019. Pharmacological Treatment for Non-alcoholic Fatty Liver Disease. *Adv Ther*, 36, 1052-1074.
- Franzen, J., Georgomanolis, T., Selich, A., Kuo, C. C., Stoger, R., Brant, L., Mulabdic, M. S., Fernandez-Rebollo, E., Grezella, C., Ostrowska, A., Begemann, M., Nikolic, M., Rath, B., Ho, A. D., Rothe, M., Schambach, A., Papantonis, A. & Wagner, W. 2021. DNA methylation changes during long-term in vitro cell culture are caused by epigenetic drift. *Commun Biol*, 4, 598.
- Freund, J. B., Goetz, J. G., Hill, K. L. & Vermot, J. 2012. Fluid flows and forces in development: functions, features and biophysical principles. *Development*, 139, 1229-45.
- Gaich, G., Chien, J. Y., Fu, H., Glass, L. C., Deeg, M. A., Holland, W. L., Kharitonov, A., Bumol, T., Schilske, H. K. & Moller, D. E. 2013. The effects of LY2405319, an FGF21 analog, in obese human subjects with type 2 diabetes. *Cell Metab*, 18, 333-40.
- Gallagher, E. P., Kunze, K. L., Stapleton, P. L. & Eaton, D. L. 1996. The kinetics of aflatoxin B1 oxidation by human cDNA-expressed and human liver microsomal cytochromes P450 1A2 and 3A4. *Toxicol Appl Pharmacol*, 141, 595-606.
- Gallego-Escuredo, J. M., Gomez-Ambrosi, J., Catalan, V., Domingo, P., Giral, M., Fruhbeck, G. & Villarroya, F. 2015. Opposite alterations in FGF21 and FGF19 levels and disturbed expression of the receptor machinery for endocrine FGFs in obese patients. *Int J Obes (Lond)*, 39, 121-9.
- Galman, C., Lundasen, T., Kharitonov, A., Bina, H. A., Eriksson, M., Hafstrom, I., Dahlin, M., Amark, P., Angelin, B. & Rudling, M. 2008. The circulating metabolic regulator FGF21 is induced by prolonged fasting and PPARalpha activation in man. *Cell Metab*, 8, 169-74.
- Garcia-Macia, M., Santos-Ledo, A., Leslie, J., Paish, H. L., Collins, A. L., Scott, R. S., Watson, A., Burgoyne, R. A., White, S., French, J., Hammond, J., Borthwick, L. A., Mann, J., Bolanos, J. P., Korolchuk, V. I., Oakley, F. & Mann, D. A. 2021. An mTORC1-Plin3 pathway is essential to activate lipophagy and protects against hepatosteatosis. *Hepatology*.
- Geltinger, F., Schartel, L., Wiederstein, M., Tevini, J., Aigner, E., Felder, T. K. & Rinnerthaler, M. 2020. Friend or Foe: Lipid Droplets as Organelles for Protein and Lipid Storage in Cellular Stress Response, Aging and Disease. *Molecules*, 25.
- Geraghty, R. J., Capes-Davis, A., Davis, J. M., Downward, J., Freshney, R. I., Knezevic, I., Lovell-Badge, R., Masters, J. R., Meredith, J., Stacey, G. N., Thraves, P., Vias, M. & Cancer Research, U. K. 2014. Guidelines for the use of cell lines in biomedical research. *Br J Cancer*, 111, 1021-46.
- Gerhart-Hines, Z., Dominy, J. E., Jr., Blattler, S. M., Jedrychowski, M. P., Banks, A. S., Lim, J. H., Chim, H., Gygi, S. P. & Puigserver, P. 2011. The cAMP/PKA pathway rapidly activates SIRT1 to promote fatty acid oxidation independently of changes in NAD(+). *Mol Cell*, 44, 851-63.
- Gieseck, R. L., 3rd, Hannan, N. R., Bort, R., Hanley, N. A., Drake, R. A., Cameron, G. W., Wynn, T. A. & Vallier, L. 2014. Maturation of induced pluripotent stem cell derived hepatocytes by 3D-culture. *PLoS One*, 9, e86372.
- Godoy, P., Hewitt, N. J., Albrecht, U., Andersen, M. E., Ansari, N., Bhattacharya, S., Bode, J. G., Bolleyn, J., Borner, C., Bottger, J., Braeuning, A., Budinsky, R. A., Burkhardt, B., Cameron, N. R., Camussi, G., Cho, C. S., Choi, Y. J., Craig Rowlands, J., Dahmen, U., Damm, G., Dirsch, O., Donato, M. T., Dong, J., Dooley, S., Drasdo, D., Eakins, R., Ferreira, K. S., Fonsato, V., Fraczek, J., Gebhardt, R., Gibson, A., Glanemann, M., Goldring, C. E., Gomez-Lechon, M. J., Groothuis, G. M., Gustavsson, L., Guyot, C., Hallifax, D., Hammad, S., Hayward, A., Haussinger, D., Hellerbrand, C., Hewitt, P., Hoehme, S., Holzthutter, H. G., Houston, J. B., Hrach, J., Ito, K., Jaeschke, H., Keitel, V., Kelm, J. M., Kevin Park, B.,

- Kordes, C., Kullak-Ublick, G. A., Lecluyse, E. L., Lu, P., Luebke-Wheeler, J., Lutz, A., Maltman, D. J., Matz-Soja, M., McMullen, P., Merfort, I., Messner, S., Meyer, C., Mwinyi, J., Naisbitt, D. J., Nussler, A. K., Olinga, P., Pampaloni, F., Pi, J., Pluta, L., Przyborski, S. A., Ramachandran, A., Rogiers, V., Rowe, C., Schelcher, C., Schmich, K., Schwarz, M., Singh, B., Stelzer, E. H., Stieger, B., Stober, R., Sugiyama, Y., Tetta, C., Thasler, W. E., Vanhaecke, T., Vinken, M., Weiss, T. S., Widera, A., Woods, C. G., Xu, J. J., Yarborough, K. M. & Hengstler, J. G. 2013. Recent advances in 2D and 3D in vitro systems using primary hepatocytes, alternative hepatocyte sources and non-parenchymal liver cells and their use in investigating mechanisms of hepatotoxicity, cell signaling and ADME. *Arch Toxicol*, 87, 1315-530.
- Godoy, P., Widera, A., Schmidt-Heck, W., Campos, G., Meyer, C., Cadenas, C., Reif, R., Stober, R., Hammad, S., Putter, L., Gianmoena, K., Marchan, R., Ghallab, A., Edlund, K., Nussler, A., Thasler, W. E., Damm, G., Seehofer, D., Weiss, T. S., Dirsch, O., Dahmen, U., Gebhardt, R., Chaudhari, U., Meganathan, K., Sachinidis, A., Kelm, J., Hofmann, U., Zahedi, R. P., Guthke, R., Bluthgen, N., Dooley, S. & Hengstler, J. G. 2016. Gene network activity in cultivated primary hepatocytes is highly similar to diseased mammalian liver tissue. *Archives of Toxicology*, 90, 2513-2529.
- Goetz, R. 2013. Metabolism: Adiponectin---a mediator of specific metabolic actions of FGF21. *Nat Rev Endocrinol*, 9, 506-8.
- Gonzalez, A., Hall, M. N., Lin, S. C. & Hardie, D. G. 2020. AMPK and TOR: The Yin and Yang of Cellular Nutrient Sensing and Growth Control. *Cell Metab*, 31, 472-492.
- Gordillo, M., Evans, T. & Gouon-Evans, V. 2015. Orchestrating liver development. *Development*, 142, 2094-108.
- Goto, T., Hirata, M., Aoki, Y., Iwase, M., Takahashi, H., Kim, M., Li, Y., Jheng, H. F., Nomura, W., Takahashi, N., Kim, C. S., Yu, R., Seno, S., Matsuda, H., Aizawa-Abe, M., Ebihara, K., Itoh, N. & Kawada, T. 2017. The hepatokine FGF21 is crucial for peroxisome proliferator-activated receptor- α agonist-induced amelioration of metabolic disorders in obese mice. *J Biol Chem*, 292, 9175-9190.
- Goulart, E., De Caires-Junior, L. C., Telles-Silva, K. A., Araujo, B. H. S., Rocco, S. A., Sforca, M., De Sousa, I. L., Kobayashi, G. S., Musso, C. M., Assoni, A. F., Oliveira, D., Caldini, E., Raia, S., Lelkes, P. I. & Zatz, M. 2019. 3D bioprinting of liver spheroids derived from human induced pluripotent stem cells sustain liver function and viability in vitro. *Biofabrication*, 12, 015010.
- Graffmann, N., Bohndorf, M., Ncube, A., Kawala, M.-A., Wruck, W., Kashofer, K., Zatloukal, K. & Adjaye, J. 2018a. Establishment and characterization of an iPSC line from a 35 years old high grade patient with nonalcoholic fatty liver disease (30–40% steatosis) with homozygous wildtype PNPLA3 genotype. *Stem Cell Research*, 31, 113-116.
- Graffmann, N., Bohndorf, M., Ncube, A., Wruck, W., Kashofer, K., Zatloukal, K. & Adjaye, J. 2018b. Establishment and characterization of an iPSC line from a 58years old high grade patient with nonalcoholic fatty liver disease (70% steatosis) with homozygous wildtype PNPLA3 genotype. *Stem Cell Res*, 31, 131-134.
- Graffmann, N., Ncube, A., Martins, S., Fiszl, A. R., Reuther, P., Bohndorf, M., Wruck, W., Beller, M., Czekelius, C. & Adjaye, J. 2021. A stem cell based in vitro model of NAFLD enables the analysis of patient specific individual metabolic adaptations in response to a high fat diet and AdipoRon interference. *Biol Open*, 10.
- Graffmann, N., Ncube, A., Wruck, W. & Adjaye, J. 2018c. Cell fate decisions of human iPSC-derived bipotential hepatoblasts depend on cell density. *PLoS One*, 13, e0200416.

- Graffmann, N., Ring, S., Kawala, M. A., Wruck, W., Ncube, A., Trompeter, H. I. & Adjaye, J. 2016. Modeling Nonalcoholic Fatty Liver Disease with Human Pluripotent Stem Cell-Derived Immature Hepatocyte-Like Cells Reveals Activation of PLIN2 and Confirms Regulatory Functions of Peroxisome Proliferator-Activated Receptor Alpha. *Stem Cells Dev*, 25, 1119-33.
- Graffmann, N., Scherer, B. & Adjaye, J. 2022. In vitro differentiation of pluripotent stem cells into hepatocyte like cells – Basic principles and current progress. *Stem Cell Research*, 61.
- Gurevich, I., Burton, S. A., Munn, C., Ohshima, M., Goedland, M. E., Czysz, K. & Rajesh, D. 2020. iPSC-derived hepatocytes generated from NASH donors provide a valuable platform for disease modeling and drug discovery. *Biol Open*, 9.
- Hannan, N. R., Fordham, R. P., Syed, Y. A., Moignard, V., Berry, A., Bautista, R., Hanley, N. A., Jensen, K. B. & Vallier, L. 2013a. Generation of multipotent foregut stem cells from human pluripotent stem cells. *Stem Cell Reports*, 1, 293-306.
- Hannan, N. R., Segeritz, C. P., Touboul, T. & Vallier, L. 2013b. Production of hepatocyte-like cells from human pluripotent stem cells. *Nat Protoc*, 8, 430-7.
- Harrison, S. A., Loomba, R., Dubourg, J., Ratziu, V. & Noureddin, M. 2023. Clinical Trial Landscape in NASH. *Clin Gastroenterol Hepatol*.
- Haussinger, D. & Kordes, C. 2019. Space of Disse: a stem cell niche in the liver. *Biol Chem*.
- Huang, Q., Zou, X., Wen, X., Zhou, X. & Ji, L. 2021. NAFLD or MAFLD: Which Has Closer Association With All-Cause and Cause-Specific Mortality?-Results From NHANES III. *Front Med (Lausanne)*, 8, 693507.
- Hussain, S. Z., Sneddon, T., Tan, X., Micsenyi, A., Michalopoulos, G. K. & Monga, S. P. S. 2004. Wnt impacts growth and differentiation in ex vivo liver development. *Experimental Cell Research*, 292, 157-169.
- Inagaki, T., Dutchak, P., Zhao, G., Ding, X., Gautron, L., Parameswara, V., Li, Y., Goetz, R., Mohammadi, M., Esser, V., Elmquist, J. K., Gerard, R. D., Burgess, S. C., Hammer, R. E., Mangelsdorf, D. J. & Kliewer, S. A. 2007. Endocrine regulation of the fasting response by PPARalpha-mediated induction of fibroblast growth factor 21. *Cell Metab*, 5, 415-25.
- Inamura, M., Kawabata, K., Takayama, K., Tashiro, K., Sakurai, F., Katayama, K., Toyoda, M., Akutsu, H., Miyagawa, Y., Okita, H., Kiyokawa, N., Umezawa, A., Hayakawa, T., Furue, M. K. & Mizuguchi, H. 2011. Efficient generation of hepatoblasts from human ES cells and iPS cells by transient overexpression of homeobox gene HEX. *Mol Ther*, 19, 400-7.
- Ingelman-Sundberg, M., Sim, S. C., Gomez, A. & Rodriguez-Antona, C. 2007. Influence of cytochrome P450 polymorphisms on drug therapies: pharmacogenetic, pharmacoepigenetic and clinical aspects. *Pharmacol Ther*, 116, 496-526.
- Jozefczuk, J., Prigione, A., Chavez, L. & Adjaye, J. 2011. Comparative analysis of human embryonic stem cell and induced pluripotent stem cell-derived hepatocyte-like cells reveals current drawbacks and possible strategies for improved differentiation. *Stem Cells Dev*, 20, 1259-75.
- Kadowaki, T. & Yamauchi, T. 2005. Adiponectin and adiponectin receptors. *Endocr Rev*, 26, 439-51.
- Kamiya, A., Kinoshita, T. & Miyajima, A. 2001. Oncostatin M and hepatocyte growth factor induce hepatic maturation via distinct signaling pathways. *FEBS Lett*, 492, 90-4.
- Kanehisa, M., Furumichi, M., Tanabe, M., Sato, Y. & Morishima, K. 2017. KEGG: new perspectives on genomes, pathways, diseases and drugs. *Nucleic Acids Res*, 45, D353-D361.

- Kanninen, L. K., Harjumaki, R., Peltoniemi, P., Bogacheva, M. S., Salmi, T., Porola, P., Niklander, J., Smutny, T., Urtti, A., Yliperttula, M. L. & Lou, Y. R. 2016. Laminin-511 and laminin-521-based matrices for efficient hepatic specification of human pluripotent stem cells. *Biomaterials*, 103, 86-100.
- Kaplowitz, N. 2005. Idiosyncratic drug hepatotoxicity. *Nat Rev Drug Discov*, 4, 489-99.
- Kaushik, S. & Cuervo, A. M. 2015. Degradation of lipid droplet-associated proteins by chaperone-mediated autophagy facilitates lipolysis. *Nat Cell Biol*, 17, 759-70.
- Kaushik, S. & Cuervo, A. M. 2016. AMPK-dependent phosphorylation of lipid droplet protein PLIN2 triggers its degradation by CMA. *Autophagy*, 12, 432-8.
- Kawala, M.-A., Bohndorf, M., Graffmann, N., Wruck, W., Zatloukal, K. & Adjaye, J. 2016a. Characterization of iPSCs derived from dermal fibroblasts from a healthy 19year old female. *Stem Cell Research*, 17, 597-599.
- Kawala, M. A., Bohndorf, M., Graffmann, N., Wruck, W., Zatloukal, K. & Adjaye, J. 2016b. Characterization of dermal fibroblast-derived iPSCs from a patient with high grade steatosis. *Stem Cell Res*, 17, 568-571.
- Kawala, M. A., Bohndorf, M., Graffmann, N., Wruck, W., Zatloukal, K. & Adjaye, J. 2016c. Characterization of dermal fibroblast-derived iPSCs from a patient with low grade steatosis. *Stem Cell Res*, 17, 547-549.
- Kaya, E., Zedginidze, A., Bechmann, L. & Canbay, A. 2022. Metabolic dysfunction-associated fatty liver disease (MAFLD) and non-alcoholic fatty liver disease (NAFLD): distinct fatty liver entities with different clinical outcomes? *Hepatobiliary Surg Nutr*, 11, 299-301.
- Keitel, V. & Haussinger, D. 2013. TGR5 in cholangiocytes. *Curr Opin Gastroenterol*, 29, 299-304.
- Khan, S. A., Sathyanarayan, A., Mashek, M. T., Ong, K. T., Wollaston-Hayden, E. E. & Mashek, D. G. 2015. ATGL-catalyzed lipolysis regulates SIRT1 to control PGC-1alpha/PPAR-alpha signaling. *Diabetes*, 64, 418-26.
- Kliwer, S. A., Umesono, K., Noonan, D. J., Heyman, R. A. & Evans, R. M. 1992. Convergence of 9-cis retinoic acid and peroxisome proliferator signalling pathways through heterodimer formation of their receptors. *Nature*, 358, 771-4.
- Kozlitina, J., Smagris, E., Stender, S., Nordestgaard, B. G., Zhou, H. H., Tybjaerg-Hansen, A., Vogt, T. F., Hobbs, H. H. & Cohen, J. C. 2014. Exome-wide association study identifies a TM6SF2 variant that confers susceptibility to nonalcoholic fatty liver disease. *Nat Genet*, 46, 352-6.
- Krawczyk, M., Rau, M., Schattenberg, J. M., Bantel, H., Pathil, A., Demir, M., Kluwe, J., Boettler, T., Lammert, F., Geier, A. & Group, N. C. S. 2017. Combined effects of the PNPLA3 rs738409, TM6SF2 rs58542926, and MBOAT7 rs641738 variants on NAFLD severity: a multicenter biopsy-based study. *J Lipid Res*, 58, 247-255.
- Lagouge, M., Argmann, C., Gerhart-Hines, Z., Meziane, H., Lerin, C., Daussin, F., Messadeq, N., Milne, J., Lambert, P., Elliott, P., Geny, B., Laakso, M., Puigserver, P. & Auwerx, J. 2006. Resveratrol improves mitochondrial function and protects against metabolic disease by activating SIRT1 and PGC-1alpha. *Cell*, 127, 1109-22.
- Lancaster, M. A. & Huch, M. 2019. Disease modelling in human organoids. *Disease Models & Mechanisms*, 12.
- Lass, A., Zimmermann, R., Haemmerle, G., Riederer, M., Schoiswohl, G., Schweiger, M., Kienesberger, P., Strauss, J. G., Gorkiewicz, G. & Zechner, R. 2006. Adipose triglyceride lipase-mediated lipolysis of cellular fat stores is activated by CGI-58 and defective in Chanarin-Dorfman Syndrome. *Cell Metab*, 3, 309-19.

- Levy, G., Bomze, D., Heinz, S., Ramachandran, S. D., Noerenberg, A., Cohen, M., Shibolet, O., Sklan, E., Braspenning, J. & Nahmias, Y. 2015. Long-term culture and expansion of primary human hepatocytes. *Nat Biotechnol*, 33, 1264-1271.
- Li, L. H., Krantz, I. D., Deng, Y., Genin, A., Banta, A. B., Collins, C. C., Qi, M., Trask, B. J., Kuo, W. L., Cochran, J., Costa, T., Pierpont, M. E. M., Rand, E. B., Piccoli, D. A., Hood, L. & Spinner, N. B. 1997. Alagille syndrome is caused by mutations in human Jagged1, which encodes a ligand for Notch1. *Nature Genetics*, 16, 243-251.
- Lichtmanegger, J., Leitzinger, C., Wimmer, R., Schmitt, S., Schulz, S., Kabiri, Y., Eberhagen, C., Rieder, T., Janik, D., Neff, F., Straub, B. K., Schirmacher, P., Dispirito, A. A., Bandow, N., Baral, B. S., Flatley, A., Kremmer, E., Denk, G., Reiter, F. P., Hohenester, S., Eckardt-Schupp, F., Dencher, N. A., Adamski, J., Sauer, V., Niemietz, C., Schmidt, H. H., Merle, U., Gotthardt, D. N., Kroemer, G., Weiss, K. H. & Zischka, H. 2016. Methanobactin reverses acute liver failure in a rat model of Wilson disease. *J Clin Invest*, 126, 2721-35.
- Listenberger, L. L., Ostermeyer-Fay, A. G., Goldberg, E. B., Brown, W. J. & Brown, D. A. 2007. Adipocyte differentiation-related protein reduces the lipid droplet association of adipose triglyceride lipase and slows triacylglycerol turnover. *J Lipid Res*, 48, 2751-61.
- Liu, C. H., Ampuero, J., Gil-Gomez, A., Montero-Vallejo, R., Rojas, A., Munoz-Hernandez, R., Gallego-Duran, R. & Romero-Gomez, M. 2018. miRNAs in patients with non-alcoholic fatty liver disease: A systematic review and meta-analysis. *J Hepatol*, 69, 1335-1348.
- Liu, Q., Yuan, B., Lo, K. A., Patterson, H. C., Sun, Y. & Lodish, H. F. 2012. Adiponectin regulates expression of hepatic genes critical for glucose and lipid metabolism. *Proc Natl Acad Sci U S A*, 109, 14568-73.
- Loewa, A., Feng, J. J. & Hedtrich, S. 2023. Human disease models in drug development. *Nature Reviews Bioengineering*.
- Loosen, S. H., Roderburg, C., Demir, M., Qvartskhava, N., Keitel, V., Kostev, K. & Luedde, T. 2022. Non-alcoholic fatty liver disease (NAFLD) is associated with an increased incidence of osteoporosis and bone fractures. *Z Gastroenterol*, 60, 1221-1227.
- Lopez-Pastor, A. R., Infante-Menendez, J., Escribano, O. & Gomez-Hernandez, A. 2020. miRNA Dysregulation in the Development of Non-Alcoholic Fatty Liver Disease and the Related Disorders Type 2 Diabetes Mellitus and Cardiovascular Disease. *Front Med (Lausanne)*, 7, 527059.
- Lucendo-Villarin, B., Meseguer-Ripolles, J., Drew, J., Fischer, L., Ma, W. S. E., Flint, O., Simpson, K., Machesky, L., Mountford, J. & Hay, D. 2020. Development of a cost effective automated platform to produce human liver spheroids for basic and applied research. *Biofabrication*.
- Lyall, M. J., Cartier, J., Thomson, J. P., Cameron, K., Meseguer-Ripolles, J., O'duibhir, E., Szkolnicka, D., Villarin, B. L., Wang, Y., Blanco, G. R., Dunn, W. B., Meehan, R. R., Hay, D. C. & Drake, A. J. 2018. Modelling non-alcoholic fatty liver disease in human hepatocyte-like cells. *Philos Trans R Soc Lond B Biol Sci*, 373.
- Ma, H., De Zwaan, E., Guo, Y. E., Cejas, P., Thiru, P., Van De Bunt, M., Jeppesen, J. F., Syamala, S., Dall'agnese, A., Abraham, B. J., Fu, D., Garrett-Engele, C., Lee, T. I., Long, H. W., Griffith, L. G., Young, R. A. & Jaenisch, R. 2022. The nuclear receptor THRβ facilitates differentiation of human PSCs into more mature hepatocytes. *Cell Stem Cell*, 29, 795-809.e11.
- Ma, X., Qu, X., Zhu, W., Li, Y. S., Yuan, S., Zhang, H., Liu, J., Wang, P., Lai, C. S., Zanella, F., Feng, G. S., Sheikh, F., Chien, S. & Chen, S. 2016. Deterministically patterned biomimetic human iPSC-derived hepatic model via rapid 3D bioprinting. *Proc Natl Acad Sci U S A*.

- Magne, J., Aminoff, A., Perman Sundelin, J., Mannila, M. N., Gustafsson, P., Hultenby, K., Wernerson, A., Bauer, G., Listenberger, L., Neville, M. J., Karpe, F., Boren, J. & Ehrenborg, E. 2013. The minor allele of the missense polymorphism Ser251Pro in perilipin 2 (PLIN2) disrupts an alpha-helix, affects lipolysis, and is associated with reduced plasma triglyceride concentration in humans. *FASEB J*, 27, 3090-9.
- Mantovani, A., Byrne, C. D., Benfari, G., Bonapace, S., Simon, T. G. & Targher, G. 2022. Risk of Heart Failure in Patients With Nonalcoholic Fatty Liver Disease: JACC Review Topic of the Week. *J Am Coll Cardiol*, 79, 180-191.
- Matz, P., Wruck, W., Fauler, B., Herebian, D., Mielke, T. & Adjaye, J. 2017. Footprint-free human fetal foreskin derived iPSCs: A tool for modeling hepatogenesis associated gene regulatory networks. *Sci Rep*, 7, 6294.
- Mcdaniell, R., Warthen, D. M., Sanchez-Lara, P. A., Pai, A., Krantz, I. D., Piccoli, D. A. & Spinner, N. B. 2006. NOTCH2 mutations cause Alagille syndrome, a heterogeneous disorder of the notch signaling pathway. *Am J Hum Genet*, 79, 169-73.
- Mcmanaman, J. L., Bales, E. S., Orlicky, D. J., Jackman, M., Maclean, P. S., Cain, S., Crunk, A. E., Mansur, A., Graham, C. E., Bowman, T. A. & Greenberg, A. S. 2013. Perilipin-2-null mice are protected against diet-induced obesity, adipose inflammation, and fatty liver disease. *J Lipid Res*, 54, 1346-59.
- Mendez-Sanchez, N., Diaz-Orozco, L. & Cordova-Gallardo, J. 2021. Redefinition of fatty liver disease from NAFLD to MAFLD raised disease awareness: Mexican experience. *J Hepatol*.
- Meseguer-Ripolles, J., Kasarinaite, A., Lucendo-Villarin, B. & Hay, D. C. 2021. Protocol for automated production of human stem cell derived liver spheres. *STAR Protocols*, 2.
- Miyajima, A., Tanaka, M. & Itoh, T. 2014. Stem/progenitor cells in liver development, homeostasis, regeneration, and reprogramming. *Cell Stem Cell*, 14, 561-74.
- Moreno, M., Lombardi, A., Silvestri, E., Senese, R., Cioffi, F., Goglia, F., Lanni, A. & De Lange, P. 2010. PPARs: Nuclear Receptors Controlled by, and Controlling, Nutrient Handling through Nuclear and Cytosolic Signaling. *PPAR Res*, 2010.
- Murphy, S. K., Yang, H., Moylan, C. A., Pang, H., Dellinger, A., Abdelmalek, M. F., Garrett, M. E., Ashley-Koch, A., Suzuki, A., Tillmann, H. L., Hauser, M. A. & Diehl, A. M. 2013. Relationship between methylome and transcriptome in patients with nonalcoholic fatty liver disease. *Gastroenterology*, 145, 1076-87.
- Nagamoto, Y., Takayama, K., Ohashi, K., Okamoto, R., Sakurai, F., Tachibana, M., Kawabata, K. & Mizuguchi, H. 2016. Transplantation of a human iPSC-derived hepatocyte sheet increases survival in mice with acute liver failure. *J Hepatol*, 64, 1068-1075.
- Ncube, A., Graffmann, N., Greulich, J., Scherer, B., Wruck, W. & Adjaye, J. 2021. Investigation of Thyroid Hormone Associated Gene-Regulatory Networks during Hepatogenesis using an Induced Pluripotent Stem Cell based Model.
- Negoita, F., Blomdahl, J., Wasserstrom, S., Winberg, M. E., Osmark, P., Larsson, S., Stenkula, K. G., Ekstedt, M., Kechagias, S., Holm, C. & Jones, H. A. 2019. PNPLA3 variant M148 causes resistance to starvation-mediated lipid droplet autophagy in human hepatocytes. *J Cell Biochem*, 120, 343-356.
- Nell, P., Kattler, K., Feuerborn, D., Hellwig, B., Rieck, A., Salhab, A., Lepikhov, K., Gasparoni, G., Thomitzek, A., Belgasmi, K., Bluthgen, N., Morkel, M., Kuppers-Munther, B., Godoy, P., Hay, D. C., Cadenas, C., Marchan, R., Vartak, N., Edlund, K., Rahnenfuhrer, J., Walter, J. & Hengstler, J. G. 2022. Identification of an FXR-modulated liver-intestine hybrid state in iPSC-derived hepatocyte-like cells. *J Hepatol*.

- Ng, S., Schwartz, R. E., March, S., Galstian, A., Gural, N., Shan, J., Prabhu, M., Mota, M. M. & Bhatia, S. N. 2015. Human iPSC-derived hepatocyte-like cells support Plasmodium liver-stage infection in vitro. *Stem Cell Reports*, 4, 348-59.
- Niemietz, C., Fleischhauer, L., Sandfort, V., Guttmann, S., Zibert, A. & Schmidt, H. H. 2018. Hepatocyte-like cells reveal novel role of SERPINA1 in transthyretin amyloidosis. *J Cell Sci*, 131.
- Oda, T., Elkahloun, A. G., Pike, B. L., Okajima, K., Krantz, I. D., Genin, A., Piccoli, D. A., Meltzer, P. S., Spinner, N. B., Collins, F. S. & Chandrasekharappa, S. C. 1997. Mutations in the human Jagged1 gene are responsible for Alagille syndrome. *Nat Genet*, 16, 235-42.
- Okada-Iwabuchi, M., Yamauchi, T., Iwabuchi, M., Honma, T., Hamagami, K., Matsuda, K., Yamaguchi, M., Tanabe, H., Kimura-Someya, T., Shirouzu, M., Ogata, H., Tokuyama, K., Ueki, K., Nagano, T., Tanaka, A., Yokoyama, S. & Kadowaki, T. 2013. A small-molecule AdipoR agonist for type 2 diabetes and short life in obesity. *Nature*, 503, 493-9.
- Omenetti, A. & Diehl, A. M. 2011. Hedgehog signaling in cholangiocytes. *Curr Opin Gastroenterol*, 27, 268-75.
- Ong, J., Serra, M. P., Segal, J., Cujba, A. M., Ng, S. S., Butler, R., Millar, V., Hatch, S., Zimri, S., Koike, H., Chan, K., Bonham, A., Walk, M., Voss, T., Heaton, N., Mitry, R., Dhawan, A., Ebner, D., Danovi, D., Nakauchi, H. & Rashid, S. T. 2018. Imaging-Based Screen Identifies Laminin 411 as a Physiologically Relevant Niche Factor with Importance for i-Hep Applications. *Stem Cell Reports*, 10, 693-702.
- Ouchi, R., Togo, S., Kimura, M., Shinozawa, T., Koido, M., Koike, H., Thompson, W., Karns, R. A., Mayhew, C. N., Mcgrath, P. S., Mccauley, H. A., Zhang, R. R., Lewis, K., Hakozaki, S., Ferguson, A., Saiki, N., Yoneyama, Y., Takeuchi, I., Mabuchi, Y., Akazawa, C., Yoshikawa, H. Y., Wells, J. M. & Takebe, T. 2019. Modeling Steatohepatitis in Humans with Pluripotent Stem Cell-Derived Organoids. *Cell Metab*, 30, 374-384 e6.
- Pastore, N., Attanasio, S., Granese, B., Castello, R., Teckman, J., Wilson, A. A., Ballabio, A. & Brunetti-Pierri, N. 2017. Activation of the c-Jun N-terminal kinase pathway aggravates proteotoxicity of hepatic mutant Z alpha1-antitrypsin. *Hepatology*, 65, 1865-1874.
- Pawella, L. M., Hashani, M., Eiteneuer, E., Renner, M., Bartenschlager, R., Schirmacher, P. & Straub, B. K. 2014. Perilipin discerns chronic from acute hepatocellular steatosis. *J Hepatol*, 60, 633-42.
- Pettinelli, P. & Videla, L. A. 2011. Up-regulation of PPAR-gamma mRNA expression in the liver of obese patients: an additional reinforcing lipogenic mechanism to SREBP-1c induction. *J Clin Endocrinol Metab*, 96, 1424-30.
- Pirola, C. J., Fernandez Gianotti, T., Castano, G. O., Mallardi, P., San Martino, J., Mora Gonzalez Lopez Ledesma, M., Flichman, D., Mirshahi, F., Sanyal, A. J. & Sookoian, S. 2014. Circulating microRNA signature in non-alcoholic fatty liver disease: from serum non-coding RNAs to liver histology and disease pathogenesis. *Gut*.
- Ramli, M. N. B., Lim, Y. S., Koe, C. T., Demircioglu, D., Tng, W., Gonzales, K. a. U., Tan, C. P., Szczerbinska, I., Liang, H., Soe, E. L., Lu, Z., Ariyachet, C., Yu, K. M., Koh, S. H., Yaw, L. P., Jumat, N. H. B., Lim, J. S. Y., Wright, G., Shabbir, A., Dan, Y. Y., Ng, H. H. & Chan, Y. S. 2020. Human Pluripotent Stem Cell-Derived Organoids as Models of Liver Disease. *Gastroenterology*, 159, 1471-1486 e12.
- Rashid, S. T., Corbineau, S., Hannan, N., Marciniak, S. J., Miranda, E., Alexander, G., Huang-Doran, I., Griffin, J., Ahrlund-Richter, L., Skepper, J., Semple, R., Weber, A., Lomas, D. A. & Vallier, L. 2010. Modeling inherited metabolic disorders of the liver using human induced pluripotent stem cells. *J Clin Invest*, 120, 3127-36.

- Rashidi, H., Alhaque, S., Szkolnicka, D., Flint, O. & Hay, D. C. 2016. Fluid shear stress modulation of hepatocyte-like cell function. *Arch Toxicol*, 90, 1757-61.
- Rashidi, H., Luu, N. T., Alwahsh, S. M., Ginai, M., Alhaque, S., Dong, H., Tomaz, R. A., Vernay, B., Vigneswara, V., Hallett, J. M., Chandrashekran, A., Dhawan, A., Vallier, L., Bradley, M., Callanan, A., Forbes, S. J., Newsome, P. N. & Hay, D. C. 2018. 3D human liver tissue from pluripotent stem cells displays stable phenotype in vitro and supports compromised liver function in vivo. *Arch Toxicol*, 92, 3117-3129.
- Ray, A., Joshi, J. M., Sundaravadivelu, P. K., Raina, K., Lenka, N., Kaveeshwar, V. & Thummer, R. P. 2021. An Overview on Promising Somatic Cell Sources Utilized for the Efficient Generation of Induced Pluripotent Stem Cells. *Stem Cell Rev Rep*, 17, 1954-1974.
- Raynaud, P., Carpentier, R., Antoniou, A. & Lemaigre, F. P. 2011. Biliary differentiation and bile duct morphogenesis in development and disease. *Int J Biochem Cell Biol*, 43, 245-56.
- Rinella, M. E., Lazarus, J. V., Ratziu, V., Francque, S. M., Sanyal, A. J., Kanwal, F., Romero, D., Abdelmalek, M. F., Anstee, Q. M., Arab, J. P., Arrese, M., Bataller, R., Beuers, U., Boursier, J., Bugianesi, E., Byrne, C., Castro Narro, G. E., Chowdhury, A., Cortez-Pinto, H., Cryer, D., Cusi, K., El-Kassas, M., Klein, S., Eskridge, W., Fan, J., Gawrieh, S., Guy, C. D., Harrison, S. A., Kim, S. U., Koot, B., Korenjak, M., Kowdley, K., Lacaille, F., Loomba, R., Mitchell-Thain, R., Morgan, T. R., Powell, E., Roden, M., Romero-Gómez, M., Silva, M., Singh, S. P., Sookoian, S. C., Spearman, C. W., Tiniakos, D., Valenti, L., Vos, M. B., Wai-Sun Wong, V., Xanthakos, S., Yilmaz, Y., Younossi, Z., Hobbs, A., Villota-Rivas, M., Newsome, P. N., Ajmeral, V., Alazawi, W., Alkhatry, M., Alkhoury, N., Allen, A., Allison, M., Alswat, K., Alvares-Da-Silva, M. R., Alves-Bezerra, M., Armstrong, M. J., Arufe, D., Aschner, P., Baffy, G., Bansal, M., Bedossa, P., Belfort, R., Berg, T., Berzigotti, A., Betel, M., Bianco, C., Brass, C., Brosgart, C. L., Brunt, E. M., Buti, M., Caldwell, S., Carr, R., Casanovas, T., Castera, L., Caussy, C., Cerda, E., Chalasani, N., Chan, W. K., Charatchoenwittaya, P., Charlton, M., Cheung, A., Chiodi, D., Chung, R., Cohen, D., Corey, K., Cotrim, H. P., Crespo, J., Dassanayake, A., Davidson, N., De Knegt, R., De Ledinghen, V., Demir, M., Diaz, S., et al. 2023. A multi-society Delphi consensus statement on new fatty liver disease nomenclature. *Journal of Hepatology*.
- Robinson, J. F., Hamilton, E. G., Lam, J., Chen, H. & Woodruff, T. J. 2020. Differences in cytochrome p450 enzyme expression and activity in fetal and adult tissues. *Placenta*, 100, 35-44.
- Roderburg, C., Kostev, K., Mertens, A., Luedde, T. & Loosen, S. H. 2022a. Non-alcoholic fatty liver disease (NAFLD) is associated with an increased incidence of extrahepatic cancer. *Gut*.
- Roderburg, C., Loosen, S., Kostev, K., Demir, M., Joerdens, M. S. & Luedde, T. 2022b. Nonalcoholic fatty liver disease is associated with a higher incidence of coeliac disease. *Eur J Gastroenterol Hepatol*, 34, 328-331.
- Romeo, S., Kozlitina, J., Xing, C., Pertsemlidis, A., Cox, D., Pennacchio, L. A., Boerwinkle, E., Cohen, J. C. & Hobbs, H. H. 2008. Genetic variation in PNPLA3 confers susceptibility to nonalcoholic fatty liver disease. *Nat Genet*, 40, 1461-5.
- Rouillard, A. D., Gundersen, G. W., Fernandez, N. F., Wang, Z., Monteiro, C. D., Mcdermott, M. G. & Ma'ayan, A. 2016. The harmonizome: a collection of processed datasets gathered to serve and mine knowledge about genes and proteins. *Database (Oxford)*, 2016.
- Saglam-Metiner, P., Devamoglu, U., Filiz, Y., Akbari, S., Beceren, G., Goker, B., Yaldiz, B., Yanasik, S., Biray Avci, C., Erdal, E. & Yesil-Celiktas, O. 2023. Spatio-temporal dynamics enhance cellular diversity, neuronal function and further maturation of human cerebral organoids. *Commun Biol*, 6, 173.

- Sathyanarayan, A., Mashek, M. T. & Mashek, D. G. 2017. ATGL Promotes Autophagy/Lipophagy via SIRT1 to Control Hepatic Lipid Droplet Catabolism. *Cell Rep*, 19, 1-9.
- Schott, M. B., Weller, S. G., Schulze, R. J., Krueger, E. W., Drizyte-Miller, K., Casey, C. A. & Mcniven, M. A. 2019. Lipid droplet size directs lipolysis and lipophagy catabolism in hepatocytes. *J Cell Biol*, 218, 3320-3335.
- Schulze, R. J., Schott, M. B., Casey, C. A., Tuma, P. L. & Mcniven, M. A. 2019. The cell biology of the hepatocyte: A membrane trafficking machine. *J Cell Biol*, 218, 2096-2112.
- Schwartz, R. E., Trehan, K., Andrus, L., Sheahan, T. P., Ploss, A., Duncan, S. A., Rice, C. M. & Bhatia, S. N. 2012. Modeling hepatitis C virus infection using human induced pluripotent stem cells. *Proc Natl Acad Sci U S A*, 109, 2544-8.
- Sentinelli, F., Capoccia, D., Incani, M., Bertocchini, L., Severino, A., Pani, M. G., Manconi, E., Cossu, E., Leonetti, F. & Baroni, M. G. 2016. The perilipin 2 (PLIN2) gene Ser251Pro missense mutation is associated with reduced insulin secretion and increased insulin sensitivity in Italian obese subjects. *Diabetes Metab Res Rev*, 32, 550-6.
- Sgodda, M., Dai, Z., Zweigerdt, R., Sharma, A. D., Ott, M. & Cantz, T. 2017. A Scalable Approach for the Generation of Human Pluripotent Stem Cell-Derived Hepatic Organoids with Sensitive Hepatotoxicity Features. *Stem Cells Dev*, 26, 1490-1504.
- Shan, J., Schwartz, R. E., Ross, N. T., Logan, D. J., Thomas, D., Duncan, S. A., North, T. E., Goessling, W., Carpenter, A. E. & Bhatia, S. N. 2013. Identification of small molecules for human hepatocyte expansion and iPS differentiation. *Nat Chem Biol*, 9, 514-20.
- Si-Tayeb, K., Lemaigre, F. P. & Duncan, S. A. 2010. Organogenesis and development of the liver. *Dev Cell*, 18, 175-89.
- Singh, R. & Cuervo, A. M. 2011. Autophagy in the cellular energetic balance. *Cell Metab*, 13, 495-504.
- Singh, R., Kaushik, S., Wang, Y., Xiang, Y., Novak, I., Komatsu, M., Tanaka, K., Cuervo, A. M. & Czaja, M. J. 2009. Autophagy regulates lipid metabolism. *Nature*, 458, 1131-5.
- Sinton, M. C., Meseguer-Ripolles, J., Lucendo-Villarin, B., Wernig-Zorc, S., Thomson, J. P., Carter, R. N., Lyall, M. J., Walker, P. D., Thakker, A., Meehan, R. R., Lavery, G. G., Morton, N. M., Ludwig, C., Tennant, D. A., Hay, D. C. & Drake, A. J. 2021. A human pluripotent stem cell model for the analysis of metabolic dysfunction in hepatic steatosis. *iScience*, 24, 101931.
- Smirnova, E., Goldberg, E. B., Makarova, K. S., Lin, L., Brown, W. J. & Jackson, C. L. 2006. ATGL has a key role in lipid droplet/adiposome degradation in mammalian cells. *EMBO reports*, 7, 106-113.
- Stefan, N. & Cusi, K. 2022. A global view of the interplay between non-alcoholic fatty liver disease and diabetes. *The Lancet Diabetes & Endocrinology*, 10, 284-296.
- Sumida, Y., Okanoue, T., Nakajima, A. & Japan Study Group Of, N. 2019. Phase 3 drug pipelines in the treatment of non-alcoholic steatohepatitis. *Hepatol Res*, 49, 1256-1262.
- Sun, D., Gao, W., Hu, H. & Zhou, S. 2022. Why 90% of clinical drug development fails and how to improve it? *Acta Pharm Sin B*, 12, 3049-3062.
- Tacke, F., Canbay, A., Bantel, H., Bojunga, J., De Laffolie, J., Demir, M., Denzer, U. W., Geier, A., Hofmann, W. P., Hudert, C., Karlas, T., Krawczyk, M., Longerich, T., Luedde, T., Roden, M., Schattenberg, J., Stefan, N., Sterneck, M., Tannapfel, A., Lorenz, P., Roeb, E. & Collaborators 2022. Updated S2k Clinical Practice Guideline on Non-alcoholic Fatty Liver Disease (NAFLD) issued by the German Society of Gastroenterology, Digestive and Metabolic Diseases (DGVS) - April 2022 - AWMF Registration No.: 021-025. *Z Gastroenterol*. 2022/09/14 ed.

- Tajima, H., Ohta, T., Shoji, Y., Watanabe, T., Makino, I., Hayashi, H., Nakagawara, H., Onishi, I., Takamura, H., Ninomiya, I., Kitagawa, H., Fushida, S., Tani, T., Fujimura, T., Kayahara, M., Arai, K., Yamashita, T., Kaneko, S. & Zen, Y. O. H. 2010. Expression of epithelial-mesenchymal transition markers in locally recurrent hepatocellular carcinoma after radiofrequency ablation. *Experimental and Therapeutic Medicine*, 1, 347-350.
- Takahashi, K., Tanabe, K., Ohnuki, M., Narita, M., Ichisaka, T., Tomoda, K. & Yamanaka, S. 2007. Induction of pluripotent stem cells from adult human fibroblasts by defined factors. *Cell*, 131, 861-72.
- Takahashi, K. & Yamanaka, S. 2006. Induction of pluripotent stem cells from mouse embryonic and adult fibroblast cultures by defined factors. *Cell*, 126, 663-76.
- Takahashi, Y., Sekine, K., Kin, T., Takebe, T. & Taniguchi, H. 2018. Self-Condensation Culture Enables Vascularization of Tissue Fragments for Efficient Therapeutic Transplantation. *Cell Rep*, 23, 1620-1629.
- Takayama, K., Inamura, M., Kawabata, K., Katayama, K., Higuchi, M., Tashiro, K., Nonaka, A., Sakurai, F., Hayakawa, T., Furue, M. K. & Mizuguchi, H. 2012a. Efficient generation of functional hepatocytes from human embryonic stem cells and induced pluripotent stem cells by HNF4alpha transduction. *Mol Ther*, 20, 127-37.
- Takayama, K., Inamura, M., Kawabata, K., Sugawara, M., Kikuchi, K., Higuchi, M., Nagamoto, Y., Watanabe, H., Tashiro, K., Sakurai, F., Hayakawa, T., Furue, M. K. & Mizuguchi, H. 2012b. Generation of metabolically functioning hepatocytes from human pluripotent stem cells by FOXA2 and HNF1alpha transduction. *J Hepatol*, 57, 628-36.
- Takayama, K., Kawabata, K., Nagamoto, Y., Kishimoto, K., Tashiro, K., Sakurai, F., Tachibana, M., Kanda, K., Hayakawa, T., Furue, M. K. & Mizuguchi, H. 2013a. 3D spheroid culture of hESC/hiPSC-derived hepatocyte-like cells for drug toxicity testing. *Biomaterials*, 34, 1781-9.
- Takayama, K., Morisaki, Y., Kuno, S., Nagamoto, Y., Harada, K., Furukawa, N., Ohtaka, M., Nishimura, K., Imagawa, K., Sakurai, F., Tachibana, M., Sumazaki, R., Noguchi, E., Nakanishi, M., Hirata, K., Kawabata, K. & Mizuguchi, H. 2014. Prediction of interindividual differences in hepatic functions and drug sensitivity by using human iPSC-derived hepatocytes. *Proc Natl Acad Sci U S A*, 111, 16772-7.
- Takayama, K., Nagamoto, Y., Mimura, N., Tashiro, K., Sakurai, F., Tachibana, M., Hayakawa, T., Kawabata, K. & Mizuguchi, H. 2013b. Long-term self-renewal of human ES/iPSC-derived hepatoblast-like cells on human laminin 111-coated dishes. *Stem Cell Reports*, 1, 322-35.
- Takebe, T., Sekine, K., Enomura, M., Koike, H., Kimura, M., Ogaeri, T., Zhang, R. R., Ueno, Y., Zheng, Y. W., Koike, N., Aoyama, S., Adachi, Y. & Taniguchi, H. 2013. Vascularized and functional human liver from an iPSC-derived organ bud transplant. *Nature*, 499, 481-4.
- Takebe, T., Sekine, K., Kimura, M., Yoshizawa, E., Ayano, S., Koido, M., Funayama, S., Nakanishi, N., Hisai, T., Kobayashi, T., Kasai, T., Kitada, R., Mori, A., Ayabe, H., Ejiri, Y., Amimoto, N., Yamazaki, Y., Ogawa, S., Ishikawa, M., Kiyota, Y., Sato, Y., Nozawa, K., Okamoto, S., Ueno, Y. & Taniguchi, H. 2017. Massive and Reproducible Production of Liver Buds Entirely from Human Pluripotent Stem Cells. *Cell Rep*, 21, 2661-2670.
- Takebe, T., Zhang, R. R., Koike, H., Kimura, M., Yoshizawa, E., Enomura, M., Koike, N., Sekine, K. & Taniguchi, H. 2014. Generation of a vascularized and functional human liver from an iPSC-derived organ bud transplant. *Nat Protoc*, 9, 396-409.

- Tan, E. H., Ma, F. J., Gopinadhan, S., Sakban, R. B. & Wang, N. D. 2007. C/EBP alpha knock-in hepatocytes exhibit increased albumin secretion and urea production. *Cell Tissue Res*, 330, 427-35.
- Tan, W., Li, Y., Lim, S. G. & Tan, T. M. 2014. miR-106b-25/miR-17-92 clusters: polycistrons with oncogenic roles in hepatocellular carcinoma. *World J Gastroenterol*, 20, 5962-72.
- Tanaka, N., Aoyama, T., Kimura, S. & Gonzalez, F. J. 2017. Targeting nuclear receptors for the treatment of fatty liver disease. *Pharmacol Ther*, 179, 142-157.
- Tanimizu, N. & Miyajima, A. 2004. Notch signaling controls hepatoblast differentiation by altering the expression of liver-enriched transcription factors. *J Cell Sci*, 117, 3165-74.
- Thomou, T., Mori, M. A., Dreyfuss, J. M., Konishi, M., Sakaguchi, M., Wolfrum, C., Rao, T. N., Winnay, J. N., Garcia-Martin, R., Grinspoon, S. K., Gorden, P. & Kahn, C. R. 2017. Adipose-derived circulating miRNAs regulate gene expression in other tissues. *Nature*, 542, 450-455.
- Tigges, J., Bielec, K., Brockerhoff, G., Hildebrandt, B., Hubenthal, U., Kapr, J., Koch, K., Teichweyde, N., Wiczorek, D., Rossi, A. & Fritsche, E. 2021. Academic application of Good Cell Culture Practice for induced pluripotent stem cells. *ALTEX*.
- Tilg, H., Moschen, A. R. & Roden, M. 2017. NAFLD and diabetes mellitus. *Nat Rev Gastroenterol Hepatol*, 14, 32-42.
- Tormos, A. M., Rius-Pérez, S., Jorques, M., Rada, P., Ramirez, L., Valverde, Á. M., Nebreda, Á. R., Sastre, J. & Taléns-Visconti, R. 2017. P38 α regulates actin cytoskeleton and cytokinesis in hepatocytes during development and aging. *PLoS ONE*, 12, 1-22.
- Tsai, T. H., Chen, E., Li, L., Saha, P., Lee, H. J., Huang, L. S., Shelness, G. S., Chan, L. & Chang, B. H. 2017. The constitutive lipid droplet protein PLIN2 regulates autophagy in liver. *Autophagy*, 13, 1130-1144.
- Tsai, W. C., Hsu, S. D., Hsu, C. S., Lai, T. C., Chen, S. J., Shen, R., Huang, Y., Chen, H. C., Lee, C. H., Tsai, T. F., Hsu, M. T., Wu, J. C., Huang, H. D., Shiao, M. S., Hsiao, M. & Tsou, A. P. 2012. MicroRNA-122 plays a critical role in liver homeostasis and hepatocarcinogenesis. *J Clin Invest*, 122, 2884-97.
- Vega, R. B., Huss, J. M. & Kelly, D. P. 2000. The coactivator PGC-1 cooperates with peroxisome proliferator-activated receptor alpha in transcriptional control of nuclear genes encoding mitochondrial fatty acid oxidation enzymes. *Mol Cell Biol*, 20, 1868-76.
- Volpato, V. & Webber, C. 2020. Addressing variability in iPSC-derived models of human disease: guidelines to promote reproducibility. *Dis Model Mech*, 13.
- Vuppalanchi, R., Marri, S., Kolwankar, D., Considine, R. V. & Chalasani, N. 2005. Is adiponectin involved in the pathogenesis of nonalcoholic steatohepatitis? A preliminary human study. *Journal of Clinical Gastroenterology*, 39, 237-242.
- Wang, Y. & Adjaye, J. 2011. A cyclic AMP analog, 8-Br-cAMP, enhances the induction of pluripotency in human fibroblast cells. *Stem Cell Rev*, 7, 331-41.
- Wang, Y., Kory, N., Basuray, S., Cohen, J. C. & Hobbs, H. H. 2019. PNPLA3, CGI-58, and Inhibition of Hepatic Triglyceride Hydrolysis in Mice. *Hepatology*.
- Warren, L., Flaks, J. G. & Buchanan, J. M. 1957. Biosynthesis of the Purines. *Journal of Biological Chemistry*, 229, 627-640.
- Wätjen, W. & Fritsche, E. 2010. Rolle des Fremdstoffmetabolismus in Pharmakologie und Toxikologie- Teil 2- Phase-II-Reaktionen. *PHARMAZEUTISCHE WISSENSCHAFT*.
- Werder, R. B., Kaserman, J. E., Packer, M. S., Lindstrom-Vautrin, J., Villacorta-Martin, C., Young, L. E., Aratyn-Schaus, Y., Gregoire, F. & Wilson, A. A. 2021. Adenine Base Editing Reduces Misfolded Protein Accumulation and Toxicity in Alpha-1 Antitrypsin Deficient Patient iPSC-Hepatocytes. *Mol Ther*.

- Wilson, A. A., Ying, L., Liesa, M., Segeritz, C. P., Mills, J. A., Shen, S. S., Jean, J., Lonza, G. C., Liberti, D. C., Lang, A. H., Nazaire, J., Gower, A. C., Mueller, F. J., Mehta, P., Ordonez, A., Lomas, D. A., Vallier, L., Murphy, G. J., Mostoslavsky, G., Spira, A., Shirihai, O. S., Ramirez, M. I., Gadue, P. & Kotton, D. N. 2015. Emergence of a stage-dependent human liver disease signature with directed differentiation of alpha-1 antitrypsin-deficient iPS cells. *Stem Cell Reports*, 4, 873-85.
- Withey, S., Gerrard, D., Leeson, H., Atkinson-Dell, R., Harrison, S., Baxter, M., Wolvetang, E. & Hanley, N. 2022. Thyroid hormone and ALK5 inhibitor improve maturation of human pluripotent stem cell derived hepatocytes.
- Wong, R. J., Aguilar, M., Cheung, R., Perumpail, R. B., Harrison, S. A., Younossi, Z. M. & Ahmed, A. 2015. Nonalcoholic steatohepatitis is the second leading etiology of liver disease among adults awaiting liver transplantation in the United States. *Gastroenterology*, 148, 547-55.
- Wruck, W., Kashofer, K., Rehman, S., Daskalaki, A., Berg, D., Gralka, E., Jozefczuk, J., Drews, K., Pandey, V., Regenbrecht, C., Wierling, C., Turano, P., Korf, U., Zatloukal, K., Lehrach, H., Westerhoff, H. V. & Adjaye, J. 2015. Multi-omic profiles of human non-alcoholic fatty liver disease tissue highlight heterogenic phenotypes. *Scientific Data*, 2, 150068.
- Wu, H., Uchimura, K., Donnelly, E. L., Kirita, Y., Morris, S. A. & Humphreys, B. D. 2018. Comparative Analysis and Refinement of Human PSC-Derived Kidney Organoid Differentiation with Single-Cell Transcriptomics. *Cell Stem Cell*, 23, 869-881 e8.
- Wu, X., Robotham, J. M., Lee, E., Dalton, S., Kneteman, N. M., Gilbert, D. M. & Tang, H. 2012. Productive hepatitis C virus infection of stem cell-derived hepatocytes reveals a critical transition to viral permissiveness during differentiation. *PLoS Pathog*, 8, e1002617.
- Yamasaki, H., Sada, A., Iwata, T., Niwa, T., Tomizawa, M., Xanthopoulos, K. G., Koike, T. & Shiojiri, N. 2006. Suppression of C/EBPalpha expression in periportal hepatoblasts may stimulate biliary cell differentiation through increased Hnf6 and Hnf1b expression. *Development*, 133, 4233-43.
- Yamashita, N., Tokunaga, E., Imori, M., Inoue, Y., Tanaka, K., Kitao, H., Saeki, H., Oki, E. & Maehara, Y. 2018. Epithelial Paradox: Clinical Significance of Coexpression of E-cadherin and Vimentin With Regard to Invasion and Metastasis of Breast Cancer. *Clin Breast Cancer*, 18, e1003-e1009.
- Yamauchi, T., Nio, Y., Maki, T., Kobayashi, M., Takazawa, T., Iwabu, M., Okada-Iwabu, M., Kawamoto, S., Kubota, N., Kubota, T., Ito, Y., Kamon, J., Tsuchida, A., Kumagai, K., Kozono, H., Hada, Y., Ogata, H., Tokuyama, K., Tsunoda, M., Ide, T., Murakami, K., Awazawa, M., Takamoto, I., Froguel, P., Hara, K., Tobe, K., Nagai, R., Ueki, K. & Kadowaki, T. 2007. Targeted disruption of AdipoR1 and AdipoR2 causes abrogation of adiponectin binding and metabolic actions. *Nat Med*, 13, 332-9.
- Younossi, Z. M., Blissett, D., Blissett, R., Henry, L., Stepanova, M., Younossi, Y., Racila, A., Hunt, S. & Beckerman, R. 2016a. The economic and clinical burden of nonalcoholic fatty liver disease in the United States and Europe. *Hepatology*, 64, 1577-1586.
- Younossi, Z. M., Koenig, A. B., Abdelatif, D., Fazel, Y., Henry, L. & Wymer, M. 2016b. Global epidemiology of nonalcoholic fatty liver disease-Meta-analytic assessment of prevalence, incidence, and outcomes. *Hepatology*, 64, 73-84.
- Yu, J., Vodyanik, M. A., Smuga-Otto, K., Antosiewicz-Bourget, J., Frane, J. L., Tian, S., Nie, J., Jonsdottir, G. A., Ruotti, V., Stewart, R., Slukvin, I. & Thomson, J. A. 2007. Induced pluripotent stem cell lines derived from human somatic cells. *Science*, 318, 1917-20.
- Yuan, Z., Zhang, X., Sengupta, N., Lane, W. S. & Seto, E. 2007. SIRT1 regulates the function of the Nijmegen breakage syndrome protein. *Mol Cell*, 27, 149-62.

- Zhang, X., Yeung, D. C., Karpisek, M., Stejskal, D., Zhou, Z. G., Liu, F., Wong, R. L., Chow, W. S., Tso, A. W., Lam, K. S. & Xu, A. 2008. Serum FGF21 levels are increased in obesity and are independently associated with the metabolic syndrome in humans. *Diabetes*, 57, 1246-53.
- Zong, Y., Panikkar, A., Xu, J., Antoniou, A., Raynaud, P., Lemaigre, F. & Stanger, B. Z. 2009. Notch signaling controls liver development by regulating biliary differentiation. *Development*, 136, 1727-39.
- Zong, Y. & Stanger, B. Z. 2011. Molecular mechanisms of bile duct development. *Int J Biochem Cell Biol*, 43, 257-64.

10 Acknowledgements:

First and foremost I would like to thank Professor Adjaye for his support of my scientific work and for his encouragement to pursue an academic career. It is a pleasure working at ISRM and exploring different fields of stem cell biology during the years.

I am very happy that Dr. Claus Kordes joined our institute during the end of my habilitation. Thank you for your advice, for giving me new insights into many aspects of physiology and disease patterns, for always thinking big and for constructively planning ahead.

Thank you Prof. Gesine Kögler for helping me to improve this work and for teaching me some strategic thinking.

Thank you Simeon for always having an open ear for all problems and for always showing a big picture. Thank you Ingo for your support in all S1 questions and beyond.

I thank all current and former members of ISRM, especially for their support and for making the institute a place where I enjoy working and look continuously forward to starting new projects. I am especially thankful that I could co-supervise so many young and eager scientists, teach them all lab techniques and always learn new things in return.

I also thank my mentors Prof. Julia Bandow, Prof. Kathrin Marcus and Prof. Sina Bartfeld who supported me throughout the years, who always had an open ear for my problems and who gave me important guidance and support in the academic world. I would also like Ekaterina Masetkina as well as the GSCN mentoring team for organizing these wonderful programs which are invaluable for career development and for finding your own way in the academic jungle. I also thank my peers from both programs, for cheering me up during times of struggle and for your encouragement.

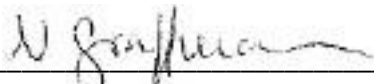
I would like to thank my friends for always being there for me and supporting my ambitions.

Finally, I would like to thank my mother Regina Riedewald-Graffmann for her tireless support during all the years. Without you always believing in me, I would not have been able to follow this path.

11 Erklärungen und eidesstattliche Versicherung

1. Hiermit erkläre ich, dass ich bei den wissenschaftlichen Arbeiten, die Gegenstand meiner Habilitationsleistung sind, ethische Grundsätze und die jeweils gültigen Empfehlungen zur Sicherung guter wissenschaftlicher Praxis durch mich beachtet wurden.

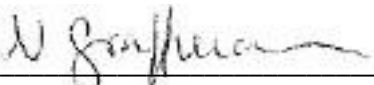
Düsseldorf, 09.10.2023



Dr. rer. nat. Nina Graffmann

2. Hiermit erkläre ich, dass keine weiteren Habilitationsverfahren eingeleitet oder erfolglos abgeschlossen worden sind.

Düsseldorf, 09.10.2023



Dr. rer. nat. Nina Graffmann

3. Hiermit versichere ich an Eides statt, dass ich die unten genannten Beiträge zu den Publikationen, die meiner Habilitationsschrift zugrunde liegen, eigenständig geleistet habe:

Establishment and characterization of an iPSC line from a 35 years old high grade patient with nonalcoholic fatty liver disease (30 – 40 % steatosis) with homozygous wildtype PNPLA3 genotype

Graffmann, N., Bohndorf, M., Ncube, A., Kawala, M.-A., Wruck, W., Kashofer, K., Zatloukal, K., and Adjaye, J.

Stem cell research (2018) 31, 113-116

and

Establishment and characterization of an iPSC line from a 58years old high grade patient with nonalcoholic fatty liver disease (70 % steatosis) with homozygous wildtype PNPLA3 genotype.

Graffmann, N., Bohndorf, M., Ncube, A., Wruck, W., Kashofer, K., Zatloukal, K., and Adjaye, J.

Stem cell research (2018) 31, 131-134.

- Performance and analysis of flow cytometry together with MB
- Editing of immunocytochemistry pictures
- Performance and interpretation of PNPLA3 Genotyping
- Preparation of the graphic
- Writing of the manuscript together with JA
- Modification of the manuscript during the review process together with JA
- Correspondence with the scientific journal together with JA
- Response to the Reviewers together with JA

Cell fate decisions of human iPSC-derived bipotential hepatoblasts depend on cell density.

Graffmann, N., Ncube, A., Wruck, W., and Adjaye, J.

PloS one (2018). 13, e0200416

- Conception of the study together with JA
- Cell culture work, molecular biological and biochemical analyses together with AN
- Data analysis together with AN and WW
- Data analysis and interpretation
- Preparation of graphics together with WW
- Writing of the manuscript together with JA

- Modification of the manuscript during the review process together with JA
- Correspondence with the scientific journal together with JA
- Response to the Reviewers together with JA

-

The published and herein discussed data are part of the Master Thesis of Audrey Ncube

Modeling Nonalcoholic Fatty Liver Disease with Human Pluripotent Stem Cell-Derived Immature Hepatocyte-Like Cells Reveals Activation of PLIN2 and Confirms Regulatory Functions of Peroxisome Proliferator-Activated Receptor Alpha.

Graffmann, N., Ring, S., Kawala, M.A., Wruck, W., Ncube, A., Trompeter, H.I., and Adjaye, J.

Stem cells and development (2016), 25, 1119-1133.

- Conception of the study together with JA
- Cell culture work, molecular biological and biochemical analyses together with SR, MAK, and AN
- Data analysis together with SR, HIT and WW
- Data interpretation together with SR, HIT, and JA
- Preparation of graphics together with SR and WW
- Writing of the manuscript together with SR, HIT and JA
- Modification of the manuscript during the review process together with SR, HIT and JA
- Correspondence with the scientific journal together with JA
- Response to the Reviewers together with JA

The published and herein discussed data are part of the Master Thesis of Sarah Ring and Marie-Ann Kawala, and the PhD thesis of Dr. Wasco Wruck

A stem cell based in vitro model of NAFLD enables the analysis of patient specific individual metabolic adaptations in response to a high fat diet and AdipoRon interference.

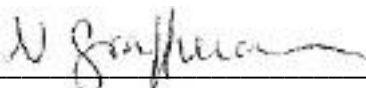
Graffmann, N., Ncube, A., Martins, S., Fizl, A. R., Reuther, P., Bohndorf, M., Wruck, W., Beller, M., Czekelius, C., and Adjaye, J.

Biol Open. (2021).

- Conception of the study together with JA
- Cell culture work, molecular biological and biochemical analyses together with AN, MB, SM, ARF

- Quantification and analysis of lipid droplets together with MB
- Data analysis together with WW
- Data interpretation together with MB, JA, and SM
- Preparation of graphics together with WW
- Writing of the manuscript together with JA
- Modification of the manuscript during the review process together with JA
- Correspondence with the scientific journal together with JA
- Response to the Reviewers together with JA

Düsseldorf, 09.10.2023

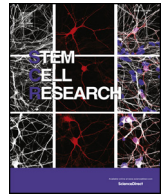


Dr. rer. nat. Nina Graffmann

12 Addendum

Selected Research Articles summarized in chapter 5.

All published under creative common licences and inserted here with friendly permission of the respective journals.



Lab resource: Stem Cell Line

Establishment and characterization of an iPSC line from a 35 years old high grade patient with nonalcoholic fatty liver disease (30–40% steatosis) with homozygous wildtype PNPLA3 genotype

Nina Graffmann^a, Martina Bohndorf^a, Audrey Ncube^a, Marie-Ann Kawala^a, Wasco Wruck^a, Karl Kashofer^b, Kurt Zatloukal^b, James Adjaye^{a,*}

^a Institute for Stem Cell Research and Regenerative Medicine, Heinrich Heine University, 40225 Düsseldorf, Germany

^b Institute of Pathology, Medical University of Graz, 8036 Graz, Austria

ABSTRACT

Nonalcoholic fatty liver disease (NAFLD) is the hepatic manifestation of the metabolic syndrome and its prevalence increases continuously. Here, we reprogrammed fibroblasts of a high grade NAFLD patient with homozygous wildtype PNPLA3 genotype. The induced pluripotent stem cells (iPSCs) were characterized by immunocytochemistry, flow cytometry, embryoid body formation, pluritest, DNA-fingerprinting and karyotype analysis.

Resource table.		Name of transgene or resistance	N/A
Unique stem cell line identifier	HHUUKDi008-A	Inducible/constitutive system	N/A
Alternative name(s) of stem cell line	S18	Date archived/stock date	N/A
Institution	Institute for Stem Cell Research and Regenerative Medicine	Cell line repository/bank	N/A
Contact information of distributor	James Adjaye, James.Adjaye@med.uni-duesseldorf.de	Ethical approval	Ethical committee University of Graz under license 20–143 ex 08/09
Type of cell line	iPSC	Resource utility	
Origin	Human	NAFLD, an increasing health and economic burden in the western world, can be modelled in vitro by using hepatocyte like cells derived from iPSCs. Being a multifactorial disease, cells from donors of different genetic backgrounds are needed to get an idea of disease progression as well as of treatment opportunities.	
Additional origin info	Age: 35 Sex: female Ethnicity: unknown	Resource details	
Cell Source	Fibroblasts	The I148M (rs738409 C > G) polymorphism in patatin-like phospholipase-3 (PNPLA3) is one of the very few SNPs that have been directly linked to nonalcoholic fatty liver disease (NAFLD) (Romeo et al., 2008). However, the mutant allele does not necessarily promote the disease phenotype and the wildtype allele is not protective against it.	
Clonality	Clonal	Here, we reprogrammed fibroblasts from a 35 year old female high	
Method of reprogramming	Episomal-based plasmid expressing OCT4, SOX2, NANOG, KLF4, c-MYC and LIN28		
Genetic Modification	No		
Type of Modification	N/A		
Associated disease	Nonalcoholic fatty liver disease (NAFLD), high grade steatosis		
Gene/locus	PNPLA3		
Method of modification	N/A		

* Corresponding author.

E-mail address: james.adjaye@med.uni-duesseldorf.de (J. Adjaye).

<https://doi.org/10.1016/j.scr.2018.07.015>

Received 6 June 2018; Accepted 13 July 2018

Available online 25 July 2018

1873-5061/ © 2018 Published by Elsevier B.V. This is an open access article under the CC BY-NC-ND license (<http://creativecommons.org/licenses/by-nc-nd/4.0/>).

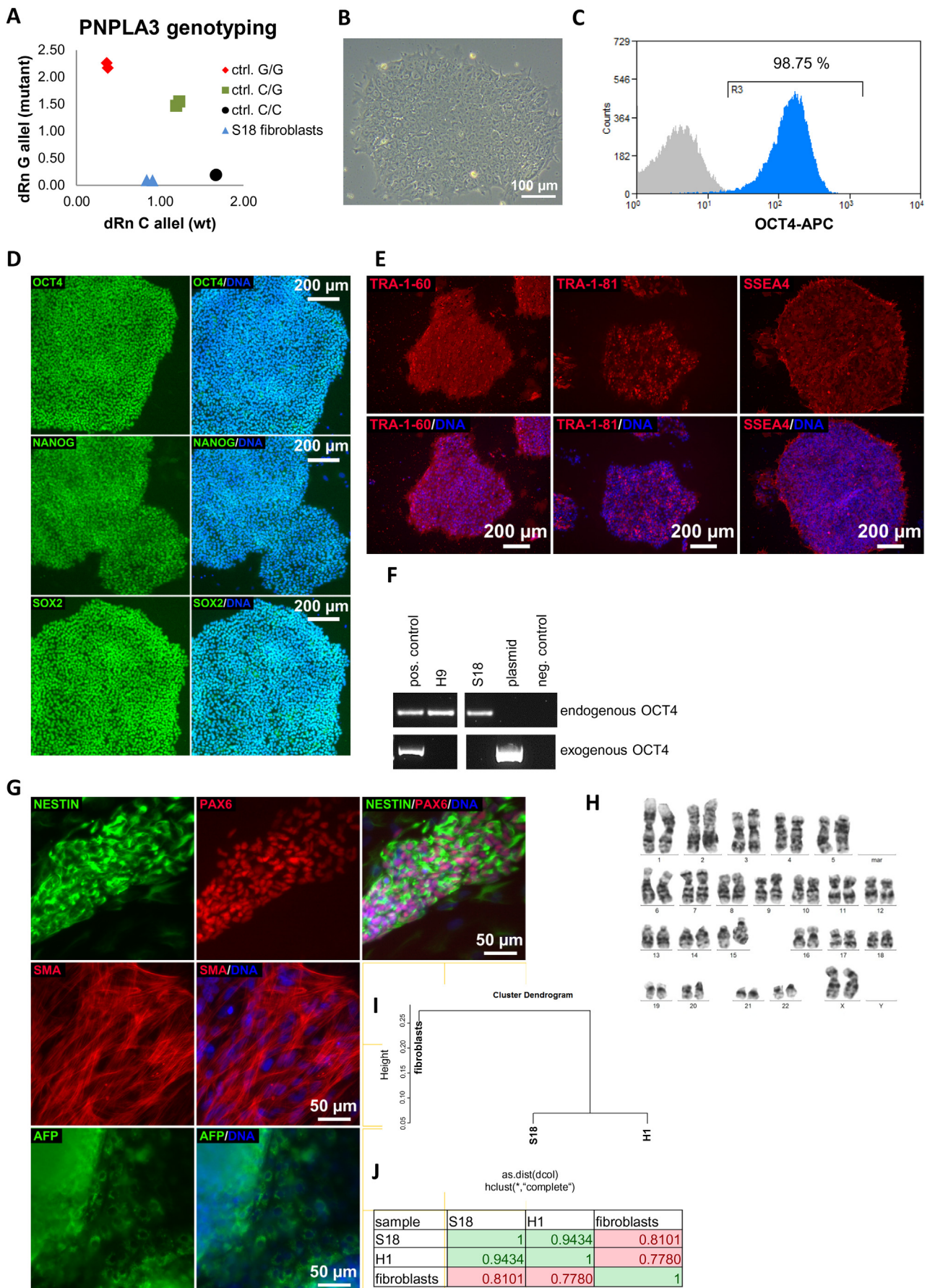


Fig. 1. Characterization of the iPSC line S18.

Table 1
Characterization and validation.

Classification	Test	Result	Data
Morphology	Photography	Normal	Fig. 1 panel B
Phenotype	Quantitative analysis: Flow cytometry	OCT 4: 98.75% positive	Fig. 1 panel C
	Qualitative analysis, immunocytochemistry	Expression of pluripotency-associated markers: OCT4, NANOG, SOX2, TRA-1-60, TRA-1-81 and SSEA4	Fig. 1 panel D and E
Genotype Identity	Karyotype (G-banding) and resolution	46 XX 150-300 Bd	Fig. 1 panel H
	Microsatellite PCR (mPCR) OR	Not tested	N/A
	STR analysis	PCR, three sites tested, matched	submitted in archive with journal
Mutation analysis (IF APPLICABLE)	TaqMan Assay	PNPLA3 I148M: homozygous wildtype	Fig. 1 panel A
	Southern Blot OR WGS	Not tested	N/A
Microbiology and virology	Mycoplasma	Mycoplasma testing by PCR	Supplementary Fig. 1
		Negative	
Differentiation potential	Embryoid body	Expression of proteins related to all 3 germ layers was assessed by immunocytochemistry:	Fig. 1 G
		Endoderm: AFP	
		Ectoderm: Nestin	
		Mesoderm: α -smoothmuscle actin	
Donor screening (OPTIONAL)	HIV 1 + 2 Hepatitis B, Hepatitis C	N/A	N/A
Genotype additional info (OPTIONAL)	Blood group genotyping	N/A	N/A
	HLA tissue typing	N/A	N/A

grade (30–40%) steatosis patient with homozygous wildtype PNPLA3 genotype (Fig. 1A) by nucleofecting two episomal-based plasmids (7F1) coding for *OCT4*, *SOX2*, *NANOG*, *LIN28*, *c-MYC* and *KLF-4*. S18 cells have the typical iPSC morphology (Fig. 1B) and express the pluripotency associated transcription factors OCT4, NANOG, SOX2 (Fig. 1C,D) as well as the characteristic surface markers SSEA-4, TRA-1-60 and TRA-1-81 (Fig. 1E). At this stage, the cells had lost the reprogramming plasmids, which was confirmed by RT-PCR with primers specific for exogenous and endogenous OCT4 (Fig. 1F). After formation of embryoid bodies (EBs), the cells differentiated spontaneously into all three germ layers and expressed AFP (endoderm), NESTIN (ectoderm), and α -smoothmuscle actin (SMA, mesoderm; Fig. 1G). They have a normal 46, XX karyotype (Fig. 1H).

Pluritest analysis revealed a high similarity to the human embryonic stem cell line H1 with a Pearson's correlation of 0.9434 (Fig. 1I,J). DNA fingerprinting was performed with the primers D7S796, D17S1290 and D21S2055 and clearly confirmed that the cells were originating from the parental fibroblast line (STR Analysis).

A PCR-based Mycoplasma contamination test was negative (Supplementary Fig. 1).

Materials and methods

Cell culture

Fibroblasts were cultured in DMEM high glucose (Gibco), supplemented with 1% Penicillin-Streptomycin (P/S, Gibco), 1% Glutamax (Gibco), and 10% fetal calf serum (Gibco) at 37 °C, 5% CO₂ and 5% O₂. iPSCs were cultured on matrigel (Corning) coated dishes in StemMACS iPS-Brew XF Medium (Miltenyi) with 1% P/S at 37 °C, 5% CO₂ and 5% O₂.

Derivation of iPSCs

Fibroblasts in the logarithmic growth phase were reprogrammed by using a combination of the two episomal based plasmids pEP4EO2SCK2MEN2L and pEP4EO2SET2K (7F1) (Yu et al., 2011) coding for *OCT4*, *SOX2*, *NANOG*, *LIN28*, *c-MYC* and *KLF-4*. 600,000 fibroblasts were resuspended in 100 μ l nucleofection solution VP1–1005 (Lonza) containing 3 μ g of each plasmid. Cells were nucleofected using the Nucleofector II (Lonza), program U-023. Afterwards, cells were plated onto one well of a matrigel coated 6 well plate in N2B27medium.

Reprogramming efficiency was enhanced by inhibiting TGF β -signaling with 0.5 μ M A-83-01, MEK-signaling with 0.5 μ M PD0325901, ROCK-signaling with 10 μ M Y-27632 and activating WNT-signaling with 3 μ M CHIR99021.

DNA fingerprinting analysis

The STR analysis was performed by PCR using primers D7S796, D10S1214, and D21S2055 (STR Analysis). For primer sequences refer to Table 2.

PNPLA3 genotyping

For PNPLA3 genotyping, genomic DNA was isolated and analyzed with the TaqMan Assay ID C-7241_10 (Applied Biosystems).

Embryoid body (EB) formation

Cells were cultured as embryoid bodies (EBs) to confirm their three-lineage differentiation potential. Sub-confluent iPSCs were transferred into a T25 flask and cultured for one week in an upright position in DMEM high glucose, containing 10% FCS, 1% P/S and 1% NEAA (Gibco). Afterwards, EBs were plated onto a gelatin coated 12-well plate and cultured for another 3–4 days.

Immunofluorescence stainings

Cells were fixed with 4% paraformaldehyde (PFA) (Polysciences). Unspecific binding sites were blocked by incubating for 2 h at room temperature (RT) in blocking buffer, consisting of 10% normal goat or donkey serum, 1% BSA, 0.5% Triton, and 0.05% Tween. Primary antibodies were diluted according to Table 2 in staining buffer (blocking buffer diluted 1:2 with PBS) and incubated overnight at 4 °C. Cells were washed 3 times with PBS/0.05% Tween. Afterwards they were incubated for 2 h at RT with secondary antibodies, diluted 1:500 in staining buffer. Nuclei were stained with Hoechst (Thermo Fisher Scientific). Cells were washed again 3 times with PBS/0.05% Tween. Images were captured using a fluorescence microscope (LSM700; Zeiss) with Zenblue software (Zeiss). Individual channel images were processed and merged with Fiji.

Table 2
Reagents details.

Antibodies used for immunocytochemistry/flow-citometry			
	Antibody	Dilution	Company Cat # and RRID
Pluripotency Markers	Rabbit anti-OCT4	1:400	Cell Signaling Technology Cat# 2840S, RRID:AB_2167691
Pluripotency Markers	Rabbit anti-SOX2	1:400	Cell Signaling Technology Cat# 3579S, RRID:AB_2195767
Pluripotency Markers	Rabbit anti-NANOG	1:800	Cell Signaling Technology Cat# 4903S, RRID:AB_10559205
Pluripotency Markers	Mouse anti-Tra-1-60	1:1000	Cell Signaling Technology Cat# 4746S, RRID:AB_2119059
Pluripotency Markers	Mouse anti-Tra-1-81	1:1000	Cell Signaling Technology Cat# 4745S, RRID:AB_2119060
Pluripotency Markers	Mouse anti-SSEA4	1:1000	Cell Signaling Technology Cat# 4755S, RRID:AB_1264259
Differentiation Markers	Goat anti-Sox17	1:50	R and D Systems Cat# AF1924, RRID:AB_355060
Differentiation Markers	Rabbit anti-AFP	1:200	Cell Signaling Technology Cat# 2137S, RRID:AB_2209744
Differentiation Markers	anti-Nestin	1:250	Sigma-Aldrich Cat# N5413, RRID:AB_1841032
Differentiation Markers	anti-aSMA	1:1000	Dako Cat# M0851, RRID:AB_2223500
Secondary antibodies	anti-mouse-Cy3	1:2000	Thermo Fisher Scientific Cat# A10521, RRID:AB_2534030
Secondary antibodies	anti-rabbit-Alexa488	1:2000	Thermo Fisher Scientific Cat# A27034, RRID:AB_2536097
Nuclear Co-Staining	Hoechst 33,258	1:5000	Thermo Fisher Scientific Cat# H3569, RRID:AB_2651133

Primers		
	Target	Forward/Reverse primer (5'-3')
Episomal plasmids	OCT4 Plasmid	OCT4ex-F 5'-AGTGAGAGGCAACCTGGAGA-3' OCT4ex- R 5'-AGGAACTGCTTCCTTCACGA-3'
Endogenous OCT4	OCT4 endogenous	OCT4end-F 5'-AGTTTGTGCCAGGGTTTTTG-3' OCT4end-R 5'-ACTTTCACCTTCCCTCCAACC-3'
e.g. House-Keeping Genes (qPCR)	NA	NA
e.g. Genotyping	PNPLA3	TaqMan SNP Genotyping Assay, Cat# 4351379, Assay ID C-7241_10
e.g. Targeted mutation analysis/sequencing	NA	NA
Fingerprinting	D7S796	TTTTGGTATTGGCCATCCTA/GAAAGGAACAGAGACAGGG
Fingerprinting	D21S2055	AACAGAACCAATAGGCTATCTATC/TACAGTAAATCACTTGGTAGGAGA
Fingerprinting	D10S1214	ATTGCCCAAACCTTTTTTG/TGAAGACCAGTCTGGGAAG
Mycoplasma	16 S rRNA gene	GGGAGCAAACAGGATTAGATACCCT/TGCACCATCTGTCACTCTGTAACTC

Flow cytometry

Cells were harvested and stained with an APC coupled OCT4 antibody (Miltenyi) for 10 min at 4 °C. Afterwards, they were washed with PBS and fixed with PFA. Analysis was performed on a CyAn ADP with Summit4.3 software (Beckman Coulter).

Karyotype analysis

Karyotype analysis was performed at the Institute of Human Genetics and Anthropology, Heinrich-Heine-University, Düsseldorf (Table 1).

Microarray-based transcriptome analysis

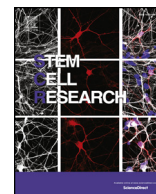
PrimeView Affymetrix microarrays were used to determine global gene expression. 1 µg of total RNA was used and all preparations were

performed by the Biologisch-medizinisches Forschungszentrum (BMFZ), Heinrich-Heine University, Düsseldorf. The dendrogram was generated using the package affy of the R/Bioconductor software (Gentleman et al., 2004).

Supplementary data to this article can be found online at <https://doi.org/10.1016/j.scr.2018.07.015>.

References

- Gentleman, R.C., Carey, V.J., Bates, D.M., Bolstad, B., Dettling, M., Dudoit, S., Ellis, B., Gautier, L., Ge, Y., Gentry, J., et al., 2004. Bioconductor: open software development for computational biology and bioinformatics. *Genome Biol.* 5, R80.
- Romeo, S., Kozlitina, J., Xing, C., Pertsemlidis, A., Cox, D., Pennacchio, L.A., Boerwinkle, E., Cohen, J.C., Hobbs, H.H., 2008. Genetic variation in PNPLA3 confers susceptibility to nonalcoholic fatty liver disease. *Nat. Genet.* 40, 1461–1465.
- Yu, J., Chau, K.F., Vodyanik, M.A., Jiang, J., Jiang, Y., 2011. Efficient feeder-free episomal reprogramming with small molecules. *PLoS One* 6, e17557.



Lab resource: Stem Cell Line

Establishment and characterization of an iPSC line from a 58 years old high grade patient with nonalcoholic fatty liver disease (70% steatosis) with homozygous wildtype PNPLA3 genotype



Nina Graffmann^a, Martina Bohndorf^a, Audrey Ncube^a, Wasco Wruck^a, Karl Kashofer^b, Kurt Zatloukal^b, James Adjaye^{a,*}

^a Institute for Stem Cell Research and Regenerative Medicine, Medical Faculty, Heinrich Heine University, 40225 Düsseldorf, Germany

^b Institute of Pathology, Medical University of Graz, 8036 Graz, Austria

ABSTRACT

Nonalcoholic fatty liver disease (NAFLD) is the hepatic manifestation of the metabolic syndrome and its prevalence increases continuously. Here, we reprogrammed fibroblasts of a high grade NAFLD patient with homozygous wildtype PNPLA3 genotype. We characterized the induced pluripotent stem cells (iPSCs) by immunocytochemistry, flow cytometry, embryoid body formation, pluritest DNA-fingerprinting, and karyotype analysis.

Resource table.

Unique stem cell line identifier	HHUUKDi007-A
Alternative name(s) of stem cell line	S11
Institution	Institute for Stem Cell Research and Regenerative Medicine
Contact information of distributor	James Adjaye, James.Adjaye@med.uni-duesseldorf.de
Type of cell line	iPSC
Origin	Human
Additional origin info	Age: 58 Sex: female Ethnicity: unknown
Cell Source	Fibroblasts
Clonality	Clonal
Method of reprogramming	Episomal-based plasmid expressing OCT4, SOX2, NANOG, KLF4, c-MYC and LIN28
Genetic Modification	No
Type of Modification	N/A
Associated disease	Nonalcoholic fatty liver disease (NAFLD), high grade steatosis
Gene/locus	PNPLA3
Method of modification	N/A
Name of transgene or resistance	N/A
Inducible/constitutive system	N/A
Date archived/stock date	N/A
Cell line repository/bank	N/A
Ethical approval	Ethical committee University of Graz under license 20–143 ex 08/09

* Corresponding author.

E-mail address: james.adjaye@med.uni-duesseldorf.de (J. Adjaye).

<https://doi.org/10.1016/j.scr.2018.07.011>

Received 4 June 2018; Accepted 13 July 2018

Available online 27 July 2018

1873-5061/ © 2018 The Authors. Published by Elsevier B.V. This is an open access article under the CC BY-NC-ND license

(<http://creativecommons.org/licenses/by-nc-nd/4.0/>).

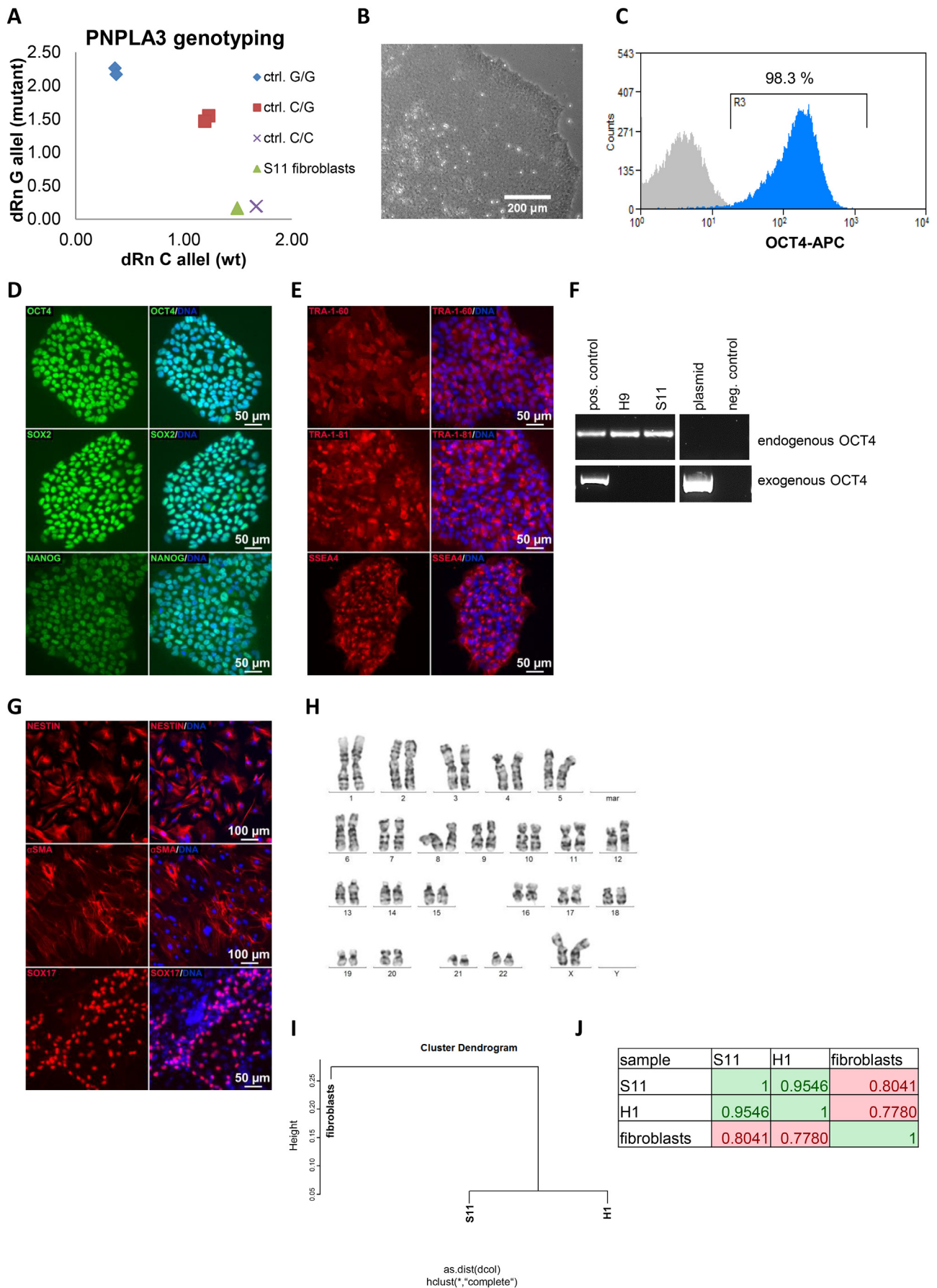


Fig. 1. Characterization of the iPSC line S11

Table 1
Characterization and validation.

Classification	Test	Result	Data
Morphology	Photography	normal	Fig. 1 B
Phenotype	Flow cytometry Immunocytochemistry	OCT 4: 98.3% positive Expression of pluripotency- associated markers: OCT4, NANOG, SOX2, TRA-1-60, TRA-1-81 and SSEA4	Fig. 1 panel C Fig. 1 panel D and E
Genotype	Karyotype (G-banding) and resolution	46 XX 150-300 Bd	Fig. 1 panel H
Identity	Microsatellite PCR (mPCR) OR STR analysis	Not tested PCR, two sites tested, matched	N/A submitted in archive with journal
Mutation analysis (IF APPLICABLE)	TaqMan Assay Southern Blot OR WGS	PNPLA3 I148M: homozygous wildtype Not tested	Fig. 1 panel A
Microbiology and virology	Mycoplasma	Mycoplasma testing by PCR Negative	Supplementary file 1
Differentiation potential	Embryoid body	Expression of proteins related to all 3 germ layers was assessed by immunocytochemistry: Endoderm: AFP Ectoderm: Nestin Mesoderm: α -smoothmuscle actin	Fig. 1 G
Donor screening (OPTIONAL)	HIV 1 + 2 Hepatitis B, Hepatitis C	N/A	N/A
Genotype additional info (OPTIONAL)	Blood group genotyping HLA tissue typing	N/A N/A	N/A N/A

Resource utility

Hepatocyte like cells derived from iPSCs serve as a valuable model for studying NAFLD, an increasing health and economic burden in the western world. Cells from donors of distinct genetic backgrounds are needed for disease modelling in order to gain insights into its etiology.

Resource details

A polymorphism in patatin-like phospholipase-3 (PNPLA3) has been associated with an increased risk in developing nonalcoholic fatty liver disease (NAFLD) (Romeo et al., 2008). The mutant I148M (rs738409 C > G) allele increases the risk of developing NAFLD in the presence of other risk factors such as an imbalance between calorie intake and expenditure. However, the wildtype allele is not protective against it and the same risk factors can promote the development of NAFLD in patients with homozygous wildtype PNPLA3 genotype.

Here, fibroblasts from a 58 year old female high grade (70%) steatosis patient with homozygous wildtype PNPLA3 genotype (Fig. 1A) were reprogrammed by nucleofecting two episomal-based plasmids (7F1) coding for *OCT4*, *SOX2*, *NANOG*, *LIN28*, *c-MYC* and *KLF-4*. S11 cells have the typical iPSC morphology (Fig. 1B). Flow cytometry and immunocytochemistry confirmed that they express the pluripotency associated transcription factors OCT4, NANOG, SOX2 (Fig. 1C,D) as well as the characteristic surface markers SSEA-4, TRA-1-60 and TRA-1-81 (Fig. 1E). These analyses were performed after RT-PCR with primers specific for exogenous and endogenous OCT4 proofed that the cells had lost the reprogramming plasmids (Fig. 1F). The cells were able to form embryoid bodies (EBs), which differentiated spontaneously into all three germ layers and expressed AFP (endoderm), NESTIN (ectoderm), and α -smoothmuscle actin (SMA, mesoderm; Fig. 1G). They have a normal 46, XX karyotype (Fig. 1H).

Global gene expression analysis was performed to determine the stem cell characteristics of the cells. This revealed a high similarity to the human embryonic stem cell line H1 with a Pearson's correlation of 0.9546 (Fig. 1I,J). DNA fingerprinting with the primers D7S796 and D21S2055 clearly confirmed that the cells originated from the parental fibroblast line (STR Analysis).

A PCR-based Mycoplasma contamination test was negative (Supplementary file 1).

Materials and methods

Cell culture

Fibroblasts were cultured in DMEM high glucose (Gibco), supplemented with 1% Penicillin-Streptomycin (P/S, Gibco), 1% Glutamax (Gibco), and 10% fetal calf serum (Gibco) at 37 °C, 5% CO₂ and 5% O₂. iPSCs were cultured on matrigel (Corning) coated dishes in StemMACS iPS-Brew XF Medium (Miltenyi) with 1% P/S at 37 °C, 5% CO₂ and 5% O₂.

Derivation of iPSCs

Fibroblasts in the logarithmic growth phase were reprogrammed by using a combination of the two episomal based plasmids pEP4EO2SCK2MEN2L and pEP4EO2SET2K (7F1) (Yu et al., 2011) coding for *OCT4*, *SOX2*, *NANOG*, *LIN28*, *c-MYC* and *KLF-4*. 600,000 fibroblasts were resuspended in 100 μ l nucleofection solution VP1–1005 (Lonza) containing 3 μ g of each plasmid. Cells were nucleofected using the Nucleofector II (Lonza), program U-023. Afterwards, cells were plated onto one well of a matrigel coated 6 well plate in N2B27medium.

Reprogramming efficiency was enhanced by inhibiting TGF β -signaling with 0.5 μ M A-83-01, MEK-signaling with 0.5 μ M PD0325901, ROCK-signaling with 10 μ M Y-27632 and activating WNT-signaling with 3 μ M CHIR99021.

DNA fingerprinting analysis

STR analysis was performed by PCR using primers D7S796 and D21S2055 (STR Analysis) (see Table 1). Primer sequences are shown in Table 2.

PNPLA3 genotyping

For PNPLA3 genotyping, genomic DNA was isolated and analyzed with the TaqMan Assay ID C-7241_10 (Applied Biosystems).

Embryoid body (EB) formation

Cells were cultured as embryoid bodies (EBs) to confirm their three-lineage differentiation potential. 70% confluent iPSCs were transferred

Table 2
Reagents details.

Antibodies used for immunocytochemistry/flow-citometry			
	Antibody	Dilution	Company Cat # and RRID
Pluripotency Markers	Rabbit anti-OCT4	1:400	Cell Signaling Technology Cat# 2840S, RRID:AB_2167691
Pluripotency Markers	Rabbit anti-SOX2	1:400	Cell Signaling Technology Cat# 3579S, RRID:AB_2195767
Pluripotency Markers	Rabbit anti-NANOG	1:800	Cell Signaling Technology Cat# 4903S, RRID:AB_10559205
Pluripotency Markers	Mouse anti-Tra-1-60	1:1000	Cell Signaling Technology Cat# 4746S, RRID:AB_2119059
Pluripotency Markers	Mouse anti-Tra-1-81	1:1000	Cell Signaling Technology Cat# 4745S, RRID:AB_2119060
Pluripotency Markers	Mouse anti-SSEA4	1:1000	Cell Signaling Technology Cat# 4755S, RRID:AB_1264259
Differentiation Markers	Goat anti-Sox17	1:50	R and D Systems Cat# AF1924, RRID:AB_355060
Differentiation Markers	Rabbit anti-AFP	1:200	Cell Signaling Technology Cat# 2137S, RRID:AB_2209744
Differentiation Markers	anti-Nestin	1:250	Sigma-Aldrich Cat# N5413, RRID:AB_1841032
Differentiation Markers	anti-aSMA	1:1000	Dako Cat# M0851, RRID:AB_2223500
Secondary antibodies	anti-mouse-Cy3	1:2000	Thermo Fisher Scientific Cat# A10521, RRID:AB_2534030
Secondary antibodies	anti-rabbit-Alexa488	1:2000	Thermo Fisher Scientific Cat# A27034, RRID:AB_2536097
Nuclear Co-Staining	Hoechst 33258	1:5000	Thermo Fisher Scientific Cat# H3569, RRID:AB_2651133
Primers			
	Target	Forward/Reverse primer (5'-3')	
Episomal plasmids	OCT4 Plasmid	OCT4ex-F 5'-AGTGTGAGAGGCAACCTGGAGA-3' OCT4ex-R 5'-AGGAACTGCTTCCTTCACGA-3'	
Endogenous OCT4	OCT4 endogenous	OCT4end-F 5'-AGTTTGTGCCAGGTTTGTG-3' OCT4end-R 5'-ACTTCACCTTCCCTCCAACC-3'	
Genotyping	PNPLA3	TaqMan SNP Genotyping Assay, Cat# 4351379, Assay ID C-7241_10	
Fingerprinting	D17S1290	GCAACAGAGCAAGACTGTC/ GGAAACAGTAAATGGCCAA	
Fingerprinting	D21S2055	AACAGAACCAATAGGCTATCTATC/ TACAGTAAATCACTTGGTAGGAGA	
Mycoplasma	16 S rRNA gene	GGGAGCAAACAGGATTAGATACCTT/ TGACCATCTGTCACCTGTGTTAACCTC	

into a T25 flask and cultured for seven days in an upright position in DMEM high glucose, with 10% FCS, 1% P/S and 1% NEAA (Gibco). EBs were plated onto a gelatin coated 12-well plate and cultured for another 3–4 days.

Immunofluorescence stainings

Cells were fixed with 4% paraformaldehyde (PFA) (Polysciences). Unspecific binding sites were blocked by incubating for 2 h at room temperature (RT) in blocking buffer, consisting of 10% normal goat or donkey serum, 1% BSA, 0.5% Triton, and 0.05% Tween. Primary antibodies (Table 2) were diluted in staining buffer (blocking buffer diluted 1:1 with PBS) and incubated overnight at 4 °C. Cells were washed 3 times with PBS/0.05% Tween. Afterwards, they were incubated for 2 h at RT with secondary antibodies, diluted 1:500 in staining buffer. Nuclei were stained with Hoechst (Thermo Fisher Scientific). Cells were washed again 3 times with PBS/0.05% Tween. Images were captured using a fluorescence microscope (LSM700; Zeiss) with Zenblue software (Zeiss). Individual channel images were processed and merged with Fiji.

Flow cytometry

Cells were harvested and stained with an APC coupled OCT4 antibody (Miltenyi) for 10 min at 4 °C. Afterwards, they were washed with PBS and fixed with PFA. Analysis was performed on a CyAn ADP with Summit4.3 software (Beckman Coulter).

Karyotype analysis

Karyotype analysis was performed at the Institute of Human Genetics and Anthropology, Heinrich-Heine-University, Düsseldorf.

Microarray-based transcriptome analysis

PrimeView Affymetrix microarrays were used to determine global gene expression. 1 µg of total RNA was used and all preparations were performed by the Biologisch-medizinisches Forschungszentrum (BMFZ), Heinrich-Heine University, Düsseldorf. The dendrogram was generated using the package affy of the R/Bioconductor software (Gentleman et al., 2004).

Appendix A. Supplementary data

Supplementary data to this article can be found online at <https://doi.org/10.1016/j.scr.2018.07.011>.

References

- Gentleman, R.C., Carey, V.J., Bates, D.M., Bolstad, B., Dettling, M., Dudoit, S., Ellis, B., Gautier, L., Ge, Y., Gentry, J., et al., 2004. Bioconductor: open software development for computational biology and bioinformatics. *Genome Biol.* 5, R80.
- Romeo, S., Kozlitina, J., Xing, C., Pertsemliadis, A., Cox, D., Pennacchio, L.A., Boerwinkle, E., Cohen, J.C., Hobbs, H.H., 2008. Genetic variation in PNPLA3 confers susceptibility to nonalcoholic fatty liver disease. *Nat. Genet.* 40, 1461–1465.
- Yu, J., Chau, K.F., Vodyanik, M.A., Jiang, J., Jiang, Y., 2011. Efficient feeder-free episomal reprogramming with small molecules. *PLoS One* 6, e17557.

Modeling Nonalcoholic Fatty Liver Disease with Human Pluripotent Stem Cell-Derived Immature Hepatocyte-Like Cells Reveals Activation of PLIN2 and Confirms Regulatory Functions of Peroxisome Proliferator-Activated Receptor Alpha

Nina Graffmann,¹ Sarah Ring,¹ Marie-Ann Kawala,¹ Wasco Wruck,¹ Audrey Ncube,¹ Hans-Ingo Trompeter,² and James Adjaye¹

Nonalcoholic fatty liver disease (NAFLD/steatosis) is a metabolic disease characterized by the incorporation of fat into hepatocytes. In this study, we developed an *in vitro* model for NAFLD based on hepatocyte-like cells (HLCs) differentiated from human pluripotent stem cells. We induced fat storage in these HLCs and detected major expression changes of metabolism-associated genes, as well as an overall reduction of liver-related microRNAs. We observed an upregulation of the lipid droplet coating protein Perilipin 2 (PLIN2), as well as of numerous genes of the peroxisome proliferator-activated receptor (PPAR) pathway, which constitutes a regulatory hub for metabolic processes. Interference with PLIN2 and PPAR α resulted in major alterations in gene expression, especially affecting lipid, glucose, and purine metabolism. Our model recapitulates many metabolic changes that are characteristic for NAFLD. It permits the dissection of disease-promoting molecular pathways and allows us to investigate the influences of distinct genetic backgrounds on disease progression.

Introduction

NONALCOHOLIC FATTY LIVER disease (NAFLD) is a widespread disease in the western hemisphere. Due to a high-fat diet and a lack of exercise, hepatocytes of NAFLD patients accumulate fat in the form of lipid droplets (LDs) [1]. This is often associated with type 2 diabetes and considered part of the metabolic syndrome [1]. Insulin resistance and obesity-associated chronic inflammation of adipose tissue are critical factors for the development and progression of NAFLD [2,3]. This is often seen as a “first hit” manifesting in the rather benign accumulation of LDs, called steatosis. A “second hit”, frequently due to an increase of reactive oxygen species-mediated stress, induces the progression toward nonalcoholic steatohepatitis (NASH), which is accompanied by liver inflammation and fibrosis [3]. Approximately, 29% of patients with NASH develop cirrhosis. Up to 27% of these further develop hepatocellular carcinoma [1].

Hepatocytes store triacylglycerides (TAGs) in LDs as a reaction to an overload with free fatty acids. These are either derived directly from the diet or result from inflammation induced lipolysis in adipose tissues [2]. The occurrence of

LDs in >5% of hepatocytes is the main diagnostic criterion for NAFLD [1].

In LDs, TAGs are enclosed by a lipid monolayer, which is encapsulated by distinct proteins, predominantly from the PAT (Perilipin/ADRP/TIP47) family [4–6]. Perilipins regulate hydrolysis of TAGs by controlling the activity of lipases and their access to LDs [7–9]. Perilipin 2 (PLIN2 or Adipophilin, ADRP) is ubiquitously expressed and plays a major role in the formation of LDs [10–12]. PLIN2 expression correlates with LD content in hepatocytes [13]. A reduction of PLIN2 expression with antisense oligonucleotides reduced liver TAG content and decreased the expression of genes involved in fatty acid and steroid metabolism in mice [14,15]. In addition, PLIN2 knockout mice develop neither obesity nor NAFLD when fed a high-fat diet because they have a higher energy turnover compared to their wild-type counterparts [16].

Nutrition and energy uptake are important factors for the development of NAFLD. However, there exist major differences between humans and mice. Various established diets reproduce effects of NAFLD/NASH in mice. Unfortunately, they fail to mirror the whole spectrum of symptoms observed in humans. While high-fat diets induce obesity and NAFLD,

¹Institute for Stem Cell Research and Regenerative Medicine and ²Institute for Transplantation Diagnostics and Cell Therapeutics, Heinrich Heine University Düsseldorf, Düsseldorf, Germany.

mice generally do not proceed toward NASH even if the diet is supplemented with fructose. To induce NASH, mice are usually fed with a methionine–choline-deficient diet. A major drawback of this diet, however, is the fact that mice do not become obese, which is a major risk-factor for NAFLD in humans [17,18]. In addition, there exist several knockout mouse models, none of which is capable of reflecting all aspects of the disease [17].

Several groups have used human hepatocarcinoma cell lines or immortalized primary hepatocytes to model NAFLD [19,20]. However, cancer-derived cell lines are of limited use for dissecting the molecular basis of NAFLD as they harbor genomic and hence functional aberrations compared to healthy primary liver cells [21,22]. The use of liver biopsy-derived primary human hepatocytes for modeling NAFLD is also limited because they can only be cultivated for a few days before the onset of dedifferentiation [23] or have to be immortalized by virus-mediated transduction with SV40. In addition, liver biopsies, especially those from the early stages, are very rare.

To overcome these limitations, we in this study aimed at dissecting the molecular basis of NAFLD using hepatocyte-like cells (HLCs), which were *in vitro* derived from human pluripotent stem cells (hPSCs). We used the human embryonic stem cell (ESC) line H1, as well as induced pluripotent stem cells (iPSCs), derived from fetal foreskin fibroblasts of a healthy individual [24,25]. We were able to monitor the accumulation of fat in the HLCs, as well as major biochemical alterations concerning lipid, glucose, and purine metabolism. Our new model system is suitable for the analysis of disease triggering factors, as well as new therapeutics.

Material and Methods

Cell culture

HepG2 cells (ATCC[®]HB-8065[™]) were cultured in DMEM low glucose with 10% FCS, 1% Penicillin/Streptomycin, and 1% GlutaMAX (Gibco). For fat induction, cells were induced with 50 μ M oleic acid (OA) (Stock solution 100 mM in ethanol). As control, cells were treated with the corresponding amount of ethanol. Fat induction was performed 24 h after passaging.

Differentiation of hPSCs into HLCs

hPSCs were cultured on Matrigel (Corning) coated plates in TeSR E8 medium (STEMCELL Technologies). Medium was changed daily and spontaneously differentiated cells were removed manually before splitting the cells. One or two days after passaging, differentiation into definitive endoderm was induced with definitive endoderm medium: 96% RPMI 1640, 2% B27 (without retinoic acid), 1% GlutaMAX (Glx), 1% Penicillin/Streptomycin (P/S) (all Gibco), 100 ng/mL Activin A (Peptidech), and for the first 3 days, 50 ng/mL WNT3A (R&D). After 5 days, medium was changed toward hepatic endoderm medium as follows: 78% Knockout DMEM, 20% Knockout serum replacement, 0.5% Glx, 1% P/S, 0.01% 2-Mercaptoethanol (all Gibco), and 1% DMSO (Sigma).

After 5 days, differentiation was continued with HLC medium as follows: 82% Leibovitz 15 medium, 8% fetal calf serum, 8% Tryptose Phosphate Broth, 1% Glx, 1% P/S (all Gibco) with 1 μ M Insulin (Sigma), 10 ng/mL hepatocyte growth factor (HGF) (Peptidech), 20 ng/mL Oncostatin M

(OSM) 209 a.a. (Immunotools), and 25 ng/mL Dexamethasone (DEX) (Sigma) (Fig. 1A). During the whole differentiation period, medium was changed daily.

Fat induction in HLCs was performed on day 12 of the differentiation process. Interference with peroxisome proliferator-activated receptor alpha (PPAR α) activity was performed by treatment with 50 μ M Fenofibrate (agonist) or 2 μ M GW6471 (antagonist, both from Cayman Chemical) in parallel with OA induction (Fig. 1C).

Liver-specific biochemical assays of HLCs

The amount of urea produced by the cells over a period of 24 h was determined from the cell culture supernatant using the QuantiChrom[™] Urea Assay Kit (BioAssay Systems) according to the manufacturer's recommendations. Cytochrome p450 3A4, 3A5, and 3A7 activity was measured with the P450-Glo[™] CYP3A4 Assay Luciferin-PFBE (Promega) using a luminometer (Lumat LB 9507; Berthold Technologies). The presence of active transporter proteins was assessed by the uptake and release of Indocyanine Green dye. Cells were incubated for 30 min with 1 mg/mL Cardiogreen (Santa Cruz Biotechnology, Inc.). Afterward, they were washed with PBS and images were captured with a light microscope (Primo Vert; Zeiss). Subsequently, cells were cultured in their usual medium for 6 h and images were again captured.

Staining of LDs

Paraformaldehyde-fixed cells were incubated for 20 min with either a 60% working solution of Oil Red O (Sigma) or with BODIPY 493/503 (1 μ g/mL; Life technologies) in PBS/0.05% Tween. After washing, images were captured with a light microscope (Primo Vert; Zeiss) or a fluorescence microscope, respectively (LSM700; Zeiss).

Immunocytochemistry

For intracellular antibody staining, paraformaldehyde-fixed cells were permeabilized and unspecific binding sites were blocked by incubating for 2 h at room temperature with blocking buffer (1 \times PBS with 10% normal goat or donkey serum, 1% BSA, 0.5% Triton, and 0.05% Tween). Afterward, blocking buffer was diluted 1:2 with 1 \times PBS and cells were incubated with the primary antibody overnight at 4°C. Cells were washed thrice with 1 \times PBS/0.05% Tween and incubated with the secondary antibody, for 2 h at room temperature. Cells were washed as above and images captured using a fluorescence microscope (LSM700; Zeiss).

Extracellular stainings were performed in the same manner without detergents. The following primary antibodies were used: Alpha Fetoprotein, Albumin (Sigma) E Cadherin (CST), HNF4 α (Abcam), SOX17 (R&D), and PLIN2 (Proteintech). For details on antibodies, see Supplementary Table S1; Supplementary Data are available online at www.liebertpub.com/scd. DNA was stained with Hoechst 33342. Individual channel images were processed and merged with Photoshop CS6.

Western blot

Cells were lysed in 1 \times RIPA buffer (50 mM Tris HCl, pH 8, 150 mM NaCl, 1% IGEPAL (NP-40), 0.1% SDS, 1 mM EDTA, and 0.5% Na-Deoxycholate) with protease inhibitors. Twenty microgram of protein was analyzed by western

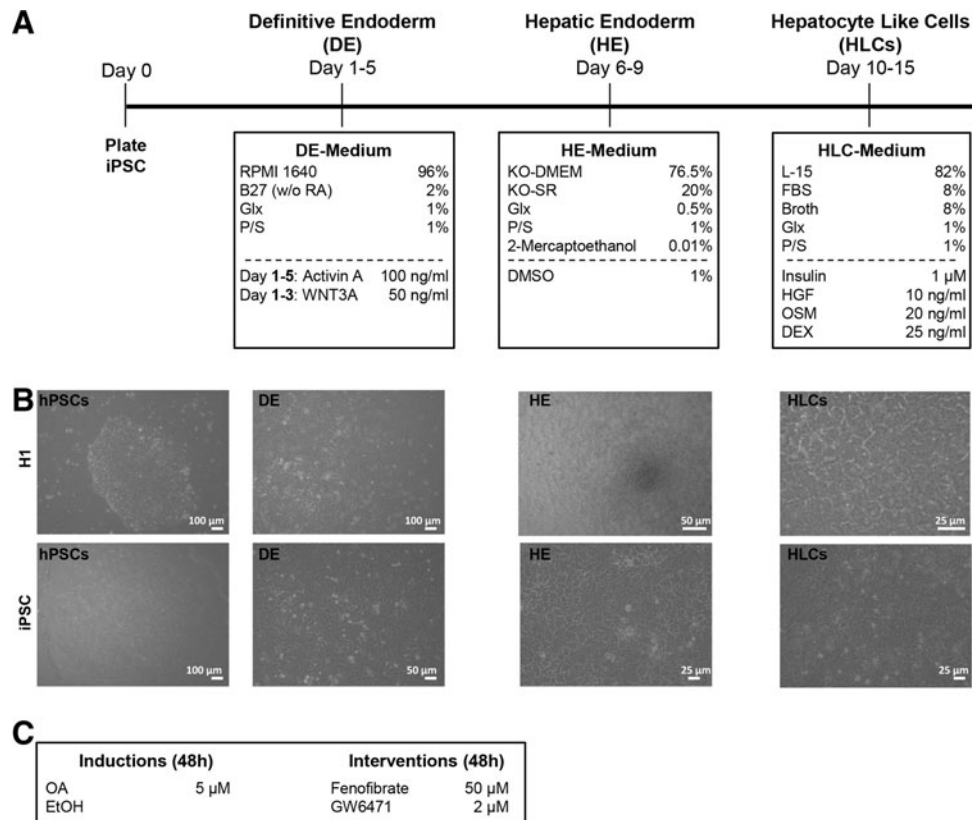


FIG. 1. Differentiation of hPSCs into HLCs. hPSCs were differentiated into HLCs using a three-step protocol (see also Materials and Methods section) (A). Morphological changes of the differentiating cells are documented for each stage. At the definitive endoderm (DE) stage, the dense cell-cell contact is lost, and cells acquire the typical endodermal morphology. The characteristic polygonal shape of hepatocytes is already evident at the hepatic endoderm (HE) stage. This morphology is even more pronounced at the HLC stage (B). Two days before the end of differentiation, steatosis was induced with 50 μ M OA, and control cells were treated with an equal volume of ethanol. To interfere with LD formation, PPAR α modulators were also added on the same day (C). HLCs, hepatocyte-like cells; hPSCs, human pluripotent stem cells; LD, lipid droplet; OA, oleic acid; PPAR α , peroxisome proliferator-activated receptor alpha.

blot with antibodies against PLIN2 (Proteintech) and ACTIN (CST). HRP coupled secondary antibodies were obtained from Abcam. Chemiluminescence was detected on a Fusion FX instrument (PeqLab) and analyzed with Fusion Capt Advance software (PeqLab) using rolling ball background correction.

RNA isolation and quantitative real-time polymerase chain reaction

For RNA isolation, up to 500,000 cells were lysed in 500 μ L TRIzol. RNA was isolated with the Direct-zolTM RNA Isolation Kit (Zymo Research) according to the user's manual, including the DNase digestion step. Reverse transcription of up to 1 μ g RNA was performed with the TaqMan Reverse Transcription (RT) Kit (Applied Biosystems). Primers were purchased from MWG; sequences are provided in Supplementary Table S2. Real-time PCR was performed in technical triplicates with Power SYBR Green Master Mix (Life technologies) on a VIIA7 or StepOnePlus (both Life technologies) machine. Mean values were normalized to actin and, subsequently, to the ethanol control. In case of siRNA experiments, data were normalized to the ethanol-treated nt siRNA sample. Experiments were carried out in biological

duplicates and are depicted as mean values (log₂) with standard error of the mean. Unpaired student's *t*-tests were performed for calculating significances.

Transcriptome and bioinformatics analysis

Microarray experiments were performed using the Affymetrix PrimeView chip (BMFZ, Düsseldorf). Details of data analysis are given in Supplementary Methods.

Liver-specific microRNA array

cDNA synthesis was carried out using the miScript II RT Kit (QIAGEN) according to the user's manual. Quantitative reverse transcription polymerase chain reaction (qRT-PCR) and data analysis were performed according to the user's manual (miScript miRNA PCR Array; QIAGEN). All values were normalized to six different housekeeping genes (snoRNA/snRNA).

microRNA target gene validation

microRNA target gene validation was performed in HEK293T cells as previously described [26,27]. In brief, 3' untranslated region (UTR) fragments of putative target

genes were cloned at the 3' end of the *Firefly* luciferase open reading frame (ORF) in dual-luciferase reporter vector pmirGLO (Promega). Ds-oligonucleotides spanning the predicted microRNA binding sites for ATL3 (hsa-miR-106b) and CPAMD8 (hsa-miR-122) were used (Supplementary Table S3), whereas the 3,406-bp EPHA7-3' UTR was represented by a 1,384-bp PCR fragment covering two predicted hsa-miR-106b binding sites (Supplementary Table S4). Normalization for effects of endogenous HEK293T microRNAs on the given 3' UTR was achieved by transfection of both empty pmirGLO, as well as pmirGLO/3' UTR, into HEK293T cells. Pairwise cotransfections of empty pmirGLO or pmirGLO/3' UTR with the microRNA mimic of interest (Supplementary Table S5) (Dharmacon) were performed. *Firefly* and *Renilla* activities were determined 24 h after transfection. All transfections were performed in at least two independent biological experiments with quadruple transfections each. Mean values with standard deviations are shown. Significances were calculated with unpaired Student's *t*-test, *** $P \leq 0.001$.

PLIN2 knockdown

PLIN2 knockdown was performed by transfecting 5 pmol PLIN2 siRNA or a nontarget (nt) control siRNA (Thermo Scientific) into 100,000 HepG2 cells using lipofectamine RNAiMAX (Life Technologies). Forty-eight hours post transfection, the cells were harvested for further analyses.

Results

Pluripotent stem cells differentiate into HLCs and show characteristic activities of liver cells

We differentiated hPSCs into HLCs using a three-step protocol, which is based on published protocols [28–30], but has been adapted in our laboratory to optimize the individual differentiation steps (Fig. 1A). We used the established ESC line H1 and an iPSC line derived from fetal foreskin fibroblasts [25] to compare two distinct hPSC lines. Morphological changes were monitored at every step of the differentiation process (Fig. 1B). ESCs and iPSCs behaved similarly during differentiation. At the definitive endoderm stage, they adopted a typical flat and elongated shape; then at the hepatic endoderm stage, cells from both sources started to adopt the polygonal shape that is characteristic for hepatocytes. At the maturation step, that is, the HLC stage, the vast majority of the cells had acquired the polygonal morphology.

Stainings with antibodies for the hepatocyte markers albumin, HNF4 α , and E-Cadherin were all positive for HLCs derived from ESCs and iPSCs (Fig. 2A). In addition, several activity tests indicated that HLCs behave like hepatocytes (Fig. 2B–D). They were able to synthesize urea (Fig. 2B) and expressed active transporters as demonstrated by their ability to take up and release indocyanine green dye (Fig. 2C). Another important characteristic of hepatocytes is the activity of phase I enzymes, for example, members of the Cytochrome p450 family, which was strongly increased in HLCs compared to undifferentiated hPSCs (Fig. 2D). Thus, we can reliably generate functional HLCs from ESCs, as well as from iPSCs, which are suitable for disease modeling.

HLCs can be induced to accumulate LDs

To analyze early steatosis in cell culture, we first established a protocol for the induction of LDs in HLCs, which is based on the addition of 50 μ M OA for 48 h into the medium. For both cell types, we observed similar increases in LD accumulation with Oil Red O and BODIPY 493/503 staining (Fig. 3A, B). *PLIN2* expression increased consistently after induction with OA (Fig. 3C). In addition, we analyzed the expression of several other genes involved in lipid metabolism to get a first impression of the immediate impact of fatty acid overload (Fig. 3C and Table 1). All factors were selected, because they were significantly regulated in liver cells of patients with high levels of steatosis compared to low-level steatosis [31]. In all cases, except for *ACADSB*, the expression changes in HLCs mirrored those observed in patient liver biopsies [31].

We decided to further focus on increased *PLIN2* expression as an indicator and marker for the induction of steatosis, because its role during progression of the disease has been analyzed extensively [13–16].

Transcriptome and associated pathway analysis of HLCs after steatosis induction

We next wanted to know how the induction of steatosis with OA affects the transcriptomes 48 h post treatment. To achieve this, we induced steatosis in HLCs derived from H1 ESCs and iPSCs as described above. Ethanol-treated cells were used as a solvent control. We found that ~13,000 genes were significantly expressed in H1- or iPSC-derived HLCs, respectively (Fig. 4A, B). In both cases, about 200 genes were exclusively expressed in the control cells, while 129 (H1) and 186 (iPSC) genes were exclusively expressed in OA-treated cells (Fig. 4A, B).

Analysis of the genes that were higher or exclusively expressed in HLCs treated with OA revealed significant enrichment of gene ontology (GO)-terms related to lipid metabolism and transport (Fig. 4C and Supplementary Table S6). As OA is dissolved in ethanol, it is not possible to completely rule out an ethanol-mediated influence on the expression of metabolically relevant genes. However, GO analysis for genes, which were exclusively expressed in ethanol-treated control cells, did not reveal any nonethanol-related metabolic pathways. Instead, pathways connected to signaling and nonhepatic development were enriched (Fig. 4C and Supplementary Table S7).

Overall, the individual regulated genes, as well as the associated GO categories and pathways, differed between both cell lines. This probably reflects innate discrepancies of the differentiation propensity of ES and iPS cells, as well as of course their different genetic background. Nonetheless, numerous genes associated with the PPAR pathway, which plays a major role in the regulation of lipid metabolism, were upregulated after OA treatment of HLCs derived from H1 or iPSCs (Supplementary Fig. S1).

Heatmap analysis of several factors involved in lipid and glucose metabolism, as well as in insulin signaling, revealed that although the absolute transcription levels of many factors differed between H1- and iPSC-derived HLCs, the OA-induced changes were frequently qualitatively similar (Fig. 4D). To get a more detailed insight into the transcriptional

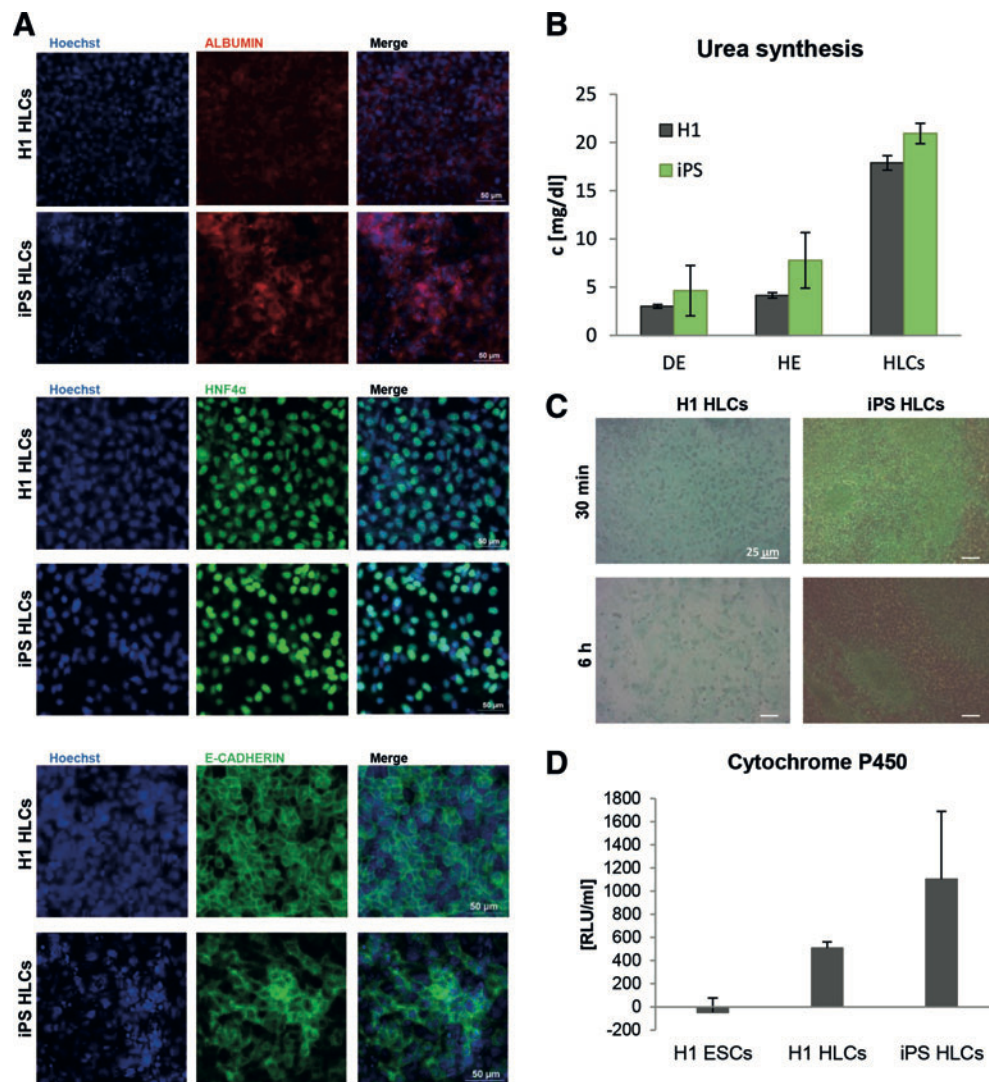


FIG. 2. Characterization of HLCs. The ES cell line H1 and iPS cells were differentiated into HLCs as described in Fig. 1. (A) HLCs derived from H1 (upper row) and iPS cells (lower row) express the liver-specific proteins Albumin, HNF4 α (scale bar 50 μ m), and E-Cadherin (scale bar 20 μ m). (B–D) HLCs have liver-specific activity. (B) Urea production increases during differentiation and reaches its maximum at the HLC. (C) HLCs take up indocyanine green dye (upper row) within 30 min and release it within 6 h (lower row). (D) HLCs have phase I enzyme activity as measured by a luminometric assay detecting Cytochrome P450 (CYP) 3A4, 3A5, and 3A7 activity. In all cases, representative experiments are shown. In (B) and (D), data represent mean value \pm standard deviation. HLCs, hepatocyte-like cells. Color images available online at www.liebertpub.com/scd

changes that occur early in steatosis, we expanded our panel of directly investigated genes (Table 1) and included more factors relevant for lipid metabolism (*CPT1A*, *CPT2*, and *HADH*). We also added *APOC2* as another lipid binding protein and *GSK3A*, which regulates glucose metabolism (Fig. 4E). Interestingly, only *CPT1A* and *APOC2* were consistently upregulated in both samples, while we observed only minor and opposed expression changes for the other factors.

Many liver-specific microRNAs are downregulated in HLCs after induction of steatosis

Next, we analyzed whether induction of steatosis in H1- and iPSC-derived HLCs alters expression of liver-specific microRNAs. To this end, we used the liver finder micro-

RNA array composed of 84 liver-related microRNAs. Interestingly, we found most microRNAs downregulated upon steatosis induction and only a few microRNAs upregulated (Fig. 5A). This finding implies that an altered microRNA expression profile is part and parcel of the early events in steatosis-induced cells, especially since the liver-specific microRNA hsa-miR-122 was among the most strongly downregulated miRNAs, together with hsa-miR-106b (Fig. 5A).

Bioinformatic target gene predictions revealed several thousand putative target genes for hsa-miRs-106b and -122 (Supplementary Table S8). Among these, we further analyzed liver-related genes *ATL3*, *EPHA7* (putative miR-106b targets), and *CPAMD8* (putative miR-122 target), which were upregulated upon steatosis induction in HLCs derived from H1 and

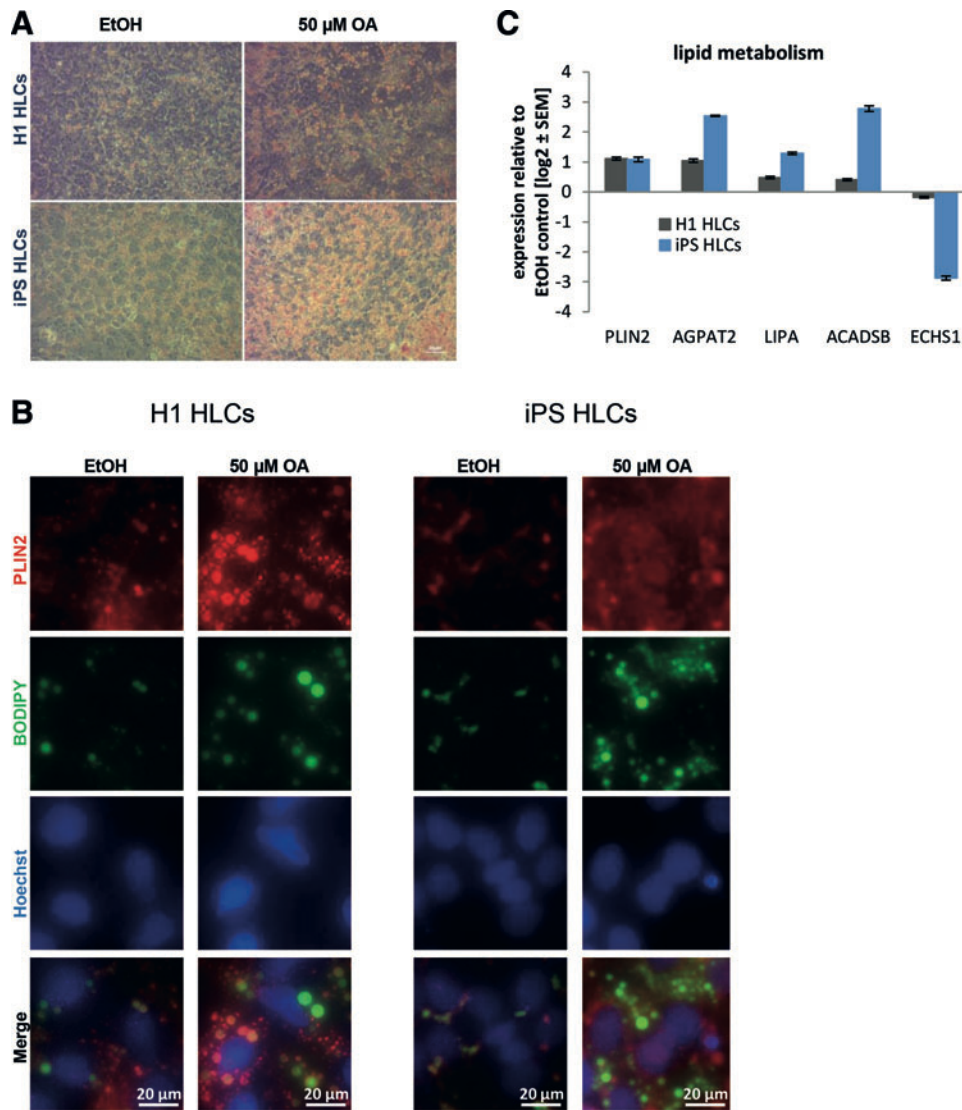


FIG. 3. Induction of steatosis in HLCs. hPSCs were differentiated into HLCs. Steatosis was induced by treatment with 50 μ M OA for 48 h. Ethanol (EtOH)-treated cells served as controls. Steatosis was monitored by Oil Red O (red) (A) or BODIPY 493/503 (green) (B) staining of LDs. The control cells treated with ethanol show limited LD accumulation, while those treated with 50 μ M OA for 48 h have abundant LDs. Scale bars: 20/50 μ m. (C) Expression of genes involved in lipid metabolism was analyzed using qRT-PCR ($n=2$). Gene expression was normalized to β -actin and, subsequently, to the control samples. For each sample, the mean \pm standard error is shown as log2 scale. HLCs, hepatocyte-like cells; hPSCs, human pluripotent stem cells; LDs, lipid droplets; OA, oleic acid; qRT-PCR, quantitative reverse transcription polymerase chain reaction. Color images available online at www.liebertpub.com/scd

iPSC (Fig. 5B). Remarkably, a significant number of miRNAs from the liver finder array were found among the predictions for these three genes (CPAMD8: 15%, ATL3: 12%, EPHA7: 44% from 84 miRNAs, see Supplementary Table S4). Luciferase reporter-based target gene validation indeed confirmed that hsa-miR-106b downregulates *ATL3* and *EPHA7*, while miR-122 targets *CPAMD8* (Fig. 5C–E).

siRNA-based suppression of PLIN2 level and function does not impair LD formation

Having characterized the impact of steatosis induction on the global gene expression, we next wanted to interfere with LD accumulation to find indications for putative treatments

for NAFLD. First, we reduced *PLIN2* expression using siRNA, because it is known that *PLIN2* plays a major role during the development of steatosis [13–16]. As the transfection efficiency of in vitro derived HLCs is very low, we decided to focus on HepG2, a hepatocellular carcinoma line, for these experiments. Forty-eight hour treatment with a *PLIN2* siRNA reduced its expression on protein level to about 33% (Fig. 6A and Supplementary Fig. S2A). Next, we induced the siRNA-treated HepG2 cells with OA for an additional 48 h. *PLIN2* siRNA reduced the expression of *PLIN2* on mRNA level to $\sim 20\%$ in the control and the OA-treated samples (Fig. 6B). However, even under siRNA knockdown conditions, *PLIN2* expression was still significantly higher in the induced sample compared to the control (Fig. 6B).

TABLE 1. NAMES AND FUNCTIONS OF THE INVESTIGATED GENES

<i>Gene symbol</i>	<i>Name</i>	<i>Function</i>	<i>Classification</i>
<i>CPT1A</i>	Carnitine palmitoyltransferase 1A	Transport acyl group of fatty acid-CoA conjugates across the mitochondrial membranes for beta-oxidation	Fatty acid catabolism
<i>CPT2</i>	Carnitine palmitoyltransferase 2	Mitochondrial fatty acid beta-oxidation	
<i>ECHS1</i>	Enoyl coenzyme A hydratase, short chain, 1, mitochondrial		
<i>HADH</i>	Hydroxyacyl-coenzyme A dehydrogenase	Mitochondrial fatty acid beta-oxidation	
<i>LIPA</i>	Lipase A, lysosomal acid, cholesterol esterase	Hydrolase of cholesteryl esters and triglycerides	
<i>ACADSB</i>	Acyl-coenzyme A dehydrogenase, short/branched chain	Dehydrogenase of acyl-CoA derivatives	
<i>ACAT1</i>	Acetyl-coenzyme A acetyltransferase 1	Ketone body metabolism	
<i>PRKAA2</i>	Protein kinase, AMP-activated, alpha 2 catalytic subunit	Regulator of FA and cholesterol biosynthesis	Regulators of metabolism
<i>PPARα</i>	Peroxisome proliferator-activated receptor alpha	Regulator of lipid and glucose metabolism	
<i>GSK3A</i>	glycogen synthase kinase 3 alpha	Regulator of glucose homeostasis	
<i>AGPAT2</i>	1-Acylglycerol-3-phosphate O-acyltransferase 2 (lysophosphatidic acid acyltransferase, beta)	Phospholipid biosynthesis	Biosynthesis
<i>HMGCR</i>	3-Hydroxy-3-methylglutaryl-coenzyme A reductase	Cholesterol synthesis	
<i>PLIN2</i>	Perilipin 2	Coats LDs	LD coating
<i>APOC2</i>	Apolipoprotein C-II	Lipid-binding protein (very low-density lipoprotein)	

LD, lipid droplet.

Contrary to our expectations, *PLIN2* knockdown did not alter the accumulation of LDs in the cells after incubation with OA (Fig. 6C). Nonetheless, microarray analysis revealed that transcriptomes of cells treated with *PLIN2* siRNA cluster away from those incubated with the nt control siRNA (Supplementary Fig. S2B, left branches). In both clusters, OA treated and control cells form separate subclusters. A detailed view on the expression of lipid and glucose metabolism related genes also confirmed that *PLIN2* siRNA treatment induced major transcriptional changes (Fig. 6E).

Numerous factors involved in lipid catabolism such as *ACADSB*, *LIPA*, and *CPT1A* were downregulated after *PLIN2* siRNA treatment. These tendencies were confirmed by qRT-PCR (Fig. 6D). However, in this study, the differences between the OA and EtOH-treated cells became more obvious. Interestingly, also *PPAR α* and γ , which regulate lipid metabolism, were downregulated after *PLIN2* knockdown (Fig. 6E). This argues in favor of an active PPAR gene regulatory network associated with steatosis. Overall, *PLIN2* knockdown modulates the expression of steatosis-related genes, but does not reduce lipid accumulation, at least in the early stage investigated.

Modulation of the lipid metabolism regulating factor PPAR α has major impact on numerous metabolism-related pathways

The hepatic nuclear receptor *PPAR α* is activated by a variety of ligands [32,33]. It regulates lipid and glucose metabolism in the liver and *PLIN2* is one of its known targets [34,35]. Transcriptome analysis revealed that many members of the *PPAR α* signaling pathway were upregulated

either in H1- or iPSC-derived HLCs after treatment with OA (Supplementary Fig. S1). Its expression was also influenced by *PLIN2* knockdown (Fig. 6D, E). As we could not transfect HLCs with siRNA against *PLIN2* to a significant level, we decided to interfere with *PPAR α* signaling by activating or inhibiting *PPAR α* action with Fenofibrate or GW6471, respectively [36].

iPSC-derived HLCs were treated for 48 h with OA and either Fenofibrate or GW6471. BODIPY staining revealed that HLCs incorporated LDs regardless of treatment with the *PPAR α* modulators (Fig. 7A). This is in line with results from Rogue et al. who showed that *PPAR α* agonist treatment reduced fat load in HepaRG cells only after a prolonged incubation of 14 days [37]. However, microarray analysis revealed that even short-term treatment with Fenofibrate and GW6471 had an impact on gene expression. The transcriptomes of HLCs incubated with either Fenofibrate or GW6471 clearly clustered away from each other (Fig. 7B).

Heatmap-based analysis of the *PPAR* pathway revealed that cells treated with Fenofibrate or GW6471 behave differently (Fig. 7C). In both cases, there were two subclusters detectable that correspond to the control cells and the OA-treated cells. We monitored the expression levels of genes important for lipid and glucose metabolism in more detail by qRT-PCR. In most cases, treatment with the agonist and the antagonist resulted in opposing changes in gene expression, as expected (Fig. 7D). Inhibition of *PPAR α* with GW6471 resulted in downregulation of genes involved in lipid catabolism, while activation using Fenofibrate reduced expression of *AGPAT2* and *HMGCR*, which are involved in biosynthesis of phospholipids and cholesterol, respectively (Fig. 7D).

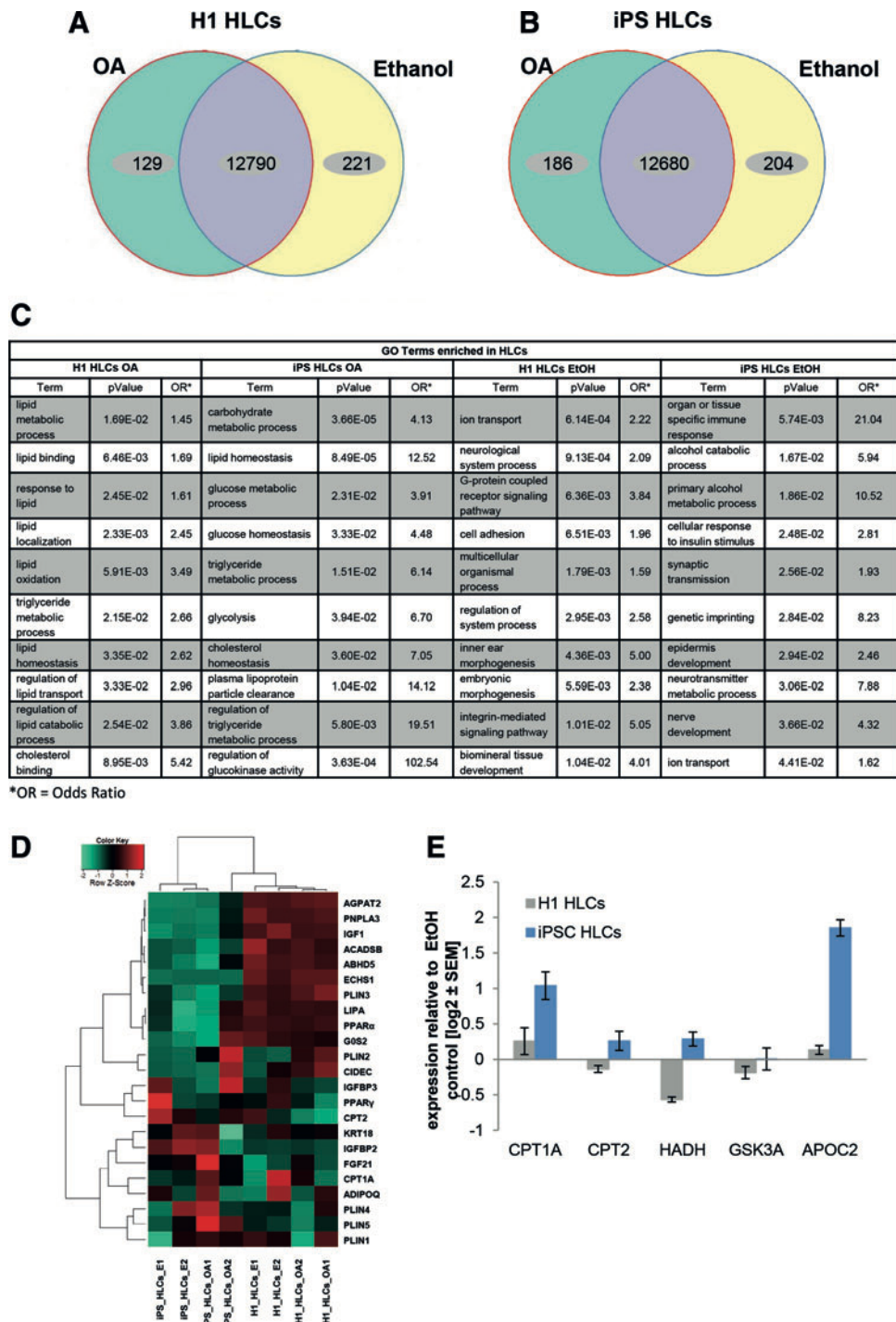


FIG. 4. Gene expression profiles of HLCs challenged with OA enable characterization of the early steps in NAFLD. Venn diagrams of genes expressed (detection P value <0.05) in H1- (A) or iPS- (B) derived HLCs ($n=2$). Green and yellow segments represent genes exclusively expressed in OA treated or control cells, respectively. Purple segments comprise genes, which are expressed under both conditions, but not necessarily with the same intensity. (C) GO-analysis of genes upregulated or exclusively expressed under OA treatment reveals an enrichment of NAFLD-related categories, while ethanol control cells predominantly express genes mapping to divergent categories. Shown are preselected significant GO-Terms; for full data set, see Supplementary Tables S6 and S7. (D) Heatmap of genes involved in insulin signaling and lipid or glucose metabolism reveals differences between H1- and iPS-derived HLCs, which might, in part, be due to their distinct genetic background. However, qualitative changes are similar between both groups, which are reflected by the formation of subclusters connected to OA treatment. (E) Expression of genes involved in lipid and glucose metabolism was analyzed using qRT-PCR ($n=2$). Gene expression was normalized to β -actin and, subsequently, to the control samples. For each sample, the mean \pm standard error of duplicate experiments is shown as \log_2 scale. GO, gene ontology; HLCs, hepatocyte-like cells; iPSC, induced pluripotent stem cell; NAFLD, nonalcoholic fatty liver disease; OA, oleic acid; qRT-PCR, quantitative reverse transcription polymerase chain reaction. Color images available online at www.liebertpub.com/scd

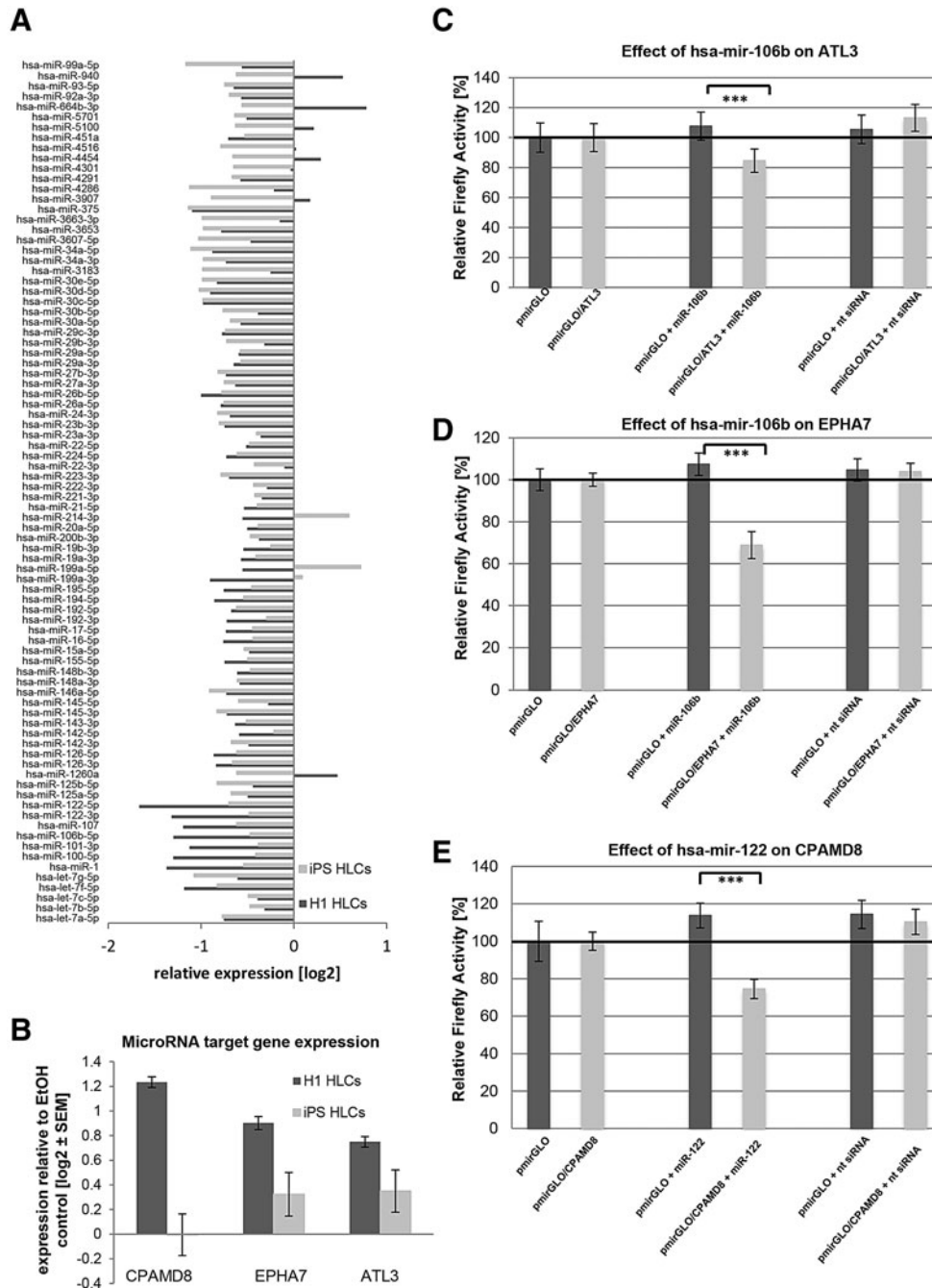


FIG. 5. Regulated expression of microRNAs upon induction of steatosis. **(A)** Expression of 84 liver-specific microRNAs from H1-HLCs (*dark gray*) and iPSC-HLCs (*light gray*) was analyzed after the induction of steatosis. MicroRNA expression was normalized to six different genes of small housekeeping RNAs. For H1-derived HLCs, biological and for iPSC-derived HLCs, technical duplicates were performed. The mean value is shown as log2 expression. With a few exceptions, all miRNAs were downregulated in steatosis-induced cells from both sources. **(B)** Expression of selected microRNA target genes was analyzed through qRT-PCR ($n = 2$). Gene expression was normalized to β -actin and, subsequently, to the control samples. For each sample, the mean \pm standard error is shown as log2 scale. **(C–E)** Validation of predicted target genes for hsa-miRNA-106b [ATL3 **(C)**, EPHA7 **(D)**] and hsa-miRNA-122 [CPAMD8 **(E)**]. To test the influence of endogenous microRNAs, empty *Firefly/Renilla* dual-reporter vector pmirGLO and pmirGLO/3' UTR (containing the 3' UTR of interest at the 3' end of the Firefly open reading frame) were each transfected into HEK293T cells ($n = 4$). Normalized *Firefly* activities were compared with those of pairwise cotransfections of these vectors with the microRNA mimic of interest (miR-106b, -122, and an unspecific siRNA negative control) to test for unspecific effects of the given microRNA-mimic in *Firefly/Renilla* per se and for validation of the particular target prediction. *Dark gray* columns show normalized *Firefly* activities from pmirGLO (mimic-co)-transfections; *light gray* columns are those from pmirGLO/3' UTR cotransfections. Percentage reductions of *Firefly* activities of pmirGLO/3' UTR compared with pmirGLO are given, as well as their statistical significances (Student's *t*-test, unpaired, $***P \leq 0.001$). All three predicted interactions were tested positive. HLCs, hepatocyte-like cells; iPSC, induced pluripotent stem cell; qRT-PCR, quantitative reverse transcription polymerase chain reaction; UTR, untranslated region.

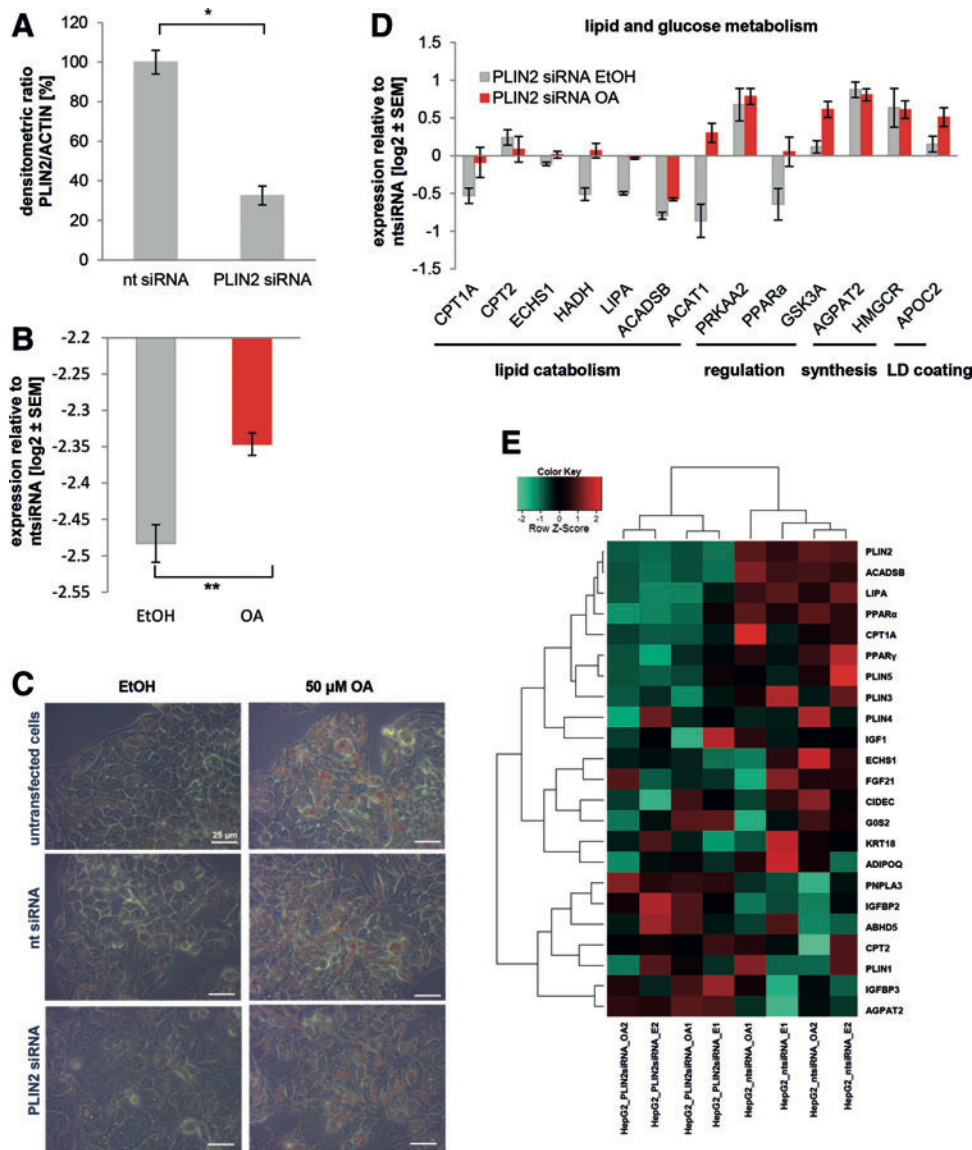


FIG. 6. Knockdown of PLIN2 in HepG2 cells does not affect LD formation, but alters gene expression. PLIN2 was knocked down in HepG2 cells by lipofectamine-mediated siRNA transfection ($n=2$). Cells were either transfected with nt siRNA or with PLIN2 siRNA. **(A)** After 48 h, PLIN2 expression was assessed by western blot and normalized to ACTIN levels. **(B)** After 48 h, steatosis was induced with 50 μ M OA for an additional 48 h. As control, cells were treated with ethanol (EtOH). Expression of PLIN2 was analyzed on mRNA level using qRT-PCR. Although levels were reduced by $\sim 80\%$ after transfection, we observed significantly increased levels after OA treatment. Gene expression was normalized to β -ACTIN and, subsequently, to the control samples. For each sample, the mean \pm standard error of duplicate experiments is shown as log₂ scale. Significances were calculated with an unpaired Student's t -test. **(C)** LD formation was monitored by Oil Red O staining. In the *upper row*, untransfected control cells are shown, followed by cells transfected with nt siRNA (*middle row*) and PLIN2 siRNA, *last row*. Ethanol-treated control cells show only minor LD accumulation (*left column*), while those treated with 50 μ M OA for 48 h have abundant LDs that are stained by Oil Red O. Scale bar: 25 μ m. Expression of genes involved and lipid or glucose metabolism **(D)** were analyzed using qRT-PCR. **(E)** Heatmap representation of genes involved in insulin signaling and lipid or glucose metabolism reveals two clusters related to treatment with either PLIN2 or the nt siRNA. LD, lipid droplet; OA, oleic acid; PLIN, Perilipin 2; qRT-PCR, quantitative reverse transcription polymerase chain reaction. Color images available online at www.liebertpub.com/scd

When we compared the number of GO-terms associated with distinct metabolic categories that were significantly regulated after PPAR α modulation, it became obvious that many were connected with glucose, lipid, and purine metabolism (Fig. 7E and Supplementary Table S9). Interestingly, genes exclusively expressed in GW6471-treated

HLCs were predominantly mapped to lipid metabolism or transport, while this category was only marginally upregulated in Fenofibrate-treated cells, indicating that inhibition of PPAR α strongly affects lipid metabolism (Fig. 7E). In contrast, expression of genes that are associated with purine metabolism was upregulated after PPAR α activation, while

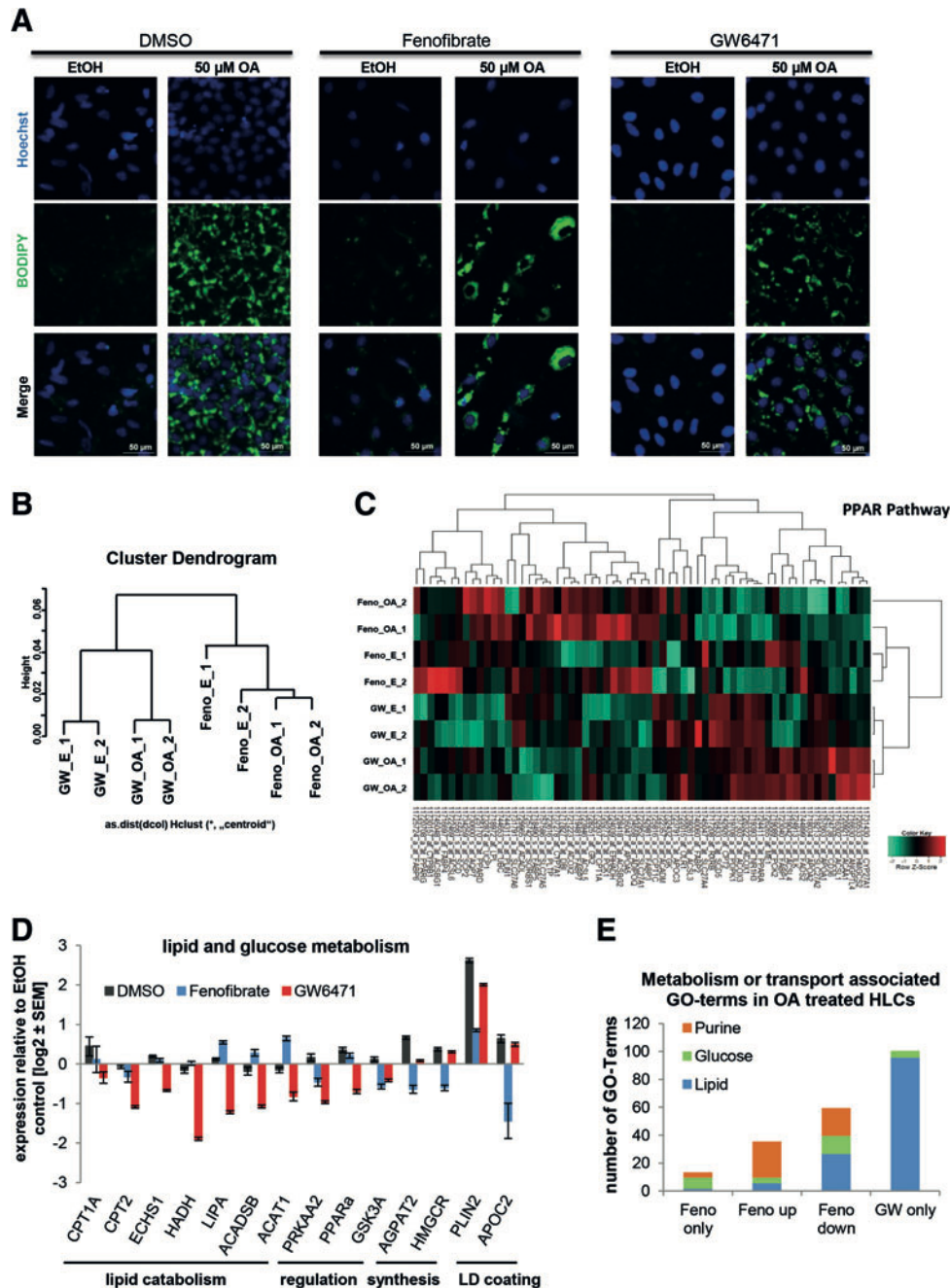


FIG. 7. PPAR α signaling has major impact on the induction of steatosis. IPSC-derived HLCs were incubated in parallel with either Fenofibrate (Feno, PPAR α agonist) or GW6471 (PPAR α antagonist) during the 48 h OA induction. **(A)** Steatosis induction was monitored by BODIPY 493/503 (green) staining of LDs. In every case, LDs increased after OA induction (right columns) compared to the control (left columns), but no differences between the different PPAR α treatments are visible. **(B)** Microarray-based transcriptome analysis revealed two distinct clusters representing Fenofibrate and GW6471 treatment and two subclusters related to OA treatment ($n=2$). **(C)** Heatmap representation of PPAR pathway genes shows distinct gene expression profiles for Fenofibrate (“F”) and GW6471 (“GW”) treated cells with qualitative changes after OA induction. Expression of genes involved in lipid or glucose metabolism **(D)** was analyzed using qRT-PCR ($n=2$). As expected, in most cases, Fenofibrate and GW6471 treatment had opposing effects on gene expression. Gene expression was normalized to β -actin and, subsequently, to the ethanol-treated control samples. For each sample, the mean \pm standard error of duplicate experiments is shown as \log_2 scale. **(E)** Significantly expressed genes from the global analysis were subdivided into genes only expressed after Fenofibrate treatment, up- or downregulated after Fenofibrate treatment, compared to GW6471 treatment or only expressed after GW6471 treatment. Then they were assigned to GOs (Supplementary Table S9). The numbers of GO-terms that were associated with lipid, glucose, or purine metabolism and transport are displayed. GO, gene ontology; HLCs, hepatocyte-like cells; LDs, lipid droplets; OA, oleic acid; PPAR α , peroxisome proliferator-activated receptor alpha; qRT-PCR, quantitative reverse transcription polymerase chain reaction. Color images available online at www.liebertpub.com/scd

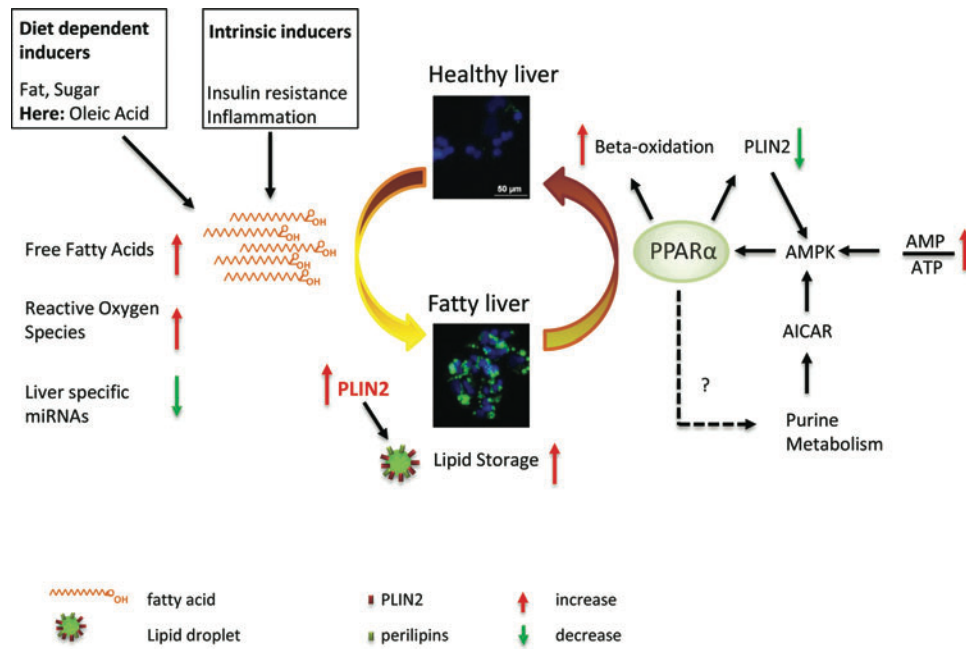


FIG. 8. Schematic overview of inducers of NAFLD and potential intervention points. The transition from a healthy liver (upper panel) toward a fatty liver (lower panel) is shown. Factors that promote NAFLD are shown on the left. Besides diet-related inducers that are in this study mimicked by OA addition to the medium, intrinsic factors like insulin resistance promote NAFLD. From a global perspective, the triggers result in increased free fatty acids and reactive oxygen species. We also observed a global downregulation of hepatic miRNAs. Eventually, every trigger results in an upregulation of PLIN2 expression and an increase in lipid storage within hepatocytes. Beneficial processes that might reduce fat content of hepatocytes are shown on the right side. In general, PPAR α activation (in our case by application of Fenofibrate) decreases the amount of stored fat by inducing β -oxidation. Besides fibrates, which activate PPAR α , it is also regulated by AMPK, which senses the low energy state of a cell as measured by the ratio between AMP and ATP. AMPK expression increases in response to PLIN2 knockdown conditions and its activity might be regulated by intermediates of purine metabolism, which is in turn regulated by PPAR α . This indicates a possible positive feedback loop that has to be verified by additional experiments. Besides PPAR α modulation, a direct reduction of PLIN2 expression could also be beneficial. AMP, adenosine monophosphate; AMPK, adenosine monophosphate-activated protein kinase; ATP, adenosine triphosphate; NAFLD, non-alcoholic fatty liver disease; OA, oleic acid; PLIN, Perilipin 2; PPAR α , peroxisome proliferator-activated receptor alpha. Color images available online at www.liebertpub.com/scd

none of the genes that were exclusively expressed in GW6471-treated cells mapped onto this GO-category.

A detailed analysis of the purine metabolic pathway demonstrated that genes associated with the early steps of purine metabolism tended to be downregulated under Fenofibrate treatment, while genes for the later steps were either upregulated or exclusively expressed during Fenofibrate treatment (Supplementary Fig. S3). This implies that PPAR α activation regulates purine metabolism.

Taken together, we have generated a robust in vitro model for NAFLD based on human PSC-derived HLCs. Upon OA induction, the cells recapitulate many features observed in NAFLD patients (LD accumulation, PLIN2 overexpression, and dysregulation of metabolic pathways) and they react to variation of PPAR α activity.

Discussion

In this study, we established a cell culture model for deciphering the molecular basis underlying early steps of LD accumulation in NAFLD, based on HLCs derived from hPSCs. We showed that ESCs and iPSCs both differentiate into HLCs that express hepatocyte-specific proteins and have characteristic hepatocyte-like biochemical functions. HLCs

could be induced to accumulate fat in LDs by incubating them with OA. Global gene expression analysis after OA induction revealed upregulation of many GO-categories associated with lipid or glucose metabolism. This effect was qualitatively similar between ESC- and iPSC-derived HLCs, but differed quantitatively due to the different genetic backgrounds of the two cell lines and the usual interdifferentiation variations. Importantly, ethanol-treated control cells had a completely different panel of genes upregulated, which mapped to GO-categories related to signaling or nonhepatic development. This indicates that expression changes observed in the OA group are not induced by the solvent ethanol, but rather by OA itself. However, for the future, it is important to compare effects of different steatosis inducing agents, for example, palmitic acid or steatogenic drugs.

After OA induction, many members of the PPAR signaling pathway, which controls lipid metabolism, were upregulated. Of the different PPAR isoforms, PPAR α is most abundant in the liver. It regulates lipid metabolism as a reaction to nutritional status and partly depends on insulin signaling [34]. In general, activation of PPAR α with fibrates is a recognized treatment for the metabolic syndrome [38] and its expression levels negatively correlate with the severity of NASH [39].

Upon induction of steatosis, expression of a panel of genes important for lipid metabolism changed in the same manner as previously observed by comparing liver biopsies from patients with high versus low levels of steatosis [31]. Among these factors, we identified *PLIN2* upregulation as a suitable marker for successful induction of steatosis. *PLIN2* is involved in the synthesis of LDs and plays an important role in the onset of steatosis. It has been shown that *PLIN2* knockout mice develop neither obesity nor steatosis [16] and the knockdown of *PLIN2* expression with an antisense oligonucleotide protected mice against the development of fatty liver [14].

To analyze the influence of *PLIN2* expression on the development of steatosis, we knocked down *PLIN2* in HepG2 cells using siRNAs. Although the knockdown was highly efficient with only 32% of protein expression remaining, we could not observe any changes in LD accumulation after induction with OA. This might be due to the short time period of only 48 h. There might still be enough *PLIN2* left for coverage of some LDs, while the shortage of *PLIN2* limits the amount of LDs that can be assembled over the long term. In addition, several other proteins are involved in LD formation. During steatosis, LDs increase in size relative to the abundance of TAGs [36]. The largest LDs are predominantly covered by *PLIN1*, which competes on the LD surface with *PLIN2* [36]. Global gene expression analysis of *PLIN2* knockdown cells revealed indeed that *PLIN1* and *PLIN4* expression was enhanced in at least two of the four samples compared to the nt siRNA samples.

Overall, we observed profound genome-wide transcriptional changes, which are reflected by the fact that the transcriptomes of *PLIN2* and nt siRNA-treated cells cluster separately from each other. Interestingly, expression levels of several factors known to have important regulatory functions on metabolism were altered after *PLIN2* knockdown. For example, *PRKAA2*, which is the catalytic subunit of adenosine monophosphate-activated protein kinase (AMPK), a sensor of nutritional level that becomes activated during fasting [40] was strongly upregulated in *PLIN2* knockdown cells, but reduced again upon OA induction. This shows that the cells still react to nutritional abundance. The lack of *PLIN2*, although it does not have a detectable influence on LDs, seems to transfer some kind of fasting signal that activates *PRKAA2* transcription. However, our data do not provide any information on *PRKAA2* activity, which has to be analyzed in the future.

In addition, *PPAR α* and γ , which regulate lipid metabolism, were downregulated in *PLIN2* siRNA-treated cells. This fits well with the predominant downregulation of lipid catabolism genes that are at least, in part, directly regulated by *PPAR α* . Our data point at the existence of a *PPAR*-gene regulatory network that depends on *PLIN2* levels. In addition, expression levels of genes important for insulin signaling were altered after *PLIN2* siRNA treatment. Interestingly, the expression of *IGFBP2* and 3, two important regulators of IGF1 signaling [41], were induced, while IGF itself was reduced. Overall, these data indicate that although *PLIN2* knockdown has no detectable effect on LD formation, it has a major impact on metabolic activities of the cell.

A knockdown of *PLIN2* was not possible in HLCs because of the low transfection efficiency in primary cells. As *PLIN2* is a target of *PPAR α* signaling [39], we interfered with

PPAR α activity using two small molecules, Fenofibrate (agonist) and GW6471 (antagonist). Again, we could not observe any changes in LD formation after treating induced HLCs with either Fenofibrate or GW6471. However, we investigated only short-term effects and it has been shown that *PPAR α* activation over a longer time period reduces steatosis in HepaRG cells [37]. Nonetheless, we observed major gene expression changes that occur as an immediate reaction toward *PPAR α* modulation accompanying OA induction. Expressed genes could be mapped to pathways related to lipid, glucose, and purine metabolism. Interestingly, the latter was not present in OA-induced HLCs, where *PPAR α* activity was reduced by GW6471. In this study, the most prominently upregulated GOs belonged to lipid metabolism. This indicates that the *PPAR α* agonist and antagonist do not simply influence gene expression in opposing directions, although we observed this for a panel of key metabolic genes, but they also modify metabolic pathways from different angles.

Genes of the purine metabolism were generally regulated in Fenofibrate-treated cells. A recent study by Asby et al. demonstrated that Aminoimidazole carboxamide ribonucleotide (AICAR), an intermediate product in de-novo purine synthesis, activates AMPK [42], which is a key regulator of metabolism that senses the nutritional state of the cell and induces *PPAR α* activity and catabolic pathways [40]. We observed that genes, which directly precede the synthesis of AICAR, were either upregulated or exclusively expressed during Fenofibrate treatment. Thus, it is possible that in addition to a direct influence on fat and glucose metabolism, *PPAR α* also indirectly enhances these pathways by regulating purine metabolism, and thus, AMPK activity.

For most of the genes that were analyzed in more detail, treatment with the *PPAR α* agonist and antagonist resulted as expected in opposing changes in expression. While GW6471-mediated inhibition of *PPAR α* resulted in downregulation of genes involved in lipid catabolism, activation using Fenofibrate reduced expression of *AGPAT2* and *HMGCR*, which are involved in biosynthesis of phospholipids and cholesterol, respectively. Thus, our HLC model can, in part, reproduce the beneficial role of *PPAR α* enhancement in patients with metabolic syndrome at least with regard to the reduced expression of lipid and cholesterol synthesizing enzymes.

In addition to major gene expression changes, we observed that the expression of most liver-specific microRNAs was downregulated as an early reaction to steatosis induction. Among the most strongly downregulated miRNAs, miR-122 is a key factor in liver development, differentiation, and homeostasis. It is elevated in the serum of NAFLD patients, while its expression levels in hepatocytes are concomitantly reduced, which is corroborated by our observations [43,44]. MiR-122a knockout mice develop steatosis and have altered levels of enzymes important for lipogenesis, LD formation, and lipid transport [45,46]. MiR-106b has not yet been associated with NAFLD, but its overexpression has been reported during development of cirrhosis and hepatocellular carcinoma [47].

Among the putative miR-106b and -122 targets predicted by at least four of the algorithms implemented in miRWalk, we confirmed *CPAMD8*, *ATL3*, and *EPHA7* as new miR-122 and miR-106b targets, respectively. None of these three proteins have been functionally associated with NAFLD. However, the validated, as well as the predicted, impact of

downregulated liver-related miRNAs on their expression together with their concordant upregulation in induced HLCs point to a functional role of these factors, but mechanisms remain to be elucidated.

We are aware of the fact that the two analyzed hPSC lines can only give a first impression of the general mechanisms of NAFLD development. To dissect these in more detail, we have generated several patient-specific iPSC lines, which are currently being characterized and which will be used in the future for more detailed analyses of the disease [48].

To summarize, our results show that hPSC-derived HLCs are a valuable in vitro model for investigating the molecular basis of the early steps of NAFLD. They accumulate LDs, and expression changes of metabolically relevant genes mirror those observed in liver biopsies of steatosis patients [31]. In addition, lipid metabolism can be regulated by modulating the activity of PPAR α . A short overview of the different processes is given in Fig. 8.

Acknowledgments

J.A. acknowledges support from the Medical faculty of the Heinrich Heine University Düsseldorf. The authors thank M. Bohndorf and S. Wehrmeyer for technical support.

Prior Conference Presentation: Part of the work was presented as a poster at the 8th International Meeting of the Stem Cell Network North Rhine-Westphalia, April 21–22, 2015, Bonn, Germany.

Author Disclosure Statement

No competing financial interests exist.

References

- Cohen JC, JD Horton and HH Hobbs. (2011). Human fatty liver disease: old questions and new insights. *Science* 332: 1519–1523.
- Perry RJ, JP Camporez, R Kursawe, PM Titchenell, D Zhang, CJ Perry, MJ Jurczak, A Abudukadier, MS Han, et al. (2015). Hepatic acetyl CoA links adipose tissue inflammation to hepatic insulin resistance and type 2 diabetes. *Cell* 160:745–758.
- Basaranoglu M, G Basaranoglu and H Senturk. (2013). From fatty liver to fibrosis: a tale of “second hit”. *World J Gastroenterol* 19:1158–1165.
- Okumura T. (2011). Role of lipid droplet proteins in liver steatosis. *J Physiol Biochem* 67:629–636.
- Thiele C and J Spandl. (2008). Cell biology of lipid droplets. *Curr Opin Cell Biol* 20:378–385.
- Greenberg AS, RA Coleman, FB Kraemer, JL McManaman, MS Obin, V Puri, QW Yan, H Miyoshi and DG Mashek. (2011). The role of lipid droplets in metabolic disease in rodents and humans. *J Clin Invest* 121:2102–2110.
- Listenberger LL, AG Ostermeyer-Fay, EB Goldberg, WJ Brown and DA Brown. (2007). Adipocyte differentiation-related protein reduces the lipid droplet association of adipose triglyceride lipase and slows triacylglycerol turnover. *J Lipid Res* 48:2751–2761.
- Sztalryd C, G Xu, H Dorward, JT Tansey, JA Contreras, AR Kimmel and C Londos. (2003). Perilipin A is essential for the translocation of hormone-sensitive lipase during lipolytic activation. *J Cell Biol* 161:1093–1103.
- Miyoshi H, SC Souza, HH Zhang, KJ Strissel, MA Christoffolete, J Kovsan, A Rudich, FB Kraemer, AC Bianco, MS Obin and AS Greenberg. (2006). Perilipin promotes hormone-sensitive lipase-mediated adipocyte lipolysis via phosphorylation-dependent and -independent mechanisms. *J Biol Chem* 281:15837–15844.
- Brasaemle DL, T Barber, NE Wolins, G Serrero, EJ Blanchette-Mackie and C Londos. (1997). Adipose differentiation-related protein is an ubiquitously expressed lipid storage droplet-associated protein. *J Lipid Res* 38:2249–2263.
- Targett-Adams P, D Chambers, S Gledhill, RG Hope, JF Coy, A Girod and J McLauchlan. (2003). Live cell analysis and targeting of the lipid droplet-binding adipocyte differentiation-related protein. *J Biol Chem* 278:15998–16007.
- Imamura M, T Inoguchi, S Ikuyama, S Taniguchi, K Kobayashi, N Nakashima and H Nawata. (2002). ADRP stimulates lipid accumulation and lipid droplet formation in murine fibroblasts. *Am J Physiol Endocrinol Metab* 283: E775–E783.
- Motomura W, M Inoue, T Ohtake, N Takahashi, M Nagamine, S Tanno, Y Kohgo and T Okumura. (2006). Up-regulation of ADRP in fatty liver in human and liver steatosis in mice fed with high fat diet. *Biochem Biophys Res Commun* 340:1111–1118.
- Imai Y, S Boyle, GM Varela, E Caron, X Yin, R Dhir, R Dhir, MJ Graham and RS Ahima. (2012). Effects of perilipin 2 antisense oligonucleotide treatment on hepatic lipid metabolism and gene expression. *Physiol Genomics* 44:1125–1131.
- Imai Y, GM Varela, MB Jackson, MJ Graham, RM Crooke and RS Ahima. (2007). Reduction of hepatosteatosis and lipid levels by an adipose differentiation-related protein antisense oligonucleotide. *Gastroenterology* 132:1947–1954.
- McManaman JL, ES Bales, DJ Orlicky, M Jackman, PS MacLean, S Cain, AE Crunk, A Mansur, CE Graham, TA Bowman and AS Greenberg. (2013). Perilipin-2-null mice are protected against diet-induced obesity, adipose inflammation, and fatty liver disease. *J Lipid Res* 54:1346–1359.
- Takahashi Y, Y Soejima and T Fukusato. (2012). Animal models of nonalcoholic fatty liver disease/nonalcoholic steatohepatitis. *World J Gastroenterol* 18:2300–2308.
- Machado MV, GA Michelotti, G Xie, TP de Almeida, J Boursier, B Bohnic, CD Guy and AM Diehl. (2015). Mouse models of diet-induced nonalcoholic steatohepatitis reproduce the heterogeneity of the human disease. *PLoS One* 10:e0127991.
- Ricchi M, MR Odoardi, L Carulli, C Anzivino, S Ballestri, A Pinetti, LI Fantoni, F Marra, M Bertolotti, et al. (2009). Differential effect of oleic and palmitic acid on lipid accumulation and apoptosis in cultured hepatocytes. *J Gastroenterol Hepatol* 24:830–840.
- De Gottardi A, M Vinciguerra, A Sgroi, M Moukil, F Ravier-Dall’Antonia, V Paziienza, P Pugnale, M Foti and A Hadengue. (2007). Microarray analyses and molecular profiling of steatosis induction in immortalized human hepatocytes. *Lab Invest* 87:792–806.
- Currie E, A Schulze, R Zechner, TC Walther and RV Farese, Jr. (2013). Cellular fatty acid metabolism and cancer. *Cell Metab* 18:153–161.
- Cantor JR and DM Sabatini. (2012). Cancer cell metabolism: one hallmark, many faces. *Cancer Discov* 2:881–898.
- Godoy P, NJ Hewitt, U Albrecht, ME Andersen, N Ansari, S Bhattacharya, JG Bode, J Bolleyn, C Borner, et al. (2013). Recent advances in 2D and 3D in vitro systems using primary hepatocytes, alternative hepatocyte sources and non-parenchymal liver cells and their use in investigating mech-

- anisms of hepatotoxicity, cell signaling and ADME. *Arch Toxicol* 87:1315–1530.
24. Thomson JA, J Itskovitz-Eldor, SS Shapiro, MA Waknitz, JJ Swiergiel, VS Marshall and JM Jones. (1998). Embryonic stem cell lines derived from human blastocysts. *Science* 282:1145–1147.
 25. Wang Y and J Adjaye. (2011). A cyclic AMP analog, 8-Br-cAMP, enhances the induction of pluripotency in human fibroblast cells. *Stem Cell Rev* 7:331–341.
 26. Iwaniuk KM, J Schira, S Weinhold, M Jung, J Adjaye, HW Muller, P Wernet and HI Trompeter. (2011). Network-like impact of MicroRNAs on neuronal lineage differentiation of unrestricted somatic stem cells from human cord blood. *Stem Cells Dev* 20:1383–1394.
 27. Trompeter HI, H Abbad, KM Iwaniuk, M Hafner, N Renwick, T Tuschl, J Schira, HW Muller and P Wernet. (2011). MicroRNAs MiR-17, MiR-20a, and MiR-106b act in concert to modulate E2F activity on cell cycle arrest during neuronal lineage differentiation of USSC. *PLoS One* 6:e16138.
 28. Hay DC, D Zhao, J Fletcher, ZA Hewitt, D McLean, A Urruticochea-Uruguén, JR Black, C Elcombe, JA Ross, R Wolf and W Cui. (2008). Efficient differentiation of hepatocytes from human embryonic stem cells exhibiting markers recapitulating liver development in vivo. *Stem Cells* 26:894–902.
 29. Hay DC, J Fletcher, C Payne, JD Terrace, RC Gallagher, J Snoeys, JR Black, D Wojtacha, K Samuel, et al. (2008). Highly efficient differentiation of hESCs to functional hepatic endoderm requires ActivinA and Wnt3a signaling. *Proc Natl Acad Sci U S A* 105:12301–12306.
 30. Jozefczuk J, A Prigione, L Chavez and J Adjaye. (2011). Comparative analysis of human embryonic stem cell and induced pluripotent stem cell-derived hepatocyte-like cells reveals current drawbacks and possible strategies for improved differentiation. *Stem Cells Dev* 20:1259–1275.
 31. Wruck W, K Kashofer, S Rehman, A Daskalaki, D Berg, E Gralka, J Jozefczuk, K Drews, V Pandey, et al. (2015). Multi-omic profiles of human non-alcoholic fatty liver disease tissue highlight heterogenic phenotypes. *Sci Data* 2:150068.
 32. McMullen PD, S Bhattacharya, CG Woods, B Sun, K Yarborough, SM Ross, ME Miller, MT McBride, EL LeCluyse, RA Clewell and ME Andersen. (2014). A map of the PPARalpha transcription regulatory network for primary human hepatocytes. *Chem Biol Interact* 209:14–24.
 33. Grygiel-Gorniak B. (2014). Peroxisome proliferator-activated receptors and their ligands: nutritional and clinical implications—a review. *Nutr J* 13:17.
 34. Pawlak M, P Lefebvre and B Staels. (2015). Molecular mechanism of PPARalpha action and its impact on lipid metabolism, inflammation and fibrosis in non-alcoholic fatty liver disease. *J Hepatol* 62:720–733.
 35. Targett-Adams P, MJ McElwee, E Ehrenborg, MC Gustafsson, CN Palmer and J McLauchlan. (2005). A PPAR response element regulates transcription of the gene for human adipose differentiation-related protein. *Biochim Biophys Acta* 1728:95–104.
 36. Pawella LM, M Hashani, E Eiteneuer, M Renner, R Bartschlagel, P Schirmacher and BK Straub. (2014). Perilipin discerns chronic from acute hepatocellular steatosis. *J Hepatol* 60:633–642.
 37. Rogue A, S Antherieu, A Vluggens, T Umbdenstock, N Claude, C de la Moureyre-Spire, RJ Weaver and A Guillouzo. (2014). PPAR agonists reduce steatosis in oleic acid-overloaded HepaRG cells. *Toxicol Appl Pharmacol* 276:73–81.
 38. Michalik L, J Auwerx, JP Berger, VK Chatterjee, CK Glass, FJ Gonzalez, PA Grimaldi, T Kadowaki, MA Lazar, et al. (2006). International Union of Pharmacology. LXI. Peroxisome proliferator-activated receptors. *Pharmacol Rev* 58:726–741.
 39. Francque S, A Verrijken, S Caron, J Prawitt, R Paumelle, B Derudas, P Lefebvre, MR Taskinen, W Van Hul, et al. (2015). PPARalpha gene expression correlates with severity and histological treatment response in patients with non-alcoholic steatohepatitis. *J Hepatol* 63:164–173.
 40. Fogarty S and DG Hardie. (2010). Development of protein kinase activators: AMPK as a target in metabolic disorders and cancer. *Biochim Biophys Acta* 1804:581–591.
 41. Yamada PM, HH Mehta, D Hwang, KP Roos, AL Hevener and KW Lee. (2010). Evidence of a role for insulin-like growth factor binding protein (IGFBP)-3 in metabolic regulation. *Endocrinology* 151:5741–5750.
 42. Asby DJ, F Cuda, M Beyaert, FD Houghton, FR Cagampang and A Tavassoli. (2015). AMPK activation via modulation of de novo purine biosynthesis with an inhibitor of ATIC homodimerization. *Chem Biol* 22:838–848.
 43. Pirola CJ, T Fernandez Gianotti, GO Castano, P Mallardi, J San Martino, M Mora Gonzalez Lopez Ledesma, D Flichman, F Mirshahi, AJ Sanyal and S Sookoian. (2015). Circulating microRNA signature in non-alcoholic fatty liver disease: from serum non-coding RNAs to liver histology and disease pathogenesis. *Gut* 64:800–812.
 44. Cermelli S, A Ruggieri, JA Marrero, GN Ioannou and L Beretta. (2011). Circulating microRNAs in patients with chronic hepatitis C and non-alcoholic fatty liver disease. *PLoS One* 6:e23937.
 45. Hsu SH, B Wang, J Kota, J Yu, S Costinean, H Kutay, L Yu, S Bai, K La Perle, et al. (2012). Essential metabolic, anti-inflammatory, and anti-tumorigenic functions of miR-122 in liver. *J Clin Invest* 122:2871–2883.
 46. Tsai WC, SD Hsu, CS Hsu, TC Lai, SJ Chen, R Shen, Y Huang, HC Chen, CH Lee, et al. (2012). MicroRNA-122 plays a critical role in liver homeostasis and hepatocarcinogenesis. *J Clin Invest* 122:2884–2897.
 47. Tan W, Y Li, SG Lim and TM Tan. (2014). miR-106b-25/miR-17-92 clusters: polycistrons with oncogenic roles in hepatocellular carcinoma. *World J Gastroenterol* 20:5962–5972.
 48. Jozefczuk J, K Kashofer, R Ummanni, F Henjes, S Rehman, S Geenen, W Wruck, C Regenbrecht, A Daskalaki, et al. (2012). A systems biology approach to deciphering the etiology of steatosis employing patient-derived dermal fibroblasts and iPS cells. *Front Physiol* 3:339.

Address correspondence to:

*Prof. James Adjaye
Institute for Stem Cell Research
and Regenerative Medicine
Heinrich Heine University Düsseldorf
Moorenstrasse 5
Düsseldorf 40225
Germany*

E-mail: james.adjaye@med.uni-duesseldorf.de

Received for publication December 16, 2015

Accepted after revision June 15, 2016

Prepublished on Liebert Instant Online June 16, 2016

RESEARCH ARTICLE

Cell fate decisions of human iPSC-derived bipotential hepatoblasts depend on cell density

Nina Graffmann, Audrey Ncube, Wasco Wruck, James Adjaye*

Institute for Stem Cell Research and Regenerative Medicine, Medical faculty, Heinrich-Heine University, Düsseldorf, Germany

* James.Adjaye@med.uni-duesseldorf.de



OPEN ACCESS

Citation: Graffmann N, Ncube A, Wruck W, Adjaye J (2018) Cell fate decisions of human iPSC-derived bipotential hepatoblasts depend on cell density. PLoS ONE 13(7): e0200416. <https://doi.org/10.1371/journal.pone.0200416>

Editor: Edward E. Schmidt, Montana State University Bozeman, UNITED STATES

Received: February 23, 2018

Accepted: June 26, 2018

Published: July 10, 2018

Copyright: © 2018 Graffmann et al. This is an open access article distributed under the terms of the [Creative Commons Attribution License](https://creativecommons.org/licenses/by/4.0/), which permits unrestricted use, distribution, and reproduction in any medium, provided the original author and source are credited.

Data Availability Statement: All relevant data are within the paper and its Supporting Information files. Additional gene expression files are available from the GEO database, accession number GSE116455. <https://www.ncbi.nlm.nih.gov/geo/query/acc.cgi?acc=GSE116455>.

Funding: N.G. acknowledges support from the Research commission of the Medical faculty of Heinrich Heine University Düsseldorf (www.medizin.hhu.de/dekanat/gremien-und-kommissionen/kommissionen/forschungskommission.html). J.A. acknowledges

Abstract

During embryonic development bipotential hepatoblasts differentiate into hepatocytes and cholangiocytes- the two main cell types within the liver. Cell fate decision depends on elaborate interactions between distinct signalling pathways, namely Notch, WNT, TGF β , and Hedgehog. Several *in vitro* protocols have been established to differentiate human pluripotent stem cells into either hepatocyte or cholangiocyte like cells (HLC/CLC) to enable disease modelling or drug screening. During HLC differentiation we observed the occurrence of epithelial cells with a phenotype divergent from the typical hepatic polygonal shape- we refer to these as endoderm derived epithelial cells (EDECs). These cells do not express the mature hepatocyte marker ALB or the progenitor marker AFP. However they express the cholangiocyte markers SOX9, OPN, CFTR as well as HNF4 α , CK18 and CK19. Interestingly, they express both E Cadherin and Vimentin, two markers that are mutually exclusive, except for cancer cells. EDECs grow spontaneously under low density cell culture conditions and their occurrence was unaffected by interfering with the above mentioned signalling pathways.

Introduction

In vitro differentiation of human pluripotent stem cells (hPSCs) into hepatocyte like cells (HLCs) or cholangiocyte like cells (CLCs) provide valuable tools for modelling hepatogenesis, studying liver-associated diseases, assessing toxicology and for drug screenings. Several protocols have been established to obtain one or the other cell type [1–10]. The success of differentiation highly depends on the quality of the pluripotent stem cells, the initial seeding density of the culture and the proliferation rate of the cells. The ultimate goal is to obtain a pure population of HLCs which have Cytochrome P450 enzyme activity and recapitulate disease associated phenotypes [4–6] or CLCs which are able to form ductal structures in a 3D culture system [7–10].

Bipotential hepatoblasts give rise to hepatocytes and cholangiocytes *in vivo* [11–13]. Hepatocytes are the most abundant cell type in the liver and responsible for metabolism, nutrient

support from the Medical faculty of Heinrich Heine University Düsseldorf. The funders had no role in study design, data collection and analysis, decision to publish, or preparation of the manuscript

Competing interests: The authors have declared that no competing interests exist.

storage and drug detoxification. Cholangiocytes are epithelial cells which line the bile ducts that draw through the liver parenchyme and transport bile into the gall bladder. Several signalling pathways have been shown to be involved in the cell fate decision making between hepatocytes and cholangiocytes.

Notch signalling is crucial for the development of cholangiocytes. Impaired Notch signalling due to *JAGGED1* (*JAG1*) or *NOTCH2* mutations causes Alagille Syndrome, a disease that manifests in the liver by a reduction of bile ducts in combination with cholestasis [14–16]. Bile ducts form during liver development next to the portal vein. Bipotential hepatoblasts are specified towards the cholangiocyte fate by Notch signalling, mediated by Notch2 [17, 18]. They form the ductal plate which is the starting point for bile-duct tubulogenesis [17]. Notch signalling in cells adjacent to this first layer of cholangiocytes induces tubulogenesis. After the first ductal structures have formed, all cells lining the duct differentiate towards cholangiocytes [17]. Interestingly, *NOTCH3* is the only family member that directs hepatoblasts towards hepatocytes [19].

Susceptibility to Notch signalling depends on transforming growth factor (TGF) β -signalling. As cells of the periportal mesenchyme are major sources for TGF β secretion, a gradient with decreasing concentrations forms along the periportal-parenchyme axis [20, 21]. Cells near the periportal region are most strongly stimulated by TGF β and they are the first to form the ductal plate as described above.

Additionally, wingless-type MMTV integration site family (WNT) signalling has been proposed to be involved in hepatic cell fate specification, however, to date contradictory results preclude an unambiguous assignment of its exact role in this process. Several studies have indicated that WNT- β -catenin signalling promotes cholangiocyte and not hepatocyte fate [22, 23], while Cordi *et al.* recently demonstrated that β -catenin is not necessary for biliary development but that its overexpression perturbs cholangiocyte differentiation as well as bile duct morphogenesis [24].

Finally, Hedgehog (Hh) is involved in the complex signalling orchestra that regulates hepatic cell fate. Bipotential hepatoblasts produce and respond to Hh ligands. This dual capacity is retained in cholangiocytes, while healthy hepatocytes lose the ability to produce Hh ligands or to react to its signals. However, upon liver injury they regain the ability to produce Hh ligands [25].

During HLC differentiation *in vitro*, we often observed cells with an epithelial but non-polygonal morphology lacking HLC characteristics occurring at areas of the dish where cell density is low. Here we set out to characterize these cells and applied distinct pathway inhibitors with the aim to reduce their appearance during HLC differentiation and maybe increase the homogeneity of HLC populations.

Materials and methods

Ethics statement

The use of iPSC lines for this study was approved by the ethics committee of the medical faculty of Heinrich-Heine University under the number 5013.

Cell culture

The human ESC line H1 was purchased from WiCell Research Institute (Madison, WI, USA), human iPSCs were generated as described in [26, 27].

hPSCs were cultured on matrigel (Corning) coated plates with Stem MACS (Miltenyi) or TSR E8 medium (Stemcell Technologies). Medium was changed on a daily basis. Spontaneously differentiated cells were removed manually if necessary. For differentiation, cells were

split onto matrigel coated plates and kept in the stem cell medium for another 16-24h. Afterwards, HLC differentiation was performed as described previously [1]. In brief, cells were first differentiated towards definitive endoderm (DE) using DE medium: 96% RPMI 1640, 2% B27 (without retinoic acid), 1% Glutamax (Glx), 1% Penicillin/Streptomycin (P/S) (all Gibco), 100 ng/ml Activin A (Peprotech) and for the first day 2.5 μ M Chir99021 (Tocris). After 5 days the medium was changed to one favouring hepatic endoderm (HE): 78% Knockout DMEM, 20% Knockout serum replacement, 0.5% Glx, 1% P/S, 0.01% 2-Mercaptoethanol (all Gibco) and 1% DMSO (Sigma), which was used for an additional 4 days. In order to induce endoderm derived epithelial cells (EDEC) differentiation, HE cells were split and plated onto matrigel coated plates on day 9 of the differentiation. Cell density has to be low to induce EDEC differentiation, which was achieved by seeding 25,000/cm² after splitting at the HE stage. On day 10 the differentiation was continued with HLC medium: 82% Leibovitz 15 medium, 8% fetal calf serum, 8% Tryptose Phosphate Broth, 1% Glx, 1% P/S (all Gibco) with 1 μ M Insulin (Sigma), 10 ng/ml hepatocyte growth factor (HGF) (Peprotech), 20 ng/ml Oncostatin M (OSM) 209 a.a. (Immunotools), 25 ng/ml Dexamethasone (DEX) (Sigma) (Fig 1A). During the course of

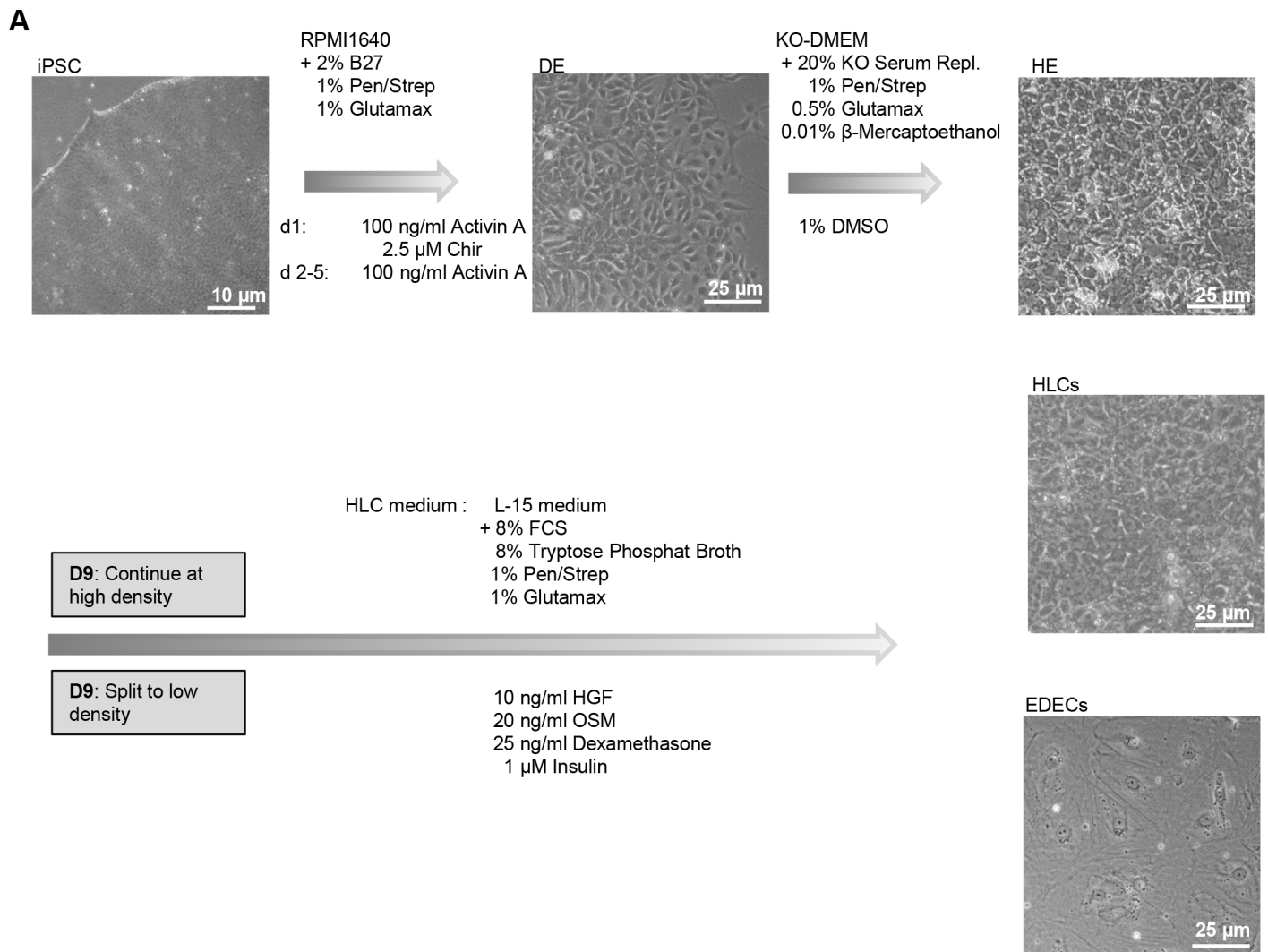


Fig 1. Differentiation of hPSCs into hepatocyte like cells (HLCs) and endoderm derived epithelial cells (EDECs). hPSCs were differentiated into hepatic endoderm (HE) which consists of bipotential hepatoblasts. Afterwards, cultures were either continued unperturbed in order to obtain HLCs, or split and replated at low density to obtain EDECs. Morphological changes were documented for each stage.

<https://doi.org/10.1371/journal.pone.0200416.g001>

differentiation towards the DE, HE and the beginning of the HLC/EDEC stage, medium was changed daily, but at later time points every other day.

In order to switch cell fate after HE stage, several signaling pathways were inhibited or activated with small molecules listed in [S1 Table](#).

Immunocytochemistry

Cells were fixed with 4% paraformaldehyde for 15 min. Unspecific binding sites were blocked by incubating 2 h at room temperature with blocking buffer (1x PBS with 10% normal goat or donkey serum, 1% BSA, 0.5% Triton and 0.05% Tween). Antibodies were diluted in blocking buffer diluted 1:2 with 1x PBS ([S2 Table](#)). Primary antibodies incubated overnight at 4°C. Cells were washed three times with 1x PBS/ 0.05% Tween and incubated with the secondary antibody for 2 h at room temperature. Cells were washed as above and images captured using a fluorescence microscope (LSM700, Zeiss). For extracellular stainings blocking and wash buffer without detergents were used. DNA was stained with Hoechst 33258 (Sigma). Individual channel images were processed and merged with Photoshop CS6 or Fiji.

RNA isolation and quantitative real time PCR (qRT-PCR). Up to 500,000 cells were lysed in 500 μ l Trizol and RNA was isolated with the Direct-zol™ RNA Isolation Kit (Zymo Research) according to the user's manual. On-column DNase digestion was performed. 500 ng of RNA were transcribed into cDNA using the TaqMan Reverse Transcription (RT) Kit (Applied Biosystems). In the case of H1 derived EDECs also cRNA obtained from Affymetrix Array preparation was transcribed into cDNA using the TaqMan RT kit with random hexamers instead of oligo-dT primers. Primers for qRT-PCR were purchased from MWG ([S3 Table](#)). Real time PCR was performed in technical triplicates of biological duplicates with Power Sybr Green Master Mix (life technologies) on a VIIA7 (life technologies). In the case of H1 derived EDECs with and without inhibitor only one biological sample was analyzed. Mean Ct values were normalized to RPS16 as a housekeeping gene and fold change was calculated relative to the controls. Results are depicted as mean values (log₂) with standard error of the mean (SEM). P-Values were calculated with two-tailed student's t-tests (** = p-value < 0.01, * = p-value < 0.05).

Transcriptome and bioinformatics analysis

Microarray experiments were performed employing the Affymetrix PrimeView chip (BMFZ, Düsseldorf). Details of data analysis are given in Supplementary materials and methods.

Biochemical activity assays

Cytochrome P450 3A4 (CYP3A4) activity was measured in technical triplicates with the respective P450 Glo assay from Promega, according to the recommendations. Supernatants were stored from every step of the differentiation process and urea content was measured in technical duplicates of biological duplicates with the QuantiChrom Urea Assay (Bioassay systems) according to the manufacturer's recommendations. Results are depicted as mean values with standard error of the mean (SEM) in case of the CYP3A4 assay and standard deviation in case of urea measurement. P-Values were calculated with two-tailed student's t-tests (** = p-value < 0.01, * = p-value < 0.05).

Results and discussion

Differentiation of hPSCs in high and low density conditions

During *in vitro* differentiation of hPSCs into hepatocyte like cells (HLCs), we frequently observed cells with atypical morphology, predominantly at the borders of densely grown

colonies. As these cells only occur at regions of low cellular density, we reasoned that they require only lose cell-cell contact in combination with enough space for growth. The cells are of endodermal origin and have an epithelial morphology but are much larger than HLCs or cholangiocyte like cells (CLCs). In order to characterize these endoderm derived epithelial cells (EDECs), we tried to produce a pure population by reducing cellular density during HLC differentiation. To this end, we differentiated two iPSC lines as well as H1 ESCs into bipotential hepatoblasts by following our recently published protocol for hepatocyte differentiation until the stage of hepatic endoderm (HE) [1]. The iPSC lines were derived from human fetal foreskin (HFF) [26] and human amniotic fluid (AF) cells [28], respectively. hPSCs changed their morphology upon induction of definitive endoderm (DE) and the typical loose and petal-like morphology became visible (Fig 1A upper row, middle panel). HE induction started after five days. At the end of this stage, the morphology of the cells resembled the typical polygonal structure of hepatocytes (Fig 1A upper row, right panel). We then either split and replated the HE cells at a low density in order to obtain an enriched population of the uncharacterized cells or we left the densely populated plates untouched for obtaining HLCs. From the next day on, culture medium was replaced with HLC medium and differentiation was continued for an additional five days. Cells cultivated at a high density only marginally changed their morphology and maintained the polygonal morphology which is typical of HLCs (Fig 1A middle row, right). However, cells split and replated at low density underwent dramatic morphological changes. They still had the typical epithelial cell-cell contact but were rather large with a flat and irregular shape. Interestingly, pronounced intracellular structures, which resemble parts of the cytoskeleton, as well as dark granula became visible (Fig 1A lowest row, right).

EDECs resemble CLCs but are Vimentin positive

The two iPSC lines as well as H1 ESCs were differentiated into HLCs and EDECs and stained for expression of characteristic markers at the respective end-stages. HLCs expressed Albumin (ALB) and Alpha Fetoprotein (AFP) as well as Cytokeratin 19 (CK19) and HNF4 α (Fig 2A–2C), while EDECs were negative for ALB and AFP but expressed high levels of CK19 as well as HNF4 α (Fig 2D–2F).

To test whether EDECs are related to cholangiocytes, we analysed the expression of characteristic markers for this cell type by immunocytochemistry. The cholangiocyte specific transcription factor SOX9 and the multifunctional protein osteopontin (OPN) were almost not present in HLCs at the protein level (Fig 3A and 3B). However, we could detect low level expression of the transporter Cystic Fibrosis Transmembrane Conductance Regulator (CFTR), but the protein was not as expected localized within the membrane, but in the cytoplasm (Fig 3C).

In contrast, EDECs expressed SOX9 as well as weak levels of OPN and they were highly positive for CFTR which is clearly localized within the cell membrane as expected in cholangiocytes (Fig 3D–3F).

Both HLCs and EDECs expressed E-Cadherin (ECAD), which is characteristic of epithelial cells (Fig 4A and 4B). However, RT-PCR revealed that they also expressed *Vimentin* (VIM, Fig 4C) an intermediate filament protein which defines mesenchymal cells. Its co-expression with ECAD has so far only been described in cancerous cells which undergo epithelial-to-mesenchymal transition [29]. EDECs were negative for *CDX2* expression, a transcription factor that is characteristic of intestinal cells (Fig 4C). GFAP, a marker for stellate cells, was only marginally expressed (Fig 4D).

HE cells which have the potential to differentiate into HLCs, CLCs and also EDECs were positive for all investigated markers that are known to be expressed in the immature stages of

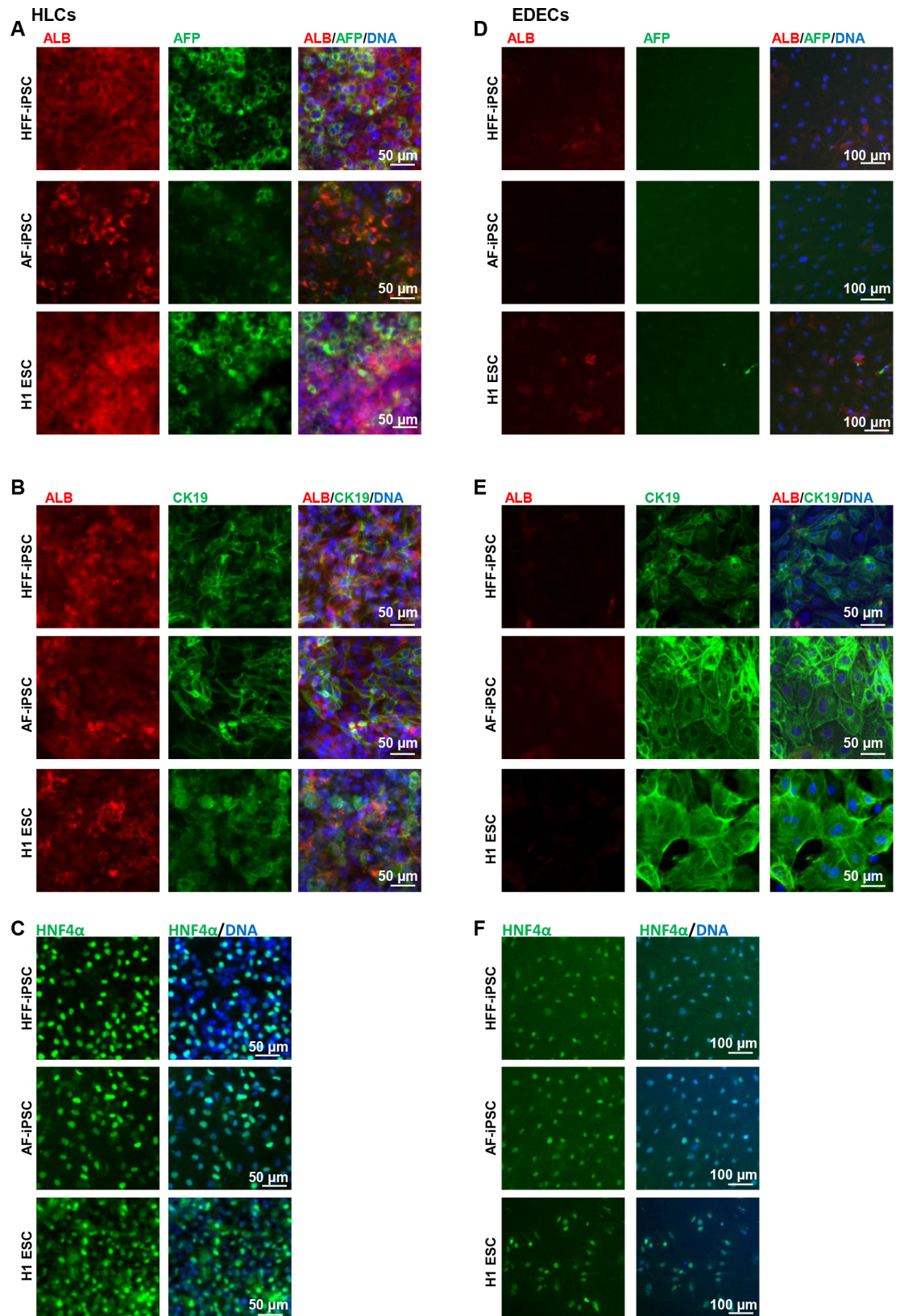


Fig 2. Expression of characteristic hepatocyte markers in HLCs and EDECs. Two iPSC lines and one ESC line were differentiated into either HLCs (A-C) or EDECs (D-F) and stained for the expression of characteristic hepatocyte markers.

<https://doi.org/10.1371/journal.pone.0200416.g002>

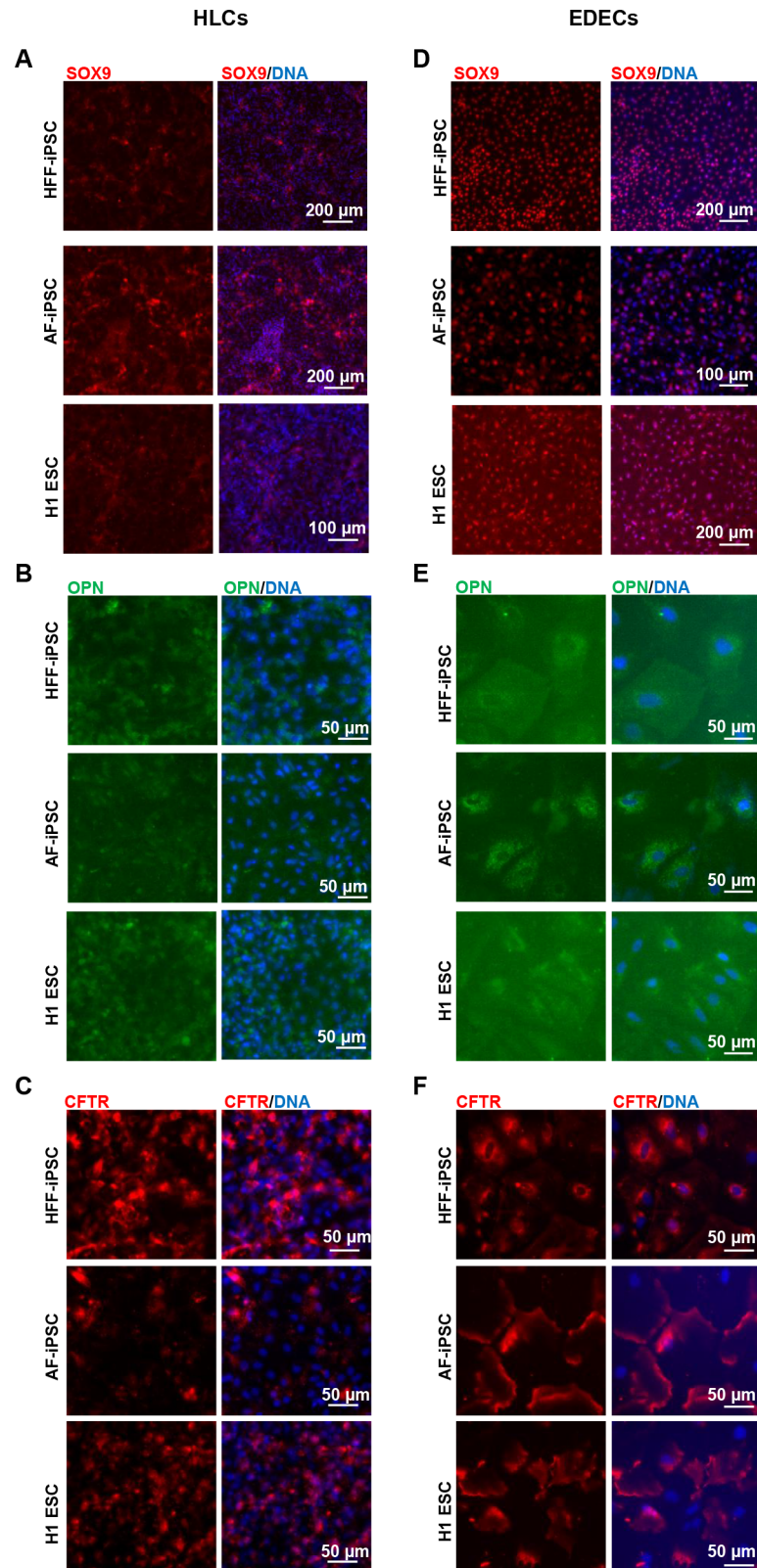


Fig 3. Expression of characteristic cholangiocyte markers in HLCs and EDECs. Two iPSC lines and one ESC line were differentiated into either HLCs (A-C) or EDECs (D-F) and stained for the expression of characteristic cholangiocyte markers.

<https://doi.org/10.1371/journal.pone.0200416.g003>

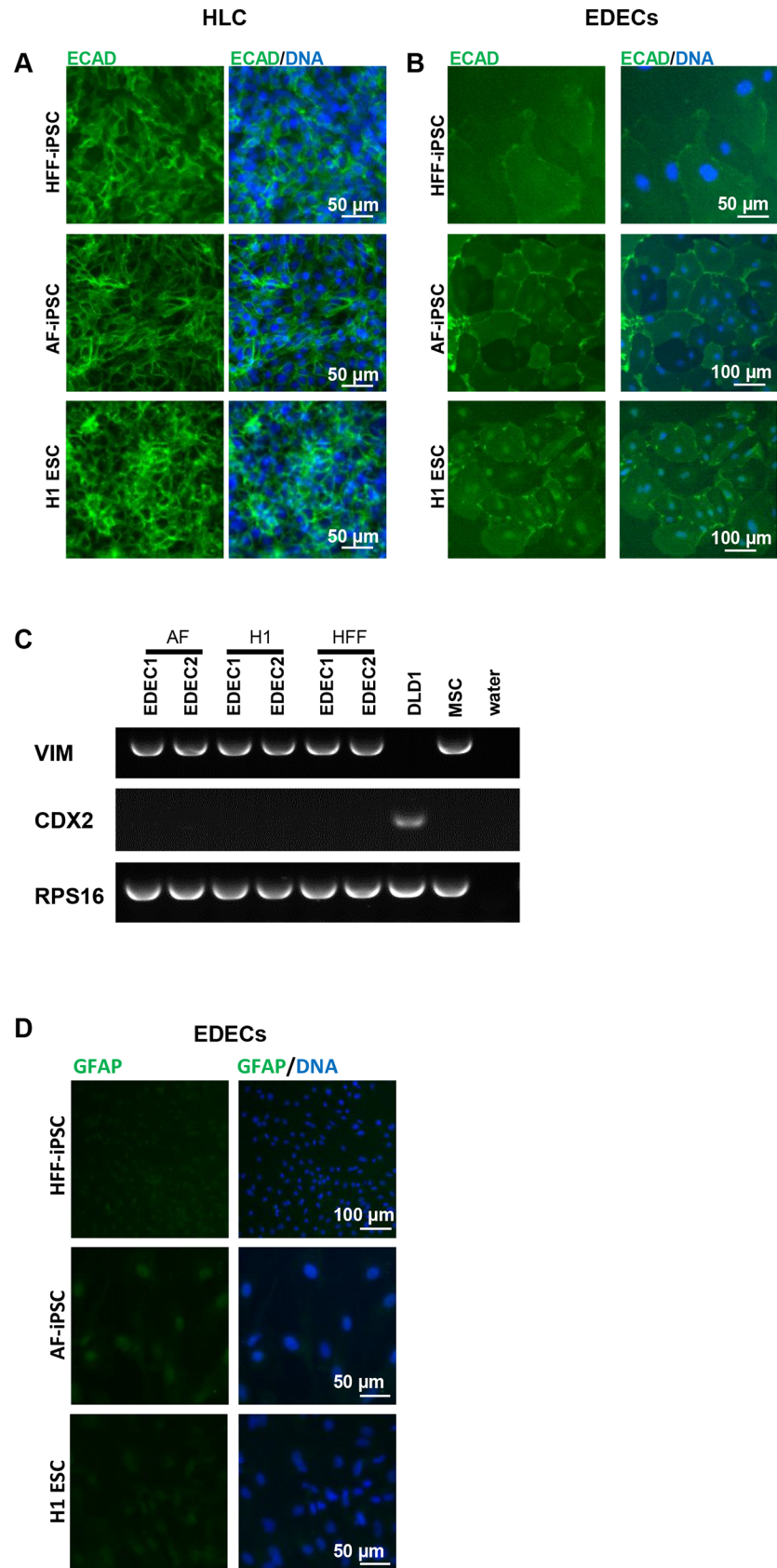


Fig 4. EDECs express a unique combination of markers. Two iPSC lines and one ESC line were differentiated into either HLCs (A) or EDECs (B-D) and marker expression was analysed. (A,B) Immunocytochemistry for ECAD. (C) Endpoint RT-PCR for *VIM* and *CDX2*. cDNA derived from mesenchymal stem cells (MSCs) and from the colon cancer line DLD1 served as positive controls for *VIM* and *CDX2* expression, respectively. (D) Immunocytochemistry for GFAP.

<https://doi.org/10.1371/journal.pone.0200416.g004>

either HLCs or EDECs, namely AFP, CK19, HNF4 α , SOX9, and ECAD (S1A–S1E Fig). However, more mature markers such as ALB, CFTR, and OPN were either inconsistently expressed or mislocalized (S1A, S1C and S1F Fig). In addition, HE cells were negative for GFAP (S1G Fig).

qRT-PCR revealed that crucial mature (*ALB*, *CYP3A4*) as well as immature (*AFP*) hepatocyte markers were significantly up-regulated in HLCs compared to EDECs and HE cells (Fig 5A–5C). Expression of *HNF4 α* , which marks early hepatic differentiation stages and mature hepatocytes, was highest in HE cells. This might imply that these cells are poised to differentiate along the hepatic lineage (Fig 5D). Compared to HE cells, EDECs expressed lower levels of *HNF4 α* (Fig 5D). Both *c/EBP α* and *PROX1*, which are transcription factors that promote HLC fate over EDEC were expressed at higher levels in HLCs than in EDECs, although in almost all cases not significantly (Fig 5E and 5F). The classic cholangiocyte marker OPN was, with the exception of AF iPSC derived cells, significantly expressed at higher levels in EDECs than in HLCs, as was the cholangiocyte-associated intermediate filament protein -CK19 (Fig 5G and 5H). Unexpectedly, EDECs expressed lower levels of the cholangiocyte specific transcription factor SOX9 than HLCs (Fig 5I).

The transcription factor FOXA2 which promotes hepatocyte fate and limits cholangiocyte proliferation was also expressed higher in most of the EDECs than in HLCs which does not support a similarity with cholangiocytes (Fig 5J). EDECs also express higher levels of CK18 than HLCs, even though this intermediate filament protein is enriched in hepatocytes (Fig 5K).

We measured cytochrome P450 (*CYP3A4*) activity as well as urea synthesis in order to check if EDECs might have hepatocyte-associated functions. HFF- and H1 derived HLCs had the highest levels of *CYP3A4* activity (S2A Fig). In both cases, HE cells showed significantly lower activity and in EDECs only minimal activity was measurable. In the case of AF-derived cells, *CYP3A4* activity was in all three stages non-significant (S2A Fig). EDECs derived from HFF-iPSCs did not produce any urea, while HLCs were highly active (S2B Fig). Overall, these data indicate that low density conditions during HLC differentiation result in cells which are morphologically and functionally clearly not hepatocytes, although they express some hepatocyte-associated markers. On the other hand they express several cholangiocyte markers in combination with Vimentin. Taken together, the pattern of marker expression implies that EDECs are an immature cell type with intermediate characteristics between HLCs and CLCs.

Interestingly, similar cell types are present in rat fetal liver where three distinct populations, comprising cells either expressing AFP, ALB and CK19, or AFP and ALB or only CK19 have been associated with distinct lineage commitment and re-population capacities [30].

Inhibition of Notch signalling does not impair EDEC formation but alters expression of key genes

Notch signalling has been described during liver development as the most important signalling pathway for the determination of cholangiocyte fate in contrast to hepatocyte [17, 18]. Therefore, we assumed that blocking Notch signalling might push cells into HLC direction even at a low density. An essential and universal step in Notch signalling is cleavage of the membrane

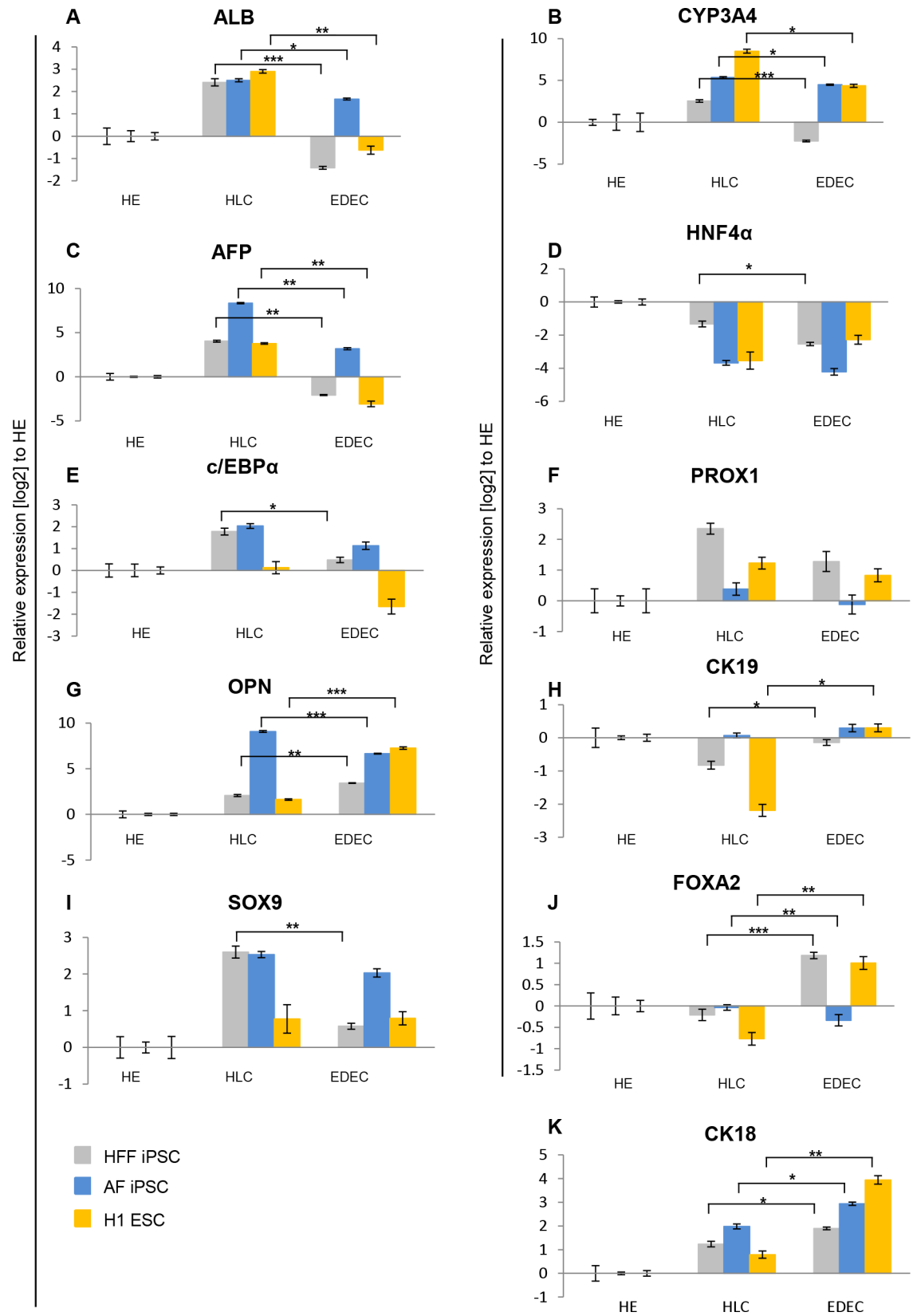


Fig 5. Temporal expression of markers during differentiation. Two iPSC lines and one ESC line were differentiated into either HLCs or EDECs and qRT-PCRs for expression of characteristic hepatocyte and cholangiocyte markers was performed. Gene expression was normalized to RPS16 and fold change was calculated relative to HE cells. Mean values of technical triplicates of biological duplicates are shown. Error bars represent SEM. P-Values were calculated with two-tailed student's t-tests (** = p-value < 0.001, * = p-value < 0.01, * = p-value < 0.05).

<https://doi.org/10.1371/journal.pone.0200416.g005>

bound Notch receptor by γ -secretase after ligand binding [31]. This creates the Notch intracellular domain which activates the transcription of specific target genes [31]. In order to prevent EDEC differentiation, we blocked Notch signalling by inhibiting γ -secretase activity. After splitting the cells and replating at low density we incubated them with two distinct γ -secretase inhibitors and continued differentiation for an additional six days. HFF-iPSC derived hepatoblasts were treated with Compound E while H1 derived hepatoblasts were incubated with γ -secretase inhibitor I. At the end of the differentiation, cells cultivated at low density predominantly adopted an EDEC phenotype, regardless of Notch inhibition, even though cells with typical HLC morphology were also visible (Fig 6A). Immunostainings confirmed the predominance of EDECs, as most cells continued to express high levels of CK19 and SOX9 as well as low levels of ECAD and OPN (Fig 6B).

We also looked in detail at the expression of several HLC and CLC specific/ enriched genes after treatment with γ -secretase inhibitors. With the exception of *c/EBP α* we observed similar regulation for all genes analysed in both cell lines, but because of the limited number of samples analysed, these expression changes are not significant (Fig 6C and 6D). Interestingly, both γ -secretase inhibitors had opposing effects on the two most characteristic cholangiocyte markers- *SOX9* and *OPN*. *SOX9* was up-regulated while *OPN* was down-regulated. Treatment with different concentrations of Compound E revealed that both effects were dose dependent (Fig 6C). *SOX9* is one of the earliest markers for cholangiocyte specification [32] and might thus not be entirely dependent on Notch signalling. *OPN*, however, is a more mature marker which is expressed later than *SOX9* [32]. It was overall only weakly expressed in our cells and its down-regulation upon γ -secretase inhibition might imply impaired maturation.

We further analysed three other transcription factors involved in hepatic cell fate determination in more detail. *PROX1* and *FOXA2* were uniformly down-regulated in iPSC and H1 derived EDECs after γ -secretase inhibition. The homeobox transcription factor *PROX1* promotes hepatocyte fate and represses biliary fate [33]. *FOXA2*, which is important for hepatocyte development is known to repress cholangiocyte proliferation [34]. The down-regulation of both factors after γ -secretase inhibition supports the immunocytochemistry-based data which shows that the cells do retain EDEC fate. Expression of *c/EBP α* changed in opposing directions after γ -secretase treatment of iPSC and H1-derived EDECs. It is known that Notch signalling down-regulates *c/EBP α* expression in cholangiocytes [35]. Thus, the dose-dependent up-regulation that we observed in iPSC-derived EDECs after treatment with Compound E would imply that Notch signalling was effectively reduced. Maybe the concentration of γ -secretase inhibitor I was not high enough to achieve similar results with the H1 derived EDECs. The transcription factor *c/EBP α* has a versatile role during development of hepatocytes and cholangiocytes. It activates on the one hand transcription of characteristic hepatocyte markers such as albumin and several enzymes of the ornithine cycle [36], while limiting hepatocyte proliferation [37] and it inhibits cholangiocyte fate by suppressing expression of the cholangiocyte determining transcription factors- *HNF6* and *HNF1 β* [38]. Thus, effects of different *c/EBP α* levels are probably not visible at this early, immature stage of our cells.

Microarray-based global gene expression analysis revealed that the transcriptomes of H1 derived HLCs cluster away from H1 derived EDECs regardless of Notch inhibition in the latter (Fig 7A). This further emphasizes the diversity of the two observed cell types. On the other

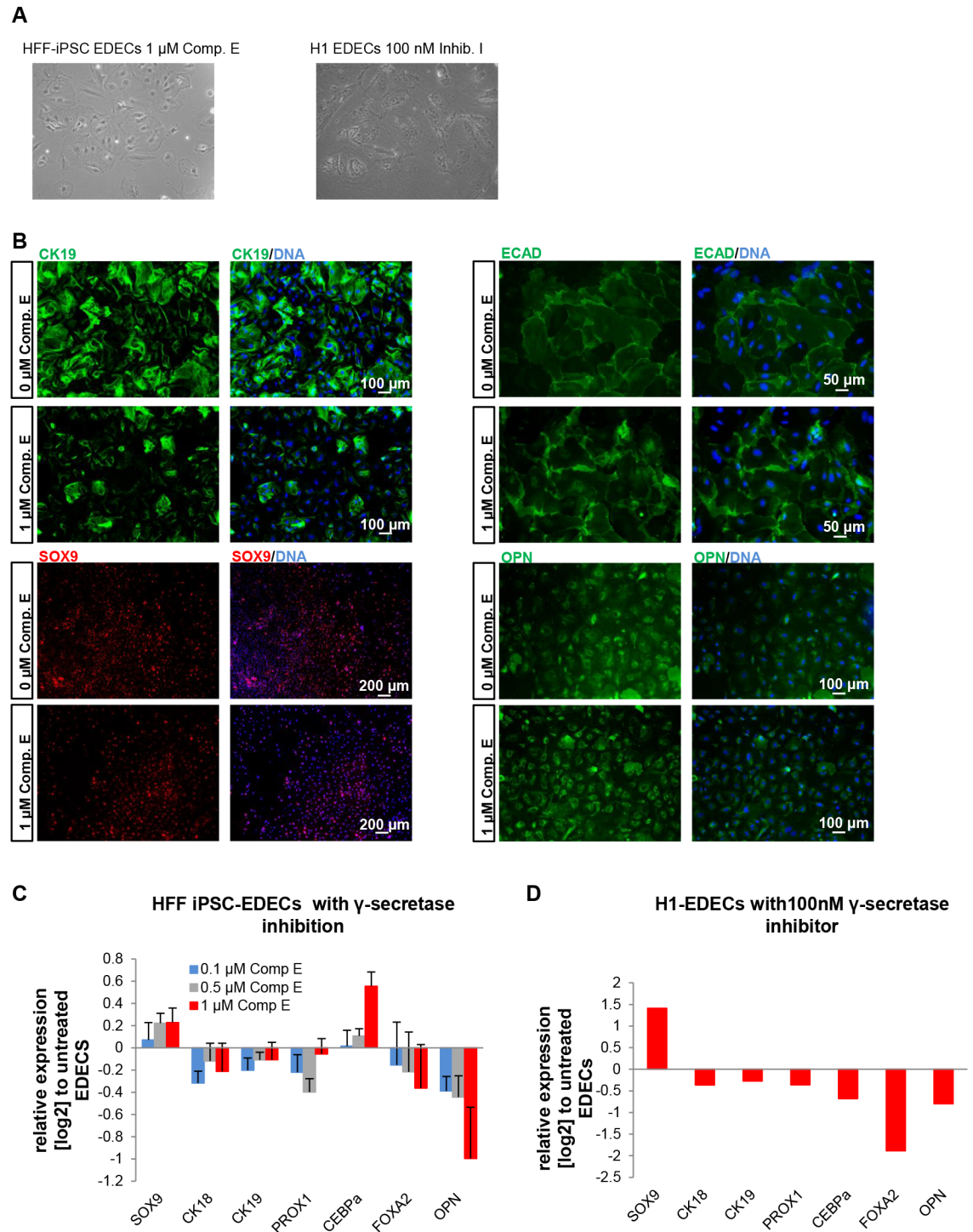


Fig 6. Inhibition of Notch signalling does not prevent EDEC development. hPSCs were differentiated into EDECs while treating them with γ -secretase inhibitors. (A) HFF derived cells treated with Compound E (left) or H1 derived cells treated with γ -secretase inhibitor I (right) adopted the EDEC morphology. (B) Immunocytochemistry for CK19, SOX9, ECAD, and OPN. (C,D) qRT-PCR for hepatocyte or cholangiocyte determining genes. Gene expression was normalized to RPS16 and fold change was calculated relative to untreated cells. Mean values of technical triplicates of biological duplicates (C) or of one sample (D) are show.

<https://doi.org/10.1371/journal.pone.0200416.g006>

hand, heatmap-based analysis of hepatocyte- and cholangiocyte- associated genes revealed a close relationship between HLCs and EDECs (Fig 7A). Many of the analysed transcription factors were expressed at similar levels in both cell populations. Interestingly, *c/EBP α* was clearly over-expressed in HLCs while *GPBAR1* and *SOX17* expression were higher in EDECs. *c/EBP α* is a transcription factor that inhibits cholangiocyte fate by suppressing expression of the cholangiocyte determining transcription factors HNF6 and HNF1 β [38]. G Protein-Coupled Bile Acid Receptor 1 (*GPBAR1* also known as *TGR5*) has been shown to be characteristic for cholangiocytes [39], while the presence of *SOX17*, an early marker for endoderm, indicates that the cells are still immature.

Surprisingly, members of the Notch signalling pathway (*NOTCH3*, *JAG2* and *DLK1,2*) were expressed at higher levels in HLCs than in EDECs. This was unexpected as it has been described that hepatocyte differentiation does not require Notch signalling. HLCs are however still immature and the presence of molecules belonging to the Notch signalling pathway might indicate that they are still able to switch cell fate towards CLCs or EDECs. In particular, the presence of *DLK1* has been described as being characteristic for bipotential hepatoblasts [40]. *NOTCH3* is the only analysed factor of this signalling pathway that is up-regulated in EDECs after treatment with the γ -secretase inhibitor. As inhibition of the γ -secretase inhibits propagation of the Notch signal cells might reduce the production of ligands which do not find a receptor counterpart, while the *NOTCH3* receptor might be up-regulated in order to compensate for low ligand density on neighbouring cells. Interestingly, *NOTCH3* is also the only family member with a positive impact on hepatocyte development [19] and its increased expression after γ -secretase inhibition might indicate that some of the cells are still or again capable of differentiating into hepatocytes.

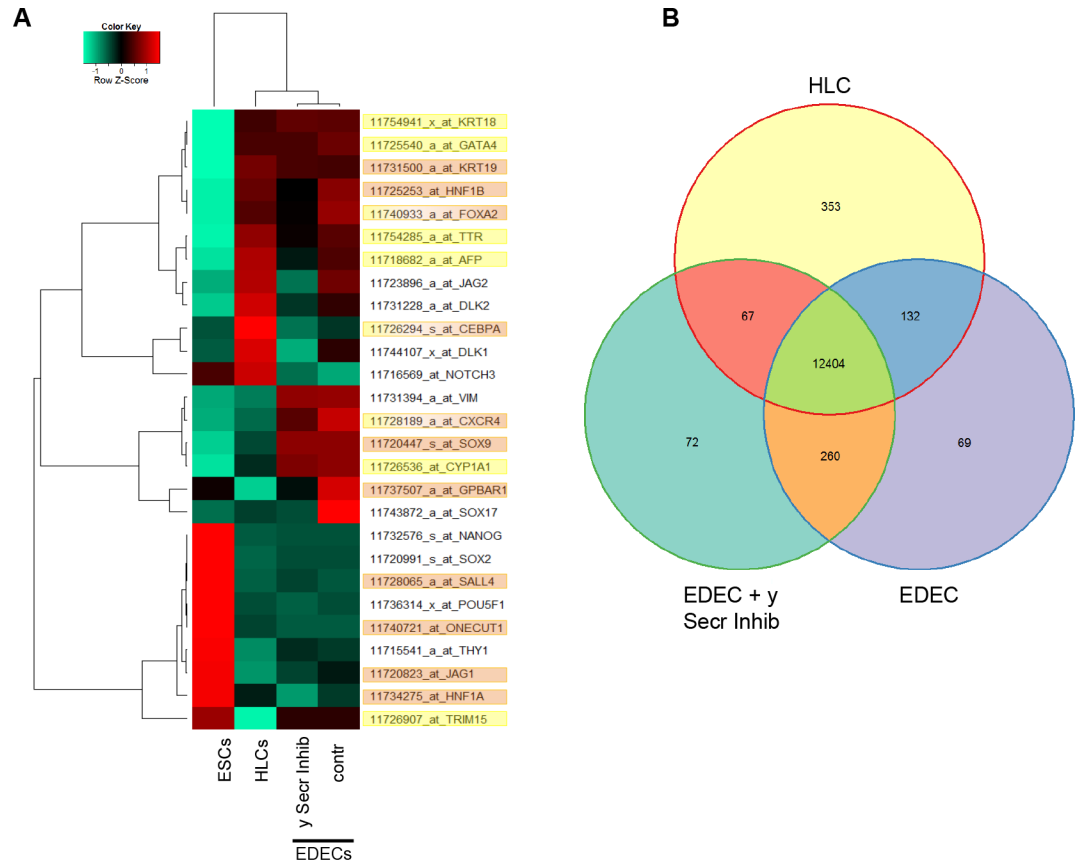
Global gene expression was compared between HLCs and EDECs with and without treatment with Notch inhibitor (Fig 7B). While 12,404 genes were expressed by all three cell types, 353 genes were only expressed in HLCs. EDECs and EDECs treated with the Notch inhibitor shared 260 genes and individually expressed 69 and 72 genes, respectively.

Genes only expressed in either HLCs (yellow) or EDECs (comprising both, untreated and treated with γ -secretase inhibitor; orange) were assigned to distinct gene ontology (GO) terms (Fig 7C, S5 Table). Interestingly, in the case of HLCs many of these terms relate to metabolic functions while in EDECs, structural features and signalling pathways are predominant. This again confirms the presence of two distinct cell types in our culture dish. There was a general tendency of EDECs expressing fewer genes related to transcription and cell cycle than HLCs while expressing more genes related to apoptosis and proliferation (S6–S8 Tables).

Analysis of differentially expressed genes between EDECs and EDECs treated with γ -secretase inhibitor I revealed that untreated cells expressed more genes related to development and differentiation in general (S9–S11 Tables). This is in line with Notch inhibition reducing the possibilities of cellular differentiation and interfering with development. In addition, γ -secretase inhibitor I treated EDECs expressed more genes related to cell cycle which mirrors the reduced differentiation/development pathways which would lead cells towards more maturity and thus less cell cycling. Interestingly, inhibition of Notch signalling resulted in a general reduction of genes associated with cell signalling affecting also other signalling pathways (S9–S11 Tables).

Inhibition of key signalling pathways does not revert cell fate

We next wanted to determine whether interference with one of the other major signalling pathways that have been described as essential for cell fate decision making between hepatocytes and cholangiocytes can revert the EDEC phenotype and push the cells into the HLC



C

GO-Categories HLC only			
Term	%	PValue	Selected Genes
lipid transport	3.08	1.53E-03	APOA4, SOAT2, APOB, APOC3, FABP1
response to nutrient levels	2.77	3.07E-02	SOAT2, CYP24A1, CYP11A1, HSD11B2
cholesterol homeostasis	2.15	6.45E-05	APOA4, SOAT2, APOB, APOC3, MTTP
Secondary metabolites biosynthesis, transport, and catabolism	2.15	1.49E-03	CYP4X1, CYP24A1, CYP2J2, CYP11A1, F5, CYP2W1, CYP19A1
protein-lipid complex remodeling	1.54	4.44E-04	APOA4, APOB, APOC3, APOC2, APOM
very-low-density lipoprotein particle assembly	0.92	4.90E-03	SOAT2, APOB, APOC3
regulation of triglyceride catabolic process	0.92	4.90E-03	APOA4, APOC3, APOC2
GO Categories EDEC only			
Term	%	PValue	Genes
cell membrane	19.30	3.61E-06	RHOJ, F2RL2, GYPB, CADM3, PEAR1, OR51D1, GLDN, UNC93A, SYT8, CD52
positive regulation of cell proliferation	5.63	1.41E-04	BMP10, NACC2, TNFSF4, TAC1, IL6R, IL34, VASH2, TNFRSF4, NTN1
channel activity	4.83	2.22E-03	GJD2, KCNJ15, AQP8, GJB3, KCNA3, AQP1, KCNJ12, ITPR1, KCNJ4, KCNS
substrate specific channel activity	4.29	8.95E-03	KCNJ15, AQP8, KCNA3, AQP1, KCNJ12, ITPR1
localization of cell	3.75	6.31E-03	CDK5R1, ITGA11, PSG2, ZEB2, CUZD1, IL6R, CCL5
regulation of MAPKKK cascade	2.14	4.94E-03	ADRB2, MAP3K5, MAPK8IP2, MAP4K1, ZEB2, IL6R, IL11

Fig 7. Gene expression analysis unravels differences and similarities between H1 derived HLCs and EDECs. (A) Heatmap representation of key genes involved in hepatic cell fate decision making or characteristic for either hepatocytes (yellow) or cholangiocytes (orange). (B) Venn diagram illustrating the numbers of genes which were expressed either by only one cell type or shared between the cell types. (C) Gene Ontology (GO) analysis of genes expressed only in HLCs (yellow) or in EDECs (with or without Notch inhibition, orange) Shown are pre-selected, significant GO-Terms, for full data set see [S4](#) and [S5](#) Tables.

<https://doi.org/10.1371/journal.pone.0200416.g007>

direction. To this end, we applied several small molecules to either induce or repress WNT, Hh, and TGFβ signalling (Fig 8A–8G). As with Notch inhibition, we did not observe changes in the phenotype and in all cases the cells were predominantly EDECs. However, the population was not pure, and we could also detect cells with typical HLC morphology. We performed

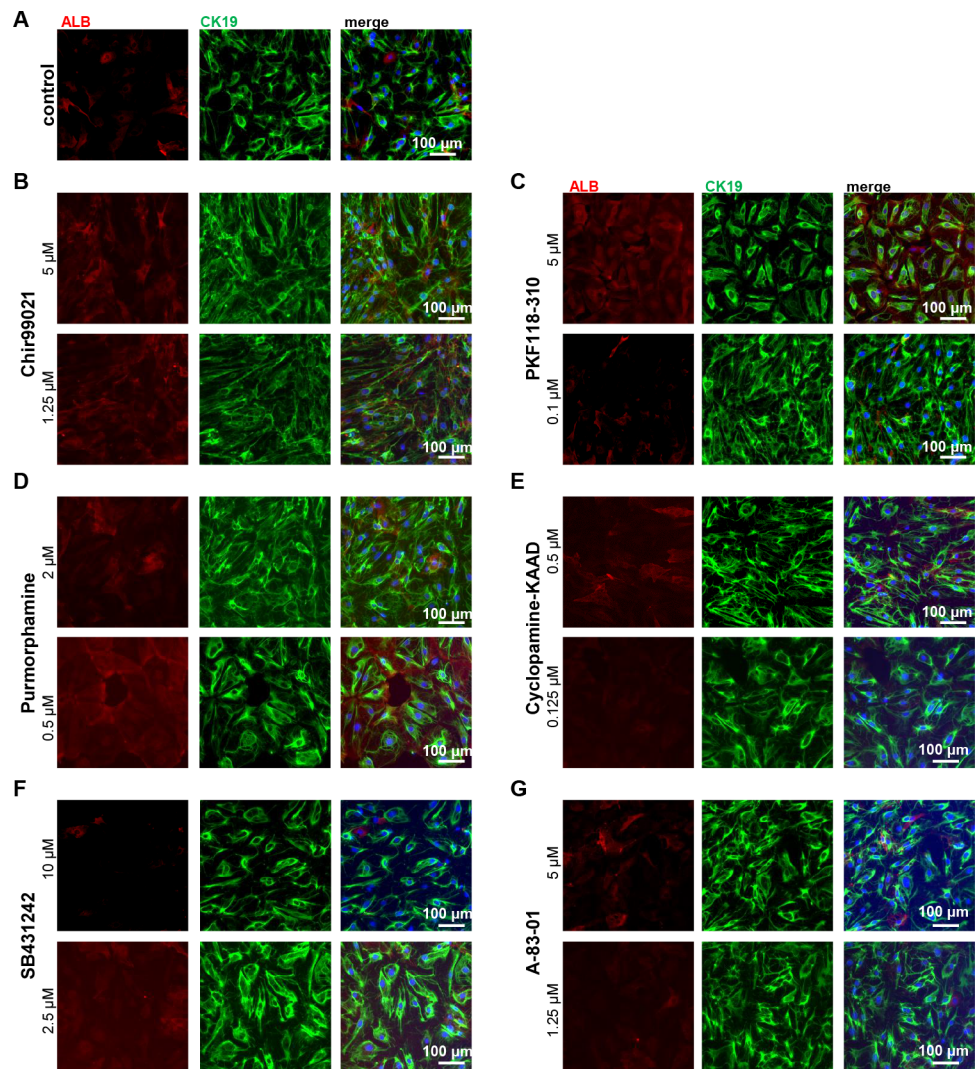


Fig 8. Interference with various signalling pathways does not change cell fate. iPSCs were differentiated into EDECs. Directly after low-density splitting, small molecules were applied in order to interfere with signalling pathways important for differentiation into hepatocytes or cholangiocytes. (A–G) Immunocytochemistry for ALB (red) and CK19 (green). (A) DMSO control, (B) activation of WNT signalling with Chir99021, (C) inhibition of WNT signaling with PKF118-310, (D) activation of Hh signalling with Purmorphamine, (E) inhibition of Hh signalling with Cyclopamine-KAAD, (F) inhibition of TGFβ signalling with SB431242, (G) inhibition of TGFβ signalling with A-83-01. Scale bar: 100 μm.

<https://doi.org/10.1371/journal.pone.0200416.g008>

immunocytochemistry-based expression analyses for ALB and CK19 in all conditions, (Fig 8B–8G) and compared it to untreated control cells (Fig 8A). This demonstrated that the majority of cells expressed high levels of CK19 and low levels of ALB. We confirmed in our transcriptome data, that the cells expressed the essential proteins for all investigated signalling pathways thus being able to react to the applied cues (S3 and S4 Fig).

Overall, it seems that splitting and replating pluripotent stem cell derived bipotential hepatoblasts at low density at the HE stage of the HLC differentiation process leads to the accumulation of EDECs. None of the applied pathway interferences was able to revert or prevent this transition. However, cell fate decision is a tightly orchestrated process with a high level of synergy between different signalling pathways. Thus, it is possible that the right interplay between the various pathways at the right time point is capable of altering cell fate. In order to determine the full potential of these cells and classify them according to already known categories of hepatic stem/progenitor cells, transplantation experiments with rats or mice after partial hepatectomy will be necessary.

As cells with EDEC morphology often appear during HLC differentiation in regions of lower cell density, it is essential to keep the cells during the whole differentiation process at a high density. The accumulation of EDECs within a population of HLCs might interfere with disease modelling or drug screenings specifically related to hepatocytes.

Supporting information

S1 Fig. Expression of characteristic markers in HE cells. Two iPSC lines and one ESC line were differentiated into HE cells and stained for characteristic hepatocyte or cholangiocyte markers.

(TIF)

S2 Fig. Biochemical activity tests. hPSC were differentiated into HLCs and EDECs. (A) CYP3A4 activity assay (B) QuantiChrome Urea Assay.

(TIF)

S3 Fig. Heatmap representation of genes involved in signalling pathways part 1. Global expression patterns of genes involved in Notch (A) and Hedgehog (B) signalling were analysed in HLCs and EDECs with and without Notch inhibitor. Genes were colour-coded according to their function. Asterisks mark the genes that are expressed above threshold in at least the EDEC sample or the EDEC sample with inhibitor.

(TIF)

S4 Fig. Heatmap representation of genes involved in signalling pathways part 2. Global expression patterns of genes involved in WNT (A) and TGF β (B) signalling were analysed in HLCs and EDECs with and without Notch inhibitor. Genes were colour-coded according to their function. Asterisks mark the genes that are expressed above threshold in at least the EDEC sample or the EDEC sample with inhibitor.

(TIF)

S1 Table. Small molecules.

(DOCX)

S2 Table. Antibodies.

(DOCX)

S3 Table. Primer sequences.

(DOCX)

S4 Table. Venn sets. The genes included in the different sets of the venn diagram shown in Fig 5D are listed in this table.

(XLS)

S5 Table. Common GO terms in H1 HLCs and EDECs. Genes expressed either in HLCs or in EDECs (regardless of inhibitor treatment) from the venn diagram (Fig 5D) were used for GO analysis. Clusters are listed in this table.

(XLSX)

S6 Table. Selected GO Categories up- and down regulated in EDECs versus HLCs.

(DOCX)

S7 Table. Comparison of gene expression between EDECs and HLCs.

(XLSX)

S8 Table. Comparison of gene expression between EDECs and EDECs treated with γ -secretase inhibitor.

(XLSX)

S9 Table. Selected GO categories up- and down regulated in EDECs with γ -secretase inhibitor versus untreated EDECs.

(DOCX)

S10 Table. GO Terms of genes expressed in both, EDECs and HLCs.

(XLSX)

S11 Table. GO Terms of genes expressed in both, EDECs and EDECs treated with γ -secretase inhibitor.

(XLSX)

Acknowledgments

Nina Graffmann acknowledges support from the Research commission of the Medical faculty of Heinrich Heine University Düsseldorf (<http://www.medizin.hhu.de/dekanat/gremien-und-kommissionen/kommissionen/forschungskommission.html>). James Adjaye acknowledges support from the Medical faculty of Heinrich Heine University Düsseldorf. We thank M. Bohndorf and S. Wehrmeyer for technical support.

Author Contributions

Conceptualization: Nina Graffmann, James Adjaye.

Data curation: Wasco Wruck.

Formal analysis: Nina Graffmann.

Funding acquisition: Nina Graffmann, James Adjaye.

Investigation: Nina Graffmann, Audrey Ncube.

Methodology: Nina Graffmann, Audrey Ncube.

Project administration: Nina Graffmann, James Adjaye.

Supervision: James Adjaye.

Validation: Nina Graffmann, Wasco Wruck.

Visualization: Nina Graffmann, Audrey Ncube, Wasco Wruck.

Writing – original draft: Nina Graffmann, James Adjaye.

References

1. Graffmann N, Ring S, Kawala MA, Wruck W, Ncube A, Trompeter HI, et al. Modeling Nonalcoholic Fatty Liver Disease with Human Pluripotent Stem Cell-Derived Immature Hepatocyte-Like Cells Reveals Activation of PLIN2 and Confirms Regulatory Functions of Peroxisome Proliferator-Activated Receptor Alpha. *Stem cells and development*. 2016; 25(15):1119–33. <https://doi.org/10.1089/scd.2015.0383> PMID: 27308945; PubMed Central PMCID: PMC4971413.
2. Siller R, Greenhough S, Naumovska E, Sullivan GJ. Small-Molecule-Driven Hepatocyte Differentiation of Human Pluripotent Stem Cells. *Stem cell reports*. 2015. <https://doi.org/10.1016/j.stemcr.2015.04.001> PMID: 25937370.
3. Hannan NR, Segeritz CP, Touboul T, Vallier L. Production of hepatocyte-like cells from human pluripotent stem cells. *Nature protocols*. 2013; 8(2):430–7. PMID: 23424751; PubMed Central PMCID: PMC3673228.
4. Cameron K, Tan R, Schmidt-Heck W, Campos G, Lyall MJ, Wang Y, et al. Recombinant Laminins Drive the Differentiation and Self-Organization of hESC-Derived Hepatocytes. *Stem cell reports*. 2015; 5(6):1250–62. <https://doi.org/10.1016/j.stemcr.2015.10.016> PMID: 26626180; PubMed Central PMCID: PMC4682209.
5. Rashid ST, Corbineau S, Hannan N, Marciniak SJ, Miranda E, Alexander G, et al. Modeling inherited metabolic disorders of the liver using human induced pluripotent stem cells. *Journal of Clinical Investigation*. 2010; 120(9):3127–36. <https://doi.org/10.1172/JCI43122> PubMed PMID: WOS:000281458800019. PMID: 20739751
6. Wilson AA, Ying L, Liesa M, Segeritz CP, Mills JA, Shen SS, et al. Emergence of a Stage-Dependent Human Liver Disease Signature with Directed Differentiation of Alpha-1 Antitrypsin-Deficient iPS Cells. *Stem cell reports*. 2015. <https://doi.org/10.1016/j.stemcr.2015.02.021> PMID: 25843048.
7. Sampaziotis F, Cardoso de Brito M, Madrigal P, Bertero A, Saeb-Parsy K, Soares FA, et al. Cholangiocytes derived from human induced pluripotent stem cells for disease modeling and drug validation. *Nature biotechnology*. 2015. <https://doi.org/10.1038/nbt.3275> PMID: 26167629.
8. Ogawa M, Ogawa S, Bear CE, Ahmadi S, Chin S, Li B, et al. Directed differentiation of cholangiocytes from human pluripotent stem cells. *Nature biotechnology*. 2015; 33(8):853–61. <https://doi.org/10.1038/nbt.3294> PMID: 26167630.
9. Dianat N, Dubois-Pot-Schneider H, Steichen C, Desterke C, Leclerc P, Raveux A, et al. Generation of functional cholangiocyte-like cells from human pluripotent stem cells and HepaRG cells. *Hepatology*. 2014; 60(2):700–14. <https://doi.org/10.1002/hep.27165> PMID: 24715669.
10. Sampaziotis F, de Brito MC, Geti I, Bertero A, Hannan NR, Vallier L. Directed differentiation of human induced pluripotent stem cells into functional cholangiocyte-like cells. *Nature protocols*. 2017; 12(4):814–27. <https://doi.org/10.1038/nprot.2017.011> PMID: 28333915.
11. Fougere-Deschatrette C, Imaizumi-Scherrer T, Strick-Marchand H, Morosan S, Charneau P, Kremsdorf D, et al. Plasticity of hepatic cell differentiation: bipotential adult mouse liver clonal cell lines competent to differentiate in vitro and in vivo. *Stem cells*. 2006; 24(9):2098–109. <https://doi.org/10.1634/stemcells.2006-0009> PMID: 16946000.
12. Miyajima A, Tanaka M, Itoh T. Stem/progenitor cells in liver development, homeostasis, regeneration, and reprogramming. *Cell stem cell*. 2014; 14(5):561–74. <https://doi.org/10.1016/j.stem.2014.04.010> PMID: 24792114.
13. Cardinale V, Wang Y, Carpino G, Cui CB, Gatto M, Rossi M, et al. Multipotent stem/progenitor cells in human biliary tree give rise to hepatocytes, cholangiocytes, and pancreatic islets. *Hepatology*. 2011; 54(6):2159–72. <https://doi.org/10.1002/hep.24590> PMID: 21809358.
14. Li LH, Krantz ID, Deng Y, Genin A, Banta AB, Collins CC, et al. Alagille syndrome is caused by mutations in human Jagged1, which encodes a ligand for Notch1. *Nature genetics*. 1997; 16(3):243–51. <https://doi.org/10.1038/ng0797-243> PubMed PMID: WOS:A1997XG60900018. PMID: 9207788
15. Oda T, Elkahlon AG, Pike BL, Okajima K, Krantz ID, Genin A, et al. Mutations in the human Jagged1 gene are responsible for Alagille syndrome. *Nature genetics*. 1997; 16(3):235–42. <https://doi.org/10.1038/ng0797-235> PMID: 9207787.
16. McDaniell R, Warthen DM, Sanchez-Lara PA, Pai A, Krantz ID, Piccoli DA, et al. NOTCH2 mutations cause Alagille syndrome, a heterogeneous disorder of the notch signaling pathway. *Am J Hum Genet*. 2006; 79(1):169–73. <https://doi.org/10.1086/505332> PMID: 16773578; PubMed Central PMCID: PMC4971413.

17. Zong Y, Panikkar A, Xu J, Antoniou A, Raynaud P, Lemaigre F, et al. Notch signaling controls liver development by regulating biliary differentiation. *Development*. 2009; 136(10):1727–39. <https://doi.org/10.1242/dev.029140> PMID: 19369401; PubMed Central PMCID: PMC2673761.
18. Geisler F, Nagl F, Mazur PK, Lee M, Zimmer-Strobl U, Strobl LJ, et al. Liver-specific inactivation of Notch2, but not Notch1, compromises intrahepatic bile duct development in mice. *Hepatology*. 2008; 48(2):607–16. <https://doi.org/10.1002/hep.22381> PMID: 18666240.
19. Ortica S, Tarantino N, Aulner N, Israel A, Gupta-Rossi N. The 4 Notch receptors play distinct and antagonistic roles in the proliferation and hepatocytic differentiation of liver progenitors. *FASEB journal: official publication of the Federation of American Societies for Experimental Biology*. 2014; 28(2):603–14. <https://doi.org/10.1096/fj.13-235903> PMID: 24145721.
20. Zong Y, Stanger BZ. Molecular mechanisms of bile duct development. *The international journal of biochemistry & cell biology*. 2011; 43(2):257–64. <https://doi.org/10.1016/j.biocel.2010.06.020> PMID: 20601079; PubMed Central PMCID: PMC2990791.
21. Raynaud P, Carpentier R, Antoniou A, Lemaigre FP. Biliary differentiation and bile duct morphogenesis in development and disease. *The international journal of biochemistry & cell biology*. 2011; 43(2):245–56. <https://doi.org/10.1016/j.biocel.2009.07.020> PMID: 19735739.
22. Decaens T, Godard C, de Reynies A, Rickman DS, Tronche F, Couty JP, et al. Stabilization of beta-catenin affects mouse embryonic liver growth and hepatoblast fate. *Hepatology*. 2008; 47(1):247–58. <https://doi.org/10.1002/hep.21952> PMID: 18038450.
23. Hussain SZ, Sneddon T, Tan X, Micsenyi A, Michalopoulos GK, Monga SPS. Wnt impacts growth and differentiation in ex vivo liver development. *Experimental Cell Research*. 2004; 292(1):157–69. <https://doi.org/10.1016/j.yexcr.2003.08.020> PMID: 14720515
24. Cordi S, Godard C, Saandi T, Jacquemin P, Monga SP, Colnot S, et al. Role of beta-catenin in development of bile ducts. *Differentiation*. 2016; 91(1–3):42–9. <https://doi.org/10.1016/j.diff.2016.02.001> PMID: 26856660; PubMed Central PMCID: PMC4803532.
25. Omenetti A, Diehl AM. Hedgehog signaling in cholangiocytes. *Current opinion in gastroenterology*. 2011; 27(3):268–75. <https://doi.org/10.1097/MOG.0b013e32834550b4> PMID: 21423008; PubMed Central PMCID: PMC3636549.
26. Wang Y, Adjaye J. A cyclic AMP analog, 8-Br-cAMP, enhances the induction of pluripotency in human fibroblast cells. *Stem cell reviews*. 2011; 7(2):331–41. <https://doi.org/10.1007/s12015-010-9209-3> PMID: 21120637.
27. Wolfrum K, Wang Y, Prigione A, Sperling K, Lehrach H, Adjaye J. The LARGE principle of cellular reprogramming: lost, acquired and retained gene expression in foreskin and amniotic fluid-derived human iPSC cells. *PloS one*. 2010; 5(10):e13703. <https://doi.org/10.1371/journal.pone.0013703> PMID: 21060825; PubMed Central PMCID: PMC2966395.
28. Drews K, Matz P, Adjaye J. Generation of iPSC lines from primary human amniotic fluid cells. *Stem cell research*. 2015; 15(3):712–4. <https://doi.org/10.1016/j.scr.2015.11.003> PMID: 26987930.
29. Chaw SY, Majeed AA, Dalley AJ, Chan A, Stein S, Farah CS. Epithelial to mesenchymal transition (EMT) biomarkers—E-cadherin, beta-catenin, APC and Vimentin—in oral squamous cell carcinogenesis and transformation. *Oral Oncol*. 2012; 48(10):997–1006. <https://doi.org/10.1016/j.oraloncology.2012.05.011> PMID: 22704062.
30. Dabeva MD, Petkov PM, Sandhu J, Oren R, Laconi E, Hurston E, et al. Proliferation and Differentiation of Fetal Liver Epithelial Progenitor Cells after Transplantation into Adult Rat Liver. *The American journal of pathology*. 2000; 156(6):2017–31. [https://doi.org/10.1016/S0002-9440\(10\)65074-2](https://doi.org/10.1016/S0002-9440(10)65074-2) PMID: 10854224
31. Andersson ER, Sandberg R, Lendahl U. Notch signaling: simplicity in design, versatility in function. *Development*. 2011; 138(17):3593–612. <https://doi.org/10.1242/dev.063610> PMID: 21828089.
32. Antoniou A, Raynaud P, Cordi S, Zong Y, Tronche F, Stanger BZ, et al. Intrahepatic bile ducts develop according to a new mode of tubulogenesis regulated by the transcription factor SOX9. *Gastroenterology*. 2009; 136(7):2325–33. <https://doi.org/10.1053/j.gastro.2009.02.051> PMID: 19403103; PubMed Central PMCID: PMC2743481.
33. Seth A, Ye J, Yu N, Guez F, Bedford DC, Neale GA, et al. Prox1 ablation in hepatic progenitors causes defective hepatocyte specification and increases biliary cell commitment. *Development*. 2014; 141(3):538–47. <https://doi.org/10.1242/dev.099481> PMID: 24449835; PubMed Central PMCID: PMC3899812.
34. Li Z, White P, Tuteja G, Rubins N, Sackett S, Kaestner KH. Foxa1 and Foxa2 regulate bile duct development in mice. *The Journal of clinical investigation*. 2009; 119(6):1537–45. <https://doi.org/10.1172/JCI38201> PMID: 19436110; PubMed Central PMCID: PMC2689124.
35. Tanimizu N, Miyajima A. Notch signaling controls hepatoblast differentiation by altering the expression of liver-enriched transcription factors. *Journal of cell science*. 2004; 117(Pt 15):3165–74. <https://doi.org/10.1242/jcs.01169> PMID: 15226394.

36. Tan EH, Ma FJ, Gopinadhan S, Sakban RB, Wang ND. C/EBP alpha knock-in hepatocytes exhibit increased albumin secretion and urea production. *Cell Tissue Res.* 2007; 330(3):427–35. <https://doi.org/10.1007/s00441-007-0505-4> PMID: 17934762.
37. Diehl AM. Roles of CCAAT/enhancer-binding proteins in regulation of liver regenerative growth. *The Journal of biological chemistry.* 1998; 273(47):30843–6. PMID: 9812973.
38. Yamasaki H, Sada A, Iwata T, Niwa T, Tomizawa M, Xanthopoulos KG, et al. Suppression of C/EBPalpha expression in periportal hepatoblasts may stimulate biliary cell differentiation through increased Hnf6 and Hnf1b expression. *Development.* 2006; 133(21):4233–43. <https://doi.org/10.1242/dev.02591> PMID: 17021047.
39. Keitel V, Haussinger D. TGR5 in cholangiocytes. *Current opinion in gastroenterology.* 2013; 29(3):299–304. <https://doi.org/10.1097/MOG.0b013e32835f3f14> PMID: 23429467.
40. Tanimizu N, Nishikawa M, Saito H, Tsujimura T, Miyajima A. Isolation of hepatoblasts based on the expression of Dlk/Pref-1. *Journal of cell science.* 2003; 116(9):1775–86. <https://doi.org/10.1242/jcs.00388> PubMed PMID: WOS:000182903600014.

RESEARCH ARTICLE

A stem cell based *in vitro* model of NAFLD enables the analysis of patient specific individual metabolic adaptations in response to a high fat diet and AdipoRon interference

Nina Graffmann¹, Audrey Ncube¹, Soraia Martins¹, Aurelian Robert Fiszl¹, Philipp Reuther², Martina Bohndorf¹, Wasco Wruck¹, Mathias Beller^{3,4}, Constantin Czekelius² and James Adjaye^{1,*}

ABSTRACT

Non-alcoholic fatty liver disease (NAFLD) is a multifactorial disease. Its development and progression depend on genetically predisposed susceptibility of the patient towards several ‘hits’ that induce fat storage first and later inflammation and fibrosis. Here, we differentiated induced pluripotent stem cells (iPSCs) derived from four distinct donors with varying disease stages into hepatocyte like cells (HLCs) and determined fat storage as well as metabolic adaptations after stimulations with oleic acid. We could recapitulate the complex networks that control lipid and glucose metabolism and we identified distinct gene expression profiles related to the steatosis phenotype of the donor. In an attempt to reverse the steatotic phenotype, cells were treated with the small molecule AdipoRon, a synthetic analogue of adiponectin. Although the responses varied between cells lines, they suggest a general influence of AdipoRon on metabolism, transport, immune system, cell stress and signalling.

KEY WORDS: NAFLD, AdipoRon, FGF21, Metabolism, Hepatocyte differentiation, Hepatocyte-like cells

INTRODUCTION

Non-alcoholic fatty liver disease (NAFLD) or steatosis is the hepatic manifestation of the metabolic syndrome and affects up to 35% of the general population in the western hemisphere, with increasing tendencies (Cohen et al., 2011). It is a multifactorial disease with sedentary lifestyle, an imbalance in calorie uptake and energy expenditure, obesity, diabetes, insulin resistance, and also genetic predisposition playing crucial roles in its development. However, so far it is poorly understood how these factors interact and why people react very differently to similar dietary conditions.

When the liver encounters a surplus of calories that is not matched by appropriate energy expenditure, it starts storing triacylglycerides in lipid droplets (LDs). This first stage is still reversible but the

accumulation of LDs in hepatocytes represents the first of several ‘hits’ that eventually impair hepatocyte function. Further hits, e.g. by inflammation or oxidative stress can lead to non-alcoholic steatohepatitis (NASH) in 30% of patients (Cohen et al., 2011). From there the disease can proceed to cirrhosis and hepatocellular carcinoma, which finally requires liver transplantation (Wong et al., 2015).

Although storage of fat in relatively inert LDs prevents lipotoxicity (Neuschwander-Tetri, 2017), it takes up a lot of space and resources in hepatocytes, thus diminishing their ability to adapt the metabolism to the bodies energy needs.

Hepatic metabolism is controlled by a complex network of signalling pathways that integrate information on nutrient availability and energy needs within the liver and peripheral organs (Bechmann et al., 2012). One of the signalling molecules that influences hepatic metabolism is adiponectin. It is an adipokine – a cytokine synthesized by adipocytes. Adiponectin levels are inversely correlated with bodyweight as well as with insulin sensitivity (Vuppalanchi et al., 2005; Wruck et al., 2015; Kadowaki and Yamauchi, 2005). It signals via two distinct receptors, adiponectin receptor (ADIPOR) 1 and 2. ADIPOR1 is ubiquitously expressed, while ADIPOR2 is predominantly present in the liver (Yamauchi et al., 2003; Felder et al., 2010). AdipoR signalling activates the key metabolic regulators 5’ adenosine monophosphate-activated protein kinase (AMPK) (predominantly via AdipoR1) and peroxisome proliferator-activated receptor (PPAR) α (predominantly via AdipoR2) (Yamauchi et al., 2007), which in turn are responsible for co-ordinating key metabolic pathways (Liu et al., 2012). In hepatocytes, adiponectin reduces gluconeogenesis and lipogenesis (Combs and Marlist, 2014). In adipocytes and skeletal muscle, it increases insulin-mediated glucose uptake and utilisation while it also stimulates insulin secretion by pancreatic beta cells in response to glucose stimulation (Ruan and Dong, 2016). Importantly, adiponectin is also capable of reducing whole body inflammation levels, mainly by stimulating M2 macrophage proliferation and activity and reducing M1 macrophage activities (Luo and Liu, 2016). However, several studies have also described a pro-inflammatory role of adiponectin, especially in the context of rheumatoid arthritis (Koskinen et al., 2011; Ehling et al., 2006).

In 2013, a small molecule with adiponectin-like function, which activates both receptors, was discovered and named AdipoRon (Okada-Iwabu et al., 2013). AdipoRon improves insulin sensitivity and reduces fasting blood glucose levels in high fat diet-induced obese mice. On a high fat diet, it reduced liver triacylglyceride levels in wild-type (wt) mice and prolonged the lifespan of *db/db* mice (Okada-Iwabu et al., 2013).

To date, most studies on NAFLD have been performed in rodents which have marked metabolic differences compared to humans (Santhekadur et al., 2018). We recently established a human *in vitro*

¹Institute for Stem Cell Research and Regenerative Medicine, Heinrich Heine University Düsseldorf, Medical faculty, Moorenstrasse 5, 40225 Düsseldorf, Germany. ²Institute of Organic Chemistry and Macromolecular Chemistry, Heinrich-Heine University Düsseldorf 40225, Düsseldorf, Germany. ³Institute for Mathematical Modeling of Biological Systems, Heinrich-Heine University Düsseldorf, Germany. ⁴Systems Biology of Lipid Metabolism, Heinrich-Heine University Düsseldorf 40225, Düsseldorf, Germany.

*Author for correspondence (James.Adjaye@med.uni-duesseldorf.de)

© N.G., 0000-0002-1229-0792; A.R.F., 0000-0002-0415-6892; M.B., 0000-0003-0987-0080; C.C., 0000-0002-2814-8686; J.A., 0000-0002-6075-6761

This is an Open Access article distributed under the terms of the Creative Commons Attribution License (<https://creativecommons.org/licenses/by/4.0>), which permits unrestricted use, distribution and reproduction in any medium provided that the original work is properly attributed.

model of NAFLD based on induced pluripotent stem cell (iPSC) derived hepatocyte like cells (HLCs) (Graffmann et al., 2016). This model allows us to (i) analyse the development of NAFLD taking into account different disease-associated genotypes that might explain the different courses of disease development, and (ii) to study the effect of potential treatments that should prevent or revert the NAFLD phenotype.

Here, we differentiated four iPSCs lines derived from donors with distinct grades of steatosis into HLCs and studied their responses to fatty acid overload and AdipoRon treatment. While all cell lines efficiently exhibited hallmarks of steatosis, the exact molecular responses to the treatment were highly variable, which can be attributed, at least in part, to variations in the individual genetic background of the donors.

RESULTS

HLCs can be derived from iPSCs of donors with distinct grades of NAFLD

In order to validate our previously published *in vitro* model of NAFLD, we differentiated four iPSC lines (Table 1) derived from donors with distinct NAFLD backgrounds into HLCs and induced fat storage by stimulation with high levels (200 μ M) of oleic acid (OA).

The CO2 control cell line was derived from a healthy donor (Kawala et al., 2016a), while the other cell lines were generated from patients with steatosis grades between 40% and 70% (Kawala et al., 2016b,c; Graffmann et al., 2018; Wruck et al., 2015). All cell lines were efficiently differentiated into HLCs (Fig. 1; Fig. S1). Immunocytochemistry showed that the cells expressed the mature hepatocyte marker Albumin (ALB) along with the more fetal marker alpha-fetoprotein (AFP). In addition, they were positive for the epithelial marker E-cadherin (ECAD) and expressed the hepatocyte specific transcription factor hepatocyte nuclear factor 4 α (HNF4 α) (Fig. 1A). Comparing the expression of key hepatocyte markers in HLCs to that of iPSCs also showed significant increases (Fig. 1B). The cells expressed *AFP* in a comparable range with fetal liver cells. *ALB* expression was significantly increased in HLCs compared to iPSCs. Expression levels of two other hepatocyte specific markers, *alpha-1-antitrypsin (A1AT)* and *Transthyretin (TTR)* were relatively close to that in adult liver-PHH and fetal liver and at least 1000 times higher than in iPSCs. All cell lines showed Cytochrome P450 (CYP) 3A activity, albeit on a low level (Fig. 1C), which is characteristic for *in vitro* derived HLCs.

HLCs derived from donors with distinct grades of steatosis can store LDs after OA induction

We added 200 μ M OA into the medium for several days to see if all cell lines were capable of storing fat in the form of LDs. We observed a significant increase of LDs after 9 days of OA induction (Fig. 2A). All four lines had low basal levels of LDs. After induction, the amount of LDs increased in all cell lines, while the pattern was clearly different. CO2 cells formed huge and clearly separated LDs, whereas S11 cells incorporated lots of tiny LDs. Both types of LDs could be observed in S08 and S12 cells.

In LDs, triacylglycerides are enclosed by a monolayer of lipids which is covered with a variety of proteins. One of them is perilipin (PLIN)2, which is characteristic for growing LDs and has been associated with the development of NAFLD (Pawella et al., 2014). Initially, all cell lines expressed low levels of PLIN2, which increased after fat induction. Especially in CO2 derived cells, the immunocytochemistry confirmed that LDs are enclosed by PLIN2 (Fig. 3A, Fig. S2). qRT-PCR corroborated the significant increase of *PLIN2* expression in all cell lines after OA treatment and revealed baseline differences in *PLIN2* levels between cell lines (Fig. 3B). LD quantification via cell profiler supported the observation that number as well as size of LDs increased (Fig. 3C) after OA treatment. Importantly, the total area covered by LDs increased in all cell lines significantly after OA treatment (Fig. 3D).

Fat storage in HLCs is not influenced by AdipoRon

The adipokine adiponectin as well as its synthetic analogue AdipoRon have many positive effects on murine metabolism, e.g. reducing gluconeogenesis, lipogenesis, and hepatic fat incorporation. We sought out to test if AdipoRon also influences LD storage and metabolism in the human iPSC-derived HLCs. To this end, we incubated HLCs for 9 days with and without 200 μ M OA and added 2 μ M AdipoRon to each condition. Visually, we could not observe any changes in LD number or structure in cells treated with AdipoRon compared to untreated cells (Figs 2A,3A; Fig. S2), while quantification indicated that AdipoRon induced an increase in LD size in CO2 cells independent of OA treatment and a decrease in OA treated S12 cells. Only in OA treated CO2 cells, *PLIN2* expression increased with OA treatment (Fig. 3B).

Mediators of Adiponectin signalling are present and active in all cell lines

Since AdipoRon treatment apparently had no effect on fat storage in HLCs, we tested if the relevant pathways, which are supposed to be influenced by AdipoRon (Fig. 4A), are actually active in HLCs.

Therefore, we first analysed the expression of the adiponectin receptors AdipoR1 and 2 in all cell lines. On the mRNA level, both receptors were present in all lines and their expression was neither influenced by OA nor by AdipoRon treatment (Fig. 4B). Interestingly, *AdipoR1* expression was significantly lower in S08 HLCs than in all other lines, independent of treatment. *AdipoR2* expression tended to be lower in CO2 cells. While both receptors were expressed in all of our cells on the mRNA level, only AdipoR2, which has been described to be the major adiponectin receptor on hepatocytes (Yamauchi et al., 2003), could be detected by western blotting (Fig. 4C).

We next wanted to know if the enzymes involved in the major signalling pathways that are influenced by AdipoRon are present in the cells. Therefore, we performed western blotting for cAMP response element-binding protein (CREB), the enzyme 5' adenosine monophosphate-activated protein (AMPK), and protein kinase beta (AKT), probing for the total protein as well as for the respective phosphorylated active forms.

Table 1. Steatosis lines

ID	Gender	Age	BMI	Steatosis grade	Diabetes type 2	Reference
CO2	F	19	21	Non-obese	Unknown	(Kawala et al., 2016a)
S08	M	61	46	Obese, high steatosis	No	(Kawala et al., 2016b)
S11	F	58	45	Obese, high steatosis	No	(Graffmann et al., 2018)
S12	F	50	35	Obese, low steatosis	No	(Kawala et al., 2016c)

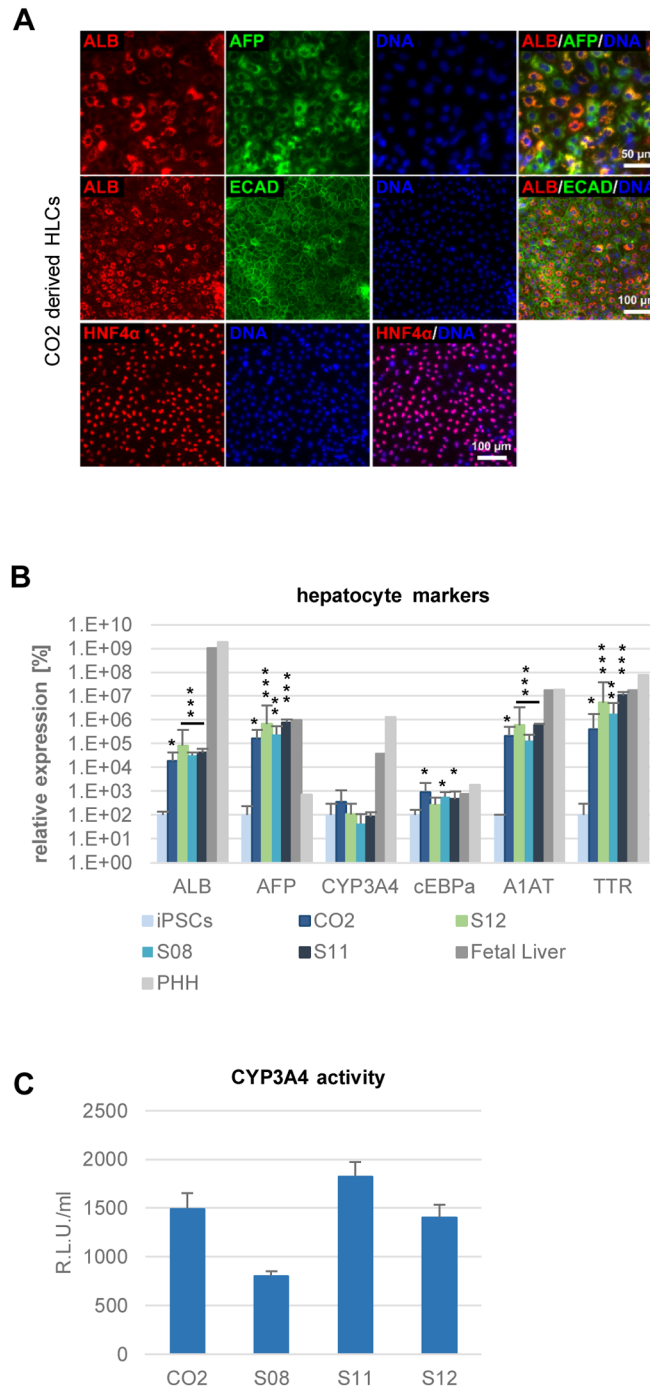


Fig. 1. Characterization of HLCs. (A) Representative immunocytochemistry of hepatocyte markers at the end of HLC differentiation for the line CO2. Cells were stained for ALB (red) and AFP (green) (upper lane), ALB (red) and ECAD (green) middle lane, HNF4 α (red) (lower lane). DNA was stained with Hoechst 33258. (B) Expression of hepatocyte markers *ALB*, *AFP*, *CYP3A4*, *cEBP α* , *A1AT*, and *TTR* was confirmed by qRT-PCR. Fold change towards iPSCs was calculated and converted into percentage. iPSCs: $n=2$, HLCs: $n=3$, PHH and fetal liver RNA: $n=1$. Data are means \pm 95% confidence interval. Significances in comparison to iPSCs were calculated with unpaired two-tailed Student's *t*-tests. * $P<0.05$, ** $P<0.01$, *** $P<0.001$. (C) CYP3A4 activity in HLCs. $n=3$, mean values \pm s.d. are shown.

In all lines, these proteins as well as their active phosphorylated counterparts were present, although with major variations between lines (Fig. 4C; Fig. S3).

Key metabolic master regulators are expressed in HLCs

We next performed qRT-PCR to see whether key metabolic regulators are expressed in our cells and how they react to the OA challenge and the AdipoRon treatment. Of special interest were the

peroxisome proliferator-activated receptor (PPAR) family members *PPAR α* and *PPAR γ* , as well as Protein Kinase AMP-Activated Catalytic Subunit Alpha (PRKAA)2, the catalytic subunit of AMPK.

Besides being involved in Adiponectin signalling, it is known that hepatic *PPAR α* gets activated by fatty acids that are released from adipocytes. It stimulates energy generating metabolic pathways, in particular β -oxidation (Pawlak et al., 2015). Here, we did not observe any substantial changes in *PPAR α* expression

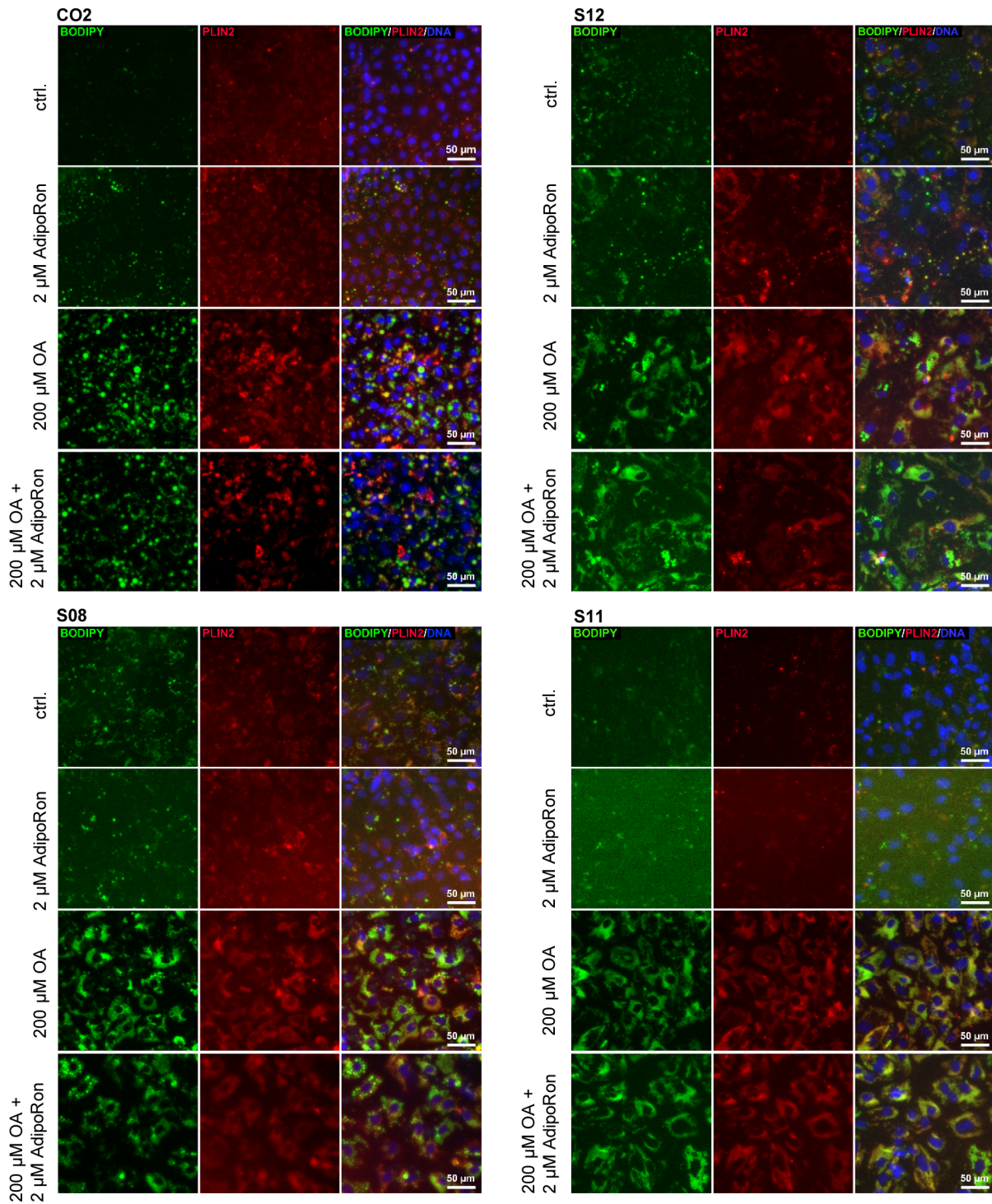


Fig. 2. Fat induction in HLCs. Representative immunocytochemistry for LDs (BODIPY 493/593, green), PLIN2 (red) and DNA (Hoechst 33258, blue) in iPSC derived HLCs.

related to OA or AdipoRon treatment. Interestingly, S08 cells had a significantly lower expression of *PPARα* with and without challenge than all other lines (Fig. 5A).

PPARy is known to increase fat storage (Medina-Gomez et al., 2007). At baseline as well as with 2 μM AdipoRon treatment alone, its expression was significantly lower in CO2 derived HLCs than in all other lines. Overall, we did not observe expression changes related to OA or AdipoRon treatment (Fig. 5A).

PPARy Coactivator-1α (*PGC1α*) is a transcriptional coactivator that interacts, amongst others, with *PPARα* and *γ*. It is involved in the upregulation of gluconeogenesis genes during fasting as well as in the induction of *β*-oxidation. It is known that, in the fed state, *PGC1α* is expressed at low levels in the liver and that expression increases during fasting (Yoon et al., 2001). In our setting, *PGC1α* was generally expressed at lower levels in CO2 and S08 cells than in S11 and S12. In the lines that expressed *PGC1α* at low levels, the

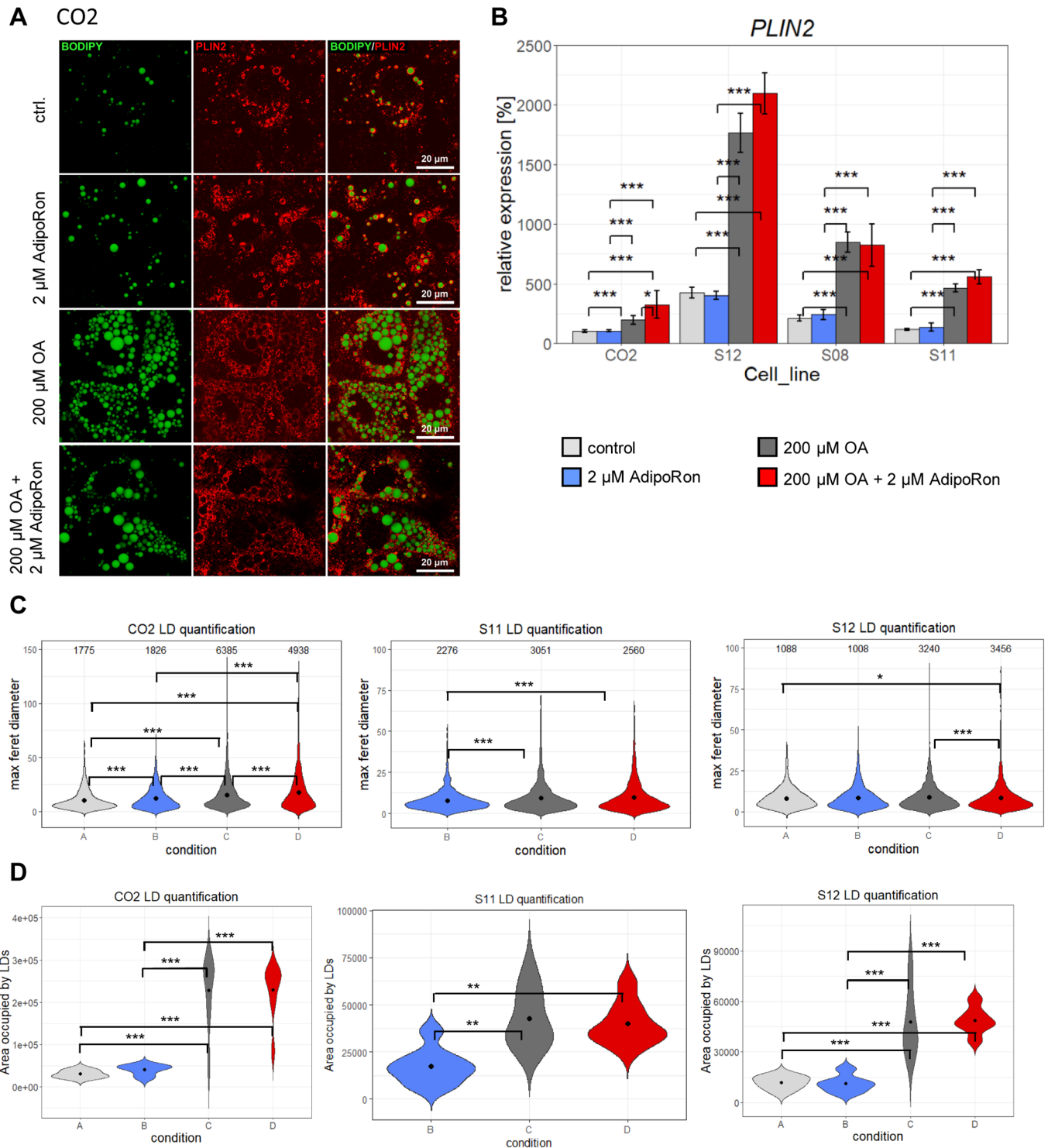


Fig. 3. LD quantification. (A) Confocal microscopy of CO2 cells. LDs (BODIPY 493/593, green), PLIN2 (red). (B) *PLIN2* expression was measured by qRT-PCR. Fold change was calculated towards CO2 control cells and converted into percentage. Mean of three biological replicates \pm 95% confidence interval is shown. Significances were calculated with ANOVA, followed by Tukey's multiple comparisons of means with 95% family wise confidence levels. Number and size of LDs as well as total area occupied by LDs were calculated via Cell Profiler 3.1.9. Due to the huge size differences of LDs, two distinct pipelines had to be used for CO2 and S11/12. Data of S08 and S11 condition A is missing due to technical issues during cell culture (C) Violin plot depicting size and number of LDs. Numbers of LDs are given within the plot. Mean values of LD size are indicated as black dots. Significances were calculated with Kruskal–Wallis test (CO2: $P < 2.2 \times 10^{-16}$, S11: $P = 2.027 \times 10^{-5}$, S12: $P = 0.002377$) followed by Wilcoxon rank test of means. (D) Total area occupied by lipid droplets. Mean values of LD size are indicated as black dots. Significances were calculated with ANOVA (CO2: $P = 1.03 \times 10^{-9}$, S11: $P = 0.000689$, S12: $P = 2.42 \times 10^{-6}$), followed by Tukey's multiple comparisons of means with 95% family wise confidence levels. *= $P < 0.05$, **= $P < 0.01$, ***= $P < 0.001$.

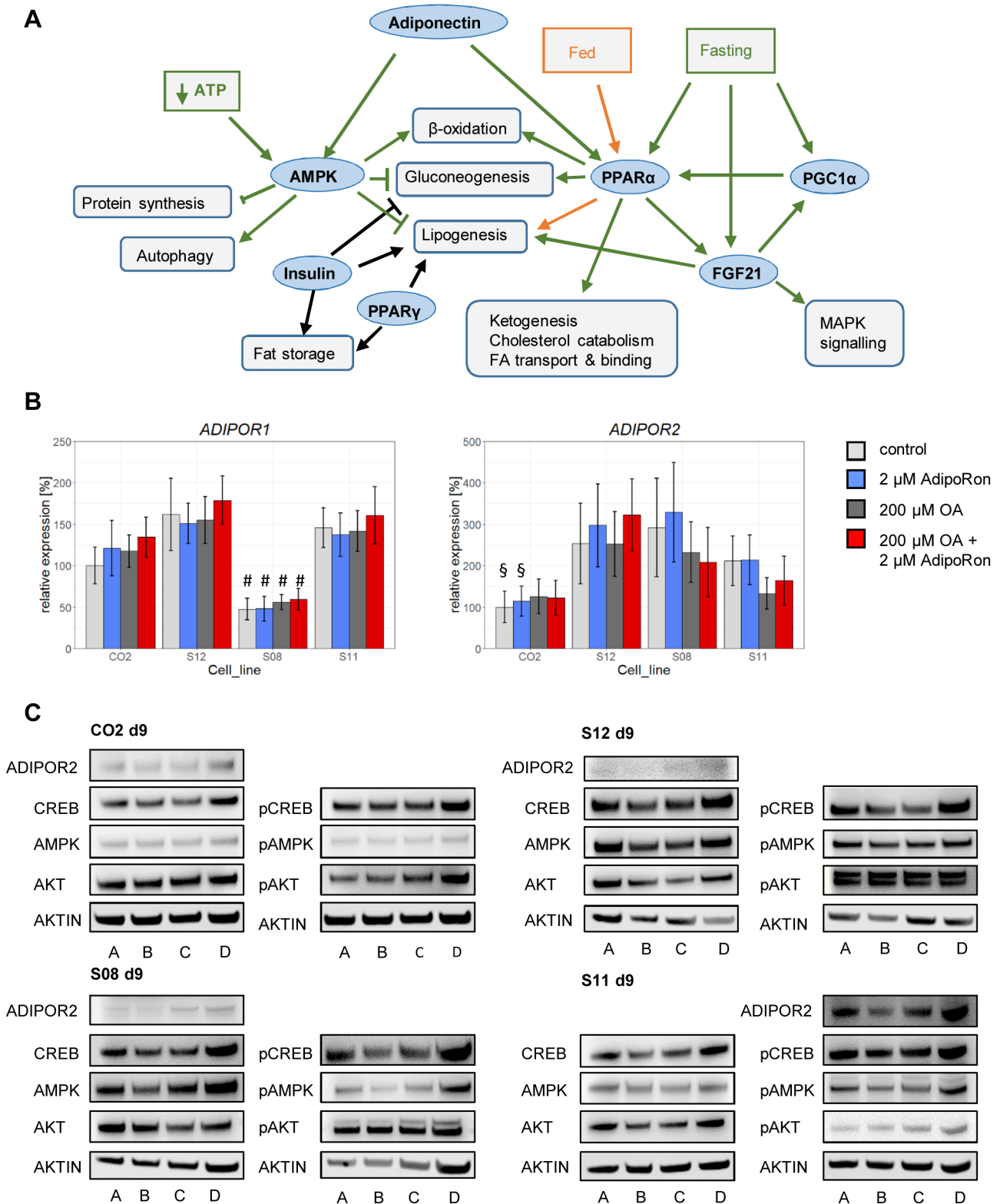


Fig. 4. Expression of metabolic master regulators in HLCs. (A) Schematic overview of relevant metabolic interactions in hepatocytes. (B) qRT-PCR for *AdipoR1* and 2. Fold change was calculated towards CO2 control cells and converted into percentage. Mean of three biological replicates +/- 95% confidence interval is shown. Significances were calculated with ANOVA, followed by Tukey's multiple comparisons of means with 95% family wise confidence levels. # = P < 0.001 when comparing same conditions between all lines; § = P < 0.01 when comparing CO2 and S08 or S12. (C) Representative western blots for AdipoR2, CREB/pCREB, AMPK/pAMPK, AKT/pAKT, and β-ACTIN. A=control, B=2 μM AdipoRon, C=200 μM OA, D=200 μM OA+2 μM AdipoRon.

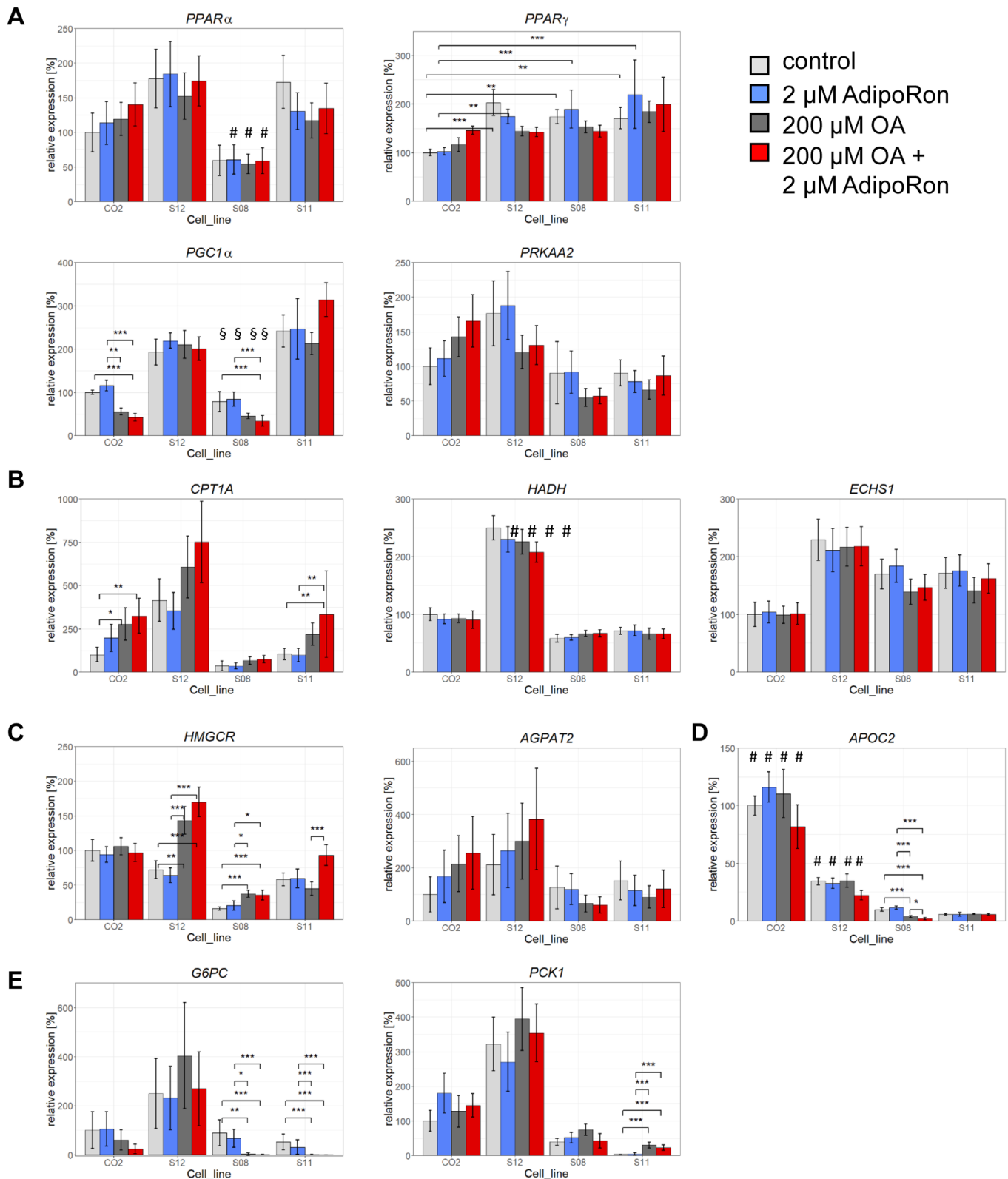


Fig. 5. Differential expression of metabolic enzymes. qRT-PCR for enzymes involved in metabolic regulation (A): *PPAR α* ($\#$ = P <0.05 when comparing same conditions between all lines), *PPAR γ* , *PGC1 α* ($\$$ = P <0.001 when comparing same conditions between S08 and S11 or S12; $\$$ = P <0.001 when comparing same conditions between S11 and S08 or CO2), *PRKAA2*, in β -oxidation (B): *CPT1A*, *HADH* ($\#$ = P <0.001 when comparing same conditions between all lines), *ECHS1*, in lipid and cholesterol metabolism (C): *HMGCR*, *AGPAT2*, in lipid export (D): *APOC2* ($\#$ = P <0.001 when comparing same conditions between all lines), in gluconeogenesis (E): *G6PC*, *PCK1*. Fold change was calculated towards CO2 control cells and converted into percentage. Mean of three biological replicates \pm 95% confidence interval is shown. Significances were calculated with ANOVA, followed by Tukey's multiple comparisons of means with 95% family wise confidence levels. *= P <0.05, **= P <0.01, ***= P <0.001.

expression was even further reduced after OA treatment independent of AdipoRon (Fig. 5A).

Finally, to assess AMPK levels, we measured *AMPK Subunit Alpha-2 (PRKAA2)* expression. Apart from its role in Adiponectin signalling, AMPK acts as a sensor of nutritional levels and reduces gluconeogenesis while it increases β -oxidation. After OA induction, *PRKAA2* expression was reduced in all cell lines except CO2, although the effect was not significant (Fig. 5A).

Enzymes involved in fatty acid and cholesterol metabolism are differentially expressed

To see if OA induction or AdipoRon treatment have any effects on downstream metabolic enzymes, we assessed the expression of lipid metabolism associated genes, which was strikingly different between cell lines. First we looked at genes involved in mitochondrial β -oxidation. Carnitine Palmitoyltransferase 1A (*CPT1A*) is the rate limiting enzyme responsible for the transport of fatty acid derived acyl-CoA across the mitochondrial membrane. In general, its expression was lower in the high steatosis lines S08 and S11 than in the low steatosis line and the control line. Interestingly, we observed a significant increase of *CPT1A* expression in CO2 and S11 cells after induction with OA alone as well as in combination with AdipoRon (Fig. 5B).

In case of Hydroxyacyl-CoA Dehydrogenase (*HADH*), which is involved in mitochondrial β -oxidation, we observed strikingly high expression levels in S12 cells in all conditions, while for Enoyl-CoA Hydratase Short Chain 1 (*ECHS1*), which also is important for this process, CO2 cells expressed remarkably low levels. For both factors, we could not observe expression changes related to OA or AdipoRon (Fig. 5B).

We also analysed the expression of genes important for cholesterol and lipid synthesis. 3-Hydroxy-3-Methylglutaryl-CoA Reductase (*HMGCR*) is involved in cholesterol synthesis. Its expression levels varied markedly between cell lines, with the lowest levels in S08 and S11 cells. Its expression was significantly upregulated in the high steatosis line S08 and the low steatosis line S12 after OA treatment independent of AdipoRon. Only in S11 cells, treatment with 2 μ M AdipoRon significantly increased *HMGCR* expression in the OA condition (Fig. 5C).

Similar to *HMGCR*, the expression of 1-Acylglycerol-3-Phosphate O-Acyltransferase 2 (*AGPAT2*), which plays a role in phospholipid biosynthesis, was highly variable in all cell lines, with S08 and S11 expressing the lowest levels of *AGPAT2* (Fig. 5C).

Finally, we analysed the expression of Apolipoprotein C2 (*APOC2*), which is involved in coating of very low-density lipoproteins (VLDL) that are secreted into the blood. Here, we observed in all conditions three to ten times higher expression levels in CO2 cells than in all other lines. We observed a significant reduction of *APOC2* expression only in S08 cells, after OA treatment, this was even further reduced upon AdipoRon stimulation (Fig. 5D).

OA treatment influences gluconeogenesis

We also wanted to know, whether there are differences in our lines with regards to the regulation of gluconeogenesis. In this regard, we analysed the expression of key genes involved in this process. Glucose-6-phosphatase (*G6PC*) is part of the catalytical complex that hydrolyses glucose 6-phosphate to glucose, the last step during gluconeogenesis. Its expression levels were generally low in all cell lines except S12. *G6PC* expression was significantly reduced in all lines except S12 after OA induction (Fig. 5E). Phosphoenolpyruvate Carboxykinase 1 (*PCK1*) catalyses the rate limiting step of gluconeogenesis, the transformation of oxaloacetate to phosphoenolpyruvate. Its

Table 2. Steatosis phenotypes

Genes	CO2 (healthy)	S12 (low steatosis)	S08 (high steatosis)	S11 (high steatosis)
PPAR α	+++	+++	+	+++
PPAR γ	++	+++	+++	+++
PGC1 α	+	+++	+	+++
PRKAA2	+++	+++	++	++
CPT1A	++	+++	+	+ / ++
HADH	+	+++	+	+
ECHS1	++	+++	++	++
HMGCR	+++	+++	+	+
AGPAT2	+++	+++	+	+
APOC2	+++	++	+	+
G6PC	++	+++	+	+
PCK1	++	+++	+	+
KLB	+++	+++	++	+

Gene expression levels according to Figs 5 and 7C.

Global gene expression profiles change after OA treatment and with AdipoRon.

expression was for all conditions highest in the low steatosis lines CO2 and S12, while it was almost undetectable in untreated S11 cells (Fig. 5E).

Taken together, the variations in the PCR data suggest the existence of cell type associated gene expression patterns that obscure the effects of OA and AdipoRon treatments at the given concentrations. Probably, a more stringent experimental approach, including age, gender and disease stage matched cells as well as a higher AdipoRon concentration will be necessary to unambiguously reveal metabolic patterns.

Nonetheless, we could identify a steatosis related phenotype (Table 2) with the high steatosis lines S11 and S08 tending to have low expression of genes involved in lipid export, fat and cholesterol synthesis as well as in gluconeogenesis, β -oxidation and FGF21 signalling.

All analyses indicated a more prominent role for OA regarding gene expression changes than for AdipoRon, at least in the selected pathways. To reveal any AdipoRon associated gene expression patterns, we performed Affymetrix Clariom S Microarray analyses for CO2 samples with and without treatment. As we saw a lot of variability in the PCR data, we restricted the microarray analysis to the cell line which has been generated from a healthy control donor in order to minimize cell line dependent or culture induce effects in the results.

Global analysis of gene expression revealed four distinct clusters, according to the four treatments (Fig. 6A). Overall, 13,834 genes were expressed in common in CO2 HLCs, independent of treatment (Fig. 6B). For every condition, we identified the exclusively expressed genes by Venn diagram analysis (Fig. 6B). 77 were only expressed in AdipoRon treated cells, 143 in cells treated with AdipoRon and OA, 83 in the OA only cells as well as in the untreated control cells. These exclusively expressed genes were related to distinct gene ontologies (GOs), indicating specific profiles of the 4 treatments (Fig. 6C). No characteristic GOs were associated with control cells. OA treated cells, on the other hand, exclusively expressed numerous genes associated with DNA replication/repair, immune reactions and metabolism. AdipoRon treatment of OA cells induced genes involved in signalling, while in the control condition, AdipoRon predominantly influenced metabolism-associated genes. For the full lists of GOs, please refer to Table S1.

In order to check the robustness of our model, we compared the differentially expressed genes between OA treated and control cells with those identified in a previous study also using iPSCs as a model

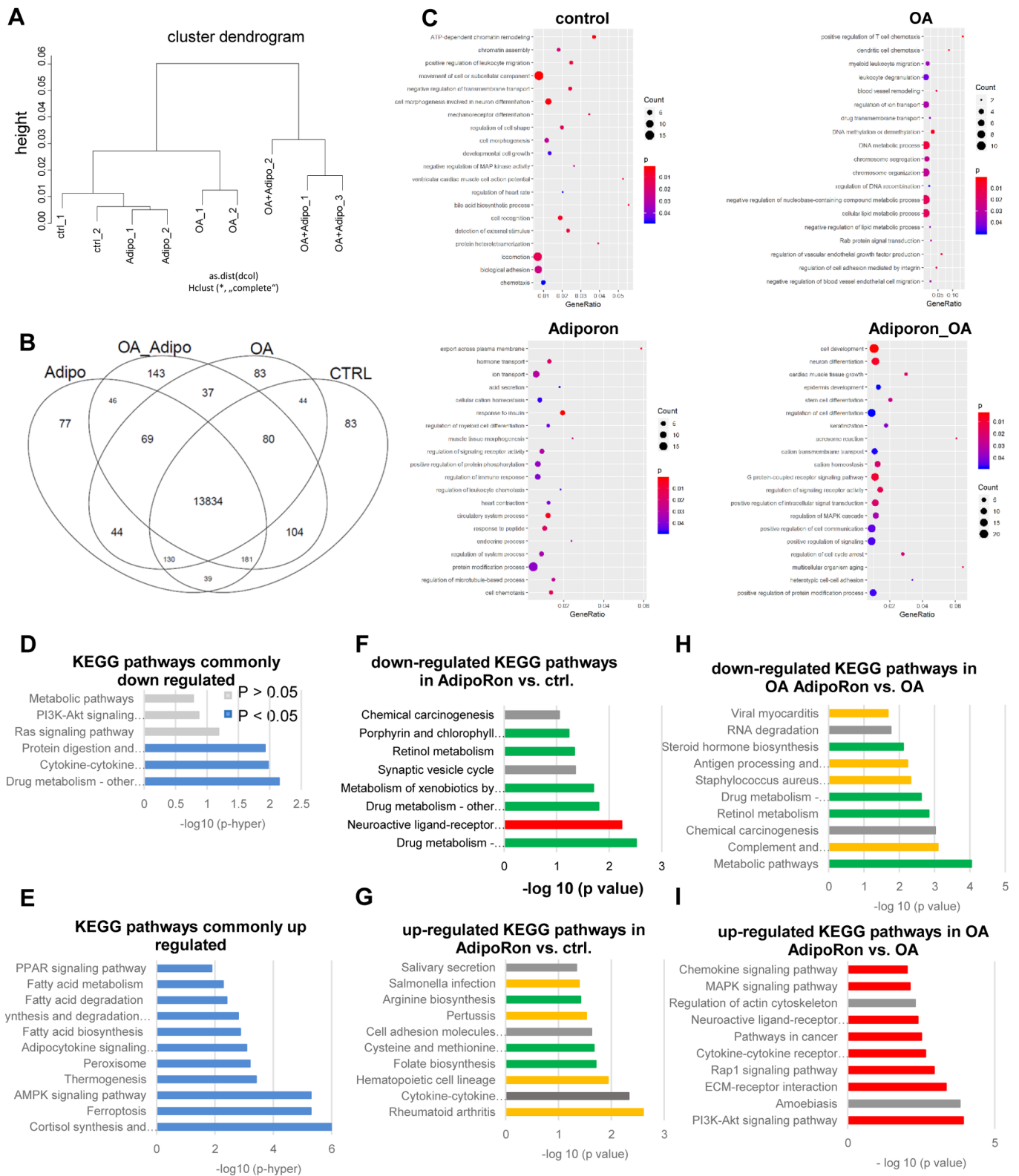


Fig. 6. Changes of global gene expression profiles after OA treatment and with AdipoRon. Transcriptome analysis was performed for all four conditions of CO2 HLCs. (A) Cells cluster according to treatment. (B) Venn diagram depicting the exclusively expressed genes for all four conditions. (C) Selected significantly enriched GOs of the exclusively expressed genes in the indicated conditions. (D,E) Comparison with published data of differentially expressed genes in iPSCs derived HLCs after OA treatment reveals common downregulated (D) and selected common upregulated (E) KEGG-pathways. (F–I) Top 10 significantly down- or upregulated KEGG pathways after AdipoRon treatment of control and OA cells. For full lists of GOs and KEGG pathways please refer to Table S1.

for NAFLD (Graffmann et al., 2016) (Fig. 6D,E). There was an overlap of 24 genes upregulated and 32 genes downregulated after OA treatment. KEGG pathway analysis revealed that the common downregulated genes were significantly associated with drug metabolism, cytokine–cytokine receptor interaction and protein digestions, while signalling and metabolic pathways were also detected although this was not significant (Fig. 6D). Importantly, the common significantly upregulated pathways were predominantly associated with metabolism as well as with adipocytokine and AMPK signalling (Fig. 6E).

Next, we checked which KEGG pathways were affected by AdipoRon treatment in the control and OA setting. In the control treatment, AdipoRon mostly affected metabolism and immune system related pathways. Interestingly, drug metabolism tended to be downregulated while metabolic pathways related to amino acid synthesis as well as pathways related to the immune system, were upregulated (Fig. 6F,G).

On the OA background, pathways related to metabolism and immune system were downregulated (Fig. 6H). The upregulated pathways in OA AdipoRon-treated cells were predominantly related to various signalling pathways (Fig. 6I).

In order to identify an AdipoRon-associated signature, we compared the common up- and downregulated genes in AdipoRon-treated control and OA cells (Fig. S4). Among the significantly upregulated pathways, we identified transmembrane transporters, drug metabolism, and glycoprotein/thyroid hormones. The significantly commonly downregulated pathways were connected to homeostasis, indicating a broad role for AdipoRon on metabolism and cell function in general.

FGF21 expression is reduced after OA treatment

Finally, we selected genes of the metabolic network involved in PPAR α and Adiponectin signalling (Fig. 4A) for heatmap analysis. Interestingly, *FGF21* expression was downregulated in OA-treated cells compared to control cells (Fig. 7A,B). FGF21 acts as a hormone in an endocrine, autocrine and paracrine manner and is tightly associated with Adiponectin and PPAR α/γ signalling (Lin et al., 2013; Goto et al., 2017; Gälman et al., 2008). FGF21 is predominantly synthesized in the liver. Its expression is regulated by PPAR α and γ . In turn, FGF21 can regulate Adiponectin as well as PPAR γ expression in feed-forward-loops (Goetz, 2013). For all cell lines except of S11 we could confirm the OA-associated reduction of FGF21 expression in western blots.

FGF21 signals via receptor dimers consisting of various FGF receptors in combination with β -KLOTHO (KLB). The common factor for signalling, *KLB*, was expressed in all cell lines independent of treatment. Similar to *AdipoR1*, its expression was significantly reduced in S08 cells (Fig. 7C).

In summary, we have shown that *in vitro* derived HLCs from various donors with distinct genetic backgrounds react similarly to OA overdose with incorporating fat and increasing *PLIN2* expression. Apart from that, there are marked differences in the gene expression profiles of the different cell lines reflecting the complex metabolic pathways that seem to play varying roles in the individual lines and could explain the differences seen in disease progression within individuals. While we could not identify a robust AdipoRon effect on an isolated factor, we saw general metabolic alterations affecting metabolism, transport, and signalling pathways.

DISCUSSION

NAFLD is a multifactorial disease that is regulated by complex interactions between genome, epigenome, and microbiome in response to certain nutritional cues. Here, we employed an iPSC

based *in vitro* model for NAFLD to assess a variety of phenotypes associated with the disease.

All our iPSC-derived HLCs from different donors accumulated LDs in response to a high fat diet. We saw substantial differences in the quantity, size, and distribution of LDs in all four cell lines, while all of them significantly upregulated *PLIN2*, a crucial LD-coating protein, in response to OA treatment. Interestingly, the cells that were derived from the healthy control donor produced the biggest LDs which even increased after AdipoRon treatment. In parallel, *PLIN2* expression levels after OA induction were lower than in all other cell lines. S11 cells, which were derived from a high steatosis patient, accumulated an uncountable amount of very tiny LDs. Also here, *PLIN2* expression was relatively low. Strikingly, S12 cells, which were derived from a low steatosis donor and showed an intermediate phenotype regarding LD size and quantity, had the highest induction of *PLIN2*. While the specific morphologies and distribution of LDs might be associated with disease severity, further investigations comparing several high-steatosis patient and healthy donor derived samples are necessary to exclude influences of age, gender, and cell culture effects.

In humans, macrovesicular steatosis, where few big LDs are formed, has a less negative impact on liver function and whole body health than microvesicular steatosis, which often is accompanied by encephalopathy and liver failure (Tandra et al., 2011). The phenotype of OA-fed CO2 cells mimics that of macrosteatosis. Low levels of *PLIN2* are associated with a lean phenotype and a reduced risk for steatosis in mice (McManaman et al., 2013). The combination of large LDs with relatively low levels of *PLIN2* expression in CO2-derived HLCs could point towards a yet unknown mechanism that protects the cells from lipid induced damage, which might be enhanced by AdipoRon treatment.

Additional indications of a healthier phenotype in CO2 cells are given by its relatively high expression of *CPT1A* and *APOC2*, possibly related to efficient burning and export of fatty acids. In contrast, gene expression patterns in the high steatosis lines indicate impaired fasting responses with low levels of *PPAR α* in S08 cells and no changes in *PGC1 α* after OA induction in S12, S11 and S08 cells. In addition, these cells seem to have an impaired capability of exporting FAs as suggested by the low levels of *APOC2* expression.

By integrating these data, we were able to identify critical metabolic constellations that suggested a more severe steatosis phenotype. High steatosis lines had a rather low expression of genes associated with gluconeogenesis, phospholipid-, and cholesterol biosynthesis with concomitant low expression of *CPT1A* indicating an additional lower capacity of β -oxidation and thus energy generation (Table 2).

Interestingly, all cells except S11 had reduced FGF21 levels after OA treatment. Normally, hepatic FGF21 expression is related to the fasting response (Gälman et al., 2008; Inagaki et al., 2007), thus low levels of FGF21 after OA overfeeding could be expected. Thus, the failure to reduce FGF21 levels in response to OA could be an additional sign of inefficient metabolic regulation in S11 cells. Interestingly, levels of PPAR α , which enhance FGF21 expression, and levels of KLB, which transfer FGF21 signalling into the cell, are within the range of the other cell lines and thus do not seem to be responsible for the failure to regulate FGF21 levels.

Taken together, our data point to an impaired reaction to nutritional cues in HLCs derived from high steatosis patients. Further comparative analysis will show if these cells really produce less glucose while also generating less energy which overall could be related to a limited capability to match the bodies energy needs which could trigger a compensatory storage of fat.

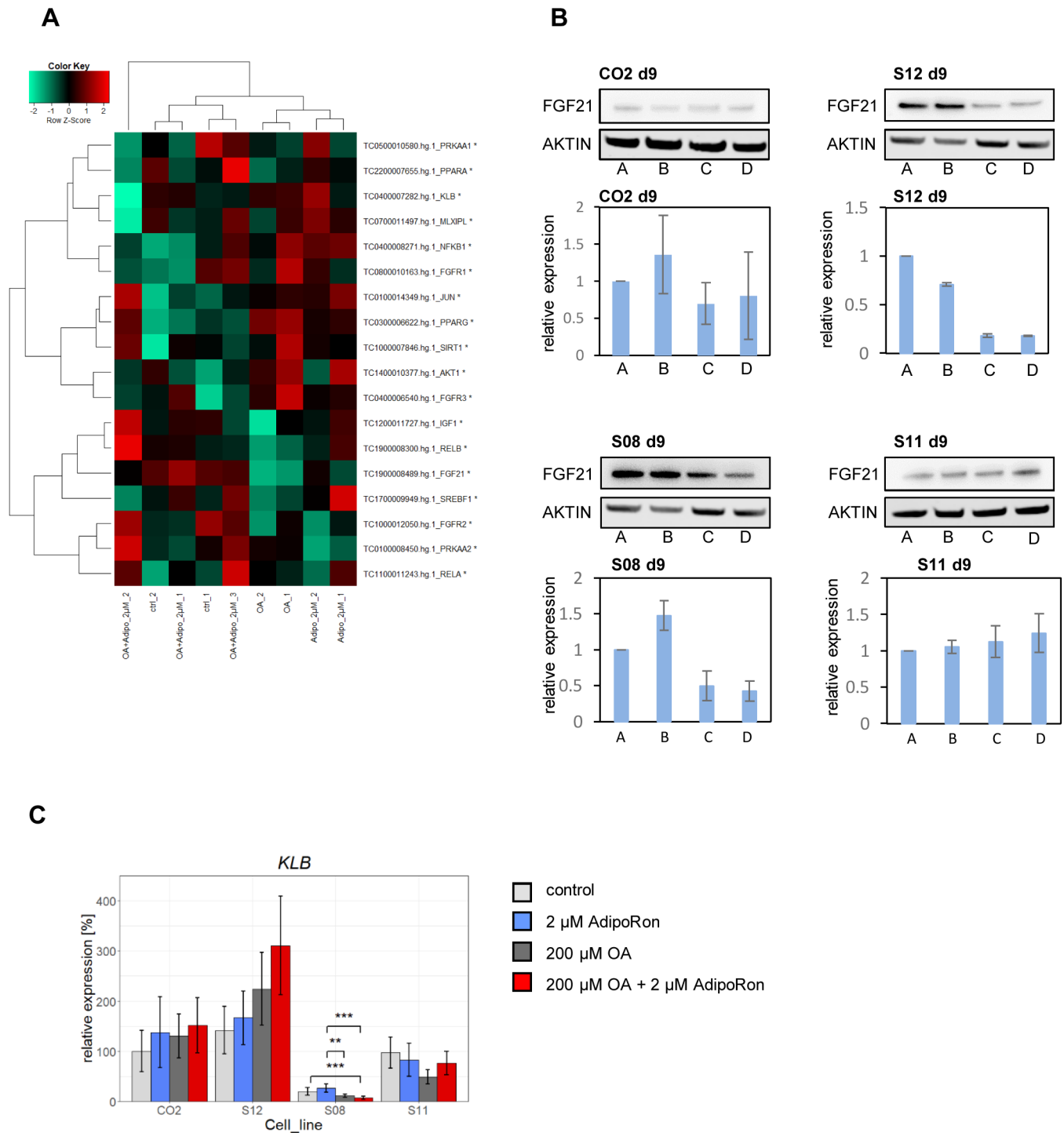


Fig. 7. FGF21 expression changes by OA treatment. (A) Heatmap analysis of genes within the Adiponectin-PPAR α metabolic network. (B) Representative western blots of three independent blots for FGF21 and β -ACTIN and quantification of FGF21 expression, normalized to control conditions. $n=3$, mean \pm s.d. is shown. A=control, B=2 μ M AdipoRon, C=200 μ M OA, D=200 μ M OA + 2 μ M AdipoRon. (C) Expression of KLB was measured by qRT-PCR. Fold change was calculated towards CO2 control cells and converted into percentage. Mean of three biological replicates \pm 95% confidence interval is shown. Significances were calculated with ANOVA, followed by Tukey's multiple comparisons of means with 95% family wise confidence levels. ***= $P<0.01$, ****= $P<0.001$.

Overall, many aspects of NAFLD can be recapitulated *in vitro*, independent of the donor's genotype. However, the distinct origin of the cells and their metabolic capacities, as well as distinct reprogramming and differentiation efficiency, have a key impact on the analyses and impede unambiguous conclusions at this stage.

In general, OA treatment had major effects on the cells, while AdipoRon effects only became visible when analysing whole transcriptome data from one single donor. Possibly, its influence might become more obvious by increasing the concentration or duration of AdipoRon treatment and including more replicates in every analysis.

The transcriptional network that regulates key metabolic processes and is supposed to be susceptible to Adiponectin signalling was active in all cells. They all expressed AdipoR2 as well as AMPK, CREB, and AKT, which were all also detectable in the phosphorylated, active form. However, we did not see reproducible disease-associated phenotypes and we were also not able to induce consistent changes in the activity levels of the analysed regulators by OA or AdipoRon treatment. This might be due to the complex interaction of several pathways and the simultaneous presence of conflicting signals that are present in the cell culture. The HLC medium contains for example insulin as well as the glucocorticoid dexamethasone which both are strong inducers of fat storage (Brown and Goldstein, 2008; Marino et al., 2016). We do not know if cells from all donors react in the same way to these molecules. Maybe higher AdipoRon concentrations are necessary to induce beneficial metabolic effects in all cell lines. In addition, it is possible that some AdipoRon related effects become only obvious in the systemic setting and cannot be reproduced in an *in vitro* model.

When analysing only the CO2 cell line, we observed influences of OA and AdipoRon on the transcriptome. The cells clustered according to the treatment. Comparison of the up- and downregulated genes after OA treatment with previously generated and published data from our system (Graffmann et al., 2016) revealed 56 overlapping genes. This number is somewhat limited due to different cell lines that were used and differences in the OA induction protocol. Nonetheless, there are commonly regulated genes. These are probably reliable as indicators for a steatotic phenotype because they were regulated in a robust way across the experiments. Interestingly, in both studies PPAR- and AMPK signalling as well as fat metabolism were upregulated, suggesting a common reproducible pattern. Especially PPAR-signalling pathways are already clinical targets for treating hyperlipidemia. So far, these medications are not approved for the treatment of NAFLD but our data support studies that claim efficiency of PPAR, agonists in this condition (Boeckmans et al., 2019; Fernandez-Miranda et al., 2008).

Analysis of the genes exclusively expressed in the four conditions revealed distinct patterns of overrepresented GOs. Most importantly, AdipoRon influenced metabolism-associated GOs in the control setting while it had an impact on signalling in the OA background. OA treatment alone induced stress in the cells, which becomes evident by many of the upregulated GOs associated with DNA repair and structure as well as to the immune system. Increased cellular stress levels are tightly connected to the progression of NAFLD to NASH and HCC (Buzzetti et al., 2016).

AdipoRon seems to have distinct functions depending on the nutritional background. As expected, it is involved in the regulation of metabolism in the control as well as in the OA setting. Interestingly, in the control AdipoRon condition, several pathways related to cysteine, methionine and folate metabolism were upregulated. Indeed, deprivation of cysteine and methionine fosters the development of NASH in mice (Rinella et al., 2008), which might be counteracted by AdipoRon. AdipoRon also influenced several pathways that are connected to the immune system, which agrees with recent publications that have described an anti-inflammatory role of Adiponectin in cardiac and adipose tissue, which also was connected to milder inflammation levels in the context of the metabolic syndrome (Jenke et al., 2013; Tsuchida et al., 2005; Frühbeck et al., 2017). Also this might help to improve health conditions of steatotic patients, as latent inflammation is a risk factor for disease progression (Tilg and Moschen, 2010). Finally, AdipoRon increased signalling pathways, many of which are involved in regulating metabolism, in OA treated cells. Although we could not confirm the AdipoRon

action in the selected pathways in our analysis, these data point to a global role of AdipoRon affecting metabolism. It is possible that higher concentrations of AdipoRon might give a clearer picture of its action. In addition, certain limitations of the cell culture setting probably also obscure AdipoRon effects. In 2D cultures, HLCs only reach limited grades of maturation, resembling fetal rather than adult cells which certainly has an impact on their metabolism. Also, differentiation efficiency varies between cell lines, introducing additional variability when comparing cells from distinct donors (Hannan et al., 2013). Recently, 3D culture models have been published, which increase maturity and might be suitable to overcome the problem of varying differentiation efficiencies (Rashidi et al., 2018; Sgodda et al., 2017). Although in this setting we face the question whether or not externally applied substances reach all cells, especially those inside the organoid, a more homogenous culture might nonetheless improve our insights into NAFLD development and metabolic regulation by AdipoRon.

Despite its limitations, the heterogeneity which we find in our cell culture samples should be taken into account when developing treatments for NAFLD patients. Although there probably exist common pathways that can be modified, every patient might react differently and personalized medicine is necessary to effectively treat this widespread disease.

MATERIALS AND METHODS

Differentiation of iPSCs into HLCs

The use of iPSC lines for this study was approved by the ethics committee of the medical faculty of Heinrich-Heine University under the number 5013. iPSCs were cultured on laminin (LN) 521 (Biolamina) coated plates in StemMACS iPSC brew medium (Miltenyi). Differentiation into HLCs was performed as described previously (Graffmann et al., 2016) with minor changes. To start the differentiation, iPSCs were passaged as single cells onto plates coated with a 3:1 mixture of LN111 and LN521. The next day, the medium was changed to definitive endoderm (DE) medium: 96% RPMI 1640, 2% B27 (without retinoic acid), 1% Glutamax (Glx), 1% Penicillin/Streptomycin (P/S) (all Gibco), 100 ng/ml Activin A (Peprotech), which was replaced daily. On the first day an additional 2.5 μ M Chir 99021 (Stemgent) was included. Afterwards the cells were cultivated for 4 days in hepatic endoderm (HE) medium with daily medium changes: 78% Knockout DMEM, 20% Knockout serum replacement, 0.5% Glx, 1% P/S, 0.01% 2-Mercaptoethanol (all Gibco) and 1% DMSO (Sigma-Aldrich). In the last step, hepatocyte-like medium was used for up to 10 days with medium change every other day: 82% Leibovitz 15 medium, 8% fetal calf serum, 8% Tryptose Phosphate Broth, 1% Glx, 1% P/S (all Gibco) with 1 μ M Insulin (Sigma-Aldrich), 10 ng/ml hepatocyte growth factor (HGF) (Peprotech), 25 ng/ml Dexamethasone (DEX) (Sigma-Aldrich).

Synthesis of AdipoRon

AdipoRon was synthesized from 4-hydroxy-benzophenone, chloroacetic acid methyl ester, and 4-amino-1-benzylpiperidine following the procedure reported by Okada-Iwabu, Yamauchi, and Iwabu (Okada-Iwabu et al., 2013; Kadowaki et al., 2015). The identity and purity of the product was double-checked by spectroscopic analysis (1 H NMR and 13 C NMR).

Fat induction and small molecule treatment

Oleic acid (Calbiochem) was bound to fatty acid free BSA (Sigma-Aldrich) and added to the cells in a final concentration of 200 μ M. AdipoRon was dissolved in DMSO and the cells were treated with a final concentration of 2 μ M. Control treatment for OA consisted in BSA and for AdipoRon in DMSO. The treatment started on day 10 of the differentiation and was continued for 5 and 9 days.

Immunocytochemistry

Cells were fixed with paraformaldehyde for 15 min at room temperature (RT). For permeabilization and blocking they were incubated for 2 h at RT with blocking buffer (1 \times PBS with 10% normal goat or donkey serum, 1% BSA,

0.5% Triton and 0.05% Tween). Blocking buffer was diluted 1:2 with 1 × PBS and cells were incubated with the primary antibody overnight at 4°C. Cells were washed three times with 1x PBS/ 0.05% Tween and incubated with the secondary antibody for 2 h at RT. To stain lipid droplets, cells were incubated with BODIPY 493/503 (1 µg/ml, Life Technologies) in PBS/0.05% Tween for 20 min and washed afterwards. DNA was stained with Hoechst 33258. Images were captured using a fluorescence microscope (LSM700, Zeiss). The following primary antibodies were used: Alpha Fetoprotein, Albumin (Sigma-Aldrich), E-cadherin (CST), HNF4 α (Abcam), SOX17 (R&D), PLIN2 (Proteintech). For details on antibodies see Table S2. Individual channel images were processed and merged with Fiji.

LD quantification

For confocal images, cells were differentiated on matrigel coated x-well tissue culture chambers (Sarstedt), except for S08, where iPSCs did not attach to the glass bottom. Similarly, one condition of S11 was lost due to attachment issues. Confocal images were analysed with Cell Profiler version 3.1.9. Due to the huge differences in LD size, separate pipelines had to be used for CO2 and S11/12 analysis. Pipelines are available upon request. Significances for LD size and numbers were calculated via Kruskal–Wallis test followed by Wilcoxon rank test and for total area occupied by ANOVA followed by Tukey’s multiple comparisons of means with 95% family wise confidence levels.

Measurement of cytochrome P450 activity

The P450-Glo™ CYP3A4 Assay Luciferin-PFBE (Promega) kit was used to measure Cytochrome P450 3A4 activity employing a luminometer (Lumat LB 9507, Berthold Technologies).

Western blot

Frozen cell pellets were lysed in 1x RIPA buffer (Sigma-Aldrich) with protease and phosphatase inhibitors (Roche, Sigma-Aldrich). 20 µg of protein were loaded into nupage 4–12% bis-tris precast gels (Thermo Fisher Scientific) and run with MES buffer. Proteins were transferred to a 0.45 µm nitrocellulose membrane (GE healthcare). Membranes were blocked with 5% milk in TBS/0.1% Tween (TBST) for 1 h at RT. Antibodies were diluted as described in Table S2. Incubation with primary antibodies was performed overnight at 4°C. Membranes were washed three times with TBST and secondary antibody incubation was performed for 1–2 h at RT followed by washing as above. In case of HRP coupled secondary antibodies, chemiluminescence was detected on a Fusion FX instrument (PeqLab). For detection of β -actin an IR dye 680 coupled secondary antibody (LICOR) was used and detection was performed on an Odyssey CLx instrument (LI-COR). Analysis was performed with Fusion Capt Advance software (PeqLab) using rolling ball background correction or with Image Studio light 5.2 software (LI-COR).

RNA isolation and quantitative reverse transcription PCR (qRT-PCR)

Cells were lysed in Trizol. RNA was isolated with the Direct-zol™ RNA Isolation Kit (Zymo Research) according to the user’s manual including a 30 min DNase digestion step. 500 ng of RNA were reverse transcribed using the TaqMan Reverse Transcription Kit (Applied Biosystems). Primer sequences are provided in Table S3. All primers were ordered from MWG.

Real time PCR was performed in technical triplicates with Power Sybr Green Master Mix (Life Technologies) on a ViiA7 (Life Technologies) machine. Mean values were normalized to *RPS16* and fold change was calculated using the indicated controls. Experiments were carried out in biological triplicates (with the exception of PHH and fetal liver which were only measures once) and are depicted as mean values with 95% confidence interval (CI). Unpaired Student’s *t*-tests were performed for calculating significances in Fig. 1, in all other cases ANOVA was used followed by Tukey’s multiple comparisons of means with 95% family wise confidence levels.

Transcriptome and bioinformatics analysis

Microarray experiments were performed on human Clariom S Arrays (Affymetrix) (BMFZ, Düsseldorf).

Data analysis

Untreated control HLCs and HLCs treated with AdipoRon, OA, and OA plus AdipoRon were hybridized on the Affymetrix Human Clariom S platform where CEL files were generated. These CEL files – regarded as the Affymetrix raw data – were read into the R/Bioconductor statistical package (Gentleman et al., 2004). The R package oligo was employed for background-correction and normalization via the Robust Multi-array Average (RMA) method (Carvalho and Irizarry, 2010). A detection *P*-value was calculated according to the method described in our previous publication by Graffmann et al. (Graffmann et al., 2016). A detection *P*-value of less than 0.05 was used to determine gene expression. Venn diagrams of expressed genes were made via the method venn from the gplots R package (Warnes et al., 2015), the dendrogram via the R function hclust. In order to determine differentially expressed genes the Bioconductor packages limma (Smyth, 2004) and qvalue (Storey, 2002) were applied.

GO and pathway analysis

Over-represented GOs were assessed with the R package GOstats (Falcon and Gentleman, 2007). For determination of over-represented KEGG pathways (Kanehisa et al., 2017) a download of pathways and associated gene symbols from March 2018 was used (Fig. 5D,E). Over-representation was calculated with the R-built-in hypergeometric test. Dot plots of most significant terms were generated via the ggplot package (Wickham, 2009). Alternatively, up- and down-regulated genes were analysed with DAVID to derive KEGG-pathways (Fig. 5F-I) (Huang et al., 2009a,b). Metascape was used to analyse the commonly up-regulated GOs and Pathways of AdipoRon treated control and OA cells (Zhou et al., 2019).

Acknowledgements

We thank Anijutta Antons and Miriam Bünning for their support with experiments.

Competing interests

The authors declare no competing or financial interests.

Author contributions

Conceptualization: N.G., J.A.; Methodology: N.G., A.N., S.M., A.R.F., P.R., M. Bohndorf, M. Beller; Software: W.W., M. Beller; Validation: W.W.; Formal analysis: N.G., W.W.; Investigation: N.G., A.N., S.M., A.R.F., M. Bohndorf; Resources: P.R., C.C.; Data curation: N.G., W.W., M. Beller; Writing - original draft: N.G., W.W., J.A.; Writing - review & editing: N.G., M. Beller, J.A.; Visualization: N.G., W.W., M. Beller; Supervision: C.C., J.A.; Project administration: J.A.; Funding acquisition: N.G., J.A.

Funding

N.G. was funded by the Forschungskommission of the Medizinische Fakultät Heinrich-Heine University Düsseldorf. J.A. was funded by the Medizinische Fakultät Heinrich-Heine University Düsseldorf.

Data availability

Data are available at the GEO database under the accession number: GSE162797, <https://www.ncbi.nlm.nih.gov/geo/query/acc.cgi?acc=GSE162797>.

Supplementary information

Supplementary information available online at <https://bio.biologists.org/lookup/doi/10.1242/bio.054189.supplemental>

References

- Bechmann, L. P., Hannivoort, R. A., Gerken, G., Hotamisligil, G. S., Trauner, M. and Canbay, A. (2012). The interaction of hepatic lipid and glucose metabolism in liver diseases. *J. Hepatol.* **56**, 952–964. doi:10.1016/j.jhep.2011.08.025
- Boeckmans, J., Natale, A., Rombaut, M., Buyl, K., Rogiers, V., De Kock, J., Vanhaecke, T. and Rodrigues, R. M. (2019). Anti-NASH drug development hitches a lift on PPAR agonism. *Cells* **9**, 37. doi:10.3390/cells9010037
- Brown, M. S. and Goldstein, J. L. (2008). Selective versus total insulin resistance: a pathogenic paradox. *Cell Metab.* **7**, 95–96. doi:10.1016/j.cmet.2007.12.009
- Buzzetti, E., Pinzani, M. and Tsochatzis, E. A. (2016). The multiple-hit pathogenesis of non-alcoholic fatty liver disease (NAFLD). *Metabolism* **65**, 1038–1048. doi:10.1016/j.metabol.2015.12.012
- Carvalho, B. S. and Irizarry, R. A. (2010). A framework for oligonucleotide microarray preprocessing. *Bioinformatics* **26**, 2363–2367. doi:10.1093/bioinformatics/btq431

- Cohen, J. C., Horton, J. D. and Hobbs, H. H. (2011). Human fatty liver disease: old questions and new insights. *Science* **332**, 1519-1523. doi:10.1126/science.1204265
- Combs, T. P. and Mariss, E. B. (2014). Adiponectin signaling in the liver. *Rev. Endocr. Metab. Disord.* **15**, 137-147. doi:10.1007/s11554-013-9280-6
- Ehling, A., Schaffler, A., Herfarth, H., Tärner, I. H., Anders, S., Distler, O., Paul, G., Distler, J., Gay, S., Scholmerich, J. et al. (2006). The potential of adiponectin in driving arthritis. *J. Immunol.* **176**, 4468-4478. doi:10.4049/jimmunol.176.7.4468
- Falcon, S. and Gentleman, R. (2007). Using GOstats to test gene lists for GO term association. *Bioinformatics* **23**, 257-258. doi:10.1093/bioinformatics/btl567
- Felder, T. K., Hahne, P., Soyak, S. M., Miller, K., Hoffinger, H., Oberkofler, H., Krempler, F. and Patsch, W. (2010). Hepatic adiponectin receptors (ADIPOR) 1 and 2 mRNA and their relation to insulin resistance in obese humans. *Int J Obes (Lond)* **34**, 846-851. doi:10.1038/ijo.2010.7
- Fernandez-Miranda, C., Perez-Carreras, M., Colina, F., Lopez-Alonso, G., Vargas, C. and Solis-Herruzo, J. A. (2008). A pilot trial of fenofibrate for the treatment of non-alcoholic fatty liver disease. *Dig. Liver Dis.* **40**, 200-205. doi:10.1016/j.dld.2007.10.002
- Frühbeck, G., Catalán, V., Rodríguez, A., Ramirez, B., Beceril, S., Salvador, J., Portincasa, P., Colina, I. and Gómez-Ambrosi, J. (2017). Involvement of the leptin-adiponectin axis in inflammation and oxidative stress in the metabolic syndrome. *Sci. Rep.* **7**, 6619. doi:10.1038/s41598-017-06997-0
- Gälman, C., Lundasen, T., Kharitonov, A., Bina, H. A., Eriksson, M., Hafström, I., Dahlin, M., Amark, P., Ångelin, B. and Rudling, M. (2008). The circulating metabolic regulator FGF21 is induced by prolonged fasting and PPAR α activation in man. *Cell Metab.* **8**, 169-174. doi:10.1016/j.cmet.2008.06.014
- Gentleman, R. C., Carey, V. J., Bates, D. M., Bolstad, B., Dettling, M., Dudoit, S., Ellis, B., Gautier, L., Ge, Y., Gentry, J. et al. (2004). Bioconductor: open software development for computational biology and bioinformatics. *Genome Biol.* **5**, R80. doi:10.1186/gb-2004-5-10-r80
- Goetz, R. (2013). Metabolism: adiponectin—a mediator of specific metabolic actions of FGF21. *Nat Rev Endocrinol* **9**, 506-508. doi:10.1038/nrendo.2013.146
- Goto, T., Hirata, M., Aoki, Y., Iwase, M., Takahashi, H., Kim, M., Li, Y., Jheng, H.-F., Nomura, W., Takahashi, N. et al. (2017). The hepatokine FGF21 is crucial for peroxisome proliferator-activated receptor- α agonist-induced amelioration of metabolic disorders in obese mice. *J. Biol. Chem.* **292**, 9175-9190. doi:10.1074/jbc.M116.767590
- Graffmann, N., Ring, S., Kawala, M.-A., Wruck, W., Ncube, A., Trompeter, H.-I. and Adjaye, J. (2016). Modeling nonalcoholic fatty liver disease with human pluripotent stem cell-derived immature hepatocyte-like cells reveals activation of PLIN2 and confirms regulatory functions of peroxisome proliferator-activated receptor α . *Stem Cells Dev.* **25**, 1119-1133. doi:10.1089/scd.2015.0383
- Graffmann, N., Bohndorf, M., Ncube, A., Wruck, W., Kashofer, K., Zatloukal, K. and Adjaye, J. (2018). Establishment and characterization of an iPSC line from a 58years old high grade patient with nonalcoholic fatty liver disease (70% steatosis) with homozygous wildtype PNPLA3 genotype. *Stem Cell Res.* **31**, 131-134. doi:10.1016/j.scr.2018.07.011
- Hannan, N. R., Segeritz, C.-P., Touboul, T. and Vallier, L. (2013). Production of hepatocyte-like cells from human pluripotent stem cells. *Nat. Protoc.* **8**, 430-437. doi:10.1038/nprot.2012.153
- Huang, D. W., Sherman, B. T. and Lempicki, R. A. (2009a). Bioinformatics enrichment tools: paths toward the comprehensive functional analysis of large gene lists. *Nucleic Acids Res.* **37**, 1-13. doi:10.1093/nar/gkn923
- Huang, D. W., Sherman, B. T. and Lempicki, R. A. (2009b). Systematic and integrative analysis of large gene lists using DAVID bioinformatics resources. *Nat. Protoc.* **4**, 44-57. doi:10.1038/nprot.2008.211
- Inagaki, T., Dutchak, P., Zhao, G., Ding, X., Gautron, L., Parameswara, V., Li, Y., Goetz, R., Mohammadi, M., Esser, V. et al. (2007). Endocrine regulation of the fasting response by PPAR α -mediated induction of fibroblast growth factor 21. *Cell Metab.* **5**, 415-425. doi:10.1016/j.cmet.2007.05.003
- Jenke, A., Wilk, S., Poller, W., Eriksson, U., Valaperti, A., Rauch, B. H., Stroux, A., Liu, P., Schultheiss, H.-P., Scheibenbogen, C. et al. (2013). Adiponectin protects against Toll-like receptor 4-mediated cardiac inflammation and injury. *Cardiovasc. Res.* **99**, 422-431. doi:10.1093/cvr/cvt118
- Kadowaki, T. and Yamauchi, T. (2005). Adiponectin and adiponectin receptors. *Endocr. Rev.* **26**, 439-451. doi:10.1210/er.2005-0005
- Kadowaki, T., Yamauchi, T., Iwabu, M., Iwabu, M., Yokoyama, S. and Honma, T. (2015). Adiponectin receptor-activating compound. EP3053911A1
- Kanehisa, M., Furumichi, M., Tanabe, M., Sato, Y. and Morishima, K. (2017). KEGG: new perspectives on genomes, pathways, diseases and drugs. *Nucleic Acids Res.* **45**, D353-D361. doi:10.1093/nar/gkw1092
- Kawala, M.-A., Bohndorf, M., Graffmann, N., Wruck, W., Zatloukal, K. and Adjaye, J. (2016a). Characterization of iPSCs derived from dermal fibroblasts from a healthy 19year old female. *Stem Cell Res* **17**, 597-599. doi:10.1016/j.scr.2016.10.002
- Kawala, M. A., Bohndorf, M., Graffmann, N., Wruck, W., Zatloukal, K. and Adjaye, J. (2016b). Characterization of dermal fibroblast-derived iPSCs from a patient with high grade steatosis. *Stem Cell Res* **17**, 568-571. doi:10.1016/j.scr.2016.10.007
- Kawala, M. A., Bohndorf, M., Graffmann, N., Wruck, W., Zatloukal, K. and Adjaye, J. (2016c). Characterization of dermal fibroblast-derived iPSCs from a patient with low grade steatosis. *Stem Cell Res* **17**, 547-549. doi:10.1016/j.scr.2016.10.004
- Koskinen, A., Juslin, S., Nieminen, R., Moilanen, T., Vuolteenaho, K. and Moilanen, E. (2011). Adiponectin associates with markers of cartilage degradation in osteoarthritis and induces production of proinflammatory and catabolic factors through mitogen-activated protein kinase pathways. *Arthritis Res. Ther.* **13**, R184. doi:10.1186/ar3512
- Lin, Z., Tian, H., Lam, K. S. L., Lin, S., Hoo, R. C. L., Konishi, M., Itoh, N., Wang, Y., Bornstein, S. R., Xu, A. et al. (2013). Adiponectin mediates the metabolic effects of FGF21 on glucose homeostasis and insulin sensitivity in mice. *Cell Metab.* **17**, 779-789. doi:10.1016/j.cmet.2013.04.005
- Liu, Q., Yuan, B., Lo, K. A., Patterson, H. C., Sun, Y. and Lodish, H. F. (2012). Adiponectin regulates expression of hepatic genes critical for glucose and lipid metabolism. *Proc. Natl. Acad. Sci. USA* **109**, 14568-14573. doi:10.1073/pnas.1211611109
- Luo, Y. and Liu, M. (2016). Adiponectin: a versatile player of innate immunity. *J Mol Cell Biol* **8**, 120-128. doi:10.1093/jmcb/mjw012
- Marino, J. S., Stechschulte, L. A., Stec, D. E., Nestor-Kalinoski, A., Coleman, S. and Hinds, T. D., Jr. (2016). Glucocorticoid receptor beta induces hepatic steatosis by augmenting inflammation and inhibition of the peroxisome proliferator-activated receptor (PPAR) α . *J. Biol. Chem.* **291**, 25776-25788. doi:10.1074/jbc.M116.752311
- McManaman, J. L., Bales, E. S., Orlicky, D. J., Jackman, M., MacLean, P. S., Cain, S., Crunk, A. E., Mansur, A., Graham, C. E., Bowman, T. A. et al. (2013). Perilipin-2-null mice are protected against diet-induced obesity, adipose inflammation, and fatty liver disease. *J. Lipid Res.* **54**, 1346-1359. doi:10.1194/jlr.M035063
- Medina-Gomez, G., Gray, S. L., Yetukuri, L., Shimomura, K., Virtue, S., Campbell, M., Curtis, R. K., Jimenez-Linan, M., Blount, M., Yeo, G. S. et al. (2007). PPAR γ 2 prevents lipotoxicity by controlling adipose tissue expandability and peripheral lipid metabolism. *PLoS Genet.* **3**, e64. doi:10.1371/journal.pgen.0030064
- Neuschwander-Tetri, B. A. (2017). Non-alcoholic fatty liver disease. *BMC Med.* **15**, 45. doi:10.1186/s12916-017-0806-8
- Okada-Iwabu, M., Yamauchi, T., Iwabu, M., Honma, T., Hamagami, K., Matsuda, K., Yamaguchi, M., Tanabe, H., Kimura-Someya, T., Shirouzu, M. et al. (2013). A small-molecule AdipoR agonist for type 2 diabetes and short life in obesity. *Nature* **503**, 493-499. doi:10.1038/nature12656
- Pawella, L. M., Hashani, M., Eiteneuer, E., Renner, M., Bartenschlager, R., Schirmacher, P. and Straub, B. K. (2014). Perilipin discerns chronic from acute hepatocellular steatosis. *J. Hepatol.* **60**, 633-642. doi:10.1016/j.jhep.2013.11.007
- Pawlak, M., Lefebvre, P. and Staels, B. (2015). Molecular mechanism of PPAR α action and its impact on lipid metabolism, inflammation and fibrosis in non-alcoholic fatty liver disease. *J. Hepatol.* **62**, 720-733. doi:10.1016/j.jhep.2014.10.039
- Rashidi, H., Luu, N. T., Alwahsh, S. M., Ginai, M., Alhaque, S., Dong, H., Tomaz, R. A., Vernay, B., Vigneswara, V., Hallett, J. M. et al. (2018). 3D human liver tissue from pluripotent stem cells displays stable phenotype in vitro and supports compromised liver function in vivo. *Arch. Toxicol.* **92**, 3117-3129. doi:10.1007/s00204-018-2280-2
- Rinella, M. E., Elias, M. S., Smolak, R. R., Fu, T., Borensztajn, J. and Green, R. M. (2008). Mechanisms of hepatic steatosis in mice fed a lipogenic methionine choline-deficient diet. *J. Lipid Res.* **49**, 1068-1076. doi:10.1194/jlr.M800042-JLR200
- Ruan, H. and Dong, L. Q. (2016). Adiponectin signaling and function in insulin target tissues. *J. Mol. Cell Biol.* **8**, 101-109. doi:10.1093/jmcb/mjw014
- Santhekadur, P. K., Kumar, D. P. and Sanyal, A. J. (2018). Preclinical models of non-alcoholic fatty liver disease. *J. Hepatol.* **68**, 230-237. doi:10.1016/j.jhep.2017.10.031
- Sgodda, M., Dai, Z., Zweigerdt, R., Sharma, A. D., Ott, M. and Cantz, T. (2017). A scalable approach for the generation of human pluripotent stem cell-derived hepatic organoids with sensitive hepatotoxicity features. *Stem Cells Dev.* **26**, 1490-1504. doi:10.1089/scd.2017.0023
- Smyth, G. K. (2004). Linear models and empirical bayes methods for assessing differential expression in microarray experiments. *Stat. Appl. Genet. Mol. Biol.* **3**, Article3. doi:10.2202/1544-6115.1027
- Storey, J. D. (2002). A direct approach to false discovery rates. *J. R. Stat. Soc. Ser. B Stat. Methodol.* **64**, 479-498. doi:10.1111/1467-9868.00346
- Tandra, S., Yeh, M. M., Brunt, E. M., Vuppalanchi, R., Cummings, O. W., Unalp-Arida, A., Wilson, L. A. and Chalasani, N. (2011). Presence and significance of microvesicular steatosis in nonalcoholic fatty liver disease. *J. Hepatol.* **55**, 654-659. doi:10.1016/j.jhep.2010.11.021
- Tilg, H. and Moschen, A. R. (2010). Evolution of inflammation in nonalcoholic fatty liver disease: the multiple parallel hits hypothesis. *Hepatology* **52**, 1836-1846. doi:10.1002/hep.24001
- Tsuchida, A., Yamauchi, T., Takekawa, S., Hada, Y., Ito, Y., Maki, T. and Kadowaki, T. (2005). Peroxisome proliferator-activated receptor (PPAR) α activation increases adiponectin receptors and reduces obesity-related inflammation in

- adipose tissue: comparison of activation of PPARalpha, PPARgamma, and their combination. *Diabetes* **54**, 3358-3370. doi:10.2337/diabetes.54.12.3358
- Vuppalanchi, R., Marri, S., Kolwankar, D., Considine, R. V. and Chalasani, N. (2005). Is adiponectin involved in the pathogenesis of nonalcoholic steatohepatitis? A preliminary human study. *J. Clin. Gastroenterol.* **39**, 237-242. doi:10.1097/01.mcg.0000152747.79773.2f
- Warnes, G. R., Bolker, B., Bonebakker, L., Gentleman, R., Liaw, W. H. A., Lumley, T., Maechler, M., Magnusson, A., Moeller, S., Schwartz, M. (2015). *gplots: Various R Programming Tools for Plotting Data*.
- Wickham, H. (2009). *Ggplot2: Elegant Graphics for Data Analysis*. Springer.
- Wong, R. J., Aguilar, M., Cheung, R., Perumpail, R. B., Harrison, S. A., Younossi, Z. M. and Ahmed, A. (2015). Nonalcoholic steatohepatitis is the second leading etiology of liver disease among adults awaiting liver transplantation in the United States. *Gastroenterology* **148**, 547-555. doi:10.1053/j.gastro.2014.11.039
- Wruck, W., Kashofer, K., Rehman, S., Daskalaki, A., Berg, D., Gralka, E., Jozefczuk, J., Drews, K., Pandey, V., Regenbrecht, C. et al. (2015). Multi-omic profiles of human non-alcoholic fatty liver disease tissue highlight heterogenic phenotypes. *Scientific Data* **2**, 150068. doi:10.1038/sdata.2015.68
- Yamauchi, T., Kamon, J., Ito, Y., Tsuchida, A., Yokomizo, T., Kita, S., Sugiyama, T., Miyagishi, M., Hara, K., Tsunoda, M. et al. (2003). Cloning of adiponectin receptors that mediate antidiabetic metabolic effects. *Nature* **423**, 762-769. doi:10.1038/nature01705
- Yamauchi, T., Nio, Y., Maki, T., Kobayashi, M., Takazawa, T., Iwabu, M., Okada-Iwabu, M., Kawamoto, S., Kubota, N., Kubota, T. et al. (2007). Targeted disruption of AdipoR1 and AdipoR2 causes abrogation of adiponectin binding and metabolic actions. *Nat. Med.* **13**, 332-339. doi:10.1038/nm1557
- Yoon, J. C., Puigserver, P., Chen, G. X., Donovan, J., Wu, Z. D., Rhee, J., Adelmant, G., Stafford, J., Kahn, C. R., Granner, D. K. et al. (2001). Control of hepatic gluconeogenesis through the transcriptional coactivator PGC-1. *Nature* **413**, 131-138. doi:10.1038/35093050
- Zhou, Y., Zhou, B., Pache, L., Chang, M., Khodabakhshi, A. H., Tanaseichuk, O., Benner, C. and Chanda, S. K. (2019). Metascape provides a biologist-oriented resource for the analysis of systems-level datasets. *Nat. Commun.* **10**, 1523. doi:10.1038/s41467-019-09234-6